Fachbereich Chemie der Universität Dortmund

# Solution- and solid-phase synthesis of monofunctionally *trans*-Pt(II) modified oligonucleotides and oligonucleotide analogues and their potential application in antigene and antisense strategy

Kathrin Susanne Schmidt

Vom Fachbereich Chemie der Universität Dortmund
zur Erlangung des akademischen Grades eines
Doktors der Naturwissenschaften
genehmigte Dissertation

| | |
|---|---|
| Referent: | Prof. Dr. B. Lippert, Dortmund |
| Korreferent: | Prof. Dr. J. Reedijk, Leiden, NL |

Die vorliegende Arbeit entstand in der Zeit von Oktober 1996 bis Februar 2001 am Lehrstuhl für Anorganische Chemie III des Fachbereichs Chemie der Universität Dortmund und am Leiden Institute of Chemistry (Leiden, Niederlande).

Mein besonderer Dank gilt meinem Lehrer

Herrn Professor Dr. B. Lippert

für seine ausgezeichnete wissenschaftliche Betreuung, sein fachliches und menschliches Engagement sowie die stets freundliche und vertrauensvolle Zusammenarbeit.

Herrn Prof. Dr. J. Reedijk danke ich herzlich für die freundliche Übernahme des Korreferates.

Mein Dank gilt ferner

allen Mitarbeiterinnen und Mitarbeitern der Arbeitskreise von Prof. Dr. B. Lippert (Universität Dortmund), Prof. Dr. J. Reedijk und Prof. Dr. J.H. van Boom (Leiden Institute of Chemistry) für die freundliche Atmosphäre, die humorvolle Zusammenarbeit sowie die immerwährende wissenschaftliche Diskussionsbereitschaft während meiner Promotionszeit,

dem Bundesland Nordrhein-Westfalen, dem Deutschen Akademischen Austauschdienst (DAAD) und Herrn Prof. Dr. J. Reedijk, Leiden Institute of Chemistry, für die finanzielle Unterstützung meiner Promotion,

Herrn Prof. Dr. J.H. van Boom (Leiden Institute of Chemistry) für seine ausgezeichnete wissenschaftliche Betreuung auf dem Gebiet der DNA- und PNA-Festphasensynthese, sein fachliches und menschliches Engagement und die stets freundliche Zusammenarbeit,

Herrn Dr. Gijs van der Marel und Herrn Dr. Dima Fillipov (Leiden Institute of Chemistry) für ihre immerwährende wissenschaftliche Diskussionsbereitschaft und die freundliche Zusammenarbeit,

Herrn Nico Meeuwenoord und Herrn Ing. Hans van den Elst (Leiden Institute of Chemistry) für die Unterweisung in HPLC, LC MS, PNA-, Peptid- und DNA-Synthese,

Herrn Dr. Matthias Janik (Universität Dortmund), Herrn Kees Erkelens und Herrn Fons Lefeber (Leiden Institute of Chemistry) für ihre Hilfe bei NMR-Fragestellungen,

Herrn Prof. Dr. Michael Linscheid (Humboldt-Universität Berlin) für die Aufname des ESI-Massenspektrums der platinverbrückten DNA-Tripelhelix,

Herrn Dr. Klaus Weisz (Freie Universität Berlin) für die Durchführung der Tieftemperaturmessungen am N1-platinierten Adenin,

Herrn Dr. Peter van Veelen (Academisch Ziekenhuis Leiden) für die Messung des MALDI-TOF Massenspektrums der platinverbrückten PNA/DNA-Duplex,

Herrn Markus Drumm (Universität Dortmund), Frau Nathalie Bleimling (Max-Planck-Institut für molekulare Physiologie, Dortmund) und Herrn Dr. Marc Boudvillain (Centre National de la Recherche Scientifique, Orléans) für die Durchführung der gelelektrophoretischen Untersuchungen,

Herrn Dr. Roland Sigel für die Berechnung der Assoziationskonstanten und die freundliche Zusammenarbeit,

Herrn Bertil Hofte und Herrn Barry Karabatak (Leiden Institute of Chemistry) für die Aufnahme zahlreicher ESI-Massenspektren,

Herrn Markus Hüffner (Universität Dortmund) für die Durchführung der Elementaranalysen,

Frau Yvonne Snellenberg, Frau Ingrid Bekooy, Frau Marianne Kooistra, Herrn John van Dijk (Leiden Institute of Chemistry), Frau Birgit Thormann und Frau Michaela Markert (Universität Dortmund) für Ihre Hilfsbereitschaft in administrativen Dingen und die freundliche Zusammenarbeit,

Frau Dr. Andrea Erxleben und Herrn Dr. Jörg Matysik für das sorgfältige Korrekturlesen und die konstruktive Kritik im Zusammenhang mit der Fertigstellung dieser Arbeit,

meinen Kolleginnen und Kollegen Herrn Markus Drumm, Frau Dr. Andrea Erxleben, Herrn Frank Glahé (thank you), Herrn Gunnar Kampf, Herrn Dr. Marc Lüth, Herrn Ralf Novak, Frau Irena Rother, Frau Dr. Gabriele Trötscher-Kaus und Herrn Michael Willermann für die freundliche Arbeitsatmosphäre und die humorvolle Zusammenarbeit,

Frau Dr. Alia, Herrn Dr. Jörg Matysik und Herrn Seiji Komeda für ihre Freundschaft,

und meiner Mutter, die mir das Chemiestudium ermöglicht hat.

# Table of contents


**A General introduction and aims of this thesis 1**

**B Main Section**

**Chapter I Crosslinking reaction of a monofunctionally *trans*-Pt(II) modified pyrimidine-rich deoxyoligonucleotide with duplex DNA 14**

1 Introduction 14

2 Choice of the oligonucleotide sequence 15
2.1 General considerations 15
2.2 UV spectroscopic analysis of the hairpin (**3**) and the unplatinated triplex (**1•3**) 18

3 Synthesis of the *trans*-$(NH_3)_2$Pt(II) crosslinked DNA triple helix **4** 20
3.1 Monofunctional platination of 5´d$(GT_2CTC_2TC)^{8-}$ (**1**) 20
3.2 Hybridization and crosslinking of *trans*-[Pt$(NH_3)_2${5´d(G-*N7*-$T_2CTC_2TC$)}Cl]$^{7-}$ (**2**) with 5´d$(GA_2GAG_2AGCT_2GCTC_2TCT_2C)^{21-}$ (**3**) 22

4 Characterization of the *trans*-$(NH_3)_2$Pt(II) crosslinked DNA triple helix **4** 24
4.1 Reversed-phase HPLC 24
4.2 ESI mass spectrometry 25
4.3 Gel electrophoresis 28
4.3.1 Denaturing 24 % PAGE gel 28
4.3.2 Hydroxyl radical footprinting 29
4.4 UV spectroscopy 31

5 Discussion 32

**Chapter II Solid-phase synthesis of monofunctionally *trans*-Pt(II) modified homopyrimidine deoxyoligonucleotides 35**

1 Introduction 35

2 Design of *trans*-Pt(II) modified building blocks for use in solid-phase DNA synthesis 36

3 Synthesis and characterization of the preplatinated building blocks *trans*-$[Pt(NH_2CH_3)_2(CHMT)\{NH_2(CH_2)_6OH\}]^+Cl^-$(**8**) and *trans*-$[Pt(NH_2CH_3)_2(CHMT)(gly\text{-}N)]^+BF_4^-$ (**9**) 39

3.1 Synthesis and characterization of *trans*-$[Pt(NH_2CH_3)_2(CHMT)Cl]$ (**7**) 40

3.2 Synthesis and characterization of *trans*-$[Pt(NH_2CH_3)_2(CHMT)\{NH_2(CH_2)_6OH\}]^+Cl^-$(**8**) 41

3.3 Synthesis and characterization of *trans*-$[Pt(NH_2CH_3)_2(CHMT)(gly\text{-}N)]^+BF_4^-$ (**9**) 42

4 Conjugation of *trans*-$[Pt(NH_2CH_3)_2(CHMT)\{NH_2(CH_2)_6OH\}]^+Cl^-$(**8**) to the 5´-terminus of homopyrimidine deoxyoligoucleotides via a phosphate bond by solid-phase DNA synthesis 46

4.1 Solution-phase test coupling experiments 46

4.1.1 Conversion of *trans*-$[Pt(NH_2CH_3)_2(CHMT)\{NH_2(CH_2)_6OH\}]^+Cl^-$(**8**) into its phosphoramidite **8a** 46

4.1.2 Condensation of *trans*-$[Pt(NH_2CH_3)_2(CHMT)\{NH_2(CH_2)_6OH\}]^+Cl^-$(**8**) with 5´-*O*-DMTr-deoxythymidine-3´-phosphoramidite (**12**) 47

4.1.3 Conclusions 50

4.2 Solid-phase coupling experiments 51

4.2.1 Optimization of conditions for the reverse coupling strategy 51

4.2.2 Conjugation of *trans*-$[Pt(NH_2CH_3)_2(CHMT)\{NH_2(CH_2)_6OH\}]^+Cl^-$(**8**) to the 5´-terminus of immobilized $dT_4$ (**16**) and $d(T_3CTC_2TC)$ (**19**) 53

4.2.3 Removal of the CHMT protecting group in **22** and **23** 55

4.2.4 Discussion 55

5 Conjugation of *trans*-[Pt($NH_2CH_3$)$_2$(CHMT)(gly-*N*)]$^+BF_4^-$ (**9**) to the 5´-terminus of homopyrimidine deoxyoligonucleotides via an amide bond by solid-phase synthesis 56
5.1 Conjugation of *trans*-[Pt($NH_2CH_3$)$_2$(CHMT)(gly-*N*)]$^+BF_4^-$ (**9**) to the 5´-terminus of immobilized 5´-functionalized d($T_2CTC_2TC$) (**28**) 56
5.2 Discussion 58

6 Conclusions 59

**Chapter III Solid-phase synthesis of monofunctionally *trans*-Pt(II) modified PNA oligomers and crosslinking reaction with a complementary oligonucleotide 60**

1 Introduction 60

2 Different methods of solid-phase PNA synthesis and design of *trans*-Pt(II) modified PNA building blocks 61

3 Solid-phase synthesis of a monofunctionally *trans*-Pt(II) modified homopyrimidine PNA pentamer 64

4 Solid-phase synthesis of monofunctionally *trans*-Pt(II) modified mixed pyrimidine / purine PNA oligomers 66
4.1 Synthesis and characterization of the preplatinated building blocks *trans*-[Pt($NH_3$)$_2$(Fmoc/N-Bhoc G)Cl]$^+BF_4^-$ (**33**) and *trans*-[Pt($NH_2CH_3$)$_2$(CHMT)(Fmoc/N-Bhoc G)]$^+BF_4^-$ (**34**) 66
4.1.1 Synthesis 66
4.1.2 Characterization of *trans*-[Pt($NH_3$)$_2$(Fmoc/N-Bhoc G)Cl]$^+BF_4^-$ (**33**) 67
4.1.2.1 NMR spectroscopy and ESI MS 67
4.1.2.2 Compatibility of *trans*-[Pt($NH_3$)$_2$(Fmoc/N-Bhoc G)Cl]$^+BF_4^-$ (**33**) with solid-phase PNA synthesis 71
4.1.3 Characterization of *trans*-[Pt($NH_2CH_3$)$_2$(CHMT)(Fmoc/N-Bhoc G)]$^+BF_4^-$ (**34**) 72
4.1.3.1 NMR spectroscopy and ESI MS 72

4.1.3.2 Compatibility of *trans*-[Pt($NH_2CH_3$)$_2$(CHMT)(Fmoc/N-Bhoc G)]$^+BF_4^-$ (**34**) with solid-phase PNA synthesis 73
4.1.4 Conclusions 74
4.2 PNA assembly on a Rink functionalized PEG-PS resin using Fmoc / N-Bhoc PNA building units 75
4.3 Conjugation of *trans*-[Pt($NH_3$)$_2$(Fmoc/N-Bhoc G)Cl]$^+BF_4^-$ (**33**) to the N-terminus of immobilized PNA oligomers 77
4.3.1 Synthesis and characterization of monofunctionally *trans*-Pt(II) modified PNA oligomers 77
4.3.2 Discussion 80

5 Synthesis and characterization of the *trans*-($NH_3$)$_2$Pt(II) crosslinked PNA / DNA double helix **47** 81
5.1 Analysis of the crosslinking reaction of *trans*-[($NH_3$)$_2$Pt(g-*N7*-attcgc)Cl]$^+$ (**43**) with the deoxyoligonucleotide 5´d(GCGAATG) (**46**) by reversed-phase HPLC 81
5.2 Characterization of the HPLC fractions by MALDI-TOF mass spectrometry 82
5.3 Characterization of the isolated *trans*-($NH_3$)$_2$Pt(II) crosslinked PNA / DNA duplex **47** by hydroxyl radical footprinting 85
5.4 Discussion 87

6 Conclusions 88

**Chapter IV Effect of Pt(II) coordination to *N1* of adenine on Hoogsteen hydrogen bonding with thymine 90**

1 Introduction 90

2 Synthesis and characterization of the chloroform-soluble complexes *trans*-[Pt($NH_2CH_3$)$_2$(CHMA)(CHMT)]$^+NO_3^-$ (**50**) and *trans*-[Pt($NH_2CH_3$)$_2$(CHMT)(TBS-ado)]$^+BF_4^-$ (**51**) 91
2.1 Synthesis 91
2.2 NMR spectroscopic characterization 93
2.2.1 *Trans*-[Pt($NH_2CH_3$)$_2$(CHMA)(CHMT)]$^+NO_3^-$ (**50**) 93

2.2.2 *Trans*-[Pt($NH_2CH_3$)$_2$(CHMT)(TBS-ado)]$^+BF_4^-$ (**51**) 99
2.3 Discussion 103

3 Investigation of hydrogen bonding interactions of the *N1*-platinated complexes **50** and **51** with 1-*N*-cyclohexylmethylthymine (**5**) 104
3.1 General considerations 104
3.2 Concentration-dependent $^1$H NMR studies in $CDCl_3$ 105
3.3 Temperature-dependent $^1$H NMR studies in $CDCl_3$ 107
3.4 Investigation of hydrogen bonding between **51** and the uridine derivative **52** within a slow exchange regime 110
3.4.1 Low temperature $^1$H NMR spectroscopy 110
3.4.2 Determination of the $^1J_{NH}$ coupling constant 115

4 Discussion 116

**C Experimental Section 118**

**D Summary 133**
**Zusammenfassung 139**

**E Appendix 145**

1 References 145

2 Overview on described compounds 155

## List of abbreviations

| | |
|---|---|
| a | $NH_3$, $NH_2CH_3$ |
| A | adenine |
| Ac | acetyl |
| $Ac_2O$ | acetic acid anhydride |
| AcOH | acetic acid |
| ado | adenosine |
| ahol | 6-amino-1-hexanol |
| aq | aqueous |
| B | nucleobase |
| Bhoc | benzhydryloxycarbonyl |
| Boc | *tert*-butyloxycarbonyl |
| Bz | benzoyl |
| c | concentration |
| C | cytosine |
| Cbz | benzyloxycarbonyl |
| CHMA | 9-*N*-cyclohexylmethyladenine |
| CHMT | 1-*N*-cyclohexylmethylthyminate |
| COSY | correlated spectroscopy |
| CPG | controlled pore glass |
| CV | column volume |
| DCM | dichloromethane |
| d | doublet, day(s) |
| dd | doublet of doublets |
| ds | double-stranded |
| dT | 2´-deoxythymidine |
| D*i*PEA | diisopropylethylamine |
| DMF | dimethylformamide |
| DMTr | dimethoxytrityl |
| DNA | deoxyribonucleic acid |
| ESI MS | electrospray ionization mass spectrometry |
| Fmoc | 9-fluorenylmethyloxycarbonyl |

| | |
|---|---|
| FPLC | fast protein liquid chromatography |
| G | guanine |
| gly | glycine |
| h | hour(s) |
| H | Hoogsteen |
| HATU | 2-(7-Azabenzotriazol-1-yl)-1,1,3,3-tetramethyluronium hexafluorophosphate |
| HMBA | p-hydroxymethylbenzoic acid |
| HMQC | heteronuclear multiple quantum coherence |
| 3-HPA | 3-hydroxy-picolinic acid. |
| HPLC | high performance liquid chromatography |
| *i*Bu | isobutyryl |
| *i*Pr | isopropyl |
| LC MS | liquid chromatography mass spectrometry |
| lys | L-lysine |
| m | multiplet |
| MALDI-TOF | matrix assisted laser desorption ionization time of flight |
| 1-MeC | 1-*N*-methylcytosine |
| 9-MeGH | 9-*N*-methylguanine |
| 1-MeT | 1-*N*-methylthyminate |
| min | minute(s) |
| MMTr | monomethoxytrityl |
| MS | mass spectrometry |
| NMP | *N*-methyl-2-pyrrolidone |
| NOESY | nuclear overhauser enhancement spectroscopy |
| *o*-NPT | ortho-nitrophenyltetrazole |
| PAGE | polyacrylamide gel electrophoresis |
| PEG-PS | polyethylene glycol derivatized polystyrene |
| $pH^*$ | uncorrected pH value, measured in $D_2O$ |
| PNA | peptide nucleic acid |
| ppm | parts per million |
| PS | polystyrene |
| pu | purine |
| pym | pyrimidine |

| | |
|---|---|
| rH | reverse Hoogsteen |
| RNA | ribonucleic acid |
| RT | room temperature |
| s | singlet |
| t | triplet |
| T | thymine |
| $t_r$ | retention time |
| TBDMS | *tert*-butyldimethylsilyl |
| TBS-ado | 2´,3´,5´-tris-(*tert*-butyldimethylsilyl)-adenosine |
| TCA | trichloroacetic acid |
| TEA | triethylamine |
| TEAA | triethylammonium acetate |
| TFA | trifluoroacetic acid |
| TFO | triplex forming oligonucleotide |
| THP | thymidine H-phosphonate |
| TMS | tetramethylsilane |
| TSP | sodium-3-(trimethylsilyl)propansulfonate |
| WC | Watson-Crick |

Capital letters stand for DNA;

Small letters stand for PNA;

PNA sequences are always written in direction from N- to C-terminus from left to right.

# A General introduction and aims of this thesis

In eukaryotic cells, the process of gene expression, which is the transformation of the genetic information stored in the base sequence of DNA into protein synthesis, is controlled by DNA-binding proteins (activators and repressors). These proteins bind via weak forces to specific DNA sequences and regulate transcription by their effect on RNA polymerase, either preventing or enhancing its binding to DNA.[1]

This observation has led to a high interest in the recognition of specific nucleic acid sequences. The design of molecules that recognize specific sequences on the DNA double helix would provide interesting tools to interfere with DNA information processing at an early stage of gene expression with high potential impact on the treatment of various diseases, including cancer, viral infections and AIDS.

In DNA, both the minor and the major grooves are sites for specific interactions. Small molecules such as synthetic polyamides containing pyrrole, hydroxypyrrole and imidazole groups recognize specific DNA base sequences from the minor groove. Some of these minor groove binders possess a specificity and affinity for DNA which is comparable to naturally occurring DNA binding proteins and are therefore successful reagents for gene regulation.[2-4]

Based on their unique formation of hydrogen bonds deoxyoligonucleotides possess a considerable potential of sequence-specific recognition. Their use as regulators for gene expression had already been demonstrated by Zamecnik und Stevenson in 1978.[5,6] Theoretically, oligonucleotides can interfere with the process of gene expression both at the level of transcription (antigene strategy) and translation (antisense strategy) (Figure 1). For sequence-specific recognition of a unique target sequence an oligonucleotide length of 12-15 nucleobases is required for statistical reasons.[7]

Within double-stranded DNA a deoxyoligonucleotide can recognize a purine-rich target sequence in the major groove through formation of Hoogsteen hydrogen bonds. The resulting structure is a (partial) DNA triple helix. Two main classes of triple helix have been characterized, which differ according to the orientation and base composition in the third strand (Figure 2). Pyrimidine-rich strands bind in a parallel fashion with regard to the central purine-rich strand, involving T•AT and $C^+$•GC triplets and a low pH for protonation of the cytosines is required (pym•pupym motif). Purine-rich oligonucleotides bind in an antiparallel orientation, including G•GC and A•AT triplets (pu•pupym motif). Formation of this triplex

motif is pH independent.[8-10] Both triplex motifs are stongly stabilized by divalent metal ions, which are necessary to screen the charge interactions between the three negatively charged phosphodiester backbones.[11,12]

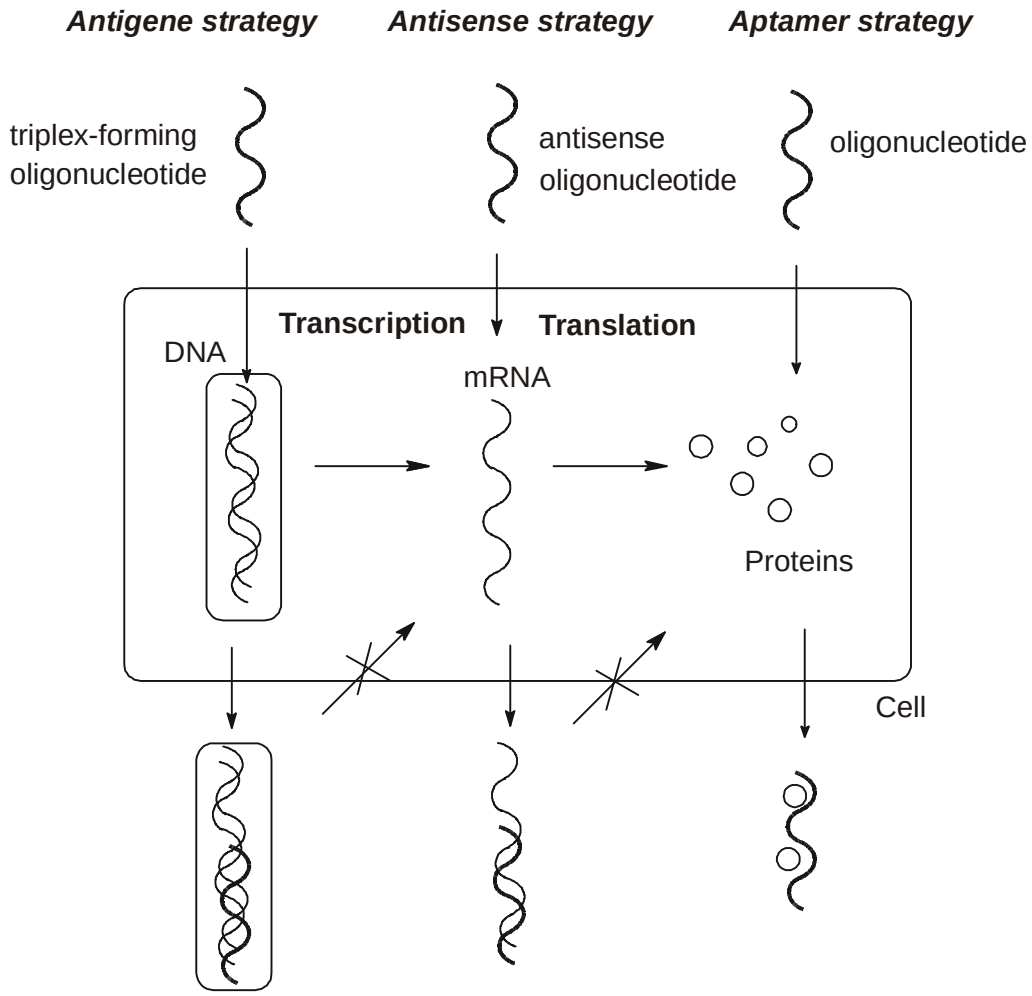


Figure 1: Process of gene expression and ways to influence the process of gene expression.

Triplex mediated specific modulation of transcription (antigene strategy) is possible, as demonstrated by an *in vitro* experiment by Cooney et al. already in 1988.[13] The process of transcription can be both inhibited and activated. E.g., triplex formation in a regulatory region of a gene can block transcription initiation by inhibiting transcription-factor binding or by interfering with formation of the initiation complex.[14-16] Alternatively, triplex formation within the transcribed region can inhibit transcription by arresting the transcription machinery during the elongation phase.[17,18] Even the activation of transcription is feasible. Recently, a TFO-peptide conjugate with the peptide being a transcriptional activator domain has been shown to activate the process of transcription.[19]

A second triplex-based strategy for altering a gene´s function is to induce a permanent change in its sequence by using TFOs to deliver site specific damage in order to generate a localized mutation. To this end, chemical reagents such as the photo-activatable psoralen have been covalently attached to TFOs. These modified TFOs have been used to direct mutations to a specific gene in cells.[20] Even in the absence of a tethered mutagen TFOs have the potential to induce mutations *in vivo*.[21-23]

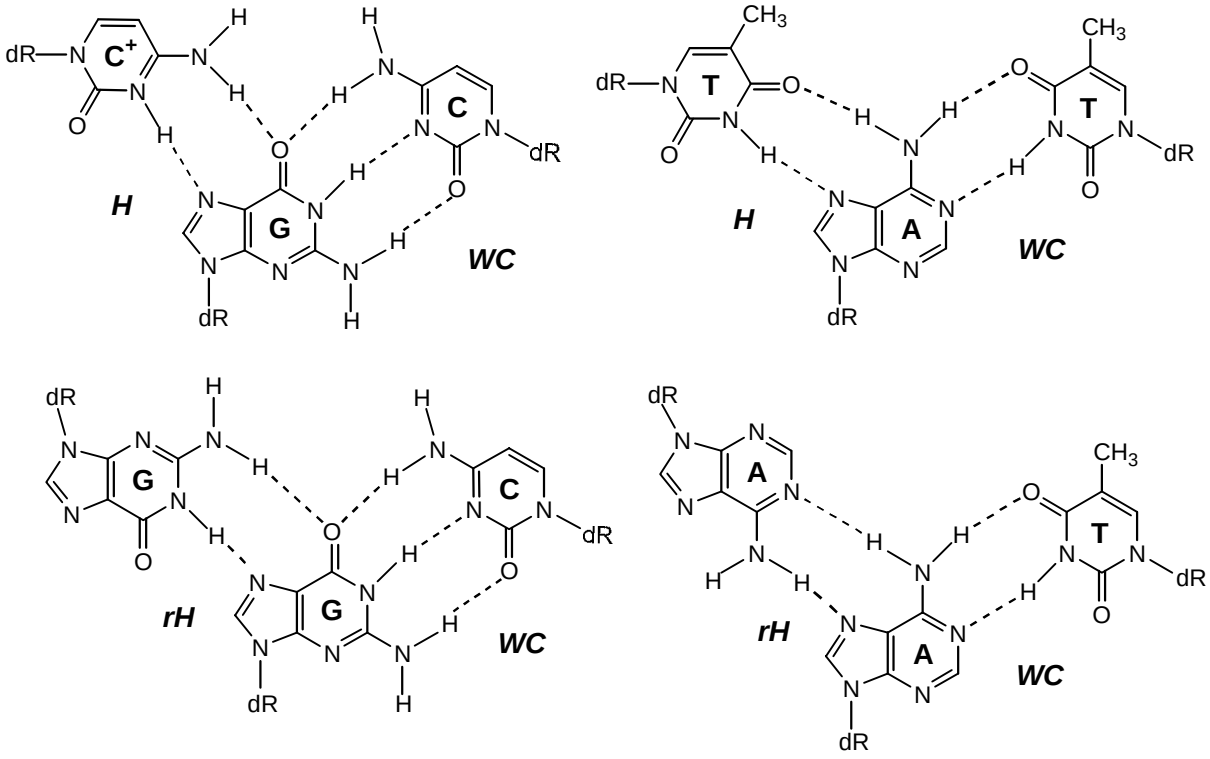


Figure 2: Base triplets involved in triplex DNA.

The residence time of a TFO on its DNA target is a determinant parameter to observe a biological response. Dissociation constants of some triple helices tend towards values comparable to values measured for transcription factors, thus affording competition with natural regulators of gene expression. Thus, the best way to obtain a long-lasting biological effect consists of irreversible linkage of the TFO to its target. More problems associated with this triplex-based approach are the pH dependence of the $C^+$•GC triplet, the general susceptibility of oligonucleotides towards enzymatic degradation and their poor cellular uptake.

In order to overcome these problems and to increase the *in vivo* stability of triplex structures, multiple approaches, involving base, sugar and backbone modifications as well as

attachment of intercalating agents, triplex-specific ligands and crosslinking agents, are currently being pursued.[24,25] Furthermore, as triplex formation is originally restricted to oligopurine sequences, attempts are made to extend the repertoire of target sequences, for example, to achieve recognition of an interrupting pyrimidine or the recognition of two oligopurine motifs located on each of the DNA strands (alternate strand recognition).[26]

Backbone modifications serve to optimize triplex stability while keeping the sequence specificity and to achieve resistance towards degradation by nucleases. Some backbone modifications are depicted in Figure 3.

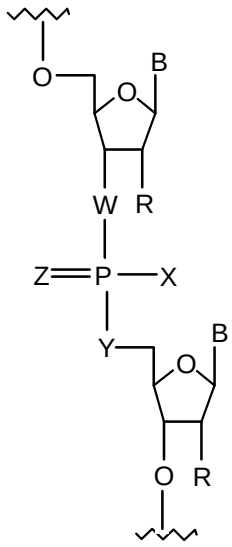

| | W | X | Y | Z | R |
|---|---|---|---|---|---|
| Phosphodiester | O | $O^-$ | O | O | H |
| Phosphorothioate | O | $S^-$ | O | O | H |
| Methylphosphonate | O | $CH_3$ | O | O | H |
| N3´→ N5´ Phosphoramidate | NH | $O^-$ | O | O | H |
| 2´-O-methyl | O | $O^-$ | O | O | $OCH_3$ |

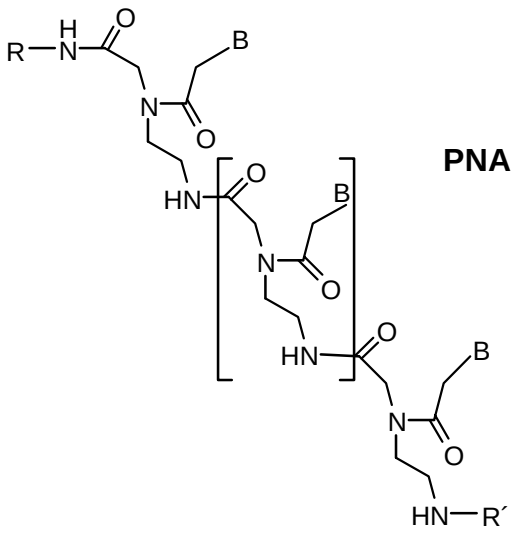


Figure 3: Oligonucleotide analogues.

For example, it has been found that the stability of triple helices involving 2´-O-alkyl oligoribonucleotides is higher than that involving oligoribonucleotides.[27,28] Furthermore, triplex forming oligo-N3´→N5´phosphoramidates seem to have promising antigene properties, both *in vitro* and in cells.[29]

A further very promising candidate in antigene strategy is the so-called peptide nucleic acid (PNA), a nuclease-resistant oligonucleotide analogue in which the deoxyribose phosphate backbone has been replaced by a homomorphous, achiral and uncharged backbone based on *N*-(2-amino-ethyl)glycine[30] (Figure 3). Hybridization of PNA to target deoxyoligonucleotides proceeds according to the Watson-Crick base pairing rules and with more stringent sequence selection as compared to hybridization of deoxyoligonucleotides.[31] In addition, PNA / deoxyoligonucleotide hybrids possess greater thermal stability as the electrostatic repulsion between the DNA and the (uncharged) PNA strand is decreased[31] and they are virtually independent of ionic strength of the medium.[32] Binding of homopyrimidine PNA to double-stranded DNA (ds DNA) results in displacement of the non-targeted Watson-Crick paired deoxyoligonucleotide strand and formation of a $(PNA)_2$ / DNA triple helix (triplex invasion complex)[33-35]. The resulting structure is a so-called P-loop in which two PNA oligomers form a $(PNA)_2$ / DNA triplex with one PNA strand binding via Watson-Crick hydrogen bonds in an antiparallel fashion to the homopurine deoxyoligonucleotide target and with the second PNA strand binding via Hoogsteen hydrogen bonds in a parallel fashion to the homopurine deoxyoligonucleotide strand. The second DNA strand is displaced (Figure 4). Once formed, these PNA / DNA-PNA triplexes are exceptionally stable.[34,36]

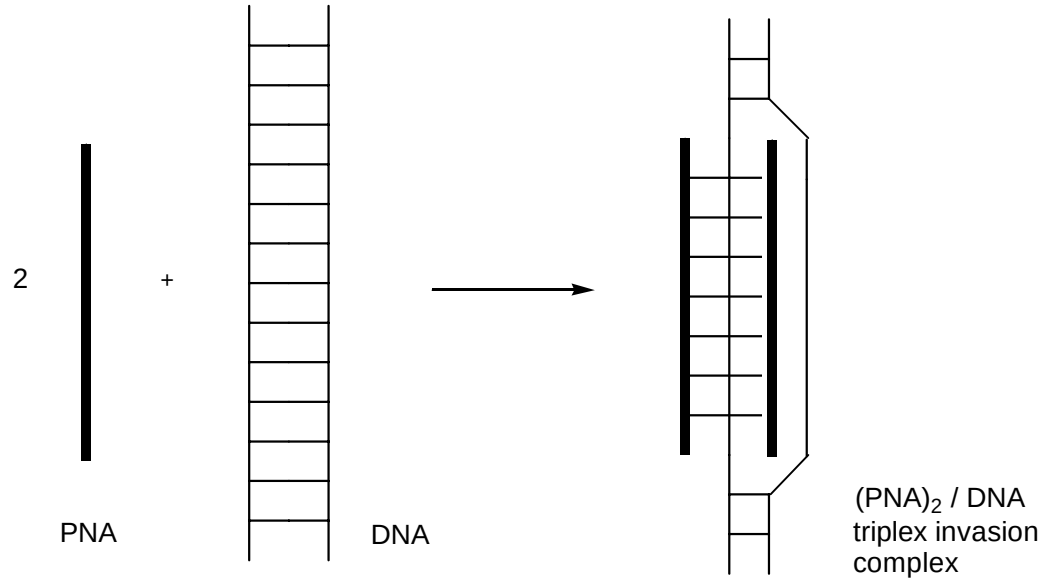


Figure 4: Formation of a $(PNA)_2$ / DNA triplex invasion complex by reaction of homopyrimidine PNA with duplex DNA.

In this way, homopurine regions of eight base pairs or more in length within double stranded DNA can be efficiently targeted.[33,35] Because two PNAs are required to form these complexes, most often bis-PNAs, in which the two PNA parts are chemically linked, are employed for targeting of ds DNA.[37] The formed $(PNA)_2$ / DNA triplex invasion complexes occlude protein binding (transcription factors, restriction enzymes) to proximal or overlapping DNA sites[38,39] and / or have sufficient stability to arrest the elongating RNA polymerase[40,41] or DNA polymerase.[42] Thus, PNAs are promising candidates for use in antigene strategy although several features like the poor cellular uptake of PNA[43] need to be optimized for an efficient *in vivo* application. E.g. covalent attachment of PNA to peptides that bind selectively to cell surface receptors can increase the cellular uptake of PNA into specific cell types.[44] Recently, it was reported that antigene effects in Burkitt´s lymphoma cells in culture were effected by a PNA 17-mer which was linked to a basic nuclear localization signal (NLS) peptide.[45] The latter mediated the transfer of the PNA-peptide conjugate across the nuclear membrane and thus afforded its nuclear penetration.[45]

Furthermore, triplex forming bis-PNAs have been employed to cause mutagenesis within a chromosomal target site in mouse cells.[46] It has been found that the majoritiy of the mutations were located in the PNA binding site and consisted mostly of single base pair insertions and deletions, suggesting that a high affinity PNA clamp constitutes a mutagenic lesion that may provoke replication slippage errors.[46] Very recently, it has been reported that the single-stranded DNA loop within a $(PNA)_2$ / DNA triplex invasion complex has the capacity to initiate transcription of a specific gene in cells,[47] which could provide a new approach for gene therapy.

Oligonucleotides can additionally interfere with the process of gene expression at the level of translation by sequence specific interaction with the messenger RNA (antisense strategy, Figure 1). The resulting structure is a mRNA-oligonucleotide duplex according to the Watson-Crick base pairing rules. The process of translation can be inhibited either by degradation of the targeted mRNA through RNase H mediated cleavage or by steric blocking of ribosomes or essential translation factors.[48,49] In the former mechanism, mRNA within the mRNA-oligonucleotide hybrid is cleaved by the enzyme RNase H. The antisense oligonucleotide is released and subsequently again available to bind another mRNA molecule. One major impediment associated with this mechanism is that for RNase H activation deoxyoligonucleotides are required. *In vivo*, deoxyoligonucleotides are rapidly degraded by nucleases and therefore their application in antisense strategy is quite limited. In order to

overcome this drawback, a plethora of chemically modified nuclease-resistent oligonucleotides has been designed but except for phosphorothioates, these are not substrates for RNase H.[48,50]

The first generation of antisense oligonucleotides was based on backbone modifications conserving the phosphorus atom present in the naturally occurring phosphodiester linkage but replacing either one or both of the non-bridging or bridging oxygen atoms[50] (e.g. phosphorothioates, methylphosphonates, Figure 3). Such modifications served to increase the stability towards enzymatic degradation. To date, phosphorothioate drugs are in various stages of clinical trials and one antisense sequence (Vitravene or ISIS 2922) has recently been approved by the FDA for treatment of CMV retinitis in AIDS patients.[51] Furthermore, oligonucleotides modified at the 2´position of the sugar[52] and N3´→5´phosphoramidates[29] are encouraging antisense candidates. Although these oligonucleotide analogues are RNase H-incompetent, they have been shown to be effective antisense reagents when targeted to the 5´-untranslated region and to the translation inition region of mRNA, where they interfere with the formation of the translation–initiation complex. Steric blockage within the coding region of mRNA is less efficient because of the unwinding action by the ribosomal complex during translation.[53-55]

PNA is a very promising candidate for use in antisense strategy due to its favourable hybridization properties with oligonucleotides and its stability against enzymatic degradation.[30] However, PNA / RNA hybrids are not substrates for RNase H.[40,56] Therefore, PNA must exert its antisense effect by direct steric blocking of ribosomes or essential translation factors. Several *in vitro* studies have shown that homopyrimidine PNAs targeted to homopurine sequences in the coding region of mRNA can even interrupt ribosome elongation at the target site by triplex formation with the mRNA target.[40,56,57] Duplex-forming mixed purine / pyrimidine PNAs were successful as antisense reagents when targeted to the AUG start codon region but not when targeted to sites within the coding region, indicating that the PNA was displaced by the moving ribosome.[55-57] Furthermore, it was shown that PNAs targeted to exon and intron sequences of RNA reduced gene expression,[54] suggesting that PNA may have even acted within the cell nucleus to inhibit RNA processing. Thus, based on its propensity to form very stable triplexes with a mRNA target, PNA is superior to other RNase H-incompetent antisense oligonucleotide analogues (e.g. 2´O-alkyl oligoribonucleotides and N3´→N5´phosphoramidates) in that it causes antisense effects not

only when targeted to the 5´- untranslated region but also when targeted to the coding region of mRNA.

In order to overcome the problem of RNase H incompetence of RNA / PNA duplexes, PNA-DNA chimeras have been synthesized.[58-60] These have been shown to hybridize efficiently with RNA. The DNA part within these chimeras suffices to activate the enzyme RNase H. RNA cleavage occurs sequence-specifically at the ribonucleotides which base pair with the DNA part of the PNA-DNA chimera.[59] Furthermore, it is also possible to attach reactive entities to PNA which effect destruction of a RNA target. Recently, a PNA-diethylenetriamine conjugate has been synthesized and shown to cleave a hybridized RNA target in a sequence-specific manner.[61]

Finally, oligonucleotides can interfere with the process of gene expression at the level of the proteins By high affinity binding of the oligonucleotides to proteins, inhibition of vital proteins, e.g. transcription factors or crucial enzymes, can be effected (aptamer strategy).[62] These aptamers originate from *in vitro* selection experiments which, starting from random sequence libraries, optimize the nucleic acids for high affinity binding to given ligands.[62]

In both the antigene and the antisense approach metal ions have been employed to effect destruction of a target sequence either by redox chemistry or hydrolysis. E.g., redox-active metal entities attached via a a linker to the 5´or 3´ terminus of an oligonucleotide, can be directed to a specific site within DNA to induce sequenc-specific cleavage. To this end, EDTA-Fe(II)[63], *o*-phen-Cu(I)[64] and cationic manganese porphyrin groups[65,66] have been attached to oligonucleotides and to PNA oligomers[66]. *In vitro* studies demonstrated that in the presence of a coreactant these oligonucleotide(analogue) metal conjugates were able to cleave double-stranded DNA in a sequence-specific manner.[63-66]

Similarly, RNA can be targeted (antisense strategy). A wide range of metal ions (e.g. Mg(II), Ca(II), Fe(III), Ni(II), Cu(II), Zn(II), Pb(II), trivalent lanthanides) is known to catalyze RNA transesterification and hydrolysis.[67] Some of these metal ions have been attached via a ligand to oligonucleotides and were shown to cleave RNA site-specifically and efficiently, thereby acting as artificial ribonucleases.[67]

The idea to use metal ions in order to link an antigene / antisense oligonucleotide and its target irreversibly in order to impair transcription or translation through hybridisational arrest of the transcription and translation machinery, is comparatively new. For this purpose, non-redox active metal species of suitable coordination geometry which are capable of forming thermodynamically stable and at the same time kinetically inert crosslinks between

oligonucleotide strands are required. Bifunctional Pt(II) compounds are well suited in this respect as shown first by Vlassov et al. as well as Chu and Orgel.[68-71]

Both the antitumor agent Cisplatin and its therapeutically inactive geometric isomer Transplatin are able to form bifunctional lesions (interstrand crosslinks) with DNA. In contrast to Cisplatin, these interstrand crosslinks occur more frequently with Transplatin [72] and, very importantly, due to its linear coordination geometry, without major distortion of the DNA double helix.[73-79] The two-dimensional NMR high resolution structure of a DNA double helix containing a *trans*-$(NH_3)_2$Pt(II) interstrand crosslink between a central G/C base pair reveals that the helix is only slightly bent (20°) towards the major groove and that no large unwinding occurs. The *trans*-$(NH_3)_2$Pt(II) interstrand crosslink causes minor distortion only, which is spread out over two base pairs on the 5´and 3´sites.[78]

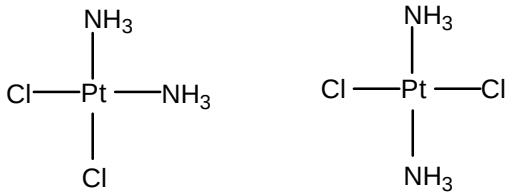


**Cisplatin** **Transplatin**

Figure 5: Structures of Cisplatin and Transplatin.

These results had been predicted by model chemistry. It was demonstrated that a linear *trans*-$a_2$Pt(II) moiety (a = $NH_3$, $NH_2CH_3$) can systematically replace a proton of a H bond within Watson-Crick and Hoogsteen A/T[80] and G/C[81-83] base pairs (compounds a - d in Figure 6). The presence of a linear *trans*-$a_2$Pt(II) moiety within these metal-modified base pairs does not significantly alter the overall structural parameters (e.g. interglycosidic distances and coplanarity of bases) compared to naturally occurring unmetallated base pairs in duplex or triplex DNA. Thus, crosslinking of two or three oligonucleotide strands by a *trans*-$a_2$Pt(II) unit is sterically feasible. As for DNA triplex structures, in principle, both the *trans*-$a_2$Pt(II) crosslinked analogue of the pym•pupym and the pu•pupym motif can be realized as demonstrated by the model nucleobase triplets d[81] and e[84] in Figure 6.

Indeed, the principle of crosslinking an oligonucleotide with its target sequence via a *trans*-$(NH_3)_2$Pt(II) unit has recently successfully been applied in antisense strategy. 2´O-methyl-oligoribonucleotides, crosslinked via a *trans*-$(NH_3)_2$Pt(II) unit to the coding

region of a mRNA target have been shown both in *in vitro* and *ex vivo* experiments to effectively arrest translation only by steric hindrance.[85-87] This result has a high impact with regard to the fact that even high affinity duplex forming oligonucleotide analogues like the N3´→N5´phosphoramidates and PNA do not arrest the elongating ribosome.[53,56] It is in fact the first example of inhibition of translation by duplex forming *occupance only* antisense oligonucleotides which are directed to the coding region of mRNA. Obviously, the *trans*-$(NH_3)_2$Pt(II) interstrand crosslink efficiently stabilizes an antisense oligonucleotide / mRNA hybrid against the translation machinery. For antisense strategy in general this means that for duplex forming RNase H incompetent antisense oligonucleotide analogues crosslinking via a *trans*-$(NH_3)_2$Pt(II) unit is a powerful new alternative to block protein synthesis at sequences downstream the AUG initiation codon.[87]

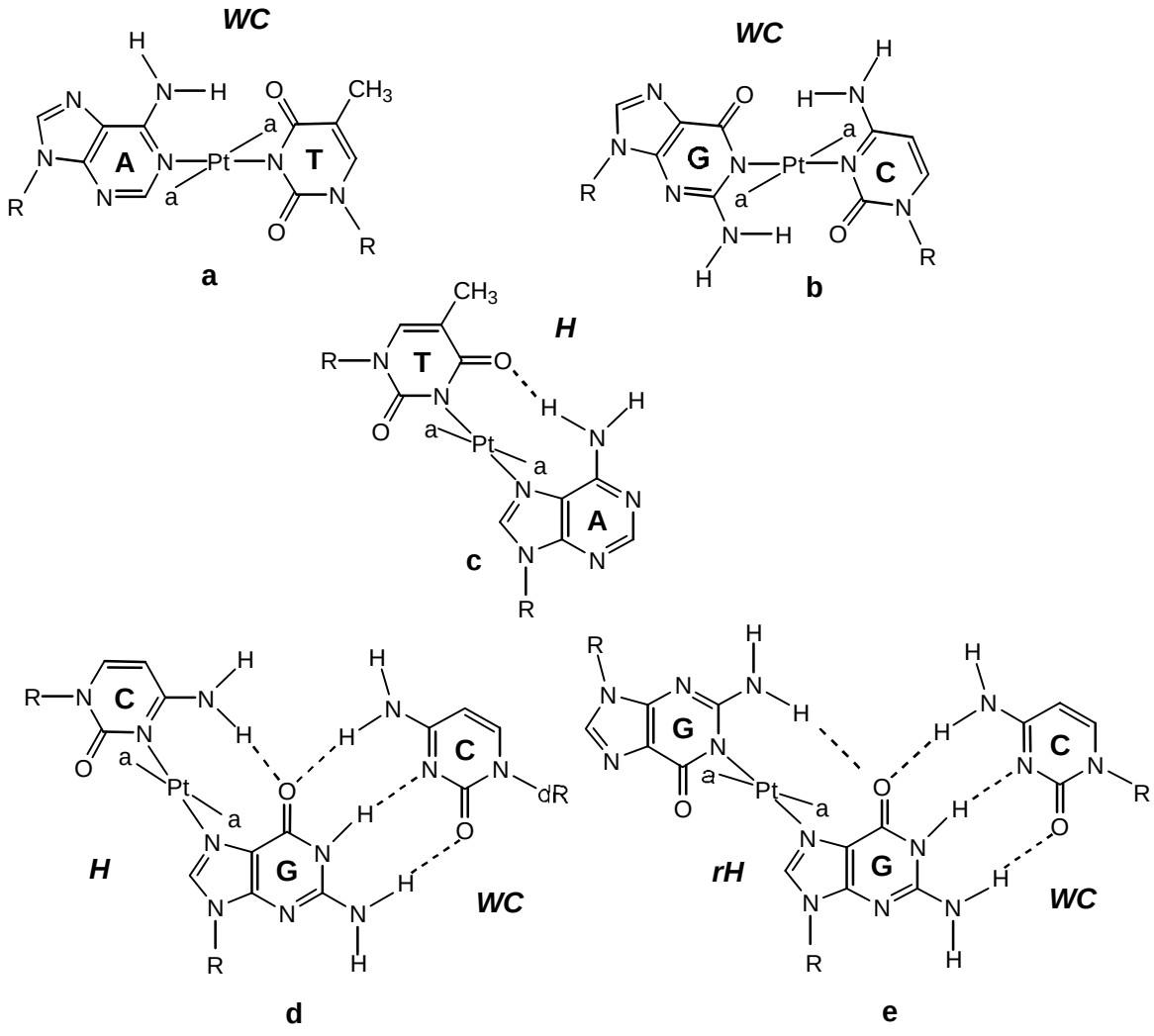


Figure 6: *trans*-$a_2$Pt(II) modified model nucleobase pairs and triplets
(a = $NH_3$, $NH_2CH_3$, R = $CH_3$, $CH_2CH_3$).

For generation of a site-specific *trans*-$a_2$Pt(II) crosslink between an oligonucleotide and its target, in principle two strategies exist. The first one is based on the observation that in the reaction of an oligonucleotide containing a 1,3 *trans*-[Pt($NH_3$)$_2$(GXG)] *intra*strand crosslink (bifunctionally *trans*-Pt(II) modified oligonucleotide) with a complementary oligonucleotide target a rearrangement from the 1,3 *trans*-[Pt($NH_3$)$_2$(GXG)] *intra*strand crosslink into a site-specific *inter*strand crosslink takes place (strategy 1, Figure 7).[88] In this way, complementary single-stranded oligonucleotides have been sequence-specifically crosslinked leading to formation of *trans*-$a_2$Pt(II) bridged Watson-Crick duplexes.[78,79] The second strategy (strategy 2, Figure 7) is based on the observation that in the reaction of a monofunctionally *trans*-Pt(II) modified deoxyoligonucleotide with a complementary single-stranded target sequence both strands are irreversibly linked at a defined site by a *trans*-Pt(II) interstrand crosslink (Figure 7, strategy 2).[89-91] This strategy allows both sequence-specific crosslinking of two[89,90] and three[91] oligonucleotide strands, leading to formation of *trans*-($NH_3$)$_2$Pt(II) crosslinked DNA duplex and triplex structures, respectively. An essential element of both strategy 1 and 2 is that sequence-specific recognition of the mono- and bifunctionally *trans*-Pt(II) modified oligonucleotide with the target strand takes place prior to formation of a *trans*-($NH_3$)$_2$Pt(II) interstrand crosslink.

It is evident that the application of this approach in antisense and antigene strategy requires an efficient synthesis of site-specifically *trans*-Pt(II) modified deoxyoligonucleotides. The synthesis of site-specifically mono- and bifunctionally *trans*-Pt(II) modified oligonucleotides by direct platination of an oligonucleotide with Transplatin or its solvent species is generally hampered by the occurrence of multiple unregiospecific platination reactions, preferrably at the endocyclic *N7* positions of the purine bases.[92] As a consequence, the desired platinated oligonucleotide can only be obtained in moderate yields. Moreover, laborious purification procedures are often required to separate it from the reaction mixture. Through fine-tuning of the pH during the platination reaction only an efficient synthesis of regiospecifically monofunctionally *trans*-Pt(II) modified pyrimidine-rich oligonucleotides containing a single guanine as the preferred Pt(II) coordination site is feasible (strategy 2, Figure 7).[89-91,93] However, also in this case, occasionally, the formation of bifunctional adducts (long-range intrastrand crosslinks) is observed, by which further crosslinking reactions with a target sequence are excluded (suicide reaction). This problem has been adressed by a protecting group strategy.[93] The complex *trans*-[Pt($NH_3$)$_2$(1-MeT)Cl] exhibits exclusive monofunctional coordination. The 1-Methylthyminate ligand (1-MeT) serves as an

acid-labile protecting group, which can be subsequently substituted by a chloro ligand (strategy 2b, Figure 7).[94-98]

The incorporation of preplatinated building blocks into an oligonucleotide by solid-phase DNA synthesis appears to be more rewarding for site-specific and sequence-independent Pt(II) modification.[99,100] This approach requires the synthesis of preplatinated building blocks which are compatible with the solid-phase DNA synthesis protocol.

Solid-phase synthesis has been extensively applied for the generation of metal-functionalyzed oligonucleotides.[101-110] In these cases, the metallated building blocks were compatible with the synthesis protocol as the metal center was protected by stable ligands. By contrast, solid-phase synthesis of metal-modified oligonucleotides with the metal center allowing for post-synthetic ligand exchange reactions (e.g. crosslinking reactions) is much more difficult since metallated building blocks that contain labile ligands (e.g. chloride) are not compatible with the automated DNA synthesis protocol.[99] Exchange of the labile chloro ligand occurs which leads to the formation of a *trans*-Pt(II) modified oligonucleotide incapable of undergoing further crosslinking reactions.[99] The solid-phase synthesis of sequence-independently monofunctionally *trans*-Pt(II) modified oligonucleotide (analogues) is therefore a major challenge.

The central aim of this thesis is the development of a solid-phase synthesis method which allows the facile preparation of sequence-independently and site-specifically monofunctionally *trans*-Pt(II) modified oligonucleotides and oligonucleotide analogues. A further aim is the investigation of the crosslinking reactions of these monofunctionally *trans*-Pt(II) modified oligonucleotide(analogues) with target oligonucleotides in order to examine their potential application for modulation of gene expression according to strategy 2 (Figure 7).

In Chapter I the crosslinking reaction of a monofunctionally *trans*-Pt(II) modified single-stranded pyrimidine-rich oligonucleotide, obtained by post-synthetic *trans*-Pt(II) modification, with double-stranded DNA is described. Chapters II and III describe novel solid-phase synthesis approaches towards the synthesis of monofunctionally *trans*-Pt(II) modified homopyrimidine deoxyoligonucleotides for potential use in antigene strategy and towards the synthesis of monofunctionally *trans*-Pt(II) modified mixed purine / pyrimidine PNA oligomers for potential use both in antisense and antigene strategy.

Chapter IV describes more subtle electronic effects like the alteration of hydrogen bonding properties of nucleobases involved in a *trans*-$a_2$Pt(II) interstrand crosslink.

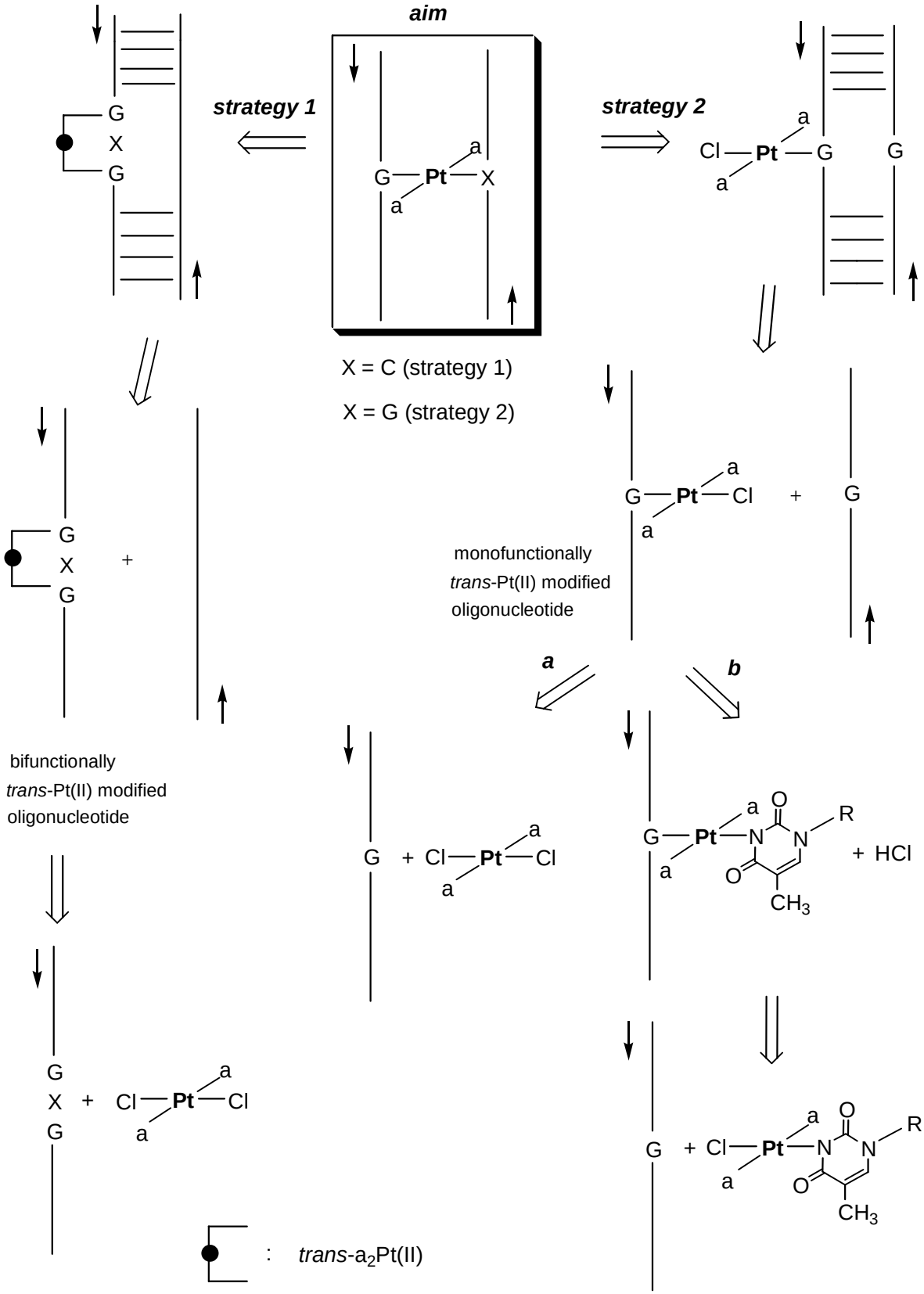


Figure 7: Different strategies to create a site-specific *trans*-$a_2$Pt(II) interstrand crosslink between sense and antisense oligonucleotide.

# B Main Section

## Chapter I Crosslinking reaction of a monofunctionally *trans*-Pt(II) modified pyrimidine-rich deoxyoligonucleotide with duplex DNA

### 1 Introduction

Recent results show that in the reaction of monofunctionally *trans*-Pt(II) modified deoxyoligonucleotides with complementary deoxyoligonucleotides initially sequence-specific recognition takes place before a *trans*-$(NH_3)_2$Pt(II) interstrand crosslink is formed at a defined site.[89,90] In this way, deoxyoligonucleotides have been crosslinked both in parallel and antiparallel fashions.[89,90] The thermal stability of the resulting *trans*-$(NH_3)_2$Pt(II) crosslinked duplexes is significantly increased compared to the respective uncrosslinked duplexes.[89,90] With respect to antisense strategy this increased thermal stability of the oligonucleotide / target hybrid means an increase in steric blockage of a given RNA target sequence against translation elongation.

Similarly, sequence-specific crosslinking of a single-stranded monofunctionally *trans*-Pt(II) modified oligonucleotide to a target sequence within duplex DNA is possible.[91] By means of gel-electrophoretic studies it has been demonstrated that a monofunctionally *trans*-Pt(II) modified pyrimidine-rich 19-mer oligonucleotide with the monofunctional *trans*-Pt(II) unit located at the 5´guanine recognizes via formation of Hoogsteen hydrogen bonds a specific homopurine sequence within a double-stranded DNA fragment consisting of two 25-mers. Subsequently, a site-specific *trans*-$(NH_3)_2$Pt(II) interstrand crosslink is formed between the third strand and the homopurine strand of the Watson-Crick duplex.[91] The resulting structure is a *trans*-$(NH_3)_2$Pt(II) crosslinked DNA triple helix of the pym•pupym motif. With respect to antigene strategy this means that permanent and irreversible steric blockage of a specific sequence within DNA should in principle be feasible.

In order to analyze the structural details of a DNA triple helix in which a Hoogsteen strand is linked via a *trans*-$(NH_3)_2$Pt(II) unit to a Watson-Crick duplex, an appropriate model

compound in sufficient amounts for NMR or X-ray analysis is required. One of the aims of this thesis is the design and synthesis of such a model compound. The complete 3D structure of this model will be determined by NMR spectroscopic methods in the group of Prof. E. Sletten, Bergen, Norway.

## 2 Choice of the oligonucleotide sequence

### 2.1 General considerations

The design of an appropriate model requires careful considerations concerning the oligonucleotide sequence and the length of the oligonucleotide. E.g. a monofunctionally platinated homopyrimidine-rich strand has to be sufficiently long to ensure efficient sequence-specific hybridization with a given homopurine tract in DNA. On the other hand, the oligonucleotide strands must not be too long since otherwise severe overlap of the NMR signals will trouble an assignment. Ideally, the crosslinking reaction should be carried out at a temperature which is far below the melting point of the triplex (dissociation of the Hoogsteen strand from the Watson-Crick duplex) but at which crosslink formation (ligand exchange reaction at the Pt(II) center) is still reasonably rapid.

The stability of parallel DNA triple helix structures according to the pym•pupym motif is not only largely dependent on the pH and the concentration of positively charged counter ions.[111] Rather the nucleobase sequence of the Hoogsteen strand is also quite important. It has been found that below pH 7.0 $C^+$•GC triples are much more stabilizing than T•AT triples and that triplex structures are most stable if the Hoogsteen strand consists of CT repeats, whereas adjacent C residues destabilize third strand binding.[112,113]

In crosslinking experiments, it has been found that efficient triplex formation of a monofunctionally platinated Hoogsteen strand with a duplex target, a major prerequisite for subsequent site-specific interstrand crosslink formation, takes place if the monofunctional *trans*-Pt(II) unit is located at a 5´guanine of the Hoogsteen strand.[91] If the monofunctionally platinated guanine residue is in the middle of the Hoogsteen strand, hybridization with the Watson-Crick duplex is less effective.[91]

Based on these considerations, the 9-mer 5´d$(GT_2CTC_2TC)^{8-}$ (**1**) has been chosen as Hoogsteen strand (Scheme 1). It contains one terminal 5´G, which can be easily

monofunctionally *trans*-Pt(II) modified.[89,93] The sequence **1** consists furthermore of four thymine and four cytosine nucleobases, which are expected to afford efficient sequence-specific recognition of the target sequence.

As a model of double-stranded DNA the hairpin sequence 5´d($GA_2GAG_2AGCT_2GCTC_2TCT_2C$)$^{21-}$ (**3**) was chosen. Here, two Watson-Crick hydrogen-bonded DNA strands are linked by a 5´CTTG loop, a structural motif which is known to encourage folding of this sequence into a highly stable two-base hairpin-loop structure.[114] The loop serves to diminish dissociation of the Watson-Crick helix and thus facilitates purification of a *trans*-$(NH_3)_2$Pt(II) crosslinked DNA triplex by HPLC under denaturing conditions.

The homopurine tract within **3** is not entirely complementary to **1** in that it contains a 5´guanine instead of a cytosine. This modification was chosen in order to increase the rate of interstrand crosslink formation between the monofunctionally platinated oligonucleotide **2** and **3** as Pt(II) has a greater affinity for guanine than for cytosine.[92]

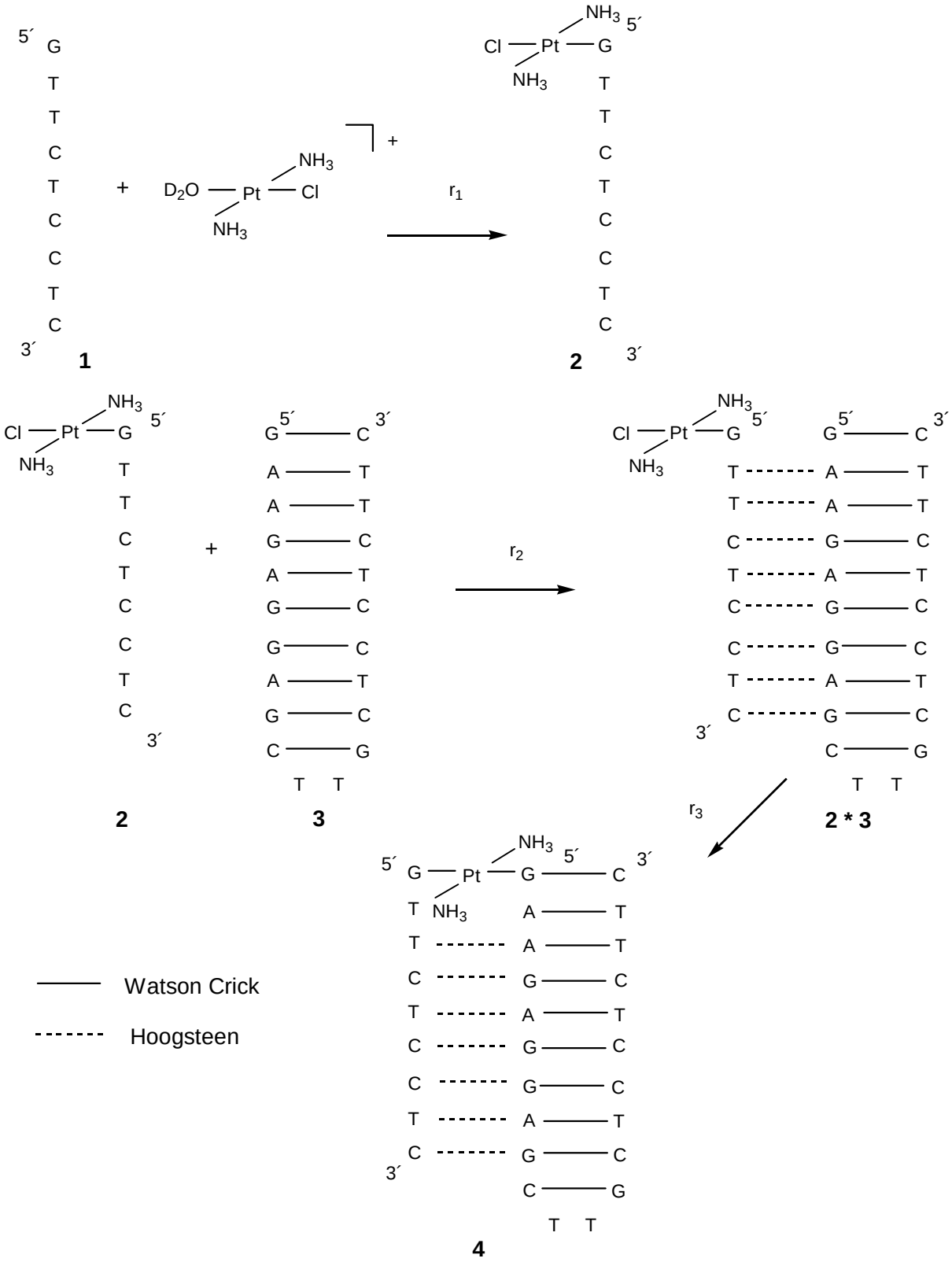


Scheme 1: Route for the synthesis of a *trans*-$(NH_3)_2Pt(II)$ crosslinked DNA triple helix;
$r_1$: monofunctional platination of **1**; $r_2$ : hybridization of **2** with **3**;
$r_3$: crosslinking reaction of **2** with **3**.

## 2.2 UV spectroscopic analysis of the hairpin (3) and the unplatinated triplex (1•3)

The viability of the described approach was first assessed by an investigation of the melting profiles of the hairpin (**3**) and the unplatinated triplex (**1•3**). Melting of highly ordered duplex and triplex structures results in disruption of base stacking which is accompagnied by an increase in UV absorption (hyperchromic effect). This feature can be exploited to determine the melting temperature: The turning point of the temperature-dependent UV absorption curve indicates the melting point.[112]

First the melting behaviour of the hairpin (**3**) and the unplatinated triplex (**1•3**) was investigated at pH 5 in a solution containing 100 mM $NaClO_4$ and 5 mM $Mg(ClO_4)_2$. Figure 1 shows the temperature-dependent UV absorption of **3** and the unplatinated triplex (**1•3**). For the hairpin (**3**) a melting point of 352 K was derived from curve a (Figure 1).

Under the same conditions the unplatinated triplex (**1•3**) exhibits a biphasic melting profile (Figure 1) with transitions at 308 K, representing dissociation of the Hoogsteen strand from the Watson-Crick duplex and 348 K, representing dissociation of the Watson-Crick duplex. Biphasic melting profiles are dependent on pH and have been observed earlier for DNA triple helices.[113,115-119] The value of 308 K for the triplex→hairpin transition compares with a value of 314 K for the same transition observed for a related DNA triplex under slightly different conditions.[113] The value of 348 K for the duplex→coil transition compares with a value of 336 K in a related hairpin sequence (containing, however, a $C_4$-loop).[113] The hyperchromicity for the transition of the unplatinated triplex (**1•3**) to the coil amounts to approximately 20 % (Figure 1).

The results suggest that at RT the unplatinated triplex (**1•3**) is intact. With respect to the aimed synthesis of a *trans*-$(NH_3)_2$Pt(II) bridged triple helix it means that hybridization of the monofunctionally *trans*-Pt(II) modified single strand **2** with the homopurine tract within **3** should also be efficient so that the crosslinking reaction of **2** with **3** at RT is expected to proceed with sequence-specific formation of an interstrand crosslink according to Scheme 1.

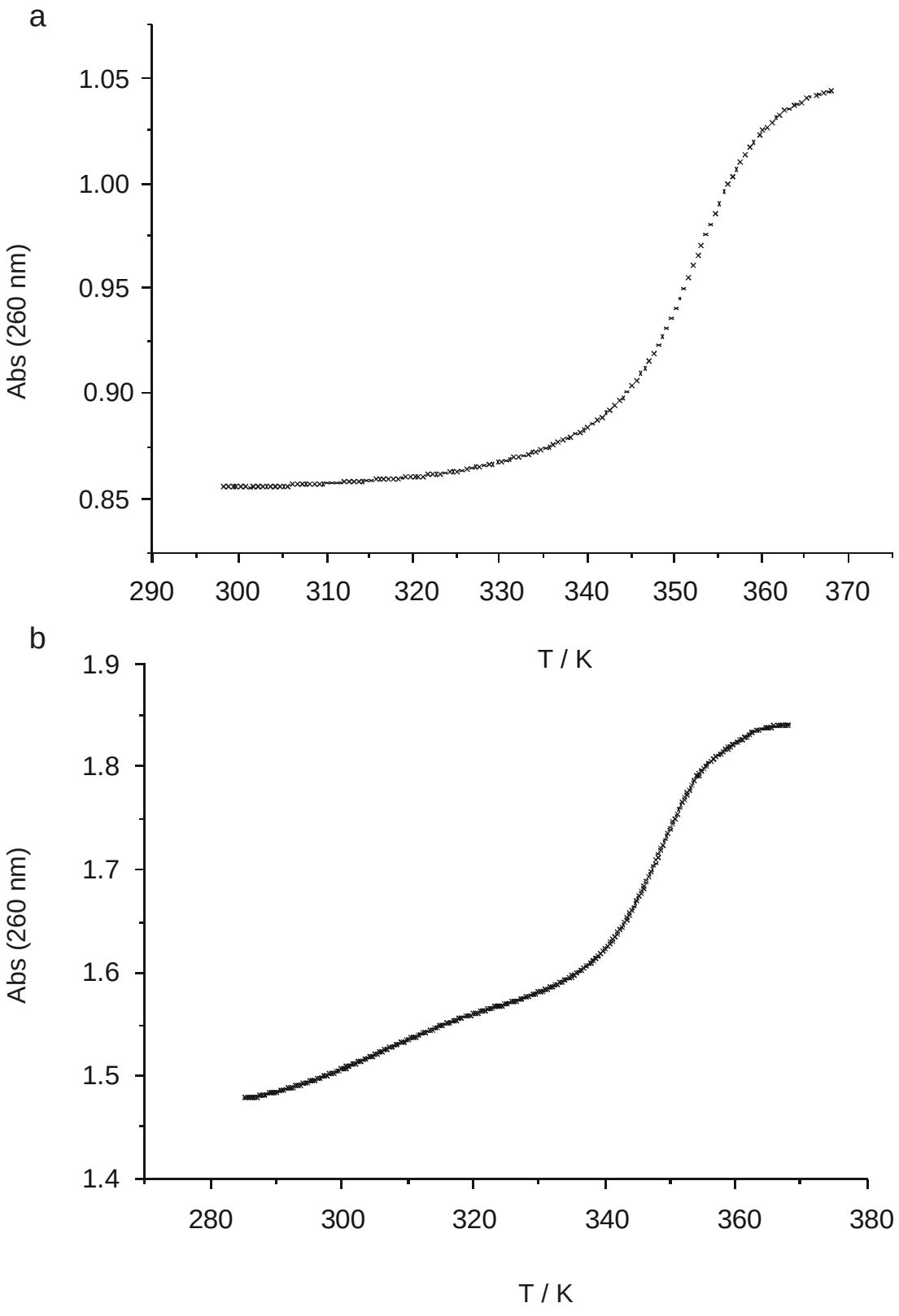


Figure 1: Melting curves of a) hairpin (**3**) and b) the unplatinated triplex (**1•3**).

## 3 Synthesis of the *trans*-$(NH_3)_2$Pt(II) crosslinked DNA triple helix 4

### 3.1 Monofunctional platination of 5´d$(GT_2CTC_2TC)^{8-}$ (1)

5´d$(GT_2CTC_2TC)^{8-}$ (**1**) was reacted with one equivalent *trans*-$[Pt(NH_3)_2(D_2O)Cl]^+$ in $D_2O$ at RT at pH$^*$ 3.2 ($r_1$, Scheme 1). Under these conditions the thymine ($pK_a = 9.9$)[121] and cytosine ($pK_a = 4.4$)[121] nucleobases are protonated so that coordination of *trans*-$[Pt(NH_3)_2(D_2O)Cl]^+$ is expected to occur primarily at the G-*N7* position. The reaction was found to be complete within 48 h as monitored by $^1$H NMR as well as ion-exchange FPLC, yielding *trans*-$[Pt(NH_3)_2\{5´d(G\text{-}N7\text{-}T_2CTC_2TC)\}Cl]^{7-}$ (**2**) (Scheme 1) as the major product.

$^1$H NMR analysis of the monofunctional platination primarily shows the appearance of one new G-H8 signal in the aromatic region at 8.58 ppm (Figure 2). In addition, further downfield a single minor signal appears at 8.73 ppm (Figure 2). In comparison with literature data the former signal is assigned to a G-H8 proton originating from *trans*-$[Pt(NH_3)_2\{5´\text{-}d(G\text{-}N7\text{-}T_2CTC_2TC)\}Cl]^{7-}$ (**2**), the latter as a G-H8 proton originating from *trans*-$[Pt(NH_3)_2\{5´d(G\text{-}N7\text{-}T_2CTC_2TC)\}_2]^{14-}$.[89] This assignment is supported by ion-exchange FPLC which shows the disappearance of the peak originating from 5´d$(GT_2CTC_2TC)^{8-}$ (**1**) (peak b, Figure 3) and the appearance of two new peaks with respective shorter and longer retention times (peaks a and c, Figure 3). The peak with the shorter retention time (peak a) must originate from a less negatively charged adduct and is therefore assigned to *trans*-$[Pt(NH_3)_2\{5´\text{-}d(G\text{-}N7\text{-}T_2CTC_2TC)\}Cl]^{7-}$ (**2**). The peak with the longer retention time (peak c) must originate from a higher negatively charged adduct and was therefore assigned to *trans*-$[Pt(NH_3)_2\{5´d(G\text{-}N7\text{-}T_2CTC_2TC)\}_2]^{14-}$.

Furthermore, $^1$H NMR spectroscopy shows, that the T-H6 resonances of the thymine residues in the vicinity of the platinated 5´guanine in **2** undergo a slight downfield shift in the $^1$H NMR (Figure 2) compared to 5´d$(GT_2CTC_2TC)^{8-}$ (**1**). This observation is probably due to decreased stacking interactions caused by the electron-withdrawing *trans*-Pt(II) entity as observed earlier.[89,93]

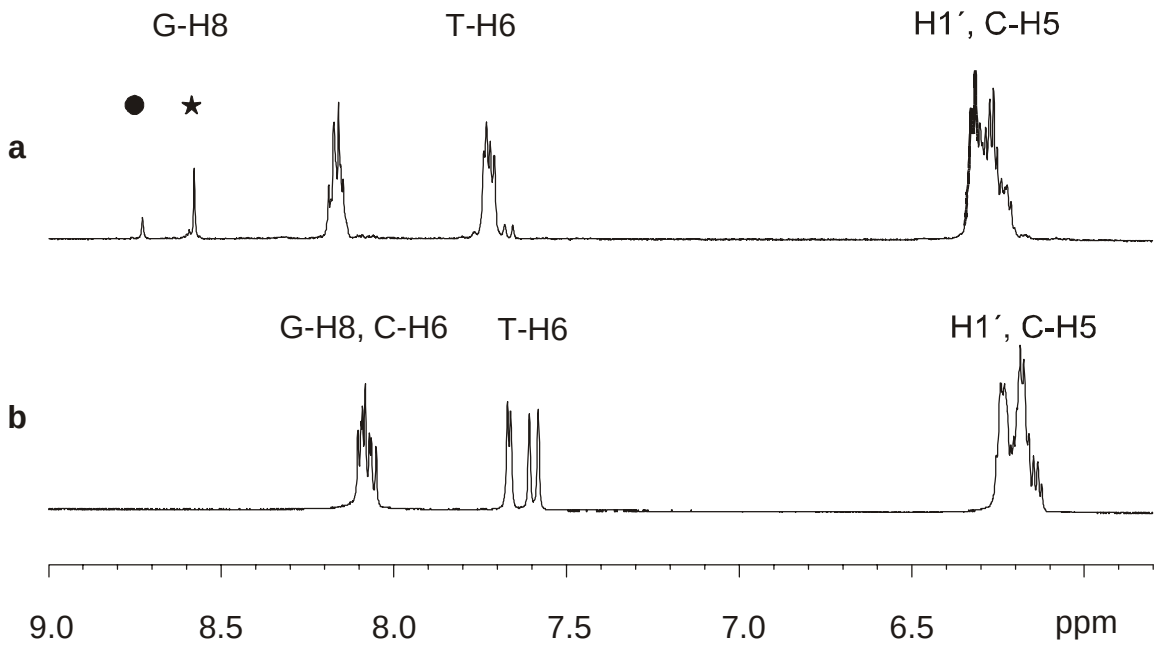


Figure 2: $^{1}$H-NMR spectra of **2** (a) and **1** (b) in $D_2O$ (pD 3.2); ★: G-H8 from **2**; ●: G-H8 from *trans*-$[Pt(NH_3)_2\{5'd(G\text{-}N7\text{-}T_2CTC_2TC)\}_2]^{14-}$.

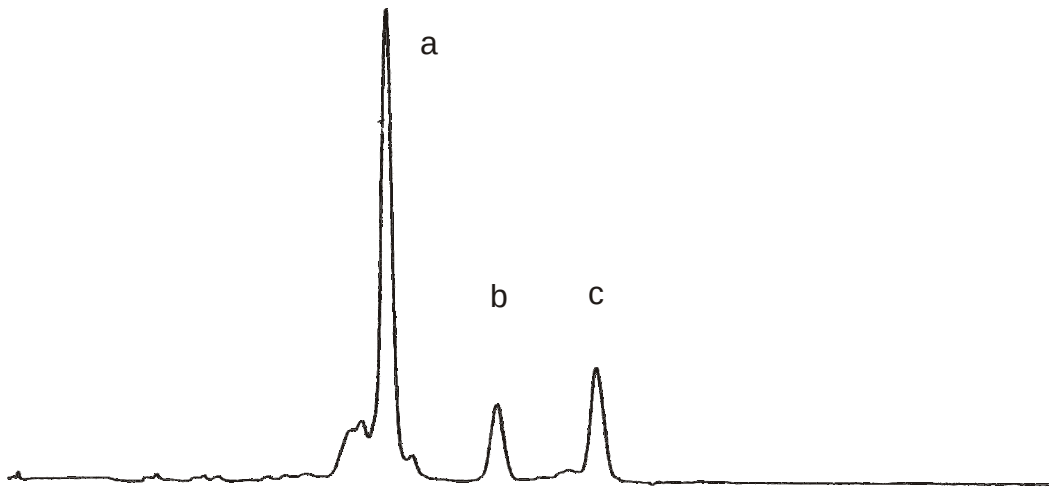


Figure 3: FPLC analysis of the monofunctional platination of **1**; peaks: a: **2**, b: **1**, c: *trans*-$[Pt(NH_3)_2\{5'd(G\text{-}N7\text{-}T_2CTC_2TC)\}_2]^{14-}$; gradient: 0→50 % B, buffers: A: 0.02 M NaOH, B: 1.2 M NaCl in 0.02 M NaOH.

## 3.2 Hybridization and crosslinking of *trans*-$[Pt(NH_3)_2\{5'\text{-}d(G\text{-}N7\text{-}T_2CTC_2TC)\}Cl]^{7-}$ (2) with $5'd(GA_2GAG_2AGCT_2GCTC_2TCT_2C)^{21-}$ (3)

The crosslinking reaction of *trans*-$[Pt(NH_3)_2\{5'd(G\text{-}N7\text{-}T_2CTC_2TC)\}Cl]^{7-}$ (**2**) with the target sequence $5'd(GA_2GAG_2AGCT_2GCTC_2TCT_2C)^{21-}$ (**3**) was carried out at $pH^*$ 4.8 in $D_2O$ at RT in the presence of 100 mM $NaClO_4$ and 5 mM $Mg(ClO_4)_2$ ($r_3$, Scheme 1). In order to drive the reaction towards the side of the products, 1.5 equivalents of the target strand **3** were applied.

$5'd(GA_2GAG_2AGCT_2GCTC_2TCT_2C)^{21-}$ (**3**) was first dissolved in a 100 mM $NaClO_4$ and 5 mM $Mg(ClO_4)_2$ solution in $D_2O$, heated, slowly cooled down to RT to ensure efficient Watson-Crick duplex formation and then added to the freeze-dried *trans*-$[Pt(NH_3)_2\{5'd(G\text{-}N7\text{-}T_2CTC_2TC)\}Cl]^{7-}$ (**2**). This procedure was expected to facilitate sequence-specific recognition of the homopurine tract within **3** by the monofunctionally platinated Hoogsteen strand *trans*-$[Pt(NH_3)_2\{5'd(G\text{-}N7\text{-}T_2CTC_2TC)\}Cl]^{7-}$ (**2**) and lead to subsequent formation of a site-specific *trans*-Pt(II) interstrand crosslink. The crosslinking reaction was monitored by ion-exchange FPLC (Figure 4) and found to be complete within 72 h, yielding one major product (peak e, Figure 4). Figure 4 shows the FPLC chromatograms of the crosslinking reaction after 22 and 71 h. It can be seen that the peak originating from the monofunctionally platinated Hoogsteen strand **2** (peak a, Figure 5) almost disappears and the height of the peak originating from the hairpin (**3**) decreases at the expense of a single new peak (peak e, Figure 4). As the FPLC chromatograms did not provide peak intensity values the half-life of *trans*-$[Pt(NH_3)_2\{5'd(G\text{-}N7\text{-}T_2CTC_2TC)\}Cl]^{7-}$ (**2**) could only roughly be estimated to be 20-25 h. Reversed-phase HPLC analysis of the reaction mixture (Figure 5) also demonstrates the presence of one major product as well as excess **3**. The main product (peak e, Figures 4 and 5) was subsequently purified by reversed-phase HPLC.

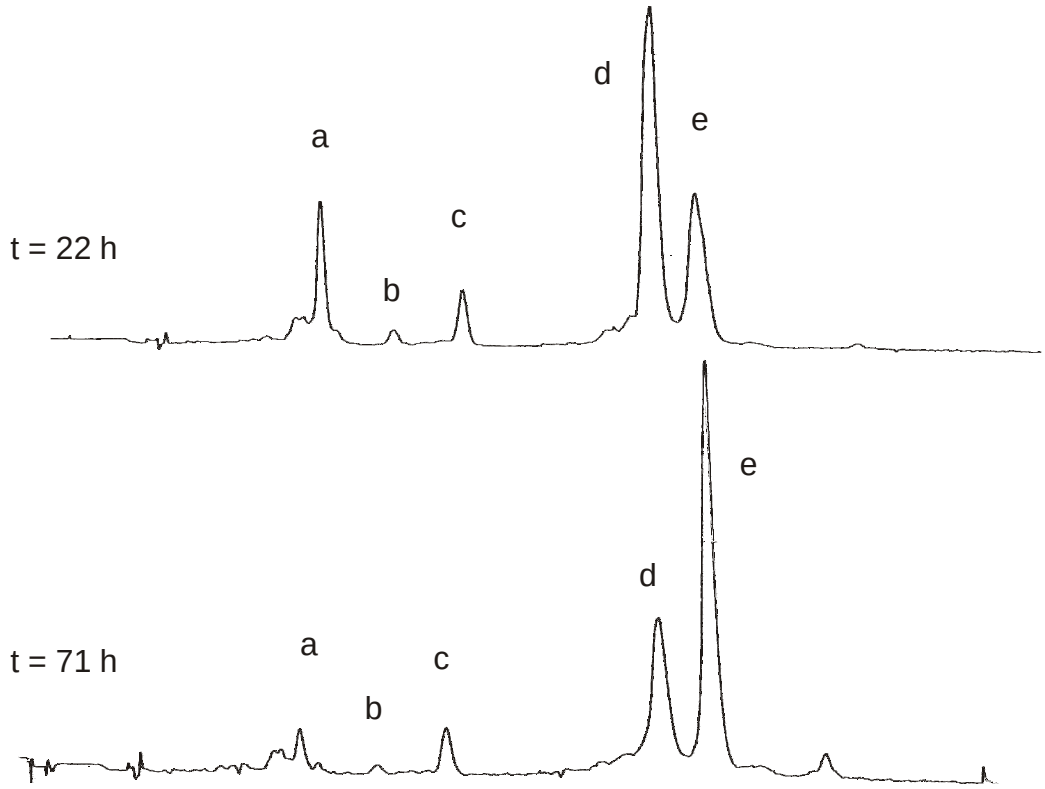


Figure 4: Ion-exchange FPLC analysis of the crosslinking reaction; peaks: a: **2**, b: **1**, c: *trans*-$[Pt(NH_3)_2\{5'd(G\text{-}N7\text{-}T_2CTC_2TC)\}_2]^{14-}$, d: **3**, e: **4**; gradient: 0→55 % B in 40 min; buffers: A: 0.02 M NaOH, B: 1.2 M NaCl in 0.02 M NaOH.

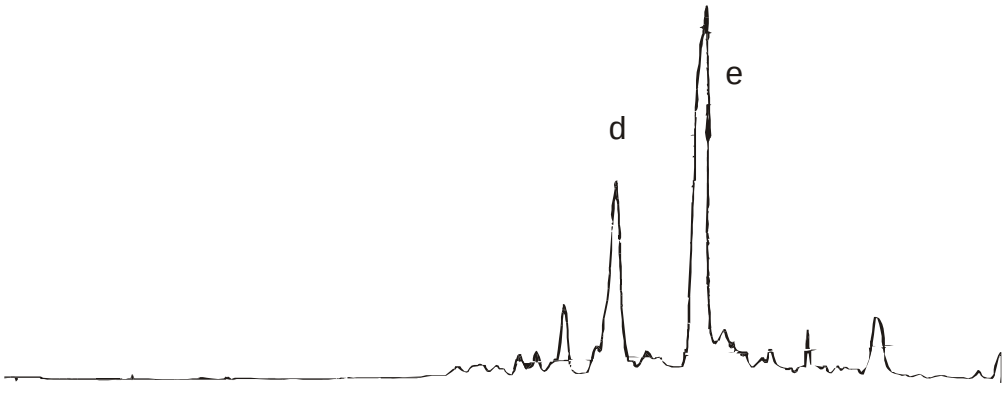


Figure 5: Reversed-phase HPLC analysis of the crosslinking reaction; d: **3**, e: **4**; gradient: 11→19 % B in 40 min; buffers: A: 50 mM TEAA, B: 50 mM TEAA in 75 % acetonitrile.

## 4 Characterization of the *trans*-$(NH_3)_2$Pt(II) crosslinked DNA triple helix 4

### 4.1 Reversed-phase HPLC

The purity of the isolated product **4** was established by reversed-phase HPLC analysis. A very smooth elution gradient in combination with a long elution time was applied to ensure efficient separation and detection of any coexisting species. The obtained HPLC chromatogram of the isolated product **4** (Figure 6) reveals a single peak with a retention time different from that of the unplatinated Hoogsteen (**1**) and hairpin (**3**) strands as proven by coelution experiments. HPLC analysis of the unplatinated, fully hybridized triplex **1•3** under the same conditions shows the appearance of two peaks belonging to the Hoogsteen (**1**) and the hairpin (**3**) strand, respectively.

Taken together, these findings strongly suggest that the isolated product **4** is neither identical with **1** nor with **3**. It is assumed that **4** is a crosslinked product. Furthermore, the isolated compound **4** is expected to be pure as different crosslinked adducts have been observed to have different retention times on a reversed-phase column.[89]

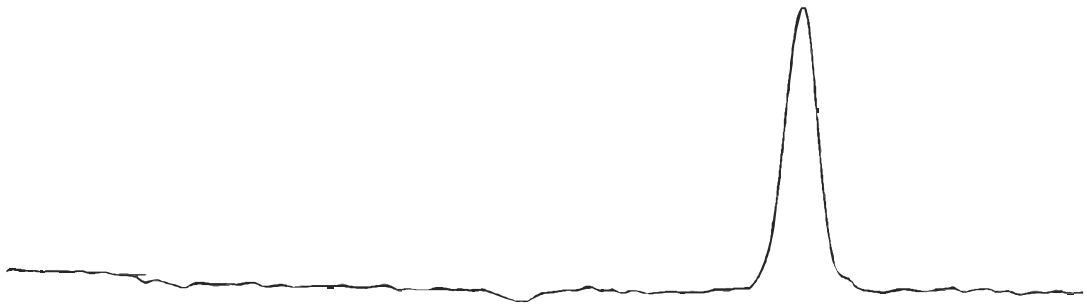

Figure 6: Reversed-phase HPLC chromatogram of the purified product **4**;
gradient: 11→18 % B in 40 min; buffers: A: 50 mM TEAA, B: 50 mM TEAA in 75 % acetonitrile.

## 4.2 ESI mass spectrometry

The isolated product **4** was subsequently characterized by ESI mass spectroscopy (Figures 7 and 8). The mass for the twofold positively charged *trans*-Pt(II) crosslinked DNA triplex **4** amounts to 9595.7 g $mol^{-1}$. In the ESI MS spectrum masses of m/z 1597, 1917, 2396 for the respective $M^{6-}/6$, $M^{5-}/5$ and $M^{4-}/4$ ions are observed. The peaks at m/z 1597 and 1917 exhibit characteristic $Na^+$ and $K^+$ adducts (Figure 7 b). A zoom scan of the peak at m/z 1917.7 (Figure 8) affords the resolution of the isotope pattern. The distance between the lines amounts to 0.2 mass units indicating that the peak at m/z 1917 belongs to a fivefold negatively charged ion. Moreover, the observed isotope pattern is in agreement with the calculated one (Figure 8).

Thus, ESI MS analysis confirms the existence of a product, where the Hoogsteen strand (**1**) is crosslinked via a *trans*-$(NH_3)_2$Pt(II) unit to the hairpin (**3**). A differentiation of linkage isomers with this method is not possible as they would have the same mass.

Furthermore, ESI MS shows, that the isolated crosslinked product is pure. Masses for the unplatinated Hoogsteen strand (**1**) and the unplatinated hairpin (**3**) are not detected in the ESI MS spectrum.

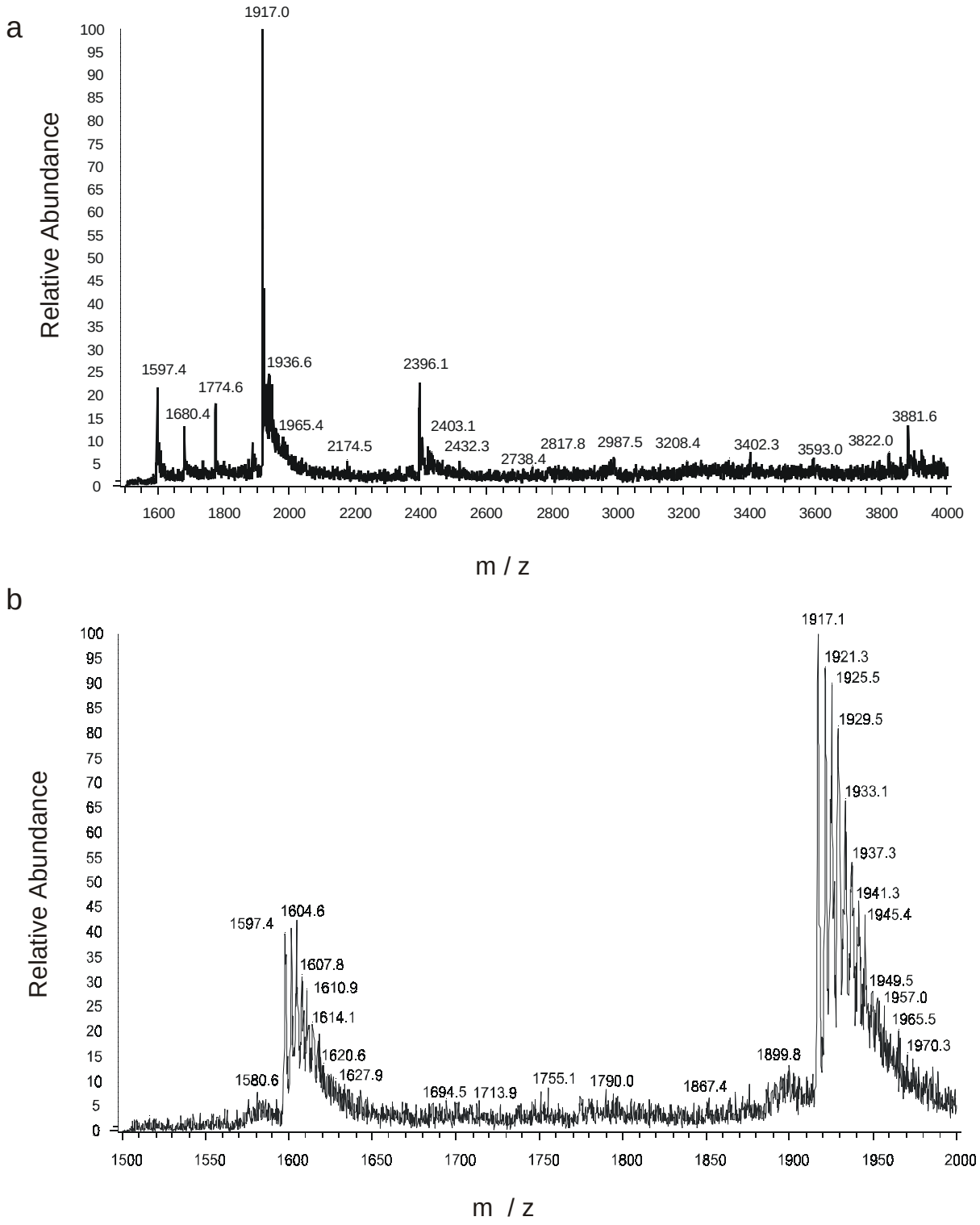


Figure 7: ESI MS spectrum of **4**.

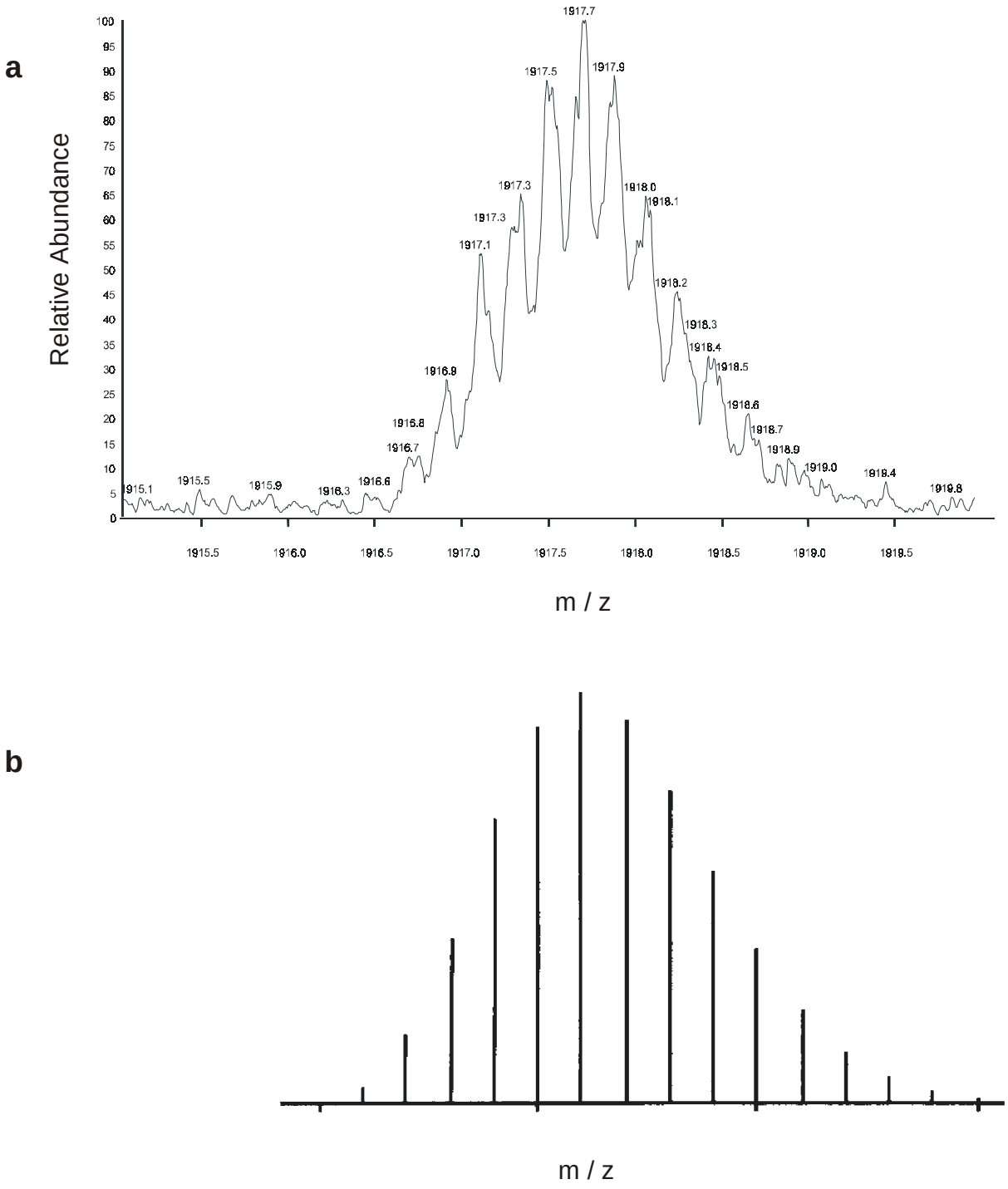


Figure 8: ESI MS spectrum of **4**; a) zoom scan of the peak at m/z 1917.7, b) theoretically calculated isotope pattern.

## 4.3 Gel electrophoresis

### 4.3.1 Denaturing 24 % PAGE gel

For a further characterization of the isolated product **4** gel electrophoresis was applied. Gel electrophoresis exploits the different mobility of differently long oligonucleotides on the gel under the influence of an electric field. Shorter oligonucleotides migrate faster, whereas longer oligonucleotides have a lower mobility.

The crosslinked isolated product **4**, the Hoogsteen (**1**) and the hairpin (**3**) strand were labelled with $^{32}$P-γ-ATP and run on a 24 % denaturing PAGE gel (Figure 9). Radioactive labelling of the isolated crosslinked product **4** was not very efficient and surprisingly, three bands have been observed on the gel, two of which can be assigned to the unplatinated Hoogsteen (**1**) and hairpin (**3**) strand. The third band represents a product with a lower mobility which could be a crosslinked product. The observation of three bands on the gel was rather unexpected in that the isolated crosslinked product had actually been shown to be pure.

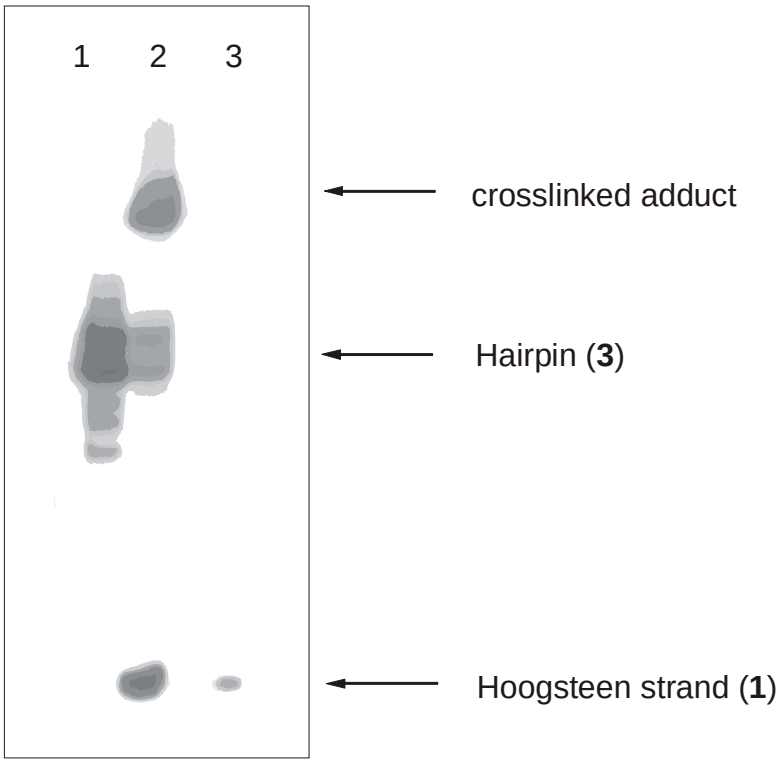


Figure 9: Autoradiogram of a denaturing 24 % polyacrylamide gel; lane 1: hairpin (**3**), lane 2: crosslinked adduct, lane 3: Hoogsteen strand (**1**).

### 4.3.2 Hydroxyl radical footprinting

For a more detailed gel-electrophoretic analysis a sample of the isolated product **4** was sent to Dr. M. Boudvillain, CNRS, Orléans, France. There, hydroxyl radical footprinting[122] was applied in order to determine the location of the *trans*-$(NH_3)_2$Pt(II) interstrand crosslink. The hydroxyl radical, generated by iron(II)-promoted reduction of hydrogen peroxide,[123] attacks the deoxyribose sugars. This results in unspecific and sequence-independent cleavage of the DNA backbone.[124]

First, the isolated product **4** was 5´ labelled with $^{32}$P-γ-ATP and loaded on a 24 % denaturing PAGE gel. Labelling occurred at both the Hoogsteen and the hairpin strand but was not very efficient, probably due to platination of the two 5´G residues. Again three bands, originating from Hoogsteen strand (**1**), hairpin strand (**3**) and a putative crosslinked product **4** were detected on the gel (not shown). The crosslinked adduct **4** was subsequently purified on the gel. Next, both the purified crosslinked adduct **4** (labelled) and the labelled hairpin (**3**) were subjected to a hydroxyl radical footprinting experiment. Conditions have been used under which on average less than one cleavage per molecule occurred. The cleavage products have been analyzed on a 24 % denaturing PAGE gel (Figure 10).

If the *trans*-$(NH_3)_2$Pt(II) unit in **4** was located between the two 5´ guanines, the shortest cleavage product of **4** would be the Hoogsteen strand containing the *trans*-$(NH_3)_2$Pt(II) unit coordinated to a single guanine residue. If one residue other than the two 5´guanine residues was involved in a *trans*-$(NH_3)_2$Pt(II) interstrand crosslink, hydroxyl radical footprinting would yield one or several fragments *shorter* than the Hoogsteen strand. From Figure 10 it is evident that the smallest major cleavage product of the crosslinked adduct migrates as a 12-mer. This is therefore assigned to the Hoogsteen strand containing the *trans*-$(NH_3)_2$Pt(II) unit coordinated to one single guanine residue. Furthermore, a band migrating exactly as the Hoogsteen strand is present, probably due to deplatination reactions during the footprinting experiment and sample handling. Additionally, there is a very faint pattern of shorter cleavage products migrating exactly as the cleavage products of the hairpin (Figure 10). This faint pattern of shorter cleavage products could arise from a crosslinked adduct with the *trans*-$(NH_3)_2$Pt(II) crosslink being located at a position different from the 5´guanine of the hairpin. However, in this case, 5´labelling of the hairpin should be much more efficient which would result in stronger bands for this adduct. The other possibility is that the faint pattern of shorter cleavage product results from the presence of a tiny amount of the hairpin (**3**) due to

deplatination reactions during the footprinting experiment and sample handling. With regard to the fact that the crosslinked adduct has been shown to be HPLC pure and thus, only one linkage isomer of **4** should be present, the second explanation is favoured.

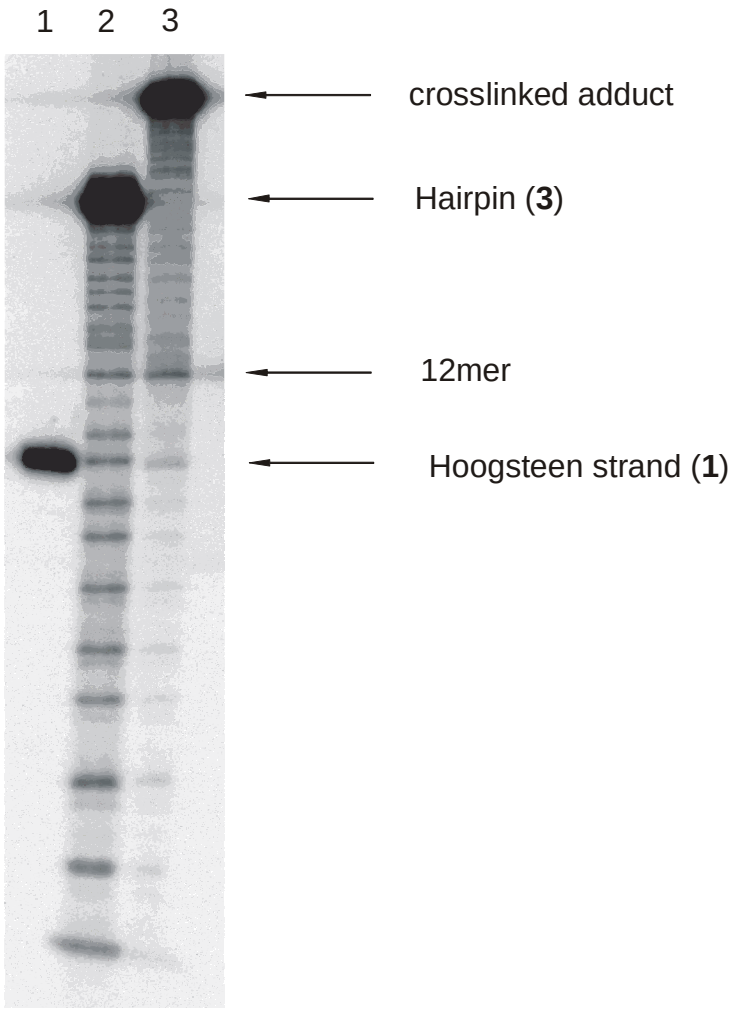


Figure 10: Autoradiogram of a 24 % denaturing PAGE gel showing the Hoogsteen strand (**1**) (lane 1) as well as the the cleavage products of the hairpin (**3**) (lane 2) and the crosslinked product **4** (lane 3) after hydroxyl radical footprinting.

### 4.4 UV spectroscopy

Finally, the melting profile of the crosslinked adduct **4** was analyzed by UV spectroscopy (Figure 11). Similarly to the melting profile of the unplatinated triplex (**1•3**) the *trans*-$(NH_3)_2Pt(II)$ crosslinked triplex **4** shows a biphasic melting behaviour. The transition at 336 K reflects dissociation of the Hoogsteen strand from the Watson-Crick duplex whereas the transition at 348 K reflects the dissociation of the Watson-Crick duplex. The hyperchromicity for the transition of the *trans*-$(NH_3)_2Pt(II)$ crosslinked triplex **4** to the coil state amounts to approximately 15 % (Figure 11).

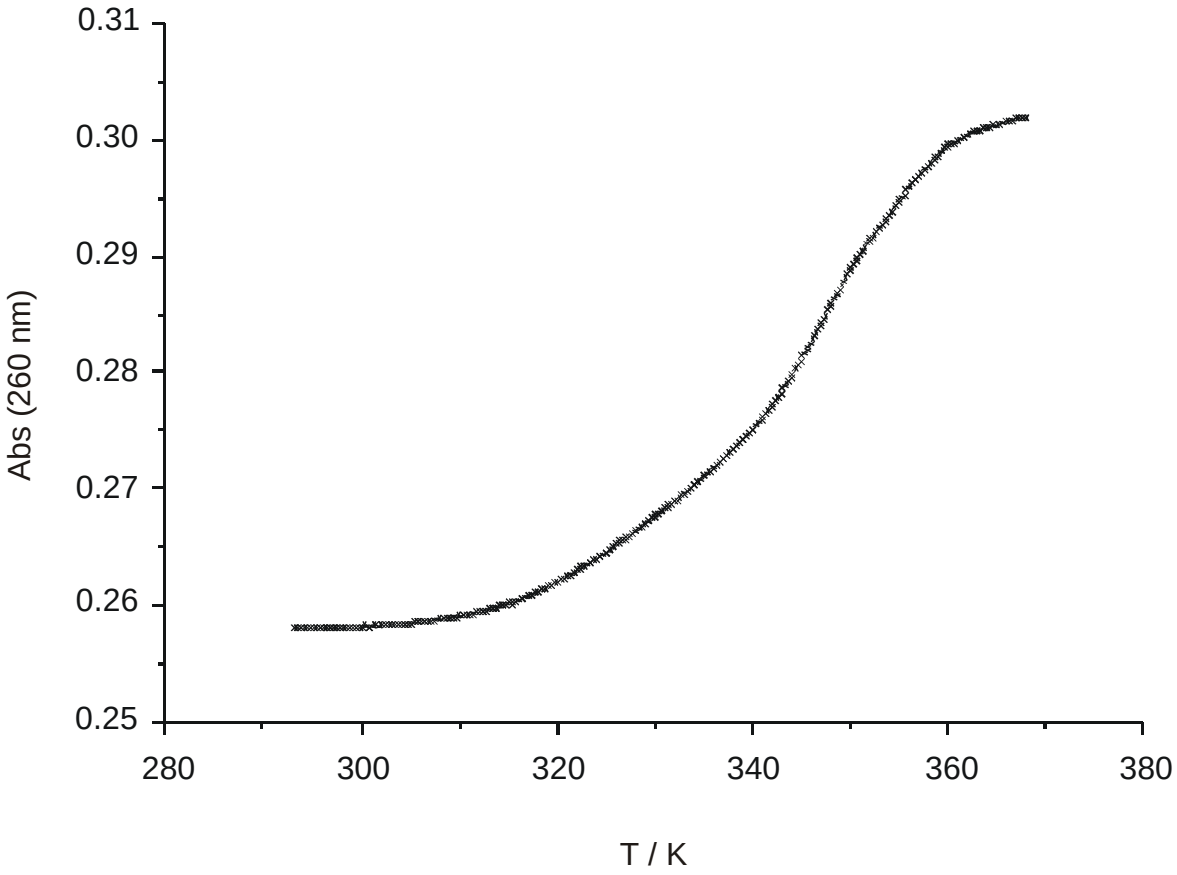


Figure 11: Melting curve of **4**.

From the melting profile of **4** it is evident that compared to the unplatinated triplex (**1•3**) the second transition at 348 K remains unaffected by the *trans*-$(NH_3)_2Pt(II)$ crosslink in **4**, while the first transition, which reflects the dissociation of the Hoogsteen strand, takes place at a significantly higher temperature ($\Delta T$ = 28 K) in **4**. Thus, binding of the Hoogsteen strand to the hairpin is significantly enhanced by the *trans*-$(NH_3)_2Pt(II)$ crosslink. This results in an

increase of the thermal stability of the DNA triple helix **4**. Similar observations have been made in case of a DNA triple helix containing a disulfide bridge between the Hoogsteen strand and the Watson-Crick duplex.[120]

The increase in thermal stabilities of crosslinked DNA triple helices has been found to result from the entropic consequences of crosslinking rather than from net enthalpic differences.[119] On the basis of configurational arguments it is evident that denaturation of a crosslinked triplex is accompagnied by a lower melting entropy than denaturation of an uncrosslinked triplex due to a more constrained final state of the denatured crosslinked triplex. Thus, for a crosslinked triplex a net entropic stabilization exists. Furthermore, from Figure 11 it is evident, that the hyperchromicity of the crosslinked triplex **4** is somewhat lower than for the unplatinated triplex (**1•3**). This observation is tentatively explained as follows: The hyperchromic effect upon melting of the triplex is a result of disruption of base stacking interactions. In case of the *trans*-$(NH_3)_2$Pt(II) crosslinked triplex **4** stacking interactions between base pairs adjacent to the crosslink are probably still partly present so that the hyperchromicity is not that pronounced as in the case of the uncrosslinked triplex (**1•3**).

## 5 Discussion

The results show that the crosslinking reaction of *trans*-$[Pt(NH_3)_2\{5'd(G\text{-}N7\text{-}T_2CTC_2TC)\}Cl]^{7-}$ (**2**) with the homopurine target within $5'd(GA_2GAG_2AGCT_2GCTC_2TCT_2C)^{21-}$ (**3**) proceeds sequence-specifically with formation of a site-specific interstrand crosslink between the two 5´guanine residues, yielding almost exclusively the *trans*-$(NH_3)_2$Pt(II) crosslinked DNA triple helix (**4**).

The *trans*-$(NH_3)_2$Pt(II) interstrand crosslink has unambiguously been determined to be located between the two 5´guanines by a hydroxyl radical footprinting experiment. However, this sequencing method does not allow for a differentiation between the two potential coordination sites G-*N7* and G-*N1* of the 5´guanine of the hairpin. It is assumed that the 5´G-*N7* position is involved in the interstrand crosslink rather than G-*N1* position. First, the G-*N1* position is protonated under the conditions of the crosslinking reaction[121] which would hamper its platination and second, it is expected to be engaged in Watson-Crick hydrogen bonding with the 3´terminal cytosine.

The crosslinking reaction leading to formation of the crosslinked triplex **4** was found to be complete within 72 h. The half-life of the monofunctional adduct **2** was roughly estimated to be 20-25 h. This value is slightly higher than results obtained in similar crosslinking reactions.[125]

In general, for formation of an interstrand crosslink two main pathways exist.[126] The first pathway implies a direct nucleophilic attack of the G residue within the purine tract of the hairpin on the platinated 5´G of the Hoogsteen strand. The second pathway proceeds through solvent-associated intermediates with the rate-limiting step being hydrolysis of the chloride ion of the monofunctional adduct. The exact mechanism, however, has not yet entirely been elucidated.[126] Studies on *trans*-$(NH_3)_2$Pt(II) interstrand crosslink formation within triplex structures have demonstrated that when the platinated G residue was located at the 5´-terminus of the Hoogsteen strand and therefore well solvent-accessible, interstrand crosslink formation took place via a solvent-associated mechanism rather than through direct nucleophilic attack.[125]

Sterically, formation of a *trans*-$(NH_3)_2$Pt(II) interstrand crosslink between the 5´G-*N7* position of the Hoogsteen strand and the 5´G-*N7* position of the central purine-rich strand requires a switch of the 5´-platinated guanine of the Hoogsteen strand from the *anti* to the *syn* conformation. Model building suggests that the two crosslinked guanine bases will adopt a head - head orientation under these circumstances.[84] Figure 12 depicts the nucleobase triple involved in such a *trans*-$(NH_3)_2$Pt(II) interstrand crosslink.

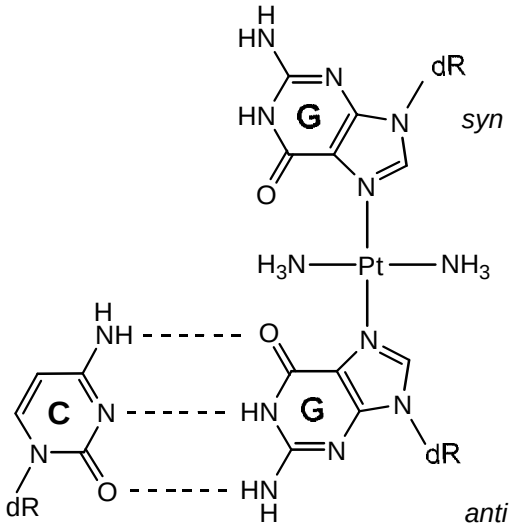


Figure 12: Nucleobase triple involved in the interstrand crosslink in **4**.

The thermal stability of the crosslinked triplex **4** is significantly higher compared to the uncrosslinked triplex (**1•3**). The UV melting profile of **4** shows that the triplex→duplex transition (dissociation of the Hoogsteen strand) occurs at a significantly higher temperature ($\Delta T$ = 28 K) whereas the hybridization of the Watson-Crick duplex remains unaffected by the presence of the *trans*-$(NH_3)_2$Pt(II) crosslink.

With respect to antigene strategy this model crosslinking reaction demonstrates that, in principle, homopurine sequences in double-stranded DNA can sequence-specifically be targeted and efficiently be sterically blocked through crosslinking of the antigene oligonucleotide via a *trans*-$(NH_3)_2$Pt(II) unit.

It is evident, that the *in vivo* application of monofunctionally *trans*-Pt(II) modified deoxyoligonucleotides is largely hampered by their instability towards enzymatic degradation. However, a potential solution to these problems is e.g. the use of nuclease-resistant oligonucleotide-analogues (cf. chapter III). Further problems can be represented by inefficient cellular uptake of these potential antigene reagents.

Furthermore, it still has to be established in how far the presence of sulfur-containing amino acids and proteins, which are known to react strongly with Pt(II) complexes,[127,128] would effect the action of monofunctionally *trans*-$(NH_3)_2$Pt(II) modified oligonucleotide(analogues) *in vivo*. However, although several features of this approach still have to be optimized, the principle to achieve long-lasting steric blockage of a DNA target sequence by an antigene oligonucleotide crosslinked via a *trans*-$(NH_3)_2$Pt(II) moiety seems reasonable and promising.

# Chapter II Solid-phase synthesis of monofunctionally *trans*-Pt(II) modified homopyrimidine deoxyoligonucleotides

## 1 Introduction

The potential use of monofunctionally *trans*-Pt(II) modified deoxyoligonucleotides in antigene and antisense strategy has been explained in the general introduction and demonstrated in chapter I of this thesis. The lack of an efficient and site-specific synthesis of these potential antisense / antigene reagents is still a major impediment for their potentially successful in *vivo* application. Among the different strategies employed, the incorporation of preplatinated building blocks into an oligonucleotide by solid-phase DNA synthesis appears to be most rewarding for the synthesis of site-specifically platinated oligonucleotides.[99,100]

The latter method was first successfully applied for the synthesis of *trans*-Pt(II) modified oligonucleotides by incorporation of the building block *trans*-[$Pt(NH_3)_2$(THP)Cl] (THP = thymidine-H-phosphonate) into deoxyoligonucleotides.[99] However, unfortunately, ligand exchange reactions at the Pt(II) center (substitution of the chloro ligand by pyridine) occurred during the synthesis protocol rendering the *trans*-Pt(II) modified oligonucleotide inactive for further crosslinking reactions.[99]

A potential solution of this problem would be the use of the thyminate protecting group mentioned earlier instead of a chloro ligand. The thyminate ligand would protect the Pt(II) center during the automated DNA synthesis protocol and could be substituted by a chloro ligand afterwards, yielding the desired monofunctionally *trans*-Pt(II) modified deoxyoligonucleotide. In *trans*-position to this thyminate ligand a suitable platinated building block would have to be coordinated either to a fully protected DNA building block (e.g THP) or, analoguously, to a ligand containing a functional group that allows conjugation of the building block to the sugar-phosphate backbone of DNA.

This chapter describes a methodology, in which two newly synthesized *trans*-Pt(II) modified building blocks, containing such thyminate protecting groups have been linked via a ligand to the 5´-terminus of the sugar phosphate backbone of an oligonucleotide using solid-phase DNA synthesis.[129]

## 2 Design of *trans*-Pt(II) modified building blocks for use in solid-phase DNA synthesis

Scheme 1 shows the synthesis cycle applied in solid-phase DNA synthesis according to the phosphoramidite method.[130] The basic steps of this protocol are:

1. Detritylation of the 5´-hydroxyl group of the terminal 2´deoxyribose, usually achieved by treatment with trichloroacetic acid (TCA) in methylene chloride.
2. Addition of a protected deoxyribonucleoside-3´phosphoramidite to the growing chain in the presence of tetrazole, followed by a capping step (not shown in Scheme 1)
3. Oxidation of the intermediate phosphite to the corresponding phosphotriester, achieved by treatment with an aqueous iodine solution in the presence of collidine.

Removal of the base protecting groups and cleavage of the oligonucleotide from the solid support is usually accomplished by treatment with concentrated aqueous ammonia at 50 °C overnight.

A suitable preplatinated building block has to be compatible with such a DNA synthesis protocol. Furthermore, an essential prerequisite is its solubility in organic solvents.

Conjugation of a preplatinated building block to the 5´-terminus of an oligonucleotide by solid-phase DNA synthesis (Scheme 2) can in principle be achieved by linkage via a phosphate bond (approach I, Scheme 1) and via an amide bond (approach II, Scheme 1). The latter approach requires 5´-terminal functionalization of an immobilized oligonucleotide by an aminolinker and the platinated building block has to contain a ligand with a free carboxyl group. For approach I (Scheme 1) the platinated building block has to contain a ligand with a free hydroxyl function via which it can be converted into the corresponding phosphoramidite (Scheme 1).[131,132]

Two potentially suitable building blocks are compounds **8** and **9** (Scheme 2). Building block **8** contains an aminohexanol ligand providing a free hydroxyl function. Building block **9** contains a glycine ligand providing a free carboxyl function. Furthermore, both **8** and **9** are coordinated to a thyminate derivative which serves to protect the Pt(II) center during the synthesis protocol and the deprotection step, and which can post-synthetically be substituted by a chloro ligand[93-98] (Scheme 1). The lipophilic cyclohexylmethyl residue at the *N1* position of the thyminate ligand affords sufficient solubility of **8** and **9** in organic solvents. In both **8** and **9** the Pt(II) center is coordinated to four nitrogen atoms, so that **8** and **9** are expected to be stable against synthesis and deprotection conditions.

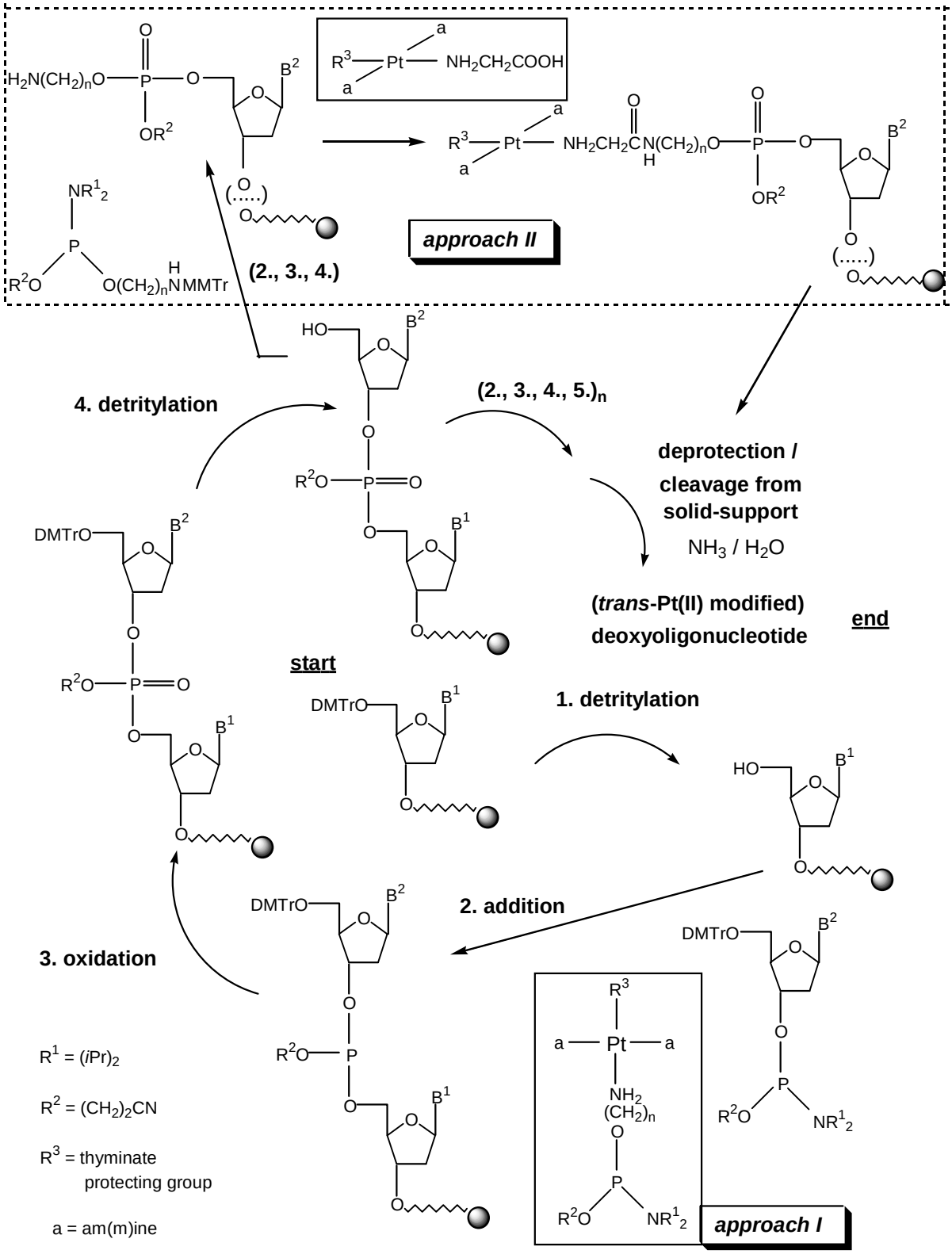


Scheme 1: Solid-phase DNA synthesis protocol (phosphoramidite method) and strategies for introduction of preplatinated building blocks (approaches I and II).

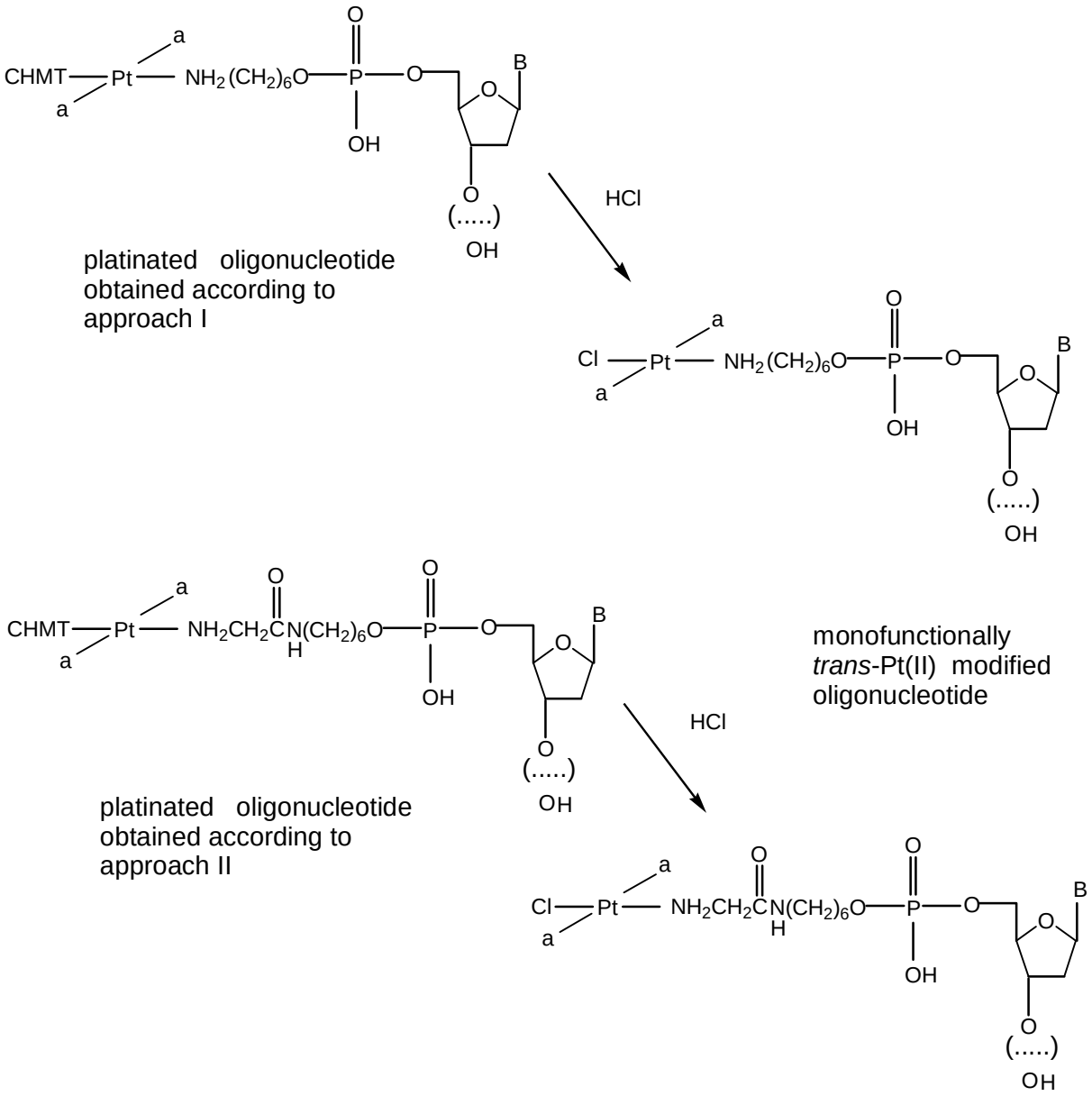


Scheme 1 (continued): Removal of the CHMT ligand and its substitution by a chloro ligand.

## 3 Synthesis and characterization of the preplatinated building blocks *trans*-$[Pt(NH_2CH_3)_2(CHMT)\{NH_2(CH_2)_6OH\}]^+Cl^-$ (**8**) and *trans*-$[Pt(NH_2CH_3)_2(CHMT)(gly\text{-}N)]^+BF_4^-$ (**9**)

Building blocks **8** and **9** have both been synthesized from *trans*-$[Pt(NH_2CH_3)_2(CHMT)Cl]$ (**7**) (Scheme 2). Synthesis and characterization of complexes **7**, **8** and **9** are described in the following sections.

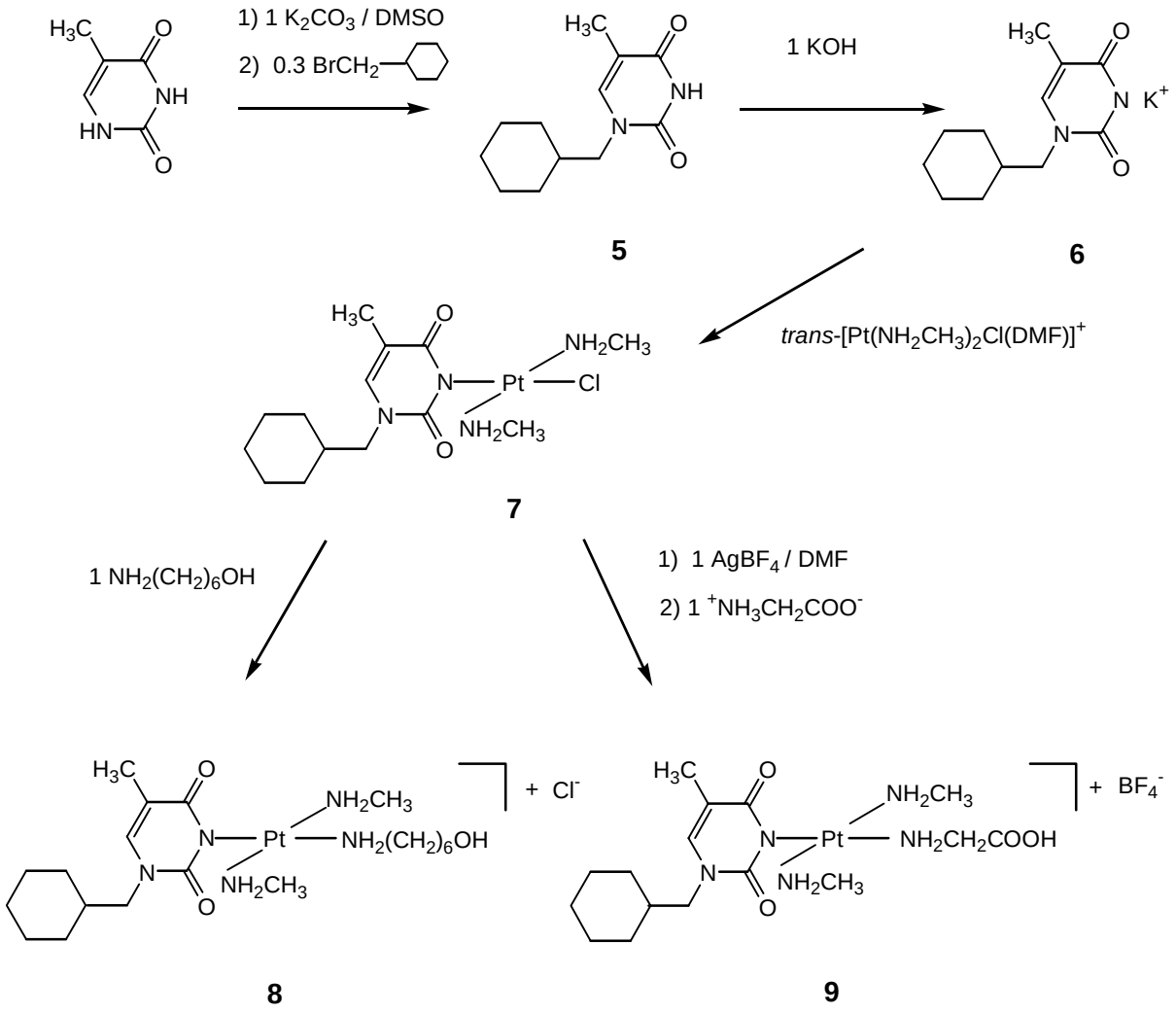


Scheme 2: Synthesis of building blocks **8** and **9**.

## 3.1 Synthesis and characterization of *trans*-[Pt($NH_2CH_3$)$_2$(CHMT)Cl] (7)

*Trans*-[Pt($NH_2CH_3$)$_2$(CHMT)Cl] (**7**) was synthesized by a slight modification of a published procedure[80] from *trans*-[Pt($NH_2CH_3$)$_2$(DMF)Cl]$^+NO_3^-$ (**7b**) and K(CHMT) (**6**) (Scheme 2). First, 1-*N*-cyclohexylmethylthymine (**5**) was synthesized from thymine and bromomethylcyclohexane in a standard alkylation reaction[133] and subsequently converted into its potassium salt **6**[134] (Scheme 2).

An interesting feature of *trans*-[Pt($NH_2CH_3$)$_2$(CHMT)Cl] (**7**) is its high solubility in chloroform. Compound **7** was analyzed by IR and NMR spectroscopy. Figure 1 shows the $^1$H NMR spectrum of **7** in $CDCl_3$. Relative to 1-*N*-cyclohexylmethylthymine (**5**), the T-H6 proton in **7** undergoes a slight upfield shift of 0.08 ppm as, compared to a proton, Pt(II) is a weaker Lewis-acid which causes a less deshielding effect on the T-H6 proton. The resonances for the amino protons of the methylamine ligands in **7** exhibit platinum satellites due to $^1$H - $^{195}$Pt coupling. The protons of the methyl groups of the methylamine ligands give rise to a triplet due to coupling with the amino protons ($^3J$ = 6.51 Hz) and similar platinum satellites are observed. The $^{195}$Pt NMR spectrum of **7** shows one signal at -2338 ppm, consistent with a $PtN_3Cl$ coordination sphere.[135,136]

The coordination of Pt(II) to the CHMT-*N3*-position is additionally evidenced by IR spectroscopy. In the double bond stretching region of the IR spectrum two characteristically split intense bands at 1660 and 1570 cm$^{-1}$ occur. They are assigned to the ν(O-C-N-C-O) vibrations, which indicate platinum binding to *N3* of the CHMT ligand.[94,96,137] In the low frequency region of the spectrum an intense band at 336.5 cm$^{-1}$ is observed and attributed to the Pt-Cl stretching vibration.

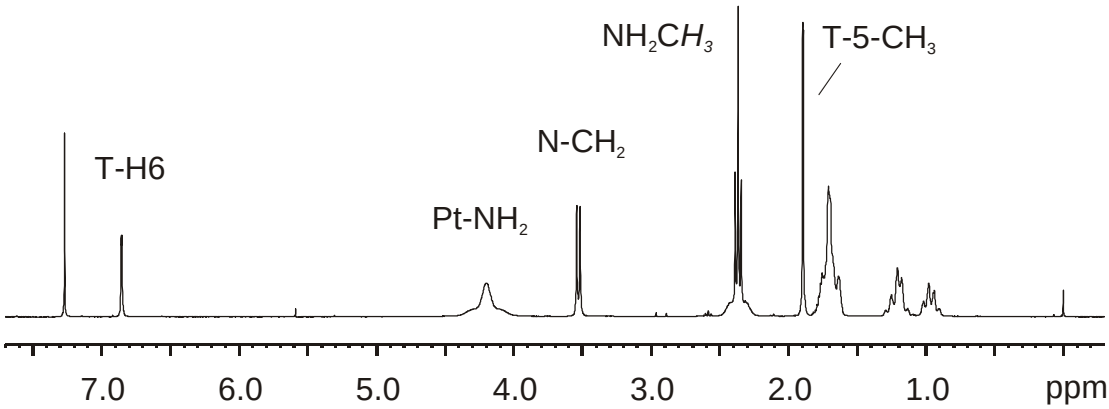


Figure 1: $^{1}$H NMR spectrum of *trans*-[Pt($NH_2CH_3$)$_2$(CHMT)Cl] (**7**) in $CDCl_3$.

### 3.2 Synthesis and characterization of *trans*-[Pt($NH_2CH_3$)$_2$(CHMT){$NH_2(CH_2)_6OH$}]$^+$Cl$^-$ (**8**)

From literature, Pt(II) complexes with both monodentate (coordination via N) and bidentate (formation of N,O chelate) coordinated 2-amino-1-ethanol are known.[138-140] In addition, complexes of the type *trans*-[Pta$_2$(1-MeT)(ama)]$^+$ [a = $NH_3$, $NH_2CH_3$ , ama = amino alcohol (2-amino-1-ethanol, 3-amino-1-propanol)], whereby Pt(II) coordinates to the amino group of the amino alcohol have been synthesized.[131] These complexes fulfil the structural requirements for use in solid-phase DNA synthesis as discussed in section 2 of this chapter, but their application is hampered by their insolubility in organic solvents. *Trans*-[Pt($NH_2CH_3$)$_2$(CHMT){$NH_2(CH_2)_6OH$}]$^+$Cl$^-$ (**8**), highly soluble in organic solvents like chloroform and dioxane, was obtained in a similar way by reaction of *trans*-[Pt($NH_2CH_3$)$_2$(CHMT)Cl] (**7**) with one equivalent of aminohexanol in a methanol / water mixture (3 d, 60°C).

Characterization of **8** was achieved by $^{1}$H and $^{195}$Pt NMR spectroscopy as well as ESI MS and IR spectroscopy. Coordination of Pt(II) to the $NH_2$ group of the aminohexanol ligand is confirmed by $^{195}$Pt NMR, which shows a single signal signal at -2616 ppm, consistent with a $PtN_4$ coordination sphere.[135,136] In addition, the $^{1}$H NMR spectrum (Figure 2) shows downfield shifts of 3.17 ppm and 0.17 ppm for the resonances of the amino group and the ζ-$CH_2$ group, respectively, compared to 1-amino-6-hexanol. The resonance for the ζ-$CH_2$ protons of the aminohexanol ligand appears as a multiplet and is significantly broadened,

possibly due to $^{1}H$-$^{195}Pt$ coupling. The protons of the methyl groups of the methylamine ligands appear as a triplet due to coupling ($^{3}J$ = 6.12 Hz) with the protons of the amino group.

The ESI MS spectrum of compound **8** shows a peak at m/z 595 for the singly positively charged ion of **8**.

Similar to the IR spectrum of **7**, in the IR spectrum of **8** two characteristically split intense bands at 1660 and 1560 $cm^{-1}$ are observed.[94,96,137]

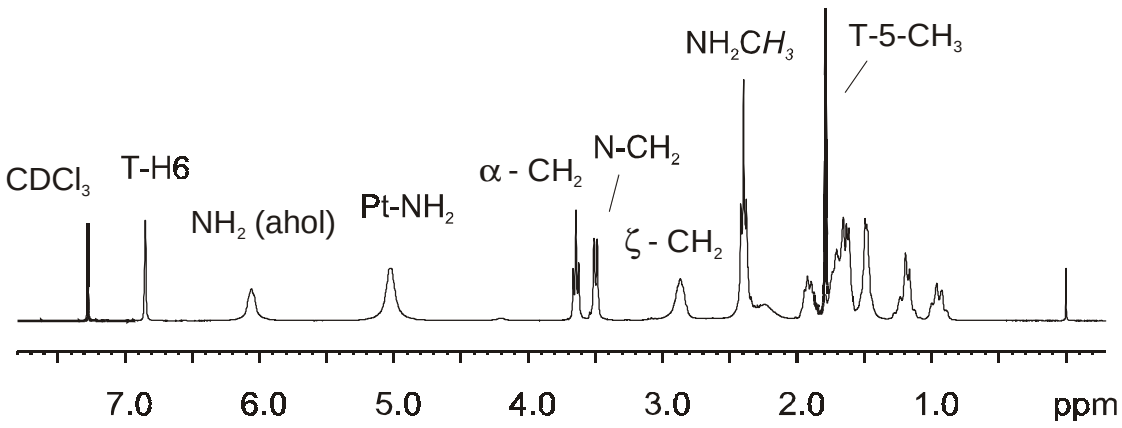


Figure 2: $^{1}H$ NMR spectrum of *trans*-$[Pt(NH_2CH_3)_2(CHMT)\{NH_2(CH_2)_6OH\}]^+Cl^-$ (**8**) in $CDCl_3$.

### 3.3 Synthesis and characterization of *trans*-$[Pt(NH_2CH_3)_2(CHMT)(gly\text{-}N)]^+BF_4^-$ (9)

Ternary complexes of *cis* and *trans*-Pt(II) with model nucleobases and glycine monodentately coordinated through the amino group have been described earlier.[141-143] Monodentate coordination of glycine to a Pt(II) complex with only one available coordination site occurs exclusively via nitrogen.[144] At a pH where the amino group ($pK_a$ = 9.8) of glycine is protonated initial coordination to an oxygen atom of the deprotonated carboxyl group ($pK_a$ = 2.35) takes place, but even in acidic solution a slow irreversible isomerization from O-bound to N-bound glycine complex takes place.[144] In organic solvents like DMF and DMSO the protonated form of the carboxylate group is favoured so that initial coordination of Pt(II) to nitrogen takes place.[145]

*Trans*-$[Pt(NH_2CH_3)_2(CHMT)(gly\text{-}N)]^+BF_4^-$ (**9**) was synthesized by reaction of *trans*-$[Pt(NH_2CH_3)_2(CHMT)(DMF)]^+BF_4^-$ (**7a**) with one equivalent of glycine in DMF with a

minimal amount of water (just allowing glycine to dissolve) at RT. The reaction proceeded smoothly and yielded exclusively the N-bound glycine complex **9** in a yield of 66 %.

Platinum binding to the amino group of glycine was confirmed by $^{195}$Pt NMR spectroscopy, which showed one single peak at -2605 ppm, consistent with a $PtN_4$ coordination sphere.[135,136] Figure 3 shows the $^{1}$H NMR spectrum of **9** in DMF-$d_7$. Surprisingly, the T-H6 and T-5-$CH_3$ resonances are doubled. In addition, the resonances for the amino protons and the methyl groups of the methylamine ligands are split. An explanation for this observation is not straightforward. Doubling of the signals seems to depend on the presence of the methylamine ligands. The $^{1}$H NMR spectrum of the water-soluble analogue **10**, which contains ammine ligands (Figure 4), does not display this phenomenon.

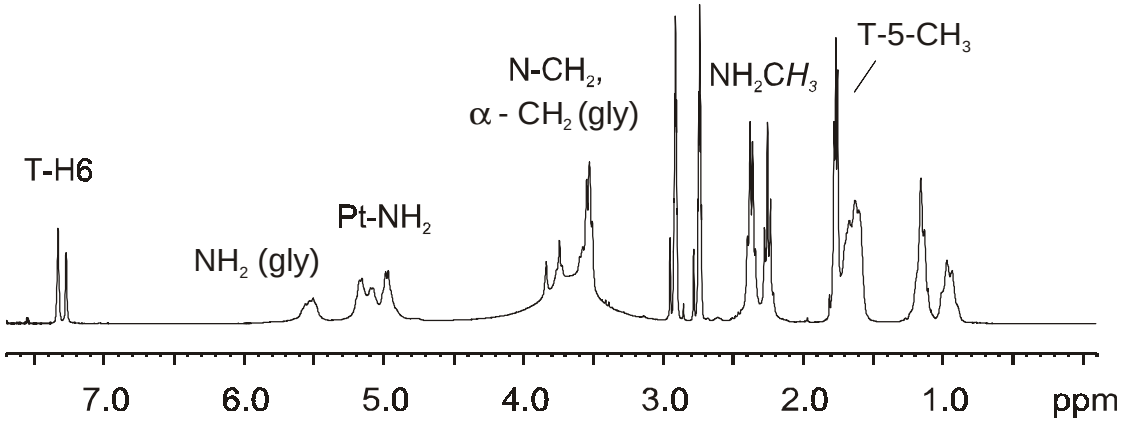


Figure 3: $^{1}$H NMR spectrum of *trans*-$[Pt(NH_2CH_3)_2(CHMT)(gly\text{-}N)]^+BF_4^-$ (**9**) in DMF-$d_7$.

The ESI MS spectrum of **9** shows a peak at m/z 553 for the onefold positively charged ion of **9**. In the IR spectrum of **9** two characteristically split intense bands at 1660 and 1560 $cm^{-1}$ are observed, similar to the IR spectrum of complex **7**.[94,96,137]

Compound **9** is highly soluble in DMF and should be suitable for an application in solid-phase DNA synthesis from this point of view. The solubility of **9** in water is rather poor.

Coordination of Pt(II) to the amino group of glycine changes the acid-base equilibrium of glycine. It is well established, that upon coordination of the electron-withdrawing Pt(II) to the amino group the acidity of neutral glycine increases dramatically.[141,142] In order to gain information on the change of the acid-base equilibrium of glycine in complexes structurally similar to **9**, the water-soluble analogue *trans*-$[Pt(NH_3)_2(1\text{-}MeT)(gly\text{-}N)]^+NO_3^-$ (**10**) was synthesized in the reaction of *trans*-$[Pt(NH_3)_2(1\text{-}MeT)(H_2O)]^+$ with one equivalent of glycine in water. Compound **10** was characterized by NMR spectroscopy. The $^{1}$H NMR spectrum of

**10** (Figure 4) shows in contrast to the $^{1}$H NMR spectrum of **9** only single resonances for the T-H6 and the T-5-$CH_3$ protons. The α-$CH_2$ resonance of the glycine ligand appears as a triplet due to $^{3}$J coupling with the amino protons of the glycine ligand which had not undergone H-D exchange as yet. The $^{195}$Pt NMR spectrum of **10** in $D_2O$ shows one signal at -2557 ppm, consistent with a $PtN_4$ coordination sphere.[135,136]

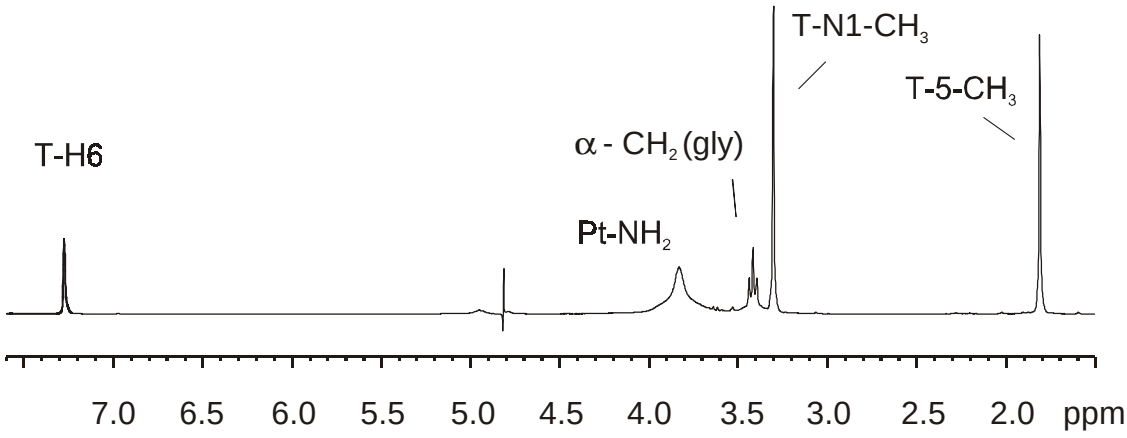


Figure 4: $^{1}$H NMR spectrum of *trans*-[$Pt(NH_3)_2$(1-MeT)(gly-*N*)]$^{+}NO_3^{-}$ (**10**) in $D_2O$ ($pH^{*}$ 5.8).

Figure 5 shows the results of the $pH^{*}$-dependent $^{1}$H NMR measurements of **10** in $D_2O$. The resonance originating from the α-$CH_2$ protons of the glycine ligand shows a marked pH dependence due to (de)protonation of the neighbouring carboxyl group. A $pK_a$ value of 3.2 has been calculated which is in agreement with results obtained for *cis*- and *trans*-[$Pta_2$(1-MeC)(gly-*N*)]$^{+}$ (a = $NH_3$, $NH_2CH_3$).[141,142] Thus, the results show that the well-established acidification of neutral glycine upon coordination of the electron-withdrawing Pt(II) to the amino group is also seen for *trans*-[$Pt(NH_3)_2$(1-MeT)(gly-*N*)]$^{+}NO_3^{-}$ (**10**). The calculated $pK_a$ value of 3.2 for deprotonation of the carboxyl group compares to that observed for *cis*- and *trans*-[$Pta_2$(1-MeC)(gly-*N*)]$^{+}$ ($pK_a$ = 2.8 and 2.5, respectively).[141,142]

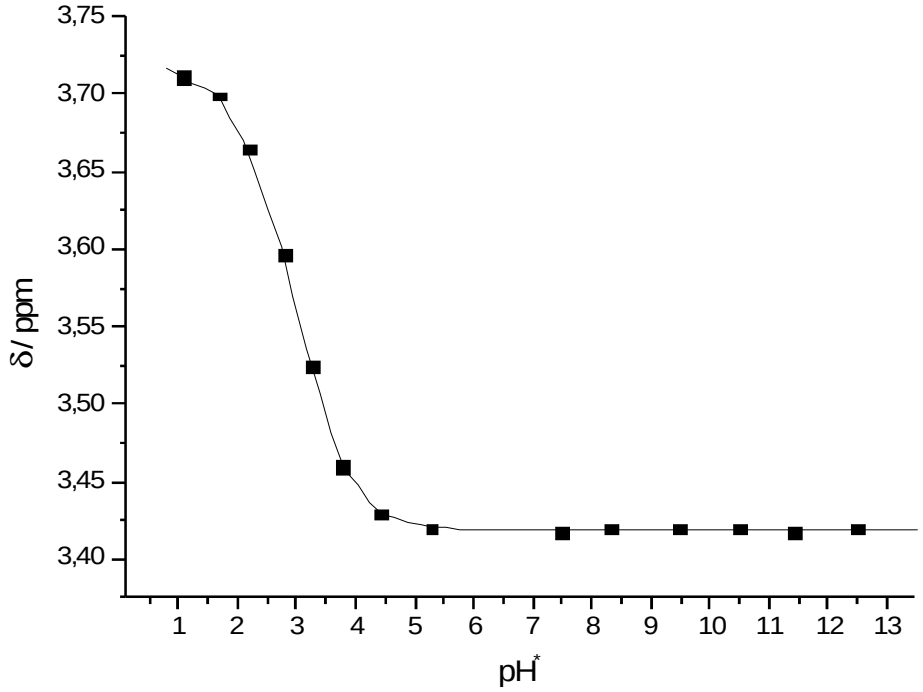


Figure 5: $pH^*$-dependence of $^1H$ NMR chemical shifts of the α-$CH_2$ (gly) protons within *trans*-$[Pt(NH_3)_2(1\text{-MeT})(\text{gly-}N)]^+NO_3^-$ (**10**).

## 4 Conjugation of *trans*-[Pt($NH_2CH_3$)$_2$(CHMT){$NH_2(CH_2)_6OH$}]$^+Cl^-$ (**8**) to the 5´-terminus of homopyrimidine deoxyoligonucleotides via a phosphate bond by solid-phase DNA synthesis

### 4.1 Solution-phase test coupling experiments

#### 4.1.1 Conversion of *trans*-[Pt($NH_2CH_3$)$_2$(CHMT){$NH_2(CH_2)_6OH$}]$^+Cl^-$ (**8**) into its phosphoramidite 8a

Incorporation of *trans*-[Pt($NH_2CH_3$)$_2$(CHMT){$NH_2(CH_2)_6OH$}]$^+Cl^-$ (**8**) into an oligonucleotide by solid-phase DNA synthesis requires its conversion into the corresponding phosphoramidite (Scheme 1). In order to investigate the feasibility of the conversion of **8** into the corresponding phosphoramidite **8a** (Scheme 3), **8** was dissolved in dioxane and reacted with chloro(N,N-diisopropyl)-β-cyanoethoxyphosphine (**11**) in the presence of triethylamine. As evidenced by $^{31}$P NMR, almost complete conversion of **8** into **8a** was achieved. In the $^{31}$P NMR spectrum two signals at 180 ppm, 148 ppm occurred, showing the presence of excess chloro(N,N-diisopropyl)-β-cyanoethoxyphosphine (**11**) and **8a**, respectively.

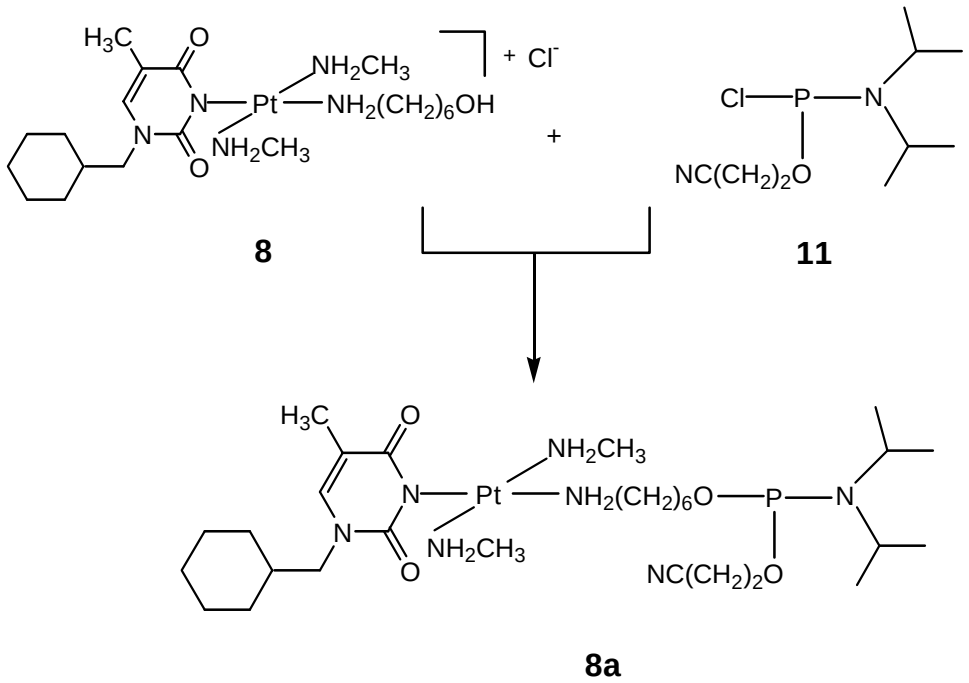


Scheme 3: Conversion of building block **8** into the corresponding phosphoramidite **8a**.

The next step, the isolation of **8a** proved to be rather troublesome. All attempts to isolate **8a** resulted in its complete degradation, as evidenced by $^{31}$P NMR spectroscopy. The instability of phosphoramidites and their sensitivity to moisture is well known.[146,147] Therefore, the required large scale synthesis of **8a** seemed not feasible. This was an incentive to test the feasibility of the reverse coupling strategy. In contrast to the normal coupling strategy (Scheme 1) the reverse coupling strategy involves initial conversion of the 5´-terminus of an immobilized oligonucleotide into a phosphoramidite (Scheme 6, conversion of **16** into **16a**) followed by a condensation reaction with the free hydroxyl group of a second reaction component.[148] Thus, application of the reverse coupling strategy does not require the synthesis of **8a** but only of building block **8**.

### 4.1.2 Condensation of *trans*-[Pt($NH_2CH_3$)$_2$(CHMT){$NH_2(CH_2)_6OH$}]$^+Cl^-$ (8) with 5´-*O*-DMTr-deoxythymidine-3´-phosphoramidite (12)

In order to establish the viability of this reverse coupling strategy a model solution-phase experiment was carried out. To this end, building block **8** was reacted with 5´*O*-DMTr-dT-3´-phosphoramidite (**12**) in the presence of *o*-NPT (Scheme 4). After oxidation and removal of the ß-cyanoethyl group this experiment should yield the coupled product **13**. Indeed, LC MS analysis of the crude product obtained in this reaction reveals the presence of **13**. Compound **13** was purified by reversed-phase HPLC and analyzed by $^1$H, $^{31}$P and $^{195}$Pt NMR as well as ESI MS.

The $^{195}$Pt NMR spectrum of **13** shows one signal at -2621 ppm, consistent with a $PtN_4$ coordination sphere.[135,136] The signal of 0.18 ppm in the $^{31}$P NMR is consistent with a phosphodiester.[149,150]

All the non-exchangeable protons in **13** could be assigned by a $^1$H, $^1$H COSY experiment (Figure 6). As expected, the H6 signal of the platinated thymine residue in **13** appears at higher field than the H6 resonance of the unplatinated thymine residue . The respective T-H6 protons of both thymine residues can be assigned through $^4$J coupling with the respective T-$CH_3$ protons. Also the other signals can be fully assigned (Figure 6).

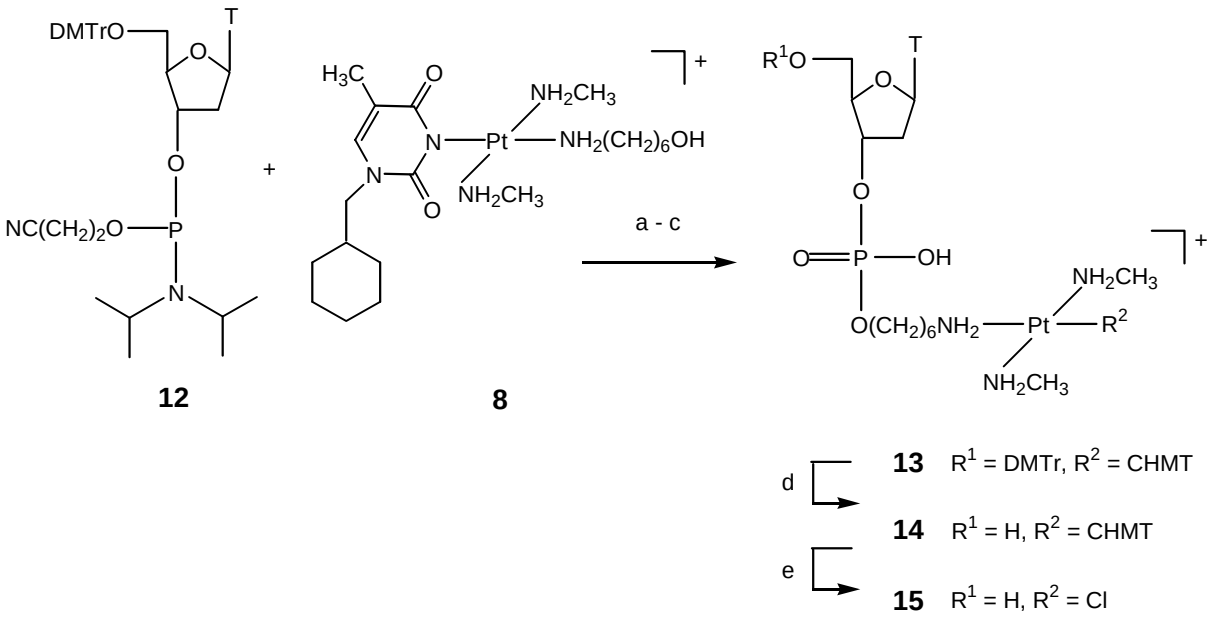


Scheme 4: Condensation reaction of building block **8** with 5´*O*-DMTr-dT-3´-phosphoramidite (**12**);
a) *o*-NPT, b) $I_2$ / collidine, c) 25 % aq $NH_3$, d) 80 % aq AcOH, e) DCl (pD 2.2).

Subsequently, compound **13** was converted into the water-soluble compound **14** by treatment of **13** with 80 % acetic acid (Scheme 4).

In order to investigate the conditions required to remove the CHMT ligand, compound **14** was subjected to DCl (pD 2.2) for several days at 40 °C and the removal of the CHMT protecting group was observed by $^1$H NMR and LC MS. Figure 7 shows the $^1$H NMR spectra obtained after various time intervals. It can be seen that in the course of time one new T-H6 resonance appears which belongs to 1-*N*-cyclohexylmethylthymine (**5**) whereas the T-H6 resonance of the platinated thymine residue of compound **14** gradually disappears. Complete removal of the CHMT ligand (conversion of **14** into **15**) is achieved after 108 h. Exchange of the CHMT ligand by a chloro ligand was additionally monitored by $^{195}$Pt NMR spectroscopy which shows one signal at -2312 ppm, consistent with a $PtN_3Cl$ coordination sphere in **15**[135,136] and by LC MS.

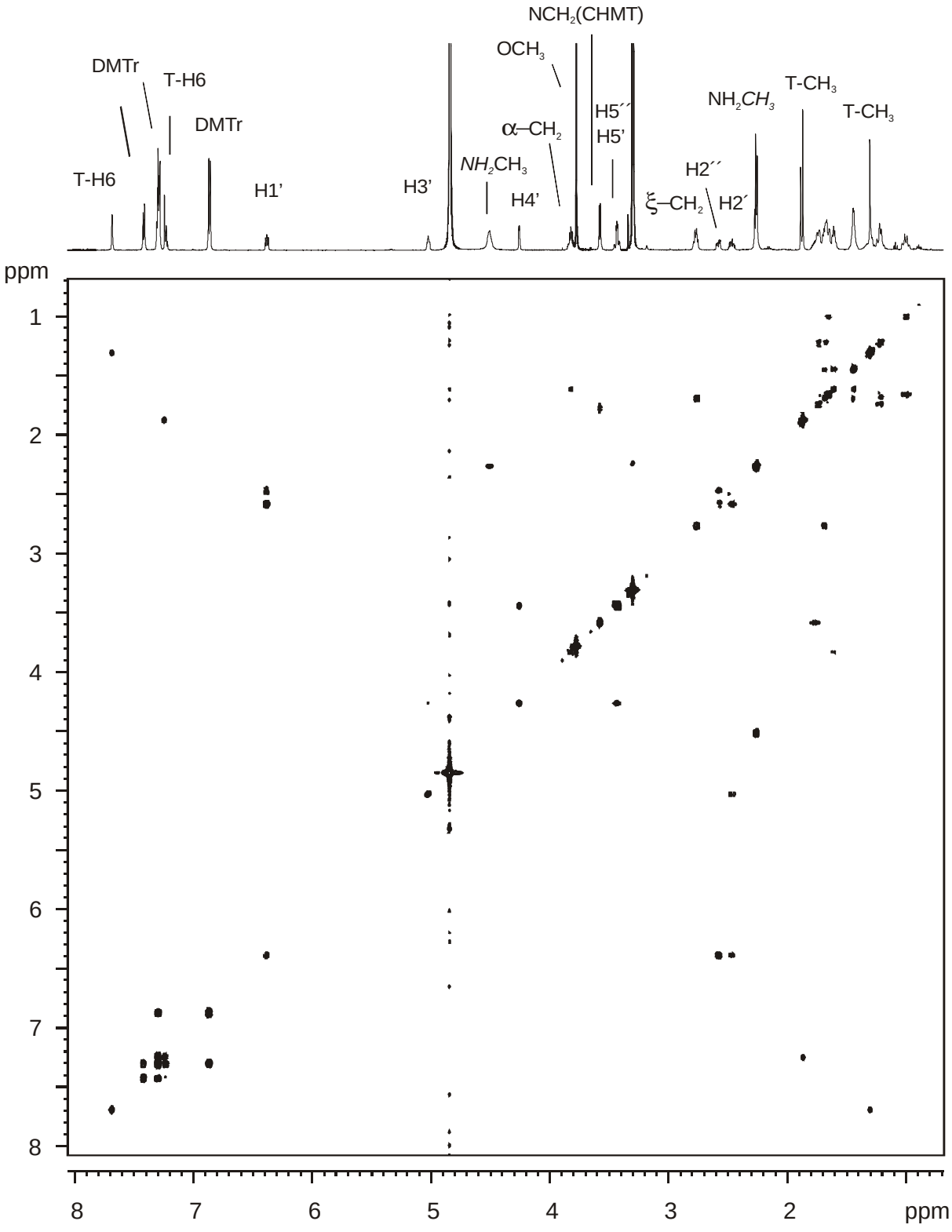


Figure 6: $^{1}H,^{1}H$ COSY spectrum of compound **13** in $CD_3OD$.

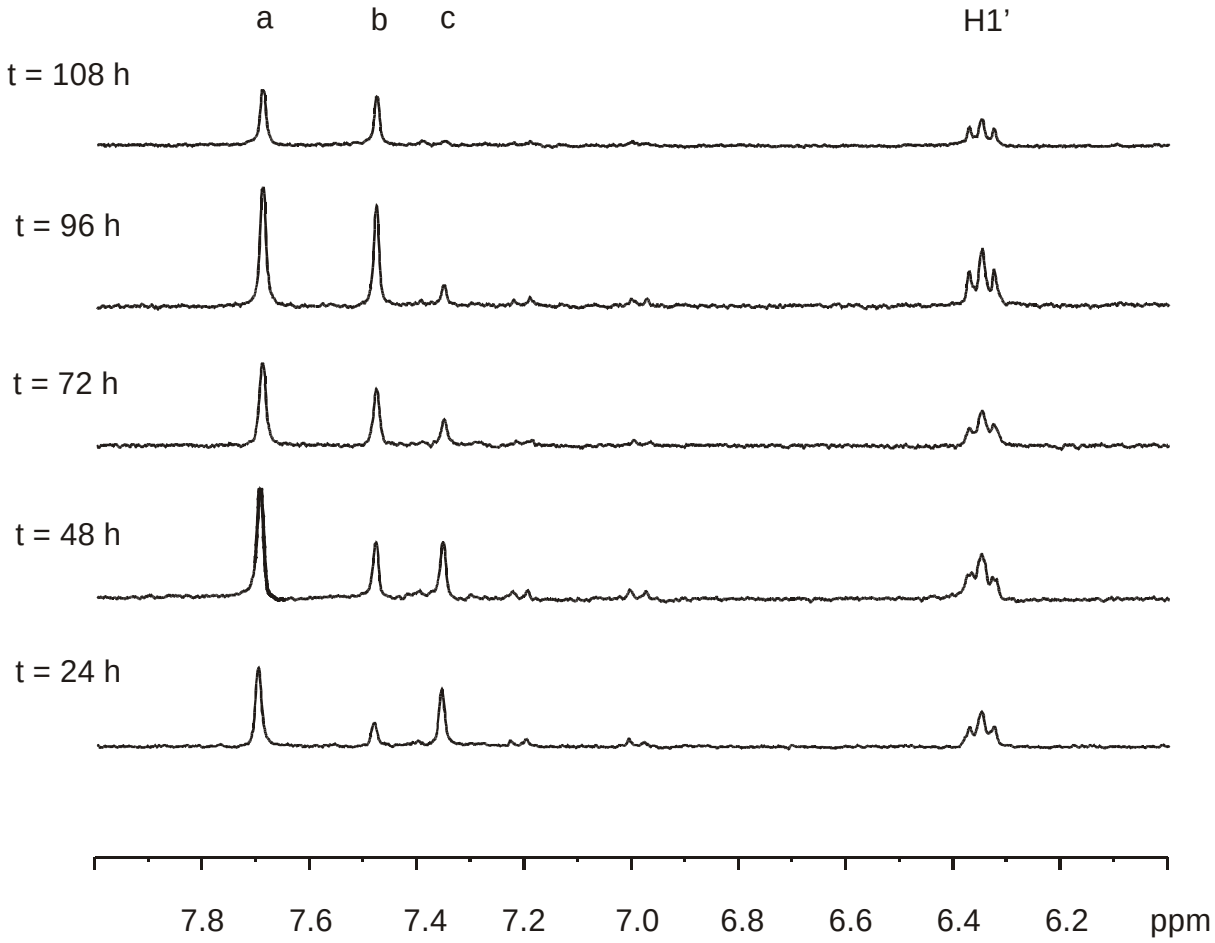


Figure 7: Conversion of **14** into **15** (followed in time); b: T-H6 resonance of 1-*N*-cyclohexylmethylthymine, c: T-H6 resonance of the platinated thymine residue of **14**, a: T-H6 resonance of the unplatinated thymine residue of **14** and **15**.

### 4.1.3 Conclusions

The results described in section 4.1 demonstrate that building block **8** can be condensed with 5´-*O*-DMTr-deoxythymidine-3´-phosphoramidite (**12**) according to the reverse coupling strategy. Furthermore, the CHMT ligand in **14** has successfully been removed and substituted by a chloro ligand (conversion of **14** into **15**). Thus, monofunctional *trans*-Pt(II) modification of an oligonucleotide according to approach I (Scheme 1) is in principle feasible. Unfortunately, for the removal of the CHMT ligand quite acidic conditions are required. As these conditions can cause depurination reactions[151] this approach would be mainly suited for the synthesis of monofunctionally *trans*-Pt(II) modified homopyrimidine oligonucleotides.

## 4.2 Solid-phase coupling experiments

### 4.2.1 Optimization of conditions for the reverse coupling strategy

A reverse coupling strategy was extensively applied in order to functionalize deoxyoligonucleotides with Hoechst 33258 minor groove binders.[152-154] This reverse coupling strategy is not routinely used as it is inherently more troublesome than the normal standard protocol. E.g., in the addition step of the standard DNA synthesis protocol, the incoming protected deoxynucleotide phosphoramidite is used in a high excess (Scheme 1). Thus, partial degradation (due to residual traces of water) does not have a dramatic effect on the yield of the desired oligonucleotide. However, if the reverse protocol is applied, degradation of the immobilized phosphoramidite has a more dramatic effect on the yield of the desired product. For a successful application of this non-standard reverse coupling strategy reaction conditions had thus first to be optimized.

In order to establish optimal conditions for conversion of the 5´-terminus of an immobilized deoxyoligonucleotide into the corresponding phosphoramidite, immobilized $dT_4$ (**16**) was assembled and phosphitylated. Subsequently, only the oxidation step was carried out (Scheme 5). After deprotection and cleavage from the solid support this protocol is expected to yield the $dT_4$-5´-terminal phosphoramidate **16b**, provided the phosphitylating step (conversion of **16** into **16a**, Scheme 5) is successful. FPLC analysis of the crude product shows the presence of one major product as well as of a minimal amount of residual $dT_4$-5´OH (evidenced by coinjection of a $dT_4$-5´OH reference sample), indicating that the 5´-terminal conversion of **16** into the phosphoramidite **16a** proceeded in approximately 70-80 % yield.

The efficiency of the coupling step was evaluated in a similar way. To this end, immobilized $dT_4$ (**16**) was phosphitylated, and the resulting immobilized phosphoramidite (**16a**) reacted with $DMTrO(CH_2)_5OH$ (**17**) in the presence of *o*-NPT, oxidized and detritylated (Scheme 5). In case of an efficient coupling of **17** to **16a** this protocol would yield the conjugate **18** after deprotection and cleavage from the solid support. FPLC analysis of the crude product shows the presence of one major product as well as of minimal amounts of residual $dT_4$-5´-OH and $dT_4$-5´-amidate (**16b**). Compound **18** was obtained in approximately 60 – 70 % yield when the phosphitylation step was carried out twice for 30 minutes each using a 1.0 M chloro(N,N-diisopropyl)-β-cyanoethoxyphosphine (**11**) / 1.2 M D*i*PEA solution

in acetonitrile and if the coupling step was carried out for 120 min using a 0.1 M solution of $DMTrO(CH_2)_5OH$ and a 0.2 M solution of *o*-NPT in acetonitrile.

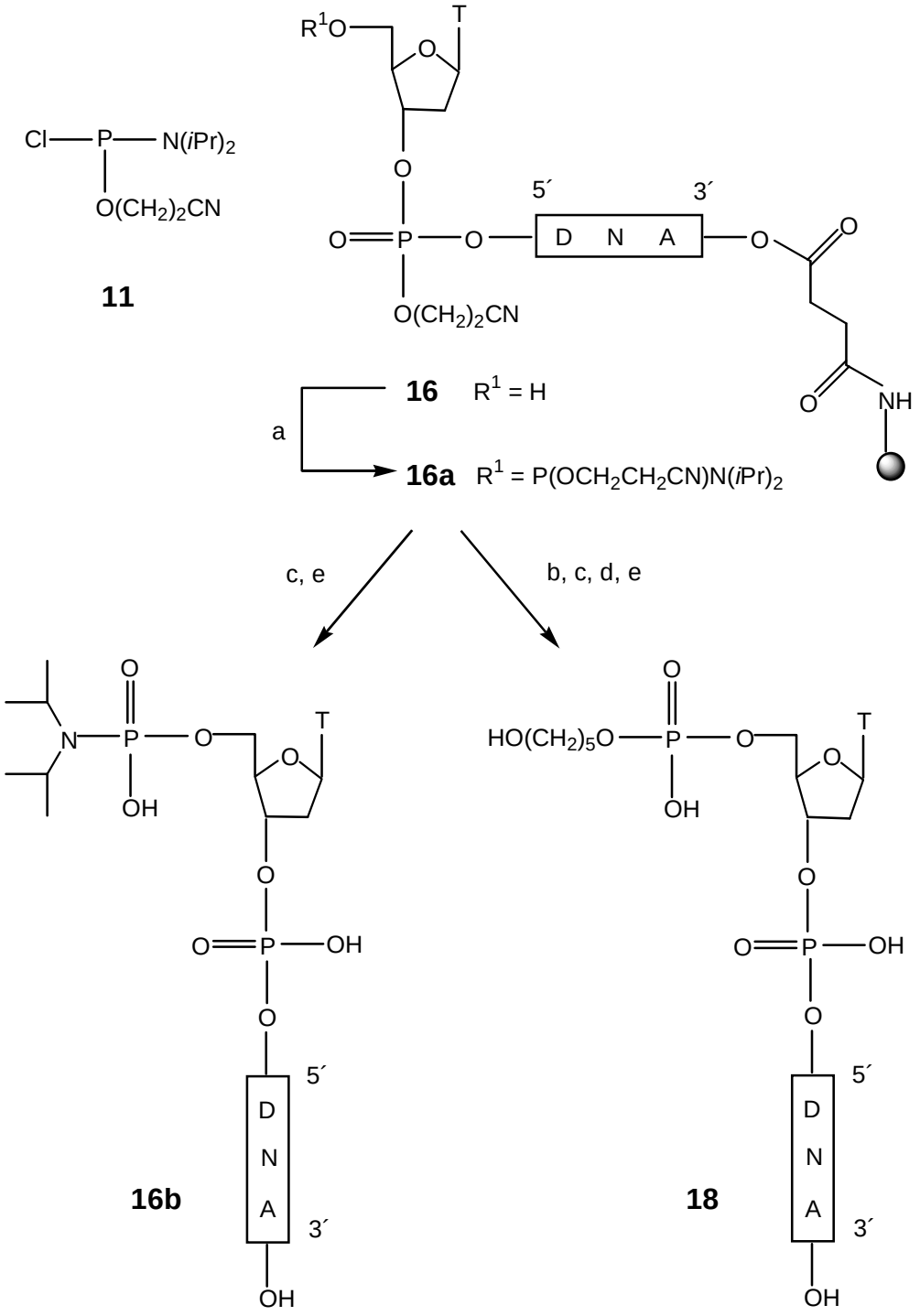


Scheme 5: Conversion of **16a** into the corresponding phosphoramidate **16b** and condensation of **16a** with **17**;
a) **11**, D*i*PEA, b) **17**, *o*-NPT, c) $I_2$ / collidine, d) TCA, e) 25 % aq $NH_3$; DNA = $dT_3$.

### 4.2.2 Conjugation of *trans*-$[Pt(NH_2CH_3)_2(CHMT)\{NH_2(CH_2)_6OH\}]^+Cl^-$ (**8**) to the 5´-terminus of immobilized $dT_4$ (**16**) and $d(T_3CTC_2TC)$ (**19**)

At this stage, $dT_4$ (**16**) and $d(T_3CTC_2TC)$ (**19**), immobilized by a 3´-O-succinyl bond to controlled pore glass (CPG) were phosphitylated with **11** (Scheme 6) according to the procedure described in section 4.2.1. The newly formed immobilized 5´-phosphoramidites **16a** and **19a** were subsequently reacted with **8** under the influence of *o*-NPT, to afford, after oxidation ($I_2$ / collidine) immobilized **20** and **21,** respectively (Scheme 6). Subjecting **20** and **21** to concentrated aqueous ammonia led to decyanoethylation and concomitant release from the solid support yielding compounds **22** and **23**. The crude reaction mixtures were analyzed by LC MS.

Table 1 shows the results obtained by LC MS for conjugation of **8** to **16a**. Three major products are observed which are assigned to the coupled product **22** in an estimated yield of 30 %, $dT_4$-5´OH (33 %) and $dT_4$-5´-phosphoramidate (**16b**) (33 %).

Table 2 shows the results obtained by LC MS for the conjugation of **8** to **19a**. According to the peak intensities of the HPLC chromatogram, the yield of **23** is estimated to be approximately 20%. Furthermore, significant amounts of $d(T_3CTC_2TC)$-5´OH as well as $d(T_3CTC_2TC)$-5´$PO_3H$ have been found.

Table 1: LC MS analysis of crude product obtained by conjugation of **8** to **16a**

| $t_r$ / min | mass | amount / % | assignment |
|---|---|---|---|
| 7.10 | 1156($M^+$), 579 ($M^{2+}$) | 33.63 | $dT_4$-5´OH |
| 10.13 | 1318($M^+$), 660($M^{2+}$) | 32.82 | **16b** |
| 12.50 | 1812 ($M^+$), 906 ($M^{2+}$) | 33.54 | **22** |

Table 2: LC MS analysis of crude product obtained by conjugation of **8** to **19a**

| $t_r$ / min | mass | amount / % | assignment |
|---|---|---|---|
| 5.76 | 1349($M^{2+}$) | 15.11 | $d(T_3CTC_2TC)$-5´$PO_3H$ |
| 7.77 | 1309($M^{2+}$) | 18.91 | $d(T_3CTC_2TC)$-5´OH |
| 8.83 | 1390($M^{2+}$), 928($M^{3+}$) | 20.61 | no |
| 11.03 | 1638($M^{2+}$), 1092($M^{3+}$) | 19.74 | **23** |
| 11.76 | multiple masses | 25.62 | no |

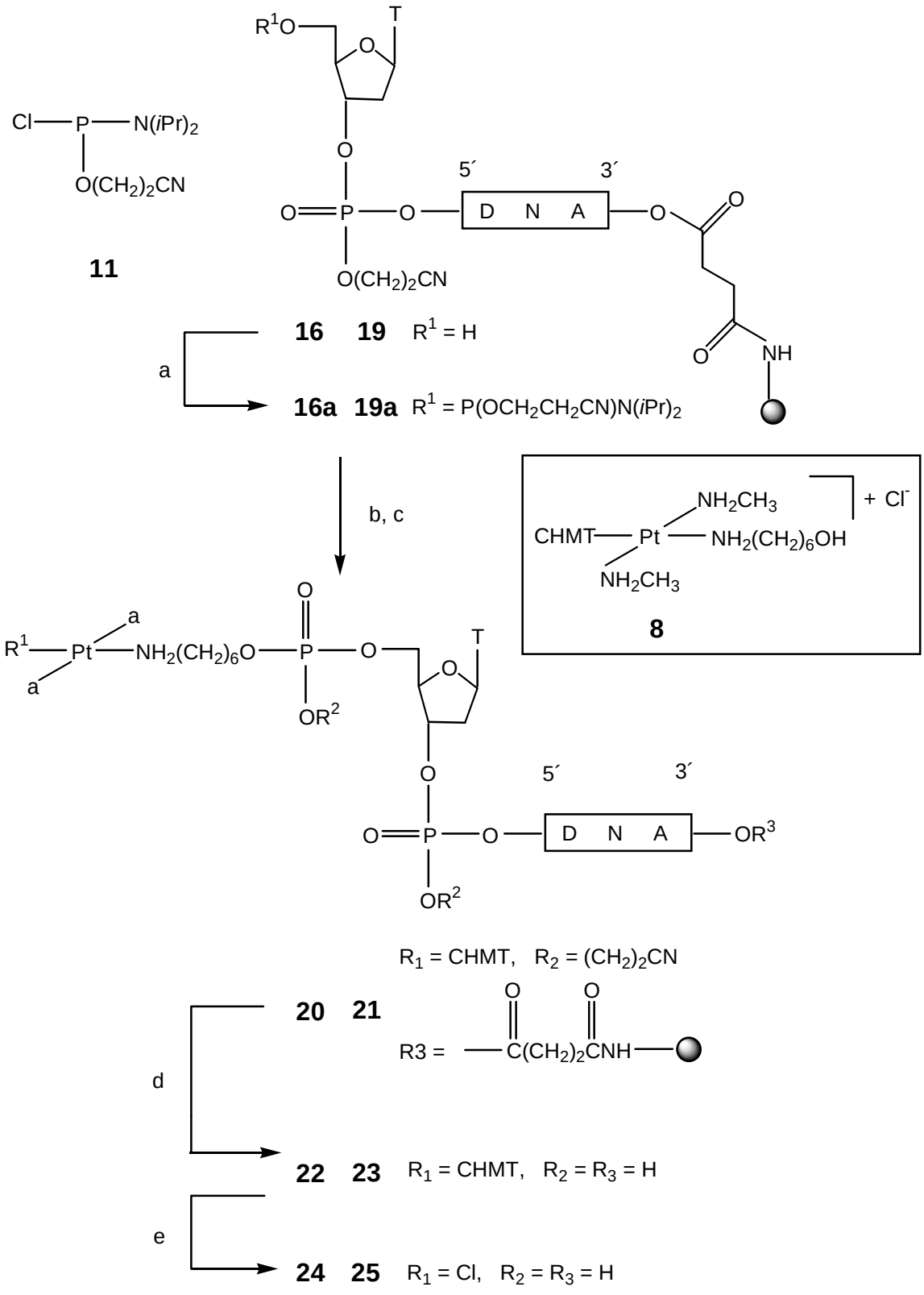


Scheme 6: Conjugation of building block **8** to the 5´-terminus of the immobilized oligonucleotides **16a** and **19a**;
a) **11**, D*i*PEA b) **8**, *o*-NPT, c) $I_2$ / collidine, d) 25 % aq $NH_3$, e) aq HCl, pH 2.3;
**16**, **20**, **22**, **24**: DNA = $dT_3$; **19**, **21**, **23**, **25**: DNA = $d(T_2CTC_2TC)$.

### 4.2.3 Removal of the CHMT protecting group in 22 and 23

The removal of the CHMT ligand and its exchange by a chloro ligand (conversion of **22** into **24** and **23** into **25**, Scheme 6) was effected by subjecting **22** and **23** to hydrochloric acid (pH 2.3) at 40 °C for 48 h to yield the monofunctionally *trans*-Pt(II) modified tetranucleotide **24** and nonanucleotide **25** as proven by LC MS.

### 4.2.4 Discussion

The results show that coupling of building block **8** to the 5´-terminus of an immobilized oligonucleotide is in principle feasible. The coupling yields of the platinated oligonucleotides **22** and **23** are in the range of 20 – 30 % and thus moderate. In the crude reaction mixtures obtained in both coupling experiments LC MS analysis reveals the presence of $dT_4$-5´OH and d($T_3CTC_2TC$)-5´OH, respectively. This indicates that the phosphitylation step (conversion of the resin-bound fully protected deoxyoligonucleotides **16** and **19** into the corresponding 5´phosphoramidites **16a** and **19a**) does not proceed in optimal yields. Furthermore, in both experiments the presence of the respective 5´-phosphoramidate and 5´-phosphate shows that conjugation of **8** to **16a** and **19a**, respectively, does not take place quantitatively.

As anticipated from the results obtained in the solution-phase test coupling reaction (section 4.1.2) the newly synthesized platinated building block **8** has been proven to be compatible with the DNA synthesis protocol. In agreement with this, in neither of the two experiments Pt(IV) adducts or Pt(II) adducts where ligand exchange has taken place during the ammonia treatment, have been detected.

The moderate yields of platinated oligonucleotides **22** and **23** of about 20-30% have to be at least partly ascribed to the inherent disadvantages of the reverse coupling strategy. Still the yields are comparable with the yields obtained in different attempts to implement platinated building blocks into oligonucleotides by means of solid-phase DNA synthesis.[99,100]

## 5 Conjugation of *trans*-[Pt($NH_2CH_3$)$_2$(CHMT)(gly-*N*)]$^+BF_4^-$ (9) to the 5´-terminus of homopyrimidine deoxyoligonucleotides via an amide bond by solid-phase synthesis

### 5.1 Conjugation of *trans*-[Pt($NH_2CH_3$)$_2$(CHMT)(gly-*N*)]$^+BF_4^-$ (9) to the 5´-terminus of immobilized 5´-functionalized d($T_2CTC_2TC$) (28)

In order to sidestep the drawbacks associated with the reverse coupling strategy applied in section 4.2 of this chapter, attempts for the conjugation of *trans*-[Pt($NH_2CH_3$)$_2$(CHMT)(gly-*N*)]$^+$ $BF_4^-$ (**9**) to the 5´-terminus of an immobilized oligonucleotide according to approach II (Scheme 1) were made. The latter strategy would be equivalent to the normal coupling strategy applied in solid-phase DNA synthesis (cf. section 2 of this chapter) in that the platinated building block **9** is activated (converted into an active ester by HATU in the presence of D*i*PEA) prior to coupling to the 5´-functionalized immobilized oligonucleotide **28**.

To this end, d($T_2CTC_2TC$) (**27**), immobilized by a 3´-O-succinyl bond to controlled pore glass (CPG) was functionalized at the 5´-terminus with the $C_6$ amino linker **26** (Scheme 7). The newly formed immobilized 5´-functionalized fully protected oligonucleotide **28** was reacted with excess **9** under the influence of HATU in the presence of D*i*PEA. Deprotection and cleavage from the solid support ($NH_3$ / $H_2O$, 12 h, RT) afforded the conjugate **29**. The crude product obtained in this coupling reaction was analyzed by LC MS (Table 3). The results show that condensation of **28** with **9** yields the coupled product **29** in almost 80 % yield. Only minor amounts of unreacted deprotected **28** have been detected by LC MS (Table 3).

Table 3: LC MS analysis of crude product obtained by conjugation of **9** to **28**

| $t_r$ | mass | amount / % | assignment |
|---|---|---|---|
| 14.40 | 1296 ($M^{2+}$) | 17.09 | **28** + Bz |
| 17.80 | 1513($M^{2+}$),1009 ($M^{3+}$) | 79.35 | **29** |
| 18.18 | 1246($M^{2+}$),831($M^{3+}$) | 3.55 | **28** |

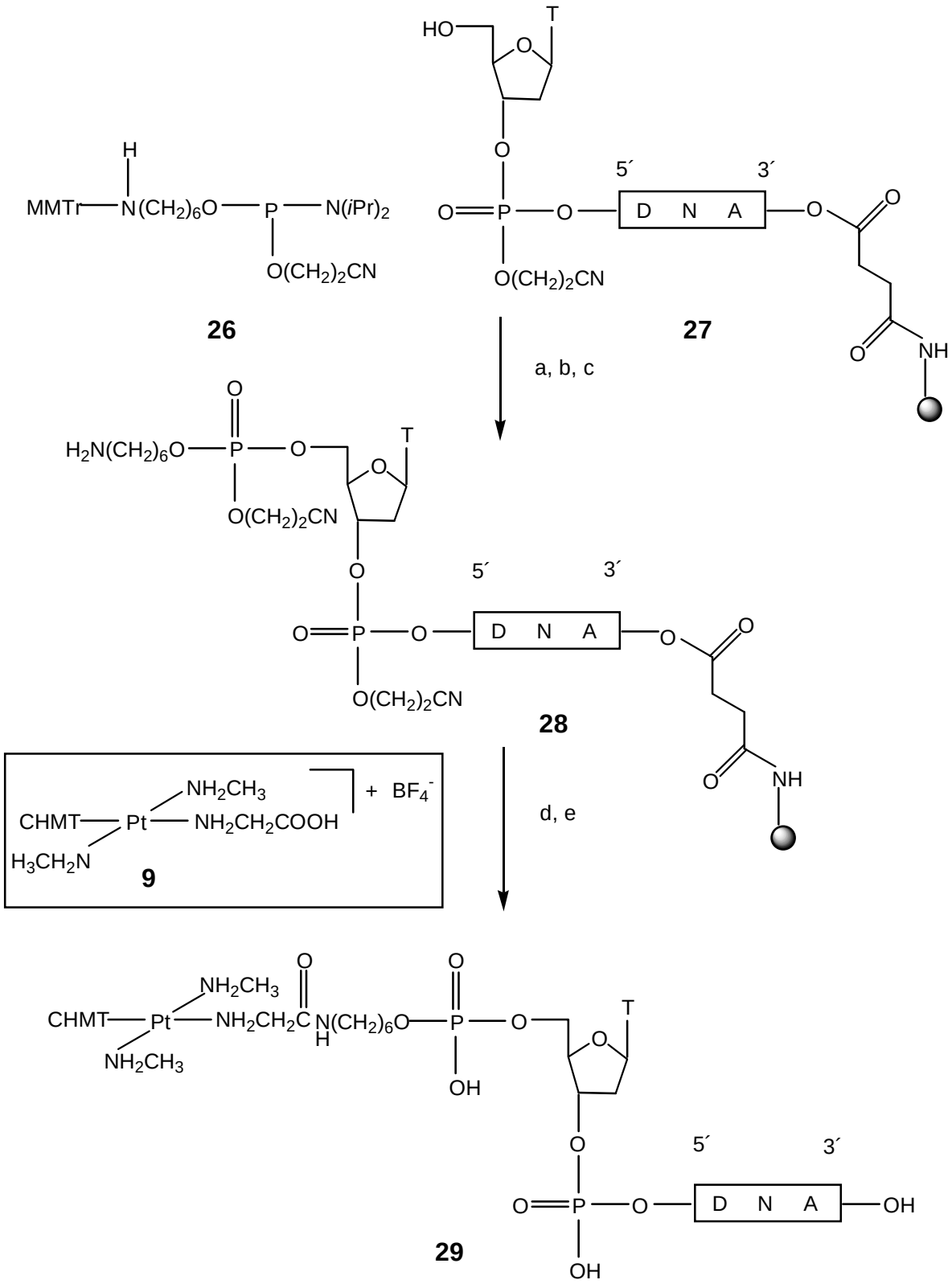


Scheme 7: Conjugation of building block **9** to the 5´-terminus of the immobilized oligonucleotide **28** yielding **29**;
a) **26**, *o*-NPT, b) $I_2$ / collidine, c) TCA, d) **9**, HATU, D*i*PEA / DMF,
e) 25 % aq $NH_3$; DNA = d(TCTC$_2$TC).

When forced ammonolysis conditions (concentrated aqueous ammonia, 50 °C, 12 h) as required for the removal of *i*Bu protecting groups of guanines,[130] were applied to **29**, complete decomposition of **29** into 5´-$NH_2CH_2CONH(CH_2)_6$O-d($T_2CTC_2TC$)-3´OH and *trans*-$[Pt(NH_2CH_3)_2(CHMT)NH_3]^+$ occurred as shown by LC MS.

## 5.2 Discussion

The results show that conjugation of building block **9** to the 5´-$NH_2$ terminus of the immobilized deoxyoligonucleotide **28** proceeds almost quantitatively and thus in a much better yield than coupling of building block **8** to the 5´-terminus of an immobilized deoxyoligonucleotide via a phosphate bond. Thus, with this approach drawbacks of the inherently more difficult reverse coupling concept as applied in section 4.2.2 of this chapter can be circumvented. Still, due to the involvement of the CHMT protecting group, this method is restricted to the synthesis of monofunctionally *trans*-Pt(II) modified homopyrimidine deoxyoligonuclotides.

While at RT the Pt(II) center in **29** withstands treatment with concentrated aqueous ammonia, forced ammonolysis conditions (50 °C, 12 h) lead to complete degradation of **29**. Obviously, at higher temperatures the $NH_3$ nucleophile attacks the Pt(II) center, resulting in the formation of 5´-$NH_2CH_2CONH(CH_2)_6$O-d($T_2CTC_2TC$)-3´OH and *trans*-$[Pt(NH_2CH_3)_2(CHMT)NH_3]^+$.

# 6 Conclusions

This chapter describes the development of two new methodologies for the solid-phase synthesis of monofunctionally *trans*-Pt(II) modified homopyrimidine deoxyoligonucleotides. The preplatinated building blocks **8** and **9** have been synthesized and conjugated via a ligand to the 5´-terminus of immobilized homopyrimidine deoxyoligonucleotides. Building block **8** has been coupled to an oligonucleotide by a phosphate bond using a reverse coupling strategy, whereas building block **9** has been conjugated to an oligonucleotide by an amide bond using a "normal" coupling strategy. While conjugation of building block **8** to the 5´-terminus of the immobilized oligonucleotides **16a** and **19a** proceeds in moderate yields, conjugation of building block **9** to the 5´-terminus of the immobilized oligonucleotide **28** occurs almost quantitatively. This observation has at least partly to be ascribed to the inherent disadvantages of the reverse coupling strategy.

After conjugation of building blocks **8** and **9** to oligonucleotides, the CHMT ligand could be substituted by a chloro ligand resulting in the formation of monofunctionally *trans*-Pt(II) modified homopyrimidine deoxyoligonucleotides with crosslinking ability.

In principle, the methodologies developed allow sequence-independent and site-specific monofunctional *trans*-Pt(II) modification of oligonucleotides. However, since for the removal of the CHMT protecting group acid treatment at a rather low pH is required, at which depurination reactions will certainly occur,[151] these methodologies are restricted to the synthesis of monofunctionally *trans*-Pt(II) modified homopyrimidine deoxyoligonucleotides with potential application mainly in antigene strategy.

A potential strategy for extending these methodologies to the synthesis of monofunctionally *trans*-Pt(II) modified mixed pyrimidine / purine oligonucleotides is feasible either by the use of a protecting group other than CHMT, which is removable at a slightly higher pH to avoid depurination,[151] or by use of a different DNA backbone which is not susceptible to acid degradation. The latter potential solution is adressed in chapter III of this thesis.

# Chapter III Solid-phase synthesis of monofunctionally *trans*-Pt(II) modified PNA oligomers and crosslinking reaction with a complementary oligonucleotide

## 1 Introduction

The solid-phase synthesis approaches towards monofunctional *trans*-Pt(II) modification of deoxyoligonucleotides described in chapter II are, due to the involvement of the thyminate protecting group, restricted to the synthesis of monofunctionally *trans*-Pt(II) modified homopyrimidine oligonucleotides for potential use mainly in antigene strategy.[129] The development of a solid-phase method allowing the synthesis of monofunctionally *trans*-Pt(II) modified oligonucleotide heterosequences, containing both pyrimidines and purines, for potential use also in antisense strategy is a further requirement.

An extension of the methods described in Chapter II to the synthesis of monofunctionally *trans*-Pt(II) modified oligonucleotide heterosequences can be achieved either by the design of a different protecting group, which is, in contrast to CHMT, removable at a slightly higher pH, where no depurination reactions within DNA occur, or by the use of an oligonucleotide analogue, which is not susceptible to acid degradation. Indeed, considering the fact that to date acid-stable backbone-modified oligonucleotide analogues exist,[48,50] the latter alternative seems quite rewarding.

One acid-stable oligonucleotide analogue is the so-called peptide nucleic acid (PNA), in which the sugar-phosphate backbone is replaced by a peptide backbone.[30] PNA strands that contain all four natural nucleobases form duplexes with RNA and single-stranded DNA targets with high affinity and sequence-specificity. Base pairing takes place according to the Watson-Crick rules with an antiparallel orientation of the strands preferred.[31]

Based on its high chemical and biological stability (e.g. stability against enzymatic degradation)[155] PNA is a very promising candidate for regulation of gene expression both in antigene and antisense strategy. The potential application of PNA in antisense strategy is based on steric blocking of ribosomes or essential translation factors, as PNA-RNA hybrids, in contrast to DNA-RNA hybrids, are not substrates for RNase H.[40,56] While triplex forming homopyrimidine PNAs targeted to the coding region of RNA efficiently interrupt ribosome elongation *in vitro*,[40,41] duplex forming mixed purine / pyrimidine PNAs do not cause

sufficient steric blockage when targeted to the coding region.[55-57] As a consequence, so far only homopurine tracts within a coding region of RNA can be blocked by triplex forming homopyrimidine PNAs, whereas this is not possible for heterosequences that are located in the coding region. A potential solution to this problem would be to enhance the stability of a PNA-RNA duplex by a *trans*-$(NH_3)_2$Pt(II) interstrand crosslink. An essential prerequisite for this approach would be a solid-phase synthesis method that allows the facile preparation of site-specifically monofunctionally *trans*-Pt(II) modified PNA oligomers.

## 2 Different methods of solid-phase PNA synthesis and design of *trans*-Pt(II) modified PNA building blocks

For solid-phase assembly of PNA basically four different methodologies exist (Scheme 1). Method I involves Boc / N-Cbz-protected PNA monomers (Scheme 1, R = Boc, PG = Cbz).[33,156-158] The Boc group provides protection of the primary amino function in the backbone and the Cbz groups protect exocyclic amino functions in the nucleobases. Removal of the Boc group (deblocking) prior to the addition step (Scheme 1), is achieved by treatment with TFA. Removal of the Cbz protecting groups and cleavage from the solid support is achieved by treatment with HF.

Furthermore, orthogonal protecting group strategies suitable for the solid-phase synthesis of DNA / PNA chimeras, have been developed, using either Fmoc / N-acyl PNA monomers[159] [method II, Scheme 1, R = Fmoc, PG = Bz (A, C) and *i*Bu (G), deblocking with 20% piperidine / DMF] or MMTr / N-acyl protected PNA monomers[58,160,161] [method III, Scheme 1, R = MMTr, PG = Bz (A, C) and *i*Bu (G), deblocking with 3% TCA/ DCM]. Removal of the N-acyl base protecting groups and release from the solid support is in both cases achieved by ammonolysis.

Method IV involves Fmoc / N-Bhoc-protected PNA monomers for solid-phase PNA assembly[162] (Scheme 1, R = Fmoc, PG = Bhoc, deblocking with 20% piperidine / DMF). Removal of the N-Bhoc groups and release from the solid support is accomplished by treatment with TFA in the presence of a scavenger (*m*-cresol).

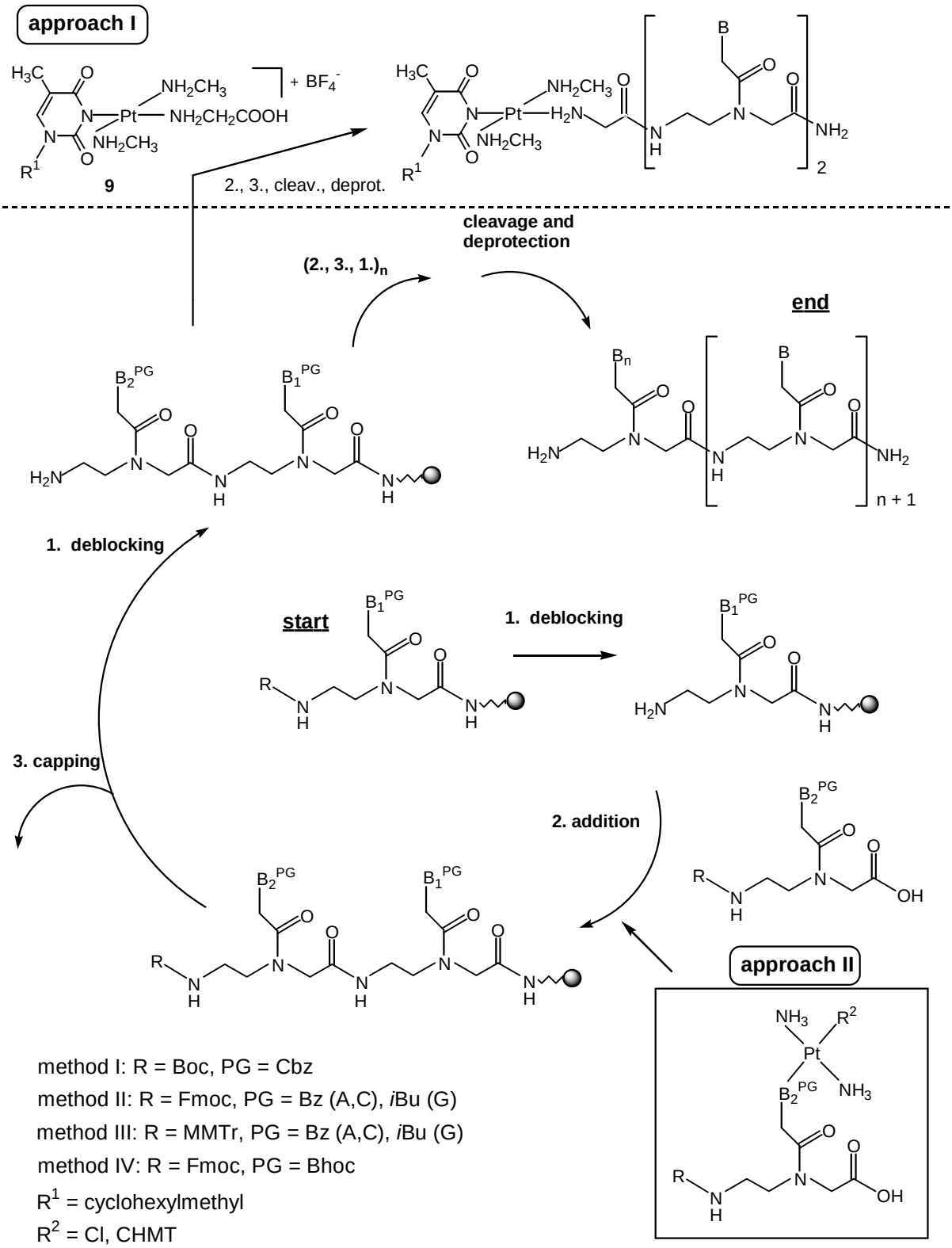


Scheme 1: Overview on the different solid-phase PNA synthesis methods and strategies for incorporation of a *trans*-$a_2$Pt(II)Cl (a = $NH_3$, $NH_2CH_3$) unit into PNA oligomers.

Scheme 1 also depicts strategies for incorporation of a *trans*-$a_2$Pt(II)Cl unit (a = $NH_3$, $NH_2CH_3$) into a PNA oligomer. Similar to the coupling strategy described in chapter II, conjugation of *trans*-[Pt($NH_2CH_3$)$_2$(CHMT)(gly-*N*)]$^+BF_4^-$ (**9**) to the N-terminal amino group of immobilized PNA seems feasible. It was expected that **9** would be compatible with the solid-phase PNA synthesis protocol according to methods II and III. The CHMT ligand would protect the Pt(II) center in **9** during solid-phase synthesis and deprotection (ammonolysis) and later on it would be substitutable by a chloro ligand upon acid treatment. A low pH, applied during removal of the CHMT ligand, would not cause depurination reactions. Thus, in principle the synthesis of monofunctionally *trans*-Pt(II) modified mixed purine / pyrimidine PNA oligomers seems feasible.

An alternative approach (approach II, Scheme 1) implies incorporation of a monofunctionally *trans*-Pt(II) functionalized protected PNA monomer into a PNA oligomer. To this end, two new preplatinated PNA building blocks **33** and **34** have been designed (Scheme 3), which were expected to be compatible with solid-phase PNA synthesis according to method IV. As for **33**, an essential element is its compatibility with the piperidine treatment step applied in method IV for removal of the Fmoc group. Piperidine is a nucleophile and could therefore replace the chloro ligand. In aprotic solvents under anhydrous conditions such as applied in method IV, however, the exchange of the chloro ligand was expected to be suppressed, as a chloride ion is not stabilized by solvent molecules in this case. Furthermore, unlike in DNA synthesis and in contrast to PNA synthesis according to methods II and III (Scheme 1) in method IV removal of the base protecting groups and cleavage from the solid support is not effected by ammonolysis but under acidic conditions with TFA. TFA is not supposed to replace the labile chloro ligand in **33**.

For the case of insufficient compatibility of **33** with the piperidine treatment step, building block **34** was synthesized. It contains a CHMT ligand instead of a chloro ligand. The former ligand would protect the Pt(II) center against piperidine and would be post-synthetically substitutable by a chloro ligand (cf. chapter II).

## 3 Solid-phase synthesis of a monofunctionally *trans*-Pt(II) modified homopyrimidine PNA pentamer

First, the feasibility of approach I (Scheme 1) was explored. To this end, the fully protected PNA pentamer $c_5$ was assembled following a well-established solid-phase synthesis protocol[161] (method II, Scheme 1). Thus, sequential elongation of glycine anchored via an ester bond to functionalized (4-hydroxymethylbenzoic acid, HMBA) polystyrene beads with Fmoc / N-acyl protected building blocks yielded resin-bound $c_5$ (**30**). It was subsequently reacted with excess **9** under the agency of the condensation reagent HATU in the presence of D*i*PEA. Afterwards, a capping procedure was carried out. Deprotection and cleavage from the solid support was effected by ammonolysis ($NH_3$ / MeOH, 12 h, 20 °C).

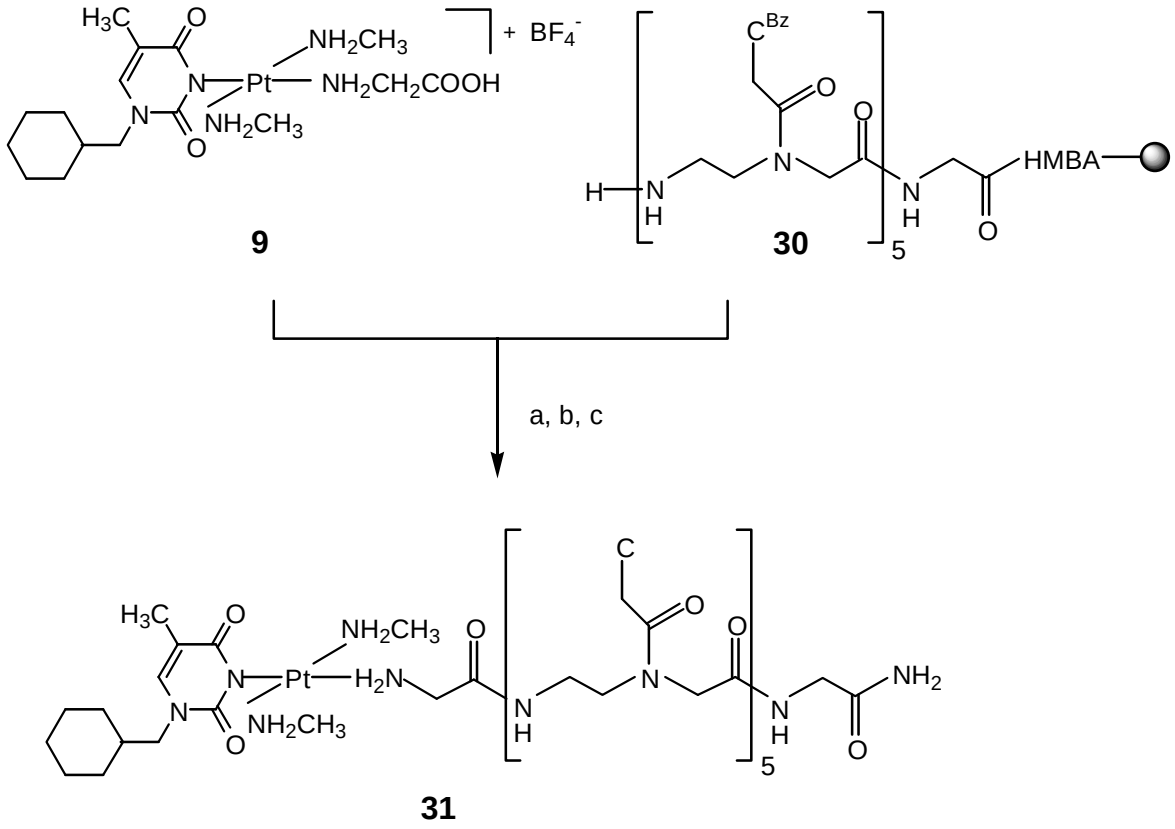


Scheme 2: Conjugation of building block **9** to immobilized $c_5$ (**30**);
a) HATU, D*i*PEA, b) cap reagent, c) $NH_3$ / MeOH.

LC MS analysis of the crude product (Table 1) reveals that conjugation of **9** to the N-terminal amino group of immobilized $c_5$ proceeded almost quantitatively. An incomplete coupling reaction of **9** to **30** would have led to the presence of acetylated (capped) $c_5$gly. LC MS analysis gives, however, no evidence for the presence of acetylated $c_5$gly.

The coupled product **31** is, however, not entirely compatible with the deprotection and cleavage conditions as evidenced by LC MS. Under mild deprotection conditions ($NH_3$ / MeOH, 12 h, RT), where removal of the Bz protecting groups is not even complete as indicated by the presence of **31** having still one or two Bz protecting groups (Table 1), deplatination reactions occur leading to formation of gly-$c_5$gly and *trans*-$[Pt(NH_2CH_3)_2(CHMT)NH_3]^+$. As in chapter II, section 5, this observation must be rationalized by a nucleophilic attack of $NH_3$ on the Pt(II) center in **31**, leading to substitution of the gly-$c_5$gly ligand in **31** by $NH_3$. However, as can be seen from Table 1, this reaction only takes place to a small extent and the desired product **31** can still be obtained in approximately 50 % yield. Subsequently, conjugate **31** was purified by reversed-phase HPLC.

Table 1: LC MS analysis of the coupling reaction of **9** with immobilized $c_5$ (**33**)

| $t_r$ | mass | amount / % | assignment |
|---|---|---|---|
| 11.24 | 694 $[M^{2+}]$ | 9.19 | gly-$c_5$gly |
| 17.67 | 1866$[M^+]$, 933$[M^{2+}]$ | 49.93 | **31** |
| 18.66 | 1971$[M^+]$, 986$[M^{2+}]$ | 19.65 | **31** + 1 Bz |
| 19.13 | 496 $[M^+]$ | 7.36 | *trans*-$[Pt(NH_2CH_3)_2(CHMT)NH_3]^+$ |
| 19.91 | 2077$[M^+]$, 1039$[M^{2+}]$ | 13.86 | **31** + 2 Bz |

The results show that the functionalization of PNA oligomers with building block **9** is feasible. However, this approach is not well suited for the synthesis of monofunctionally *trans*-Pt(II) modified mixed purine / pyrimidine PNA oligomers, as the forced ammonolysis conditions required for removal of the G-*i*Bu protecting groups[130] are not compatible with building block **9**. As in section 5 of chapter II, at higher temperatures the observed ligand exchange reaction would take place to a much larger extent. For this reason this approach was not further pursued. Instead, the feasibility of approach II (Scheme 1) involving the newly synthesized building blocks **33** and **34** (Scheme 3) was explored in more detail.

# 4 Solid-phase synthesis of monofunctionally *trans*-Pt(II) modified mixed pyrimidine / purine PNA oligomers

## 4.1 Synthesis and characterization of the preplatinated building blocks *trans*-$[Pt(NH_3)_2(Fmoc/N\text{-}Bhoc\ G)Cl]^+BF_4^-$ (33) and *trans*-$[Pt(NH_2CH_3)_2(CHMT)(Fmoc/N\text{-}Bhoc\ G)]^+BF_4^-$ (34)

### 4.1.1 Synthesis

*Trans*-$[Pt(NH_3)_2(Fmoc/N\text{-}Bhoc\ G)Cl]^+BF_4^-$ (**33**) was synthesized by reacting *trans*-$[Pt(NH_3)_2(DMF)Cl]^+BF_4^-$ with one equivalent Fmoc/N-Bhoc G (**32**) in DMF at RT (Scheme 3). The reaction proceeded almost instantaneously without the formation of much side products giving *trans*-$[Pt(NH_3)_2(Fmoc/N\text{-}Bhoc\ G)Cl]^+BF_4^-$ (**33**) in 75 % yield.

*Trans*-$[Pt(NH_2CH_3)_2(CHMT)(Fmoc/N\text{-}Bhoc\ G)]^+BF_4^-$ (**34**) was synthesized by reacting *trans*-$[Pt(NH_2CH_3)_2(CHMT)(DMF)]^+BF_4^-$ (**7a**) with one equivalent Fmoc/N-Bhoc G (**32**) in DMF at RT (Scheme 3). The reaction was complete within two days affording **34** in 80 % yield.

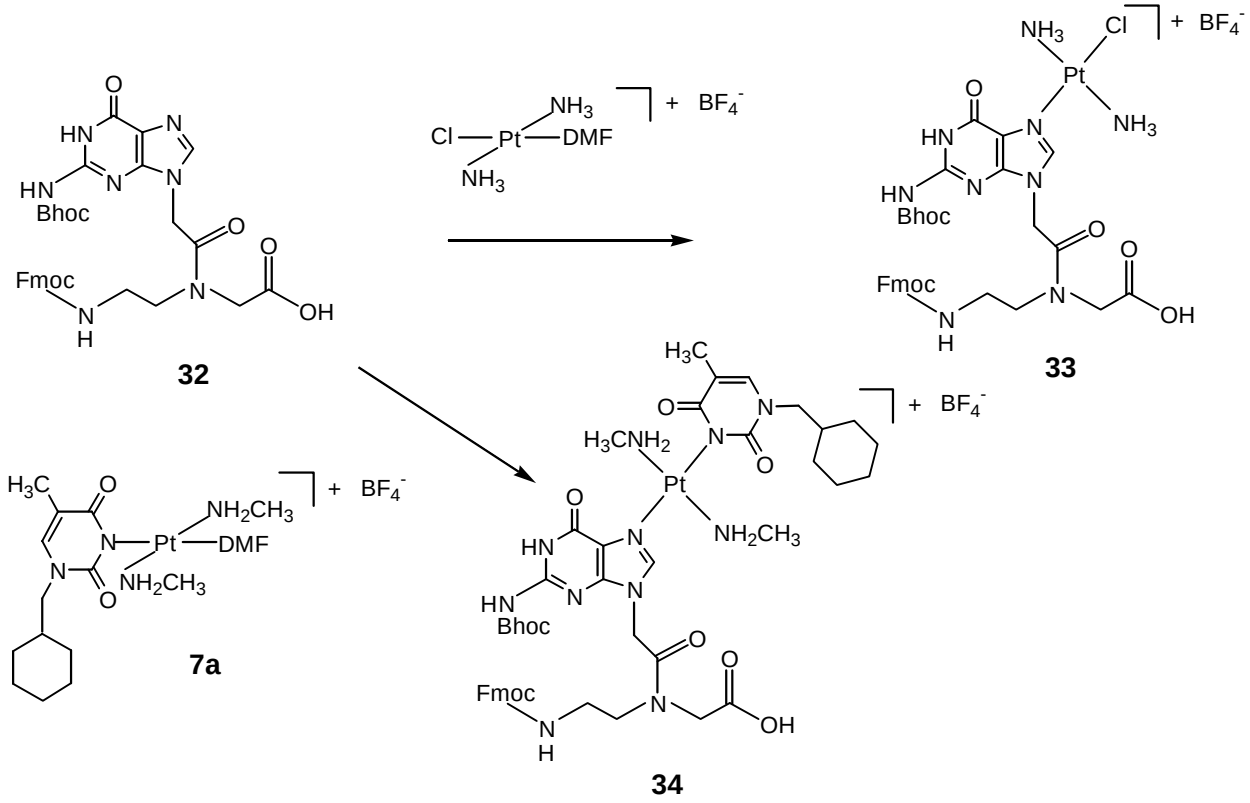


Scheme 3: Synthesis of the platinated PNA building blocks **33** and **34**.

### 4.1.2 Characterization of *trans*-[Pt(NH$_3$)$_2$(Fmoc/N-Bhoc G)Cl]$^+$BF$_4^-$ (33)

#### 4.1.2.1 NMR spectroscopy and ESI MS

*Trans*-[Pt(NH$_3$)$_2$(Fmoc/N-Bhoc G)Cl]$^+$BF$_4^-$ (**33**) was characterized by ESI MS as well as NMR spectroscopy. The ESI MS spectrum shows a peak at m/z 1006 for the singly positively charged ion of **33**. Calculated and found isotope pattern are in perfect agreement. The $^{195}$Pt NMR spectrum of **33** in DMF-d$_7$ shows one signal with a chemical shift of -2289 ppm, which is consistent with a PtN$_3$Cl coordination sphere.[135,136] Coordination of Pt(II) to the G-*N7* position in **33** is evidenced by a characteristic lowfield shift of the G-H8 resonance of 0.87 ppm in the $^1$H NMR[163] compared to the free ligand Fmoc/N-Bhoc G (**32**). Similarly, the G-N9-CH$_2$ protons are shifted to lower field by 0.19 ppm. The NOESY spectrum of **33** (not shown) displays crosspeaks between the G-H8 proton and the G-N9-CH$_2$ protons as well as between the G-H8 proton and the protons of the NH$_3$ ligands. Furthermore, $^1$H NMR spectroscopy in DMF-d$_7$ at RT shows both for Fmoc/N-Bhoc G (**32**) and *trans*-[Pt(NH$_3$)$_2$(Fmoc/N-Bhoc G)Cl]$^+$BF$_4^-$ (**33**) two signals for the respective methylene (G-N9-CH$_2$) protons (Figures 2 and 3). This observation is explained by hindered rotation about the tertiary amide bond. Due to restricted rotation around the tertiary amide bond **32** and **33** exist in both a *cis*- and a *trans*-conformation.[157,164] In the *cis*-conformation, the side chain carbonyl group points towards the glycine placing the methylene protons in proximity to the 2-aminoethyl protons[164] (Figure 1).

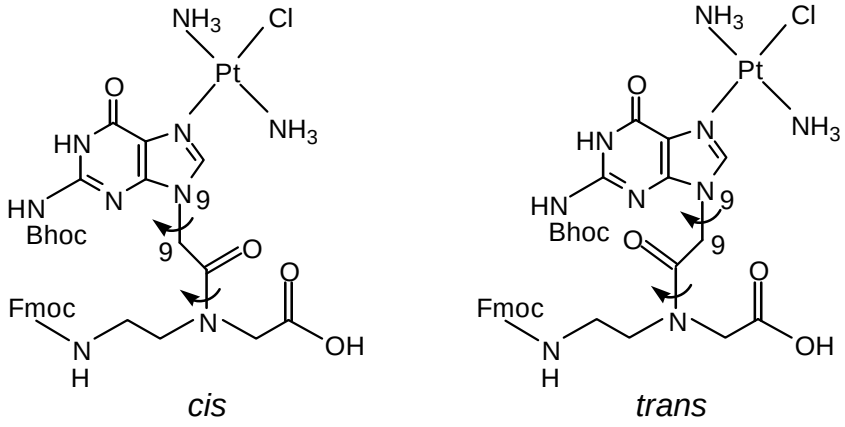


Figure 1: *Cis*- and *trans*- conformers of **33**.

At 297 K *trans*-[Pt($NH_3$)$_2$(Fmoc/N-Bhoc G)Cl]$^+$$BF_4^-$ (**33**) exists as a 57:43 *cis* : *trans* and Fmoc/N-Bhoc G (**32**) as a 61:39 *cis* : *trans* mixture of the two amide rotamers as gauged by the integrals of the $^1$H NMR signals.

Temperature-dependent $^1$H NMR measurements in DMF-$d_7$ reveal that the two G-N9-$CH_2$ resonances of Fmoc/N-Bhoc G (**32**) merge at around 357 K, whereas for *trans*-[Pt($NH_3$)$_2$(Fmoc/N-Bhoc G)Cl]$^+$$BF_4^-$ (**33**) no coalescence is observed until this temperature (Figures 2 and 3). These data suggest that in **33** the rotational barrier of the interconversion between the *cis* and *trans* conformation is increased.

The respective G-H8 resonances of both **32** and **33** are doubled up to 338 K (Figures 2 and 3). Coalescence of these resonances occurs for both **32** and **33** already at 338 K and does not coincide with the coalescence of the methylene proton resonances. This suggests that below 338 K the nucleobase rotation around the G-N9-C9 bond in **32** and **33** is also slow on the NMR time-scale. If this rotation was fast, only one G-H8 resonance should be observed, regardless of *cis*- and *trans*- conformation. This might lead to the conclusion that in addition to restricted rotation around the tertiary amide bond in **32** and **33** also the nucleobase rotation around the G-N9-C9 bond is restricted to some extent.

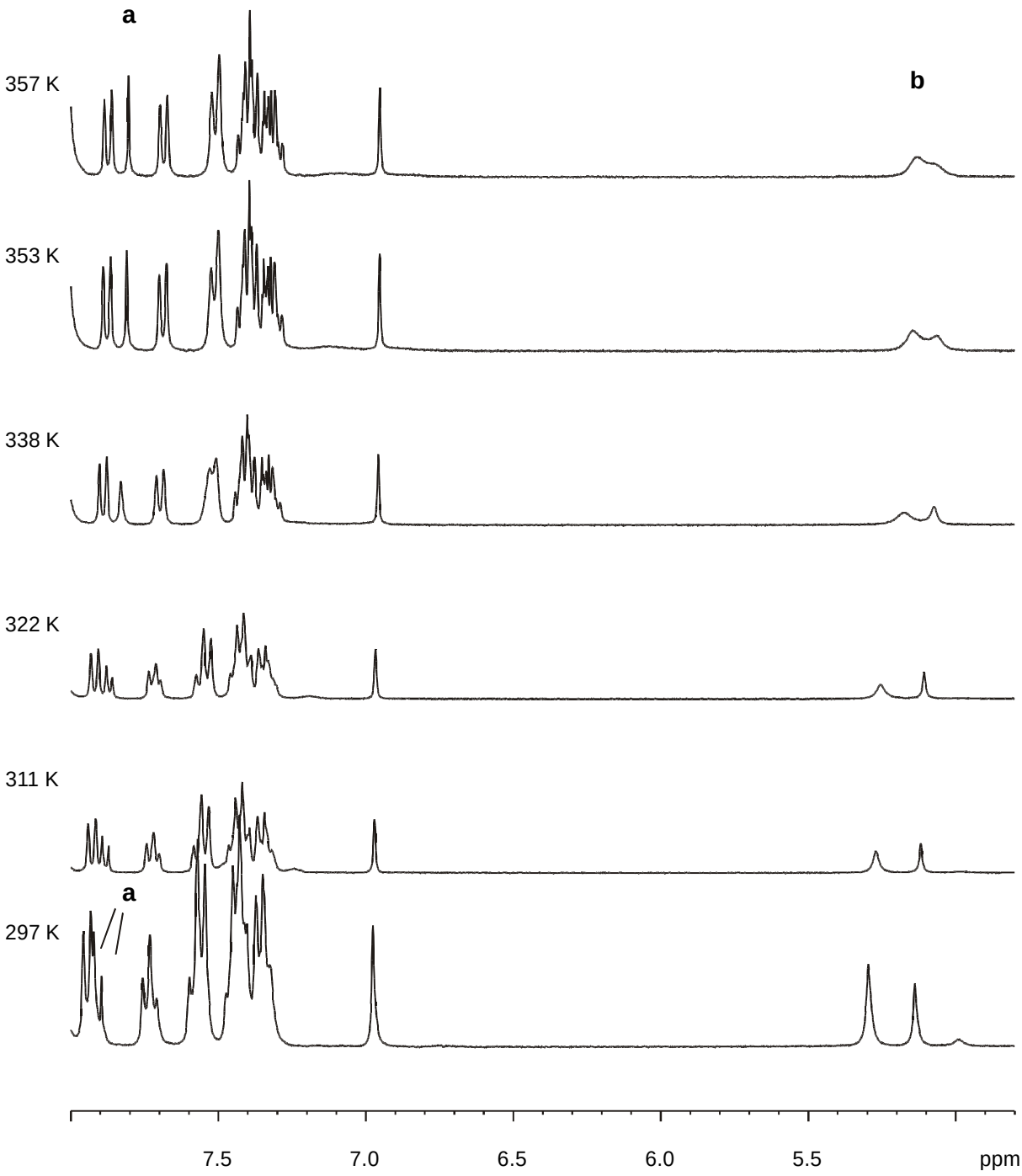


Figure 2: Temperature-dependent $^{1}H$ NMR spectra of **32** in DMF-$d_7$;
a: G-H8 resonance, b: G-N9-$CH_2$ resonances.

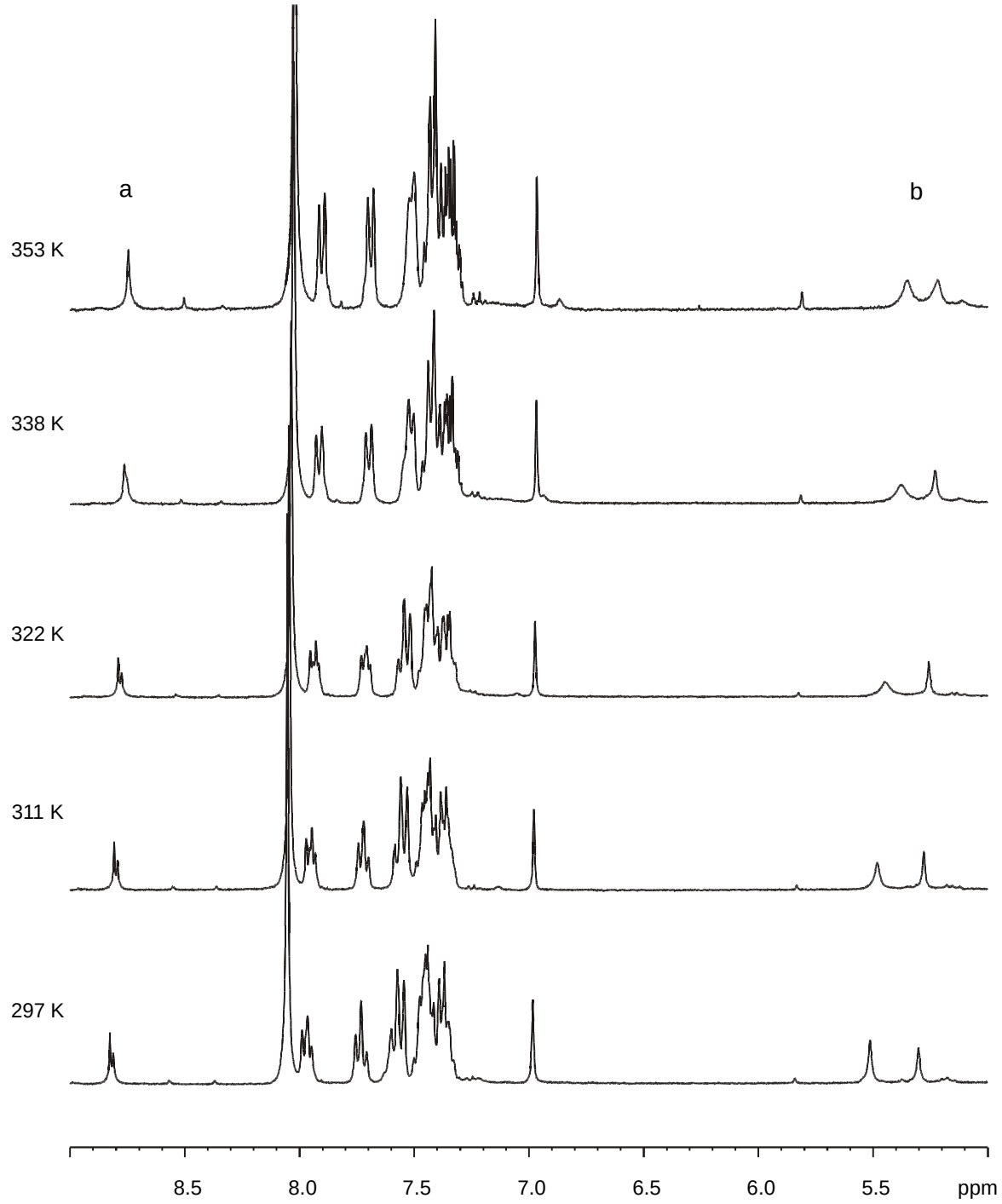


Figure 3: Temperature-dependent $^{1}H$ NMR spectra of **33** in DMF-$d_7$;
a: G-H8 resonance, b: G-N9-$CH_2$ resonances.

#### 4.1.2.2 Compatibilty of *trans*-$[Pt(NH_3)_2(Fmoc/N\text{-}Bhoc\ G)Cl]^+BF_4^-$ (33) with solid-phase PNA synthesis

The compatibility of *trans*-$[Pt(NH_3)_2(Fmoc/N\text{-}Bhoc\ G)Cl]^+BF_4^-$ (**33**) with the solid-phase PNA synthesis protocol according to method IV (Scheme 1) is essential. No ligand exchange reactions at the Pt(II) center (e.g. substitution of the chloro ligand by piperidine) may occur as in this case a platinated PNA conjugate would have no crosslinking ability. The compatibility of **33** with the solid-phase PNA synthesis protocol according to method IV (Scheme 1) was assessed by subjecting **33** to the various reagents of this synthesis protocol. $^{195}$Pt NMR spectroscopy was applied to probe changes in the coordination sphere of the Pt(II) center in **33**.

First, **33** was treated with a 20 % solution of piperidine in DMF, which normally serves to remove the N-terminal Fmoc group (Scheme 1). This reagent is most critical for building block **33**, as piperidine is a nucleophile and could therefore replace the labile chloro ligand. However, in a dry aprotic solvent (e.g. dry DMF) this ligand exchange reaction is expected to be rather slow. In agreement with this assumption, $^{195}$Pt NMR shows up to approximately one hour no ligand exchange reactions. After several hours an additional $^{195}$Pt NMR signal at -2396 ppm is observed, indicating most probably substitution of the chloro ligand by piperidine.

Second, building block **33** was subjected to a mixture of TFA / *m*-cresol (4 / 1, v/v), used normally for removal of the Bhoc protecting groups and cleavage from the solid support (Scheme 1). After one hour $^{195}$Pt NMR spectroscopy shows exclusively the original signal at -2290 ppm, indicating that the Pt(II) center in **33** is not effected by these two reagents.

Third, to a solution of **33** in DMF a mixture of one equivalent of HATU and two equivalents D*i*PEA was added. These reagents normally effect conjugation of a protected PNA monomer to the 5´-terminus of immobilized PNA (Scheme 1). Even after one day at RT, only the original signal at -2290 ppm is observed in the $^{195}$Pt NMR spectrum indicating that ligand exchange did not occur.

Fourth, **33** was treated with capping solution (acetic acid anhydride / D*i*PEA). Again, $^{195}$Pt NMR spectroscopy shows full compatibility of **33** with this reagent.

### 4.1.3 Characterization of *trans*-[Pt($NH_2CH_3$)$_2$(CHMT)(Fmoc/N-Bhoc G)]$^+BF_4^-$ (34)

#### 4.1.3.1 NMR spectroscopy and ESI MS

*N7*-platination within *trans*-[Pt($NH_2CH_3$)$_2$(CHMT)(Fmoc/N-Bhoc G)]$^+BF_4^-$ (**34**) is verified in the $^1$H NMR spectrum by the characteristic downfield shift of the G-H8 resonance of 1.03 ppm.[163] Similar to building block **33** the G-H8 resonance in **34** is also doubled which suggests that, as in **33**, there is restriction of the nucleobase rotation. The $^{195}$Pt NMR spectrum of **34** displays one signal at -2476 ppm, consistent with a $PtN_4$ coordination sphere.[135,136]

The ESI MS spectrum shows compound **34** as the singly positively charged ion of **34** at m/z 1219.

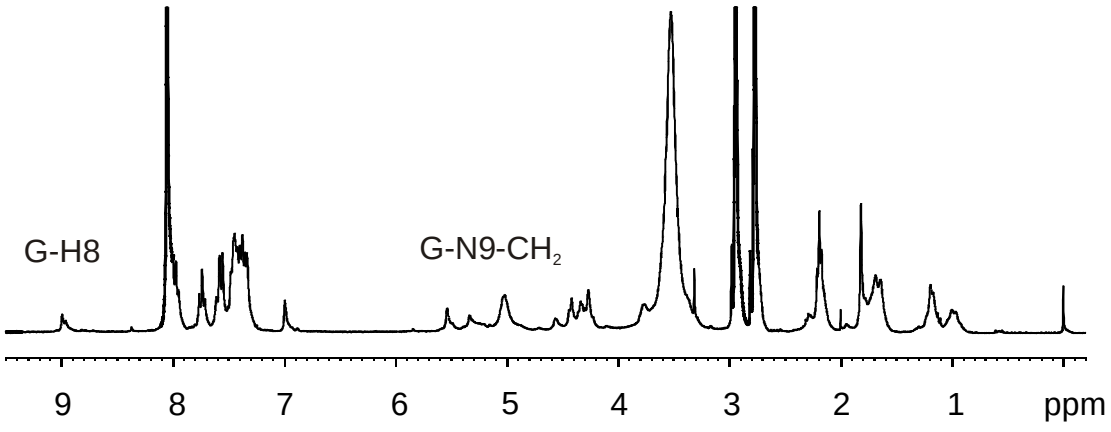


Figure 4: $^1$H NMR spectrum of **34** in DMF-$d_7$.

### 4.1.3.2 Compatibility of *trans*-[Pt($NH_2CH_3$)$_2$(CHMT)(Fmoc/N-Bhoc G)]$^+BF_4^-$ (34) with solid-phase PNA synthesis

As the Pt(II) center in *trans*-[Pt($NH_2CH_3$)$_2$(CHMT)(Fmoc/N-Bhoc G)]$^+BF_4^-$ (**34)** is surrounded by four nitrogen atoms, **34** was expected to be stable against HATU / D*i*PEA, piperidine / DMF and acetic anhydride / D*i*PEA. However, TFA treatment was supposed to remove at least partly the acid-labile CHMT ligand.

In order to study the effect of TFA on the CHMT ligand *trans*-[Pt($NH_2CH_3$)$_2$(CHMT)(Fmoc/N-Bhoc G)]$^+BF_4^-$ (**34**) was subjected to a TFA / *m*-cresol (4/1, v/v) solution at RT for 1 h. The $^{195}$Pt NMR spectrum of the freeze-dried sample shows two signals at –2119 ppm and –2483 ppm, consistent with $PtN_3O$ and $PtN_4$ coordination spheres,[135,136] respectively. In combination with ESI MS, the latter signal is assigned to originate from compound **34a** and the former from compound **34b**. Thus, TFA treatment effects not only removal of the Bhoc base protecting group resulting in formation of **34a** but also partly the removal of the CHMT ligand and its exchange for a TFA ligand resulting in formation of **34b**. According to the integrals of the $^{195}$Pt NMR signals the removal of the CHMT ligand is approximately 50 %.

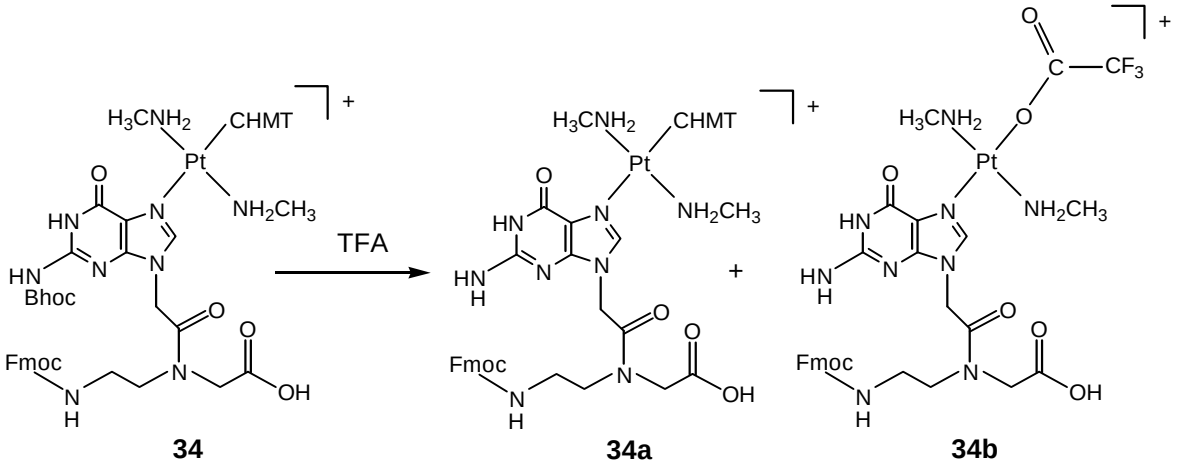


Scheme 4: Partial removal of the CHMT ligand upon treatment of **34** with TFA.

### 4.1.4 Conclusions

The synthesized building blocks *trans*-[Pt($NH_3$)$_2$(Fmoc/N-Bhoc G)Cl]$^+$$BF_4^-$ (**33**) and *trans*-[Pt($NH_2CH_3$)$_2$(CHMT)(Fmoc/N-Bhoc G)]$^+$$BF_4^-$ (**34**) are potentially suitable for an application in solid-phase PNA synthesis according to method IV (Scheme 1). Both **33** and **34** show the required high solubility in DMF. Building block **33** has been shown to be completely compatible with the solid-phase PNA synthesis protocol according to method IV (Scheme I). Building block **34** is not entirely stable against TFA as indicated by a partial removal of the CHMT ligand and its exchange with TFA (Scheme 4). The latter observation does, however, not represent a major problem. Exchange of the CHMT ligand by TFA can be circumvented by using HCl instead of TFA for deprotection and cleavage from the solid support in method IV. In this case the CHMT ligand would be replaced by a chloro ligand which would lead directly to the formation of the desired monofunctionally *trans*-Pt(II) modified PNA oligomer.

## 4.2 PNA assembly on a Rink functionalized PEG-PS resin using Fmoc / N-Bhoc building units

The application of approach II (Scheme 1) requires solid-phase PNA synthesis conditions according to method IV (Scheme 1) involving Fmoc / N-Bhoc protected PNA monomers. The standard protocol for a common Expedite 8909 DNA synthesizer involves polyethylene glycol polystyrene (PEG-PS) resin as solid support which is functionalized with a Fmoc-Pal or Fmoc-Xal linker.[162] As a consequence of the higher costs of these linkers and the fact that solid-phase PNA synthesis has to be carried out for practical reasons on a peptide synthesizer, the PNA synthesis protocol was slightly modified. Instead of a Pal or Xal linker the commonly in peptide synthesis employed Fmoc-Rink linker[165] was used.

Thus, first, PEG-PS resin was functionalized with a Fmoc-Rink linker (Scheme 5). In order to evaluate the efficiency of this functionalized resin the PNA sequence gattcgc was assembled. Thus, sequential elongation of Rink anchored via an amide bond to PEG-PS resin with Fmoc / N-Bhoc protected PNA monomers yielded the resin-bound gattcgc (**35**) (Scheme 5). Deprotection and cleavage from the solid support, achieved by treatment with TFA / water (9/1, v/v) at RT for 45 min, yielded crude **36**.

LC MS analysis of the crude product (Table 1) shows that the main product is the desired PNA 7-mer gattcgc (**36**). Only a small amount (7.5 %) of the PNA 6-mer attcgc is detected. The coupling efficiency is thus rather good. Furthermore, the presence of minor amounts of gattcgc with re-bound benzhydryl cation (bhc) shows that the use of a scavenger is required which prevents the highly reactive benzhydryl cation formed during TFA treatment from re-binding to the electron-rich aromatic rings.

Table 2: LC MS analysis of crude product of gattcgc test synthesis

| $t_r$ | mass | amount / % | assignment |
|---|---|---|---|
| 18.65 | 1953 ($M^+$), 977 ($M^{2+}$) | 76.87 | Ac-gattcgc (**36**) |
| 20.75 | 1662 ($M^+$) | 7.54 | Ac-attcgc |
| 21.45 | 1060 ($M^{2+}$) | 15.58 | Ac-gattcgc (**36**) + bhc |

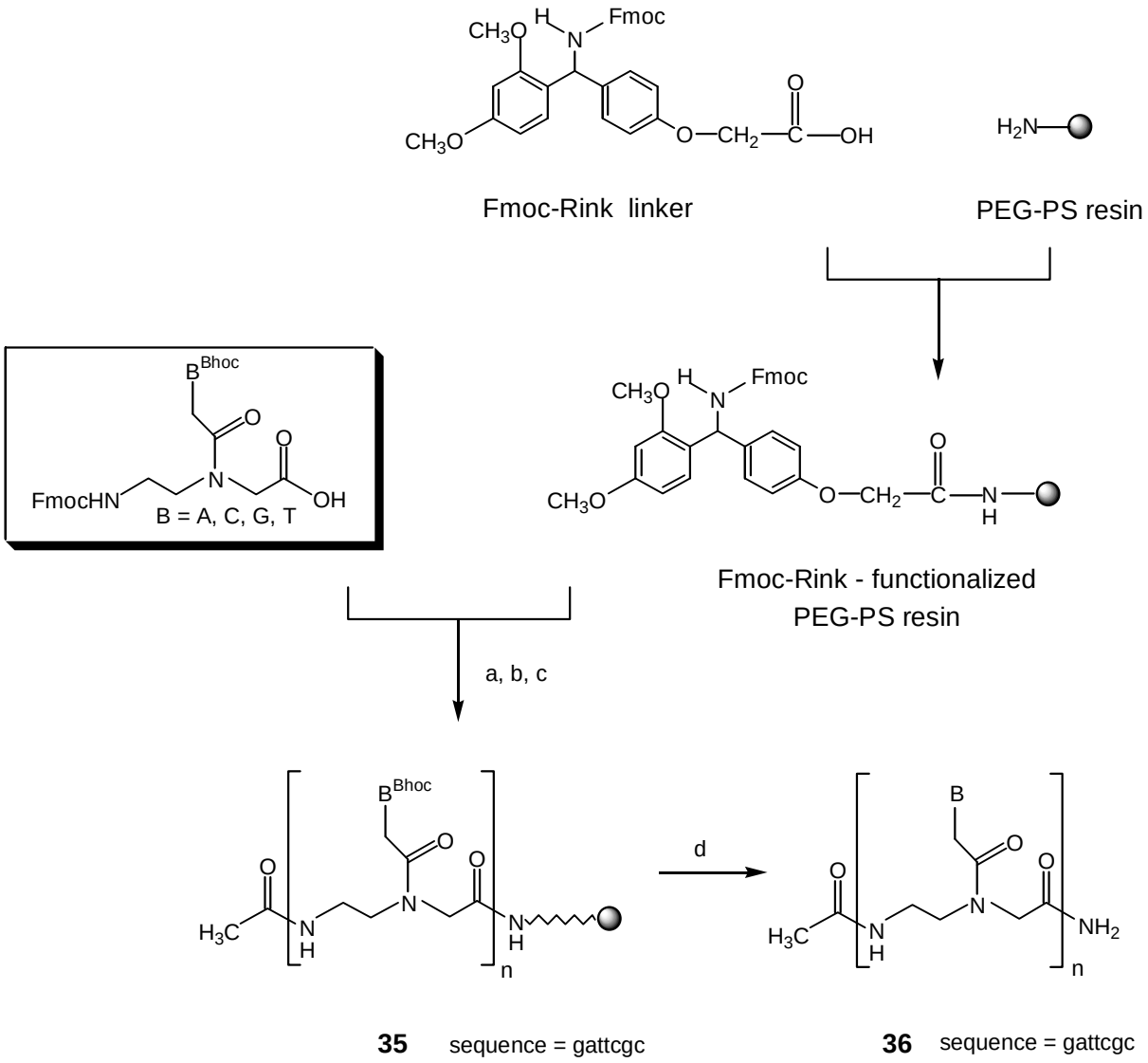


Scheme 5: Solid-phase PNA synthesis using Rink-functionalized PEG-PS resin and Fmoc / N-Bhoc protected PNA monomers;
a) piperidine / DMF, b) HATU / D*i*PEA, c) $Ac_2O$ / D*i*PEA, d) TFA / *m*-cresol.

## 4.3 Conjugation of *trans*-[Pt(NH$_3$)$_2$(Fmoc/N-Bhoc G)Cl]$^+$BF$_4^-$ (33) to the N-terminus of immobilized PNA oligomers

### 4.3.1 Synthesis and characterization of monofunctionally *trans*-Pt(II) modified PNA oligomers

In order to explore the feasibility of approach II (Scheme 1) in combination with building block **33**, the PNA oligomer attcgc has been assembled according to the method described in section 4.2 of this chapter. The resulting resin-bound, fully protected PNA oligomer attcgc (**37**) was reacted with excess **33** under the agency of the coupling reagent HATU in the presence of D*i*PEA (Scheme 6). Afterwards a capping procedure was carried out. Deprotection and cleavage from the solid support was subsequently effected by treatment with TFA in the presence of *m*-cresol. The crude reaction mixture was analyzed by LC MS (Table 3). The HPLC chromatogram shows two main peaks with retention times of 13.41 and 13.67 min, respectively. In combination with ESI MS, the peak at 13.41 min can be assigned as capped (acetylated) attcgc. The peak at 13.67 min yields peaks at m/z 2215.2, 1108.6 and 738.8 in the ESI MS, which can be assigned as the $M^+$, $M^{2+}$ and $M^{3+}$ ions of the monofunctionally platinated PNA oligomer *trans*-[(NH$_3$)$_2$Pt(g-*N7*-attcgc)Cl]$^+$ (**43**) (Table 3). Compound **43** was subsequently purified by reversed-phase HPLC and its purity was established by LC MS (Figure 5).

In order to establish the reproducibility of this approach two more coupling experiments with different PNA oligomers were carried out. To this end, the PNA / peptide conjugate attcgc-lys (**38**) and the PNA oligomer atctcagc (**39**) were assembled and similarly reacted with excess **33** under the agency of the coupling reagent HATU in the presence of D*i*PEA (Scheme 6). Afterwards a capping procedure was carried out. Deprotection and cleavage from the solid support was subsequently achieved by treatment with TFA in the presence of *m*-cresol. LC MS analysis of the crude reaction mixtures (Tables 4 and 5) reveals that the respective main products in both experiments are the monofunctionally *trans*-Pt(II) modified PNA oligomers **44** and **45**. The major side products in both experiments are the respective capped (acetylated) PNA (n-1)-mers Ac-attcgc-lys and Ac-atctcagc. The monofunctionally *trans*-Pt(II) modified PNA oligomers **44** and **45** have similarly been purified by reversed-phase HPLC. The purity of **44** and **45** was again established by LC MS.

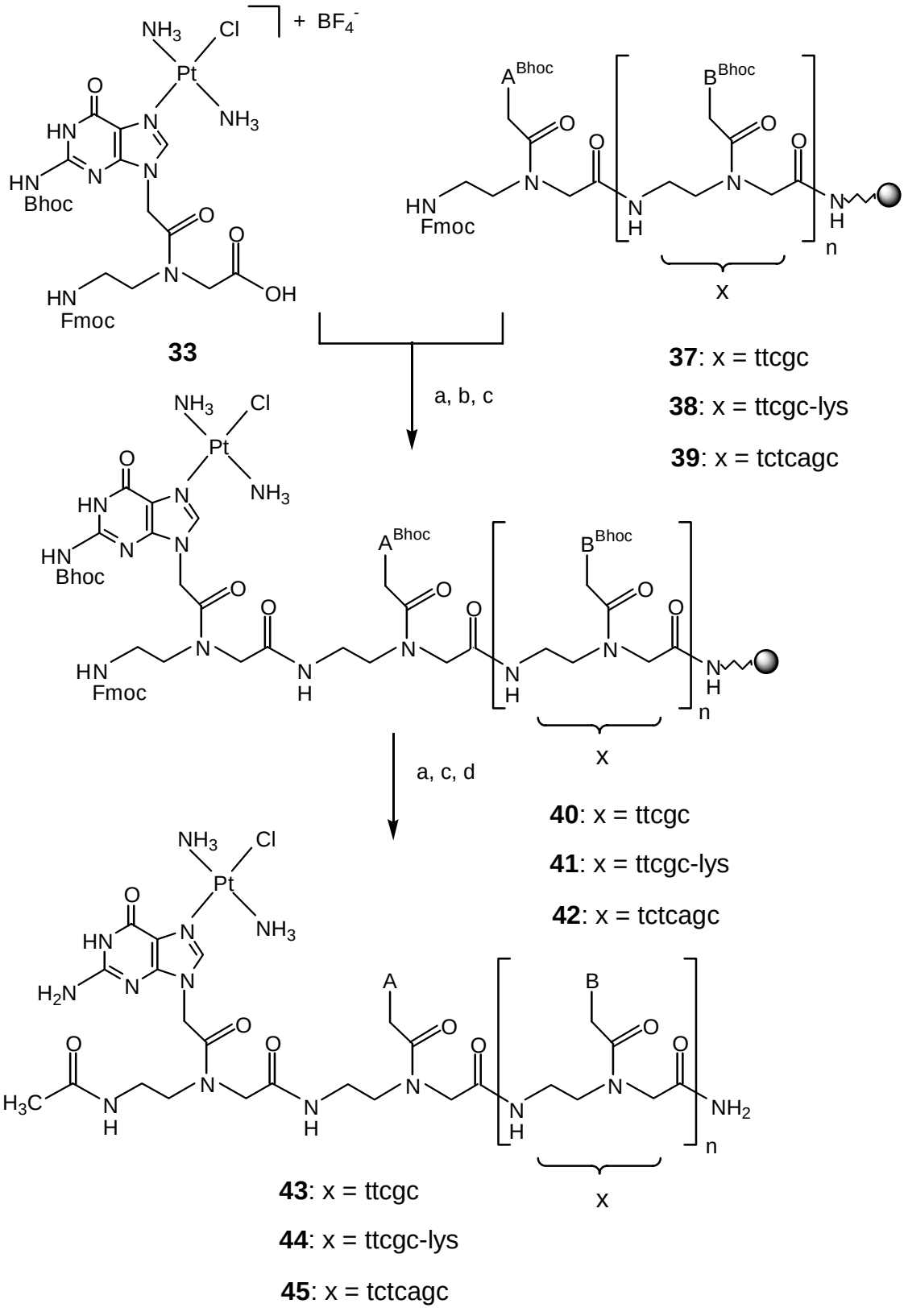


Scheme 6: Solid-phase synthesis of the monofunctionally *trans*-Pt(II) modified PNA oligomers **43**, **44** and **45**; a) piperidine / DMF, b) HATU / D*i*PEA, c) $Ac_2O$ / D*i*PEA, d) TFA / *m*-cresol.

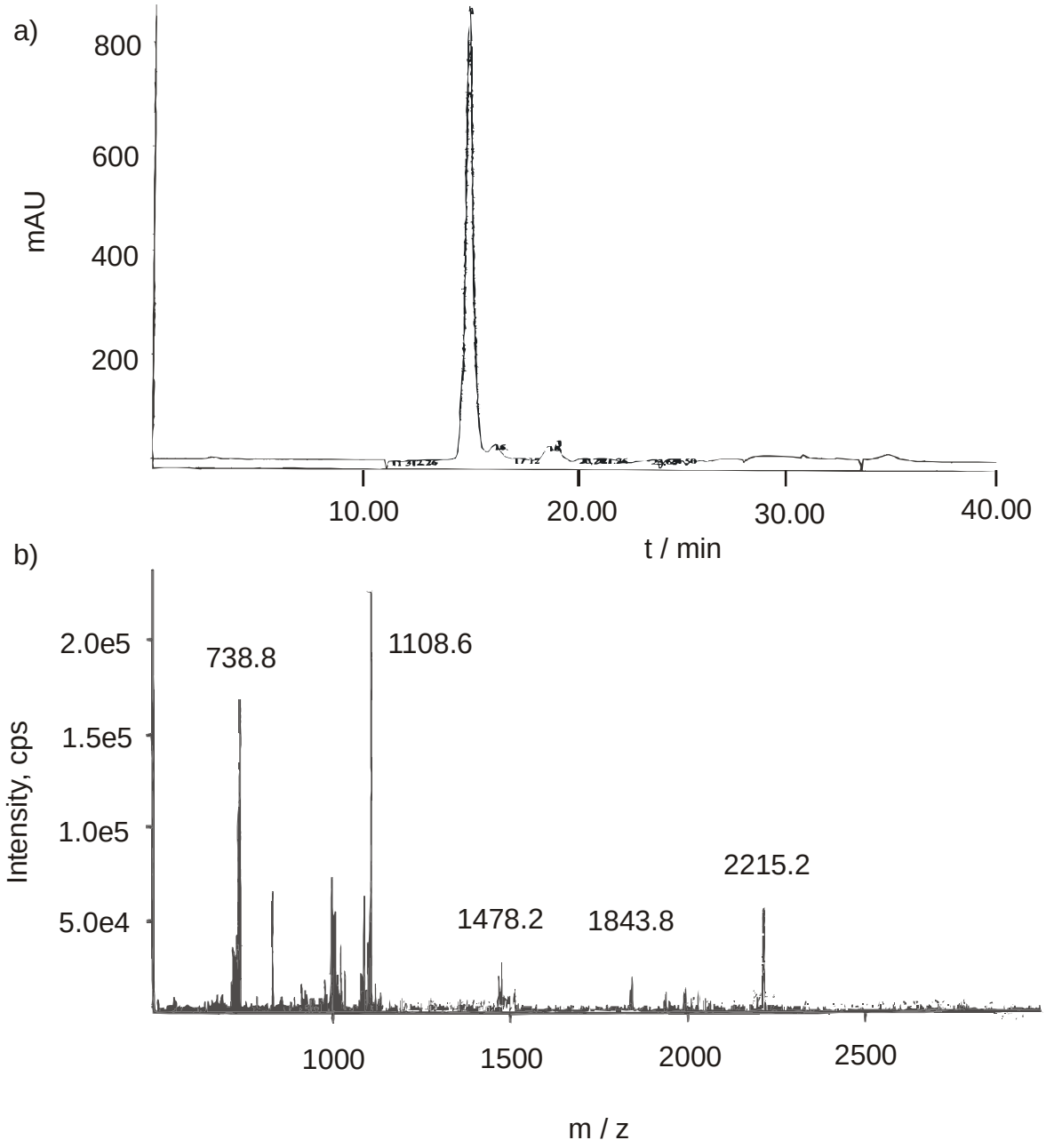


Figure 5: LC MS analysis of the purified monofunctionally *trans*-Pt(II) modified PNA oligomer **43**; a) reversed-phase HPLC chromatogram, b) ESI MS spectrum.

Table 3: LC MS analysis of crude product obtained by conjugation of **33** to **37**

| $t_r$ | mass | amount / % | assignment |
|---|---|---|---|
| 13.41 | 1662 ($M^+$), 831 ($M^{2+}$) | 31.11 | Ac-attcgc |
| 13.67 | 2215 ($M^+$), 1108 ($M^{2+}$) 739 ($M^{3+}$) | 67.89 | **43** |

Table 4: LC MS analysis of crude product obtained by conjugation of **33** to **38**

| $t_r$ | mass | amount / % | assignment |
|---|---|---|---|
| 17.41 | 1790 ($M^+$), 895 ($M^{2+}$) | 52.15 | Ac-attcgc-lys |
| 18.16 | 1172 ($M^{2+}$), 782 ($M^{3+}$) | 47.85 | **44** |

Table 5: LC MS analysis of crude product obtained by conjugation of **33** to **39**

| $t_r$ | mass | amount / % | assignment |
|---|---|---|---|
| 14.74 | 1094 ($M^{2+}$), 730 ($M^{3+}$), | 41.08 | Ac-atctcagc |
| 15.26 | 2741 ($M^+$), 1371 ($M^{2+}$), 914 ($M^{3+}$) | 42.62 | **45** |

### 4.3.2 Discussion

The results described in this section demonstrate that an efficient synthesis of monofunctionally *trans*-Pt(II) modified PNA oligomers is feasible by conjugation of **33** to the N-terminus of immobilized PNA. Tables 3, 4 and 5 show that in all coupling experiments the respective monofunctionally *trans*-Pt(II) modified PNA oligomer is obtained as the major product. As major side product the respective capped PNA (n-1)-mers (Ac-atctcagc, Ac-attcgc and Ac-attcgc-lys) are detected. This indicates that coupling of **33** to immobilized PNA is less effective than coupling of the unplatinated Fmoc / N-Bhoc-PNA monomers. The reason for this is not entirely clear. One explanation could be a less effective preactivation reaction (HATU / D*i*PEA mediated formation of an active ester). The *trans*-$(NH_3)_2$Pt(II)Cl moiety in **33** might exert steric hindrance on the carboxyl group and thereby "shield" it against conversion into the active ester. Another explanation could be the acidification of the G-NH(1) proton due to *N7*-platination.[166] This acidified G-NH(1) proton could interfere with the preactivation step in that it partly neutralizes the reaction mixture so that quantitative conversion of the carboxyl group into the active ester is prevented. Nevertheless, despite this

lower coupling efficiency, the desired monofunctionally *trans*-Pt(II) modified PNA oligomers **43**, **44** and **45** could be obtained in reasonably high yields (40–60 %) by this solid-phase approach.

Building block **33** proved entirely compatible with the applied synthesis protocol in that exchange of the chloro ligand was not observed. The presence of platinated PNA adducts, in which the chloro ligand was exchanged by e.g. piperidine was ruled out by LC MS.

The monofunctionally *trans*-Pt(II) modified PNA oligomers **43**, **44** and **45** have successfully been purified by reversed-phase HPLC. The conjugates **43**, **44** and **45** were stable and performed no suicide reactions (long range intrastrand crosslinks). Thus, this solid-phase method allows the convenient site-specific and sequence-independent monofunctional *trans*-Pt(II) modification of PNA oligomers.

# 5 Synthesis and characterization of the *trans*-$(NH_3)_2$Pt(II) crosslinked PNA / DNA double helix 47

## 5.1 Analysis of the crosslinking reaction of *trans*-[$(NH_3)_2$Pt(g-*N7*-attcgc)Cl]$^+$ (43) with the deoxyoligonucleotide 5´d(GCGAATG) (46) by reversed-phase HPLC

An essential prerequisite for the potential application of the synthesized monofunctionally *trans*-Pt(II) modified PNA oligomers **43**, **44** and **45** in antisense strategy is their sequence-specific crosslinking reaction with a complementary RNA target. In a model experiment, the crosslinking ability of *trans*-[$(NH_3)_2$Pt(g-*N7*-attcgc)Cl]$^+$ (**43**) with the deoxyoligonucleotide target 5´d(GCGAATG) (**46**) was investigated. Instead of a RNA target a DNA target was applied in order to avoid problems with hydrolysis of RNA. The deoxyoligonucleotide **46** is not entirely complementary to the base sequence in **43** in that it contains a 3´-terminal guanine instead of a cytosine. This modification was chosen in order to increase the rate of interstrand crosslink formation between **43** and **46** as Pt(II) has a greater affinity for guanine than for cytosine.[92]

The structure of a DNA / PNA duplex has been described in detail earlier.[167] It is a right handed Watson-Crick base paired helix with a wide and deep major groove and a narrow and shallow minor groove. An antiparallel orientation of the strands is preferred and the duplex has elements of both A- and B-form DNA. E.g., the DNA backbone torsion angles are close to

those in A-DNA while the base-sugar moieties of the DNA strand are in a B-like conformation with anti-glycosidic torsion angles and sugars predominantly near the C2´endo range.[167]

Thus, the reaction of *trans*-[$(NH_3)_2$Pt(g-*N7*-attcgc)Cl]$^+$ (**43**) with 5´d(GCGAATG) (**46**) at neutral pH in water at RT should lead to the formation of the *trans*-$(NH_3)_2$Pt(II) crosslinked PNA / DNA duplex **47** with antiparallel orientation of the strands (Scheme 7). The *trans*-$(NH_3)_2$Pt(II) interstrand crosslink would be located between the platinated N-terminal guanine of *trans*-[$(NH_3)_2$Pt(g-*N7*-attcgc)Cl]$^+$ (**43**) and the 3´guanine of 5´d(GCGAATG) (**46**). Furthermore, the formation of the *trans*-$(NH_3)_2$Pt(II) interstrand crosslink requires the rotation of the platinated guanine around the N9-C9 bond in **43**, analoguously to the anti→syn rotation of a nucleobase within a deoxyoligonucleotide.[89] The two guanines involved in an interstrand crosslink would under these circumstances most likely adopt a head-tail arrangement as previously shown in a *trans*-$(NH_3)_2$Pt(II) crosslinked antiparallel DNA duplex.[89]

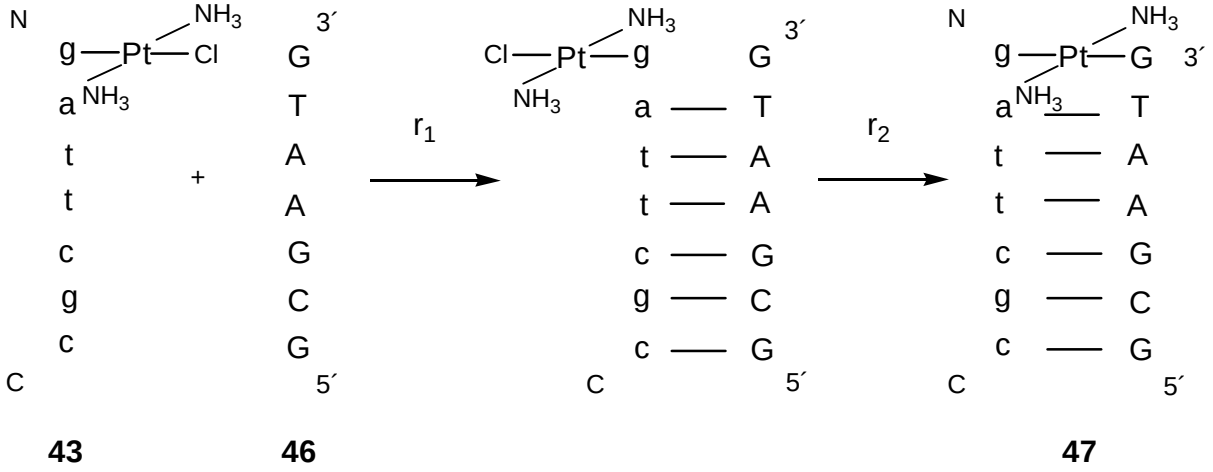


Scheme 7: Crosslinking reaction of **43** with **46**.

*Trans*-[$(NH_3)_2$Pt(g-*N7*-attcgc)Cl]$^+$ (**43**) was reacted with 5´d(GCGAATG) at pH 6.5 in water at RT. Figure 6 shows the reversed-phase HPLC chromatogram after 11 d. After 11 d the different components of the reaction mixture were separated by reversed-phase HPLC and analyzed by MALDI-TOF mass spectrometry.

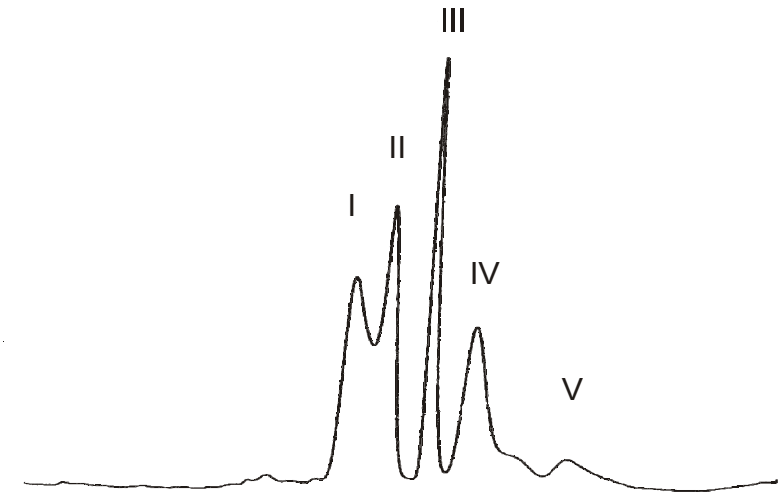


Figure 6: Reversed-phase HPLC chromatogram of the crosslinking reaction of **43** with **46**; gradient: 0→23 % B in 30 min; buffers: A: 50 mM TEAA, B: 50 mM TEAA in 75 % acetonitrile.

## 5.2 Characterization of the HPLC fractions by MALDI-TOF mass spectrometry

The HPLC fractions of the crosslinking reaction have been analyzed by matrix assisted laser desorption time of flight mass spectrometry (MALDI-TOF MS).

According to MALDI-TOF MS analysis (Figure 7), the HPLC fractions I, II and III contain unreacted 5´d(GCGAATG) (**46**). Fraction IV contains a product with a mass of 2178.6 which can be assigned either to **43** with the chloro ligand being removed during the MALDI-TOF experiment (fragmentation) or to a product resulting from a suicide reaction (formation of an intrastrand crosslink within **43**). Fraction V contains a product with a mass of 4325.07 which corresponds to a PNA / DNA hybrid containing a *trans*-$(NH_3)_2Pt(II)$ interstrand crosslink. Additionally, in fraction V the masses for the unplatinated gattcgc (**36**) and the unplatinated 5´d(GCGAATG) (**46**) are detected, probably due to fragmentation of the crosslinked product **47** during the MALDI-TOF experiment (Figure 7).

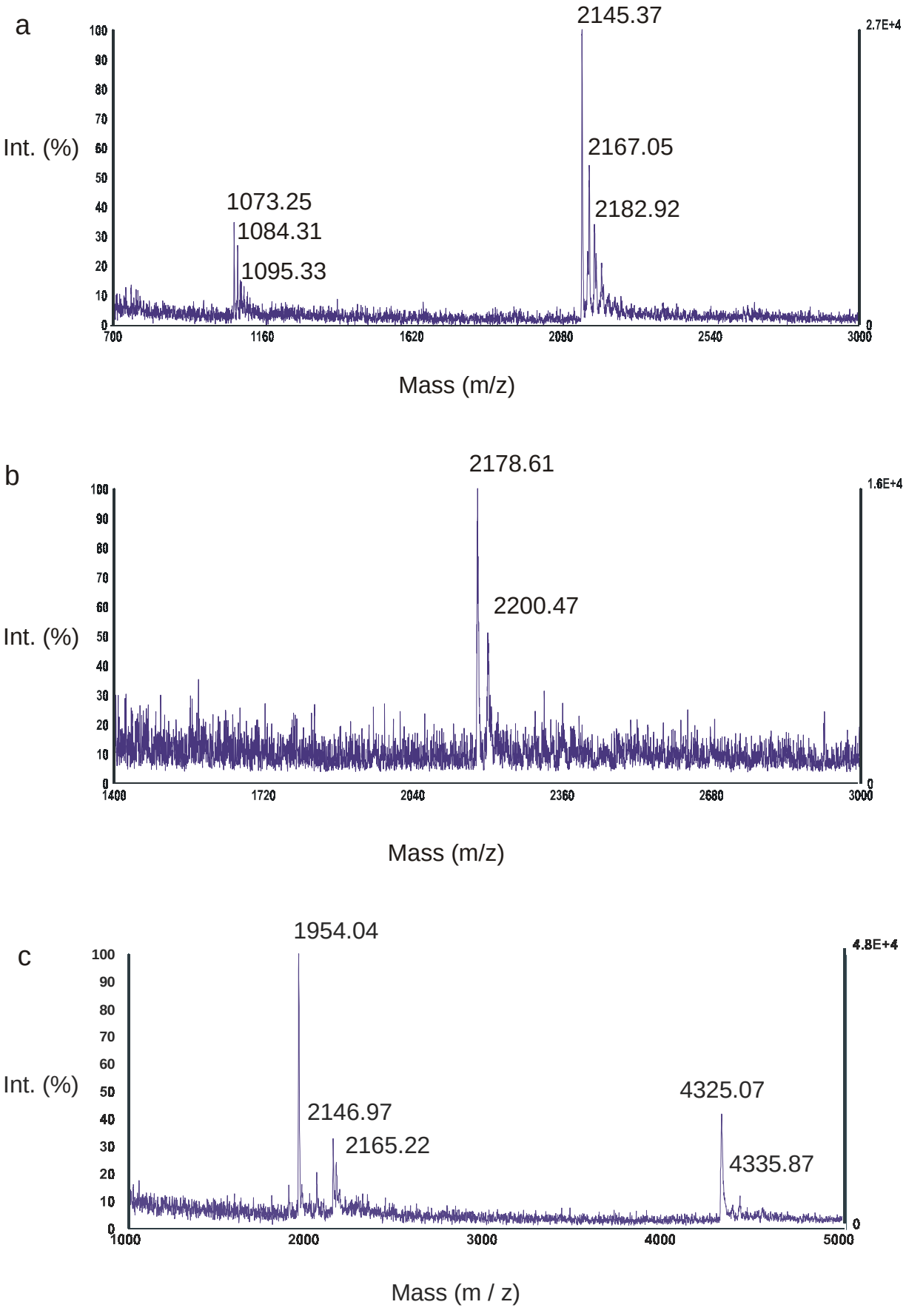


Figure 7: MALDI-TOF spectra of HPLC fractions I (a), IV (b) and V (c).

Thus, MALDI-TOF analysis confirms the presence of a DNA / PNA hybrid containing a *trans*-$(NH_3)_2$Pt(II) unit but gives no information on the location of the interstrand crosslink. For the determination of the location of the interstrand crosslink a gel-electrophoretic sequencing experiment has to be carried out.

## 5.3 Characterization of the isolated *trans*-$(NH_3)_2$Pt(II) crosslinked PNA / DNA duplex 47 by hydroxyl radical footprinting

The location of the *trans*-$(NH_3)_2$Pt(II) interstrand crosslink within **47** can be determined by a sequencing experiment involving hydroxyl radical mediated strand cleavage[122] of the deoxyoligonucleotide moiety in **47**. To this end, a sample of HPLC fraction V was labelled with $^{32}$P-γ-ATP and subjected to a hydroxyl radical footprinting experiment performed by Dr. M. Boudvillain, CNRS Orléans, France. Conditions have been used under which on average less than one cleavage per molecule occurred. The cleavage products have been analyzed on a denaturing 24 % polyacrylamide gel (Figure 8). Lane 1 represents the isolated crosslinked PNA / DNA duplex **47** after hydroxyl radical footprinting. Lanes 2 and 3 represent 5´d(GCGAATG) (**46**) after and without hydroxyl radical footprinting, respectively. Since hydroxyl radical mediated strand cleavage yields oligonucleotide-3´-phosphate and -3´-phosphoglycolate fragments,[122,124] for cleavage of every residue in **46** two distinct bands are observed. Hydroxyl radical footprinting of the 5´labelled *trans*-[Pt$(NH_3)_2$(g-*N7*-attcgc){3´d(G-*N7*-TAAGCG)}] (**47**) should yield the same cleavage products as the 5´labelled 5´d(GCGAATG) (**46**). As can be seen from Figure 8, for **47** there are two bands for every residue. Only for the 3´G one of the bands has disappeared. Furthermore, a band for the unplatinated 7-mer **46** is seen. The latter observation could be explained by the occurrence of deplatination reactions during the footprinting experiment and sample handling. For the former observation, however, an explanation is not immediately evident. Cleavage of the 3´G residue within **47** might be less efficient due to the steric constraints caused by the *trans*-$(NH_3)_2$Pt(II) interstrand crosslink. The site containing the *trans*-$(NH_3)_2$Pt(II) interstrand crosslink could be distorted to such an extent that the H4´ and H5´ sugar protons, which represent the preferential sites for attack by the hydroxyl radical,[124] are sterically less available for an attack by the hydroxyl radical. Furthermore, it is possible that the PNA part in **47** causes similar effects.

In conclusion, the results of the hydroxyl radical footprinting experiment strongly suggest that the *trans*-$(NH_3)_2Pt(II)$ interstrand crosslink in **47** is located between the N-terminal guanine of the PNA strand and the 3´G of 5´d(GCGAATG) (**46**).

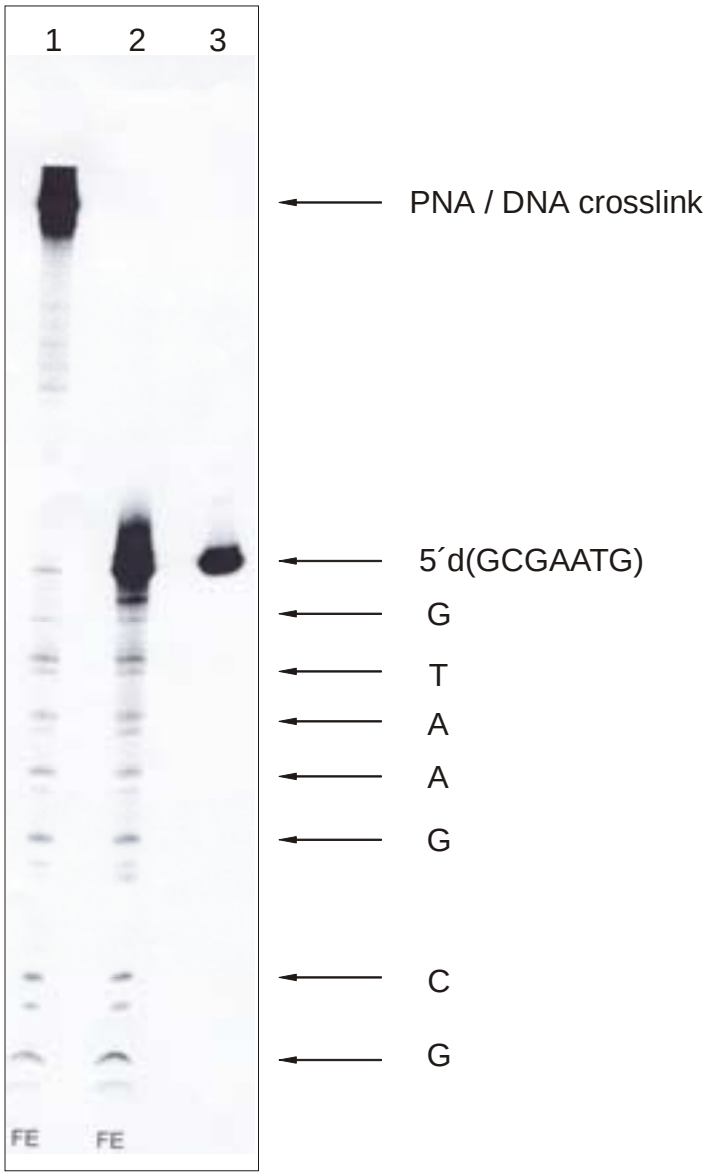


Figure 8: Autoradiogram of a denaturing 24 % polyacrylamide gel;
lane 1: PNA / DNA crosslink after hydroxyl radical footprinting,
lane 2: 5´d(GCGAATG) after hydroxyl radical footprinting,
lane 3: 5´d(GCGAATG) reference.

## 5.4 Discussion

The results of section 5 show that the monofunctionally *trans*-Pt(II) modified PNA oligomer **43** performs a crosslinking reaction with the complementary deoxyoligonucleotide **46** yielding a *trans*-$(NH_3)_2$Pt(II) crosslinked PNA / DNA duplex as shown by MALDI-TOF analysis. Gel-electrophoretic studies strongly suggest that the *trans*-$(NH_3)_2$Pt(II) interstrand crosslink within the PNA / DNA duplex is located between the N-terminal guanine of the PNA part and the 3´guanine of the oligonucleotide 5´d(GCGAATG) (**46**). The crosslinking reaction between **43** and **46**, however, is slow and proceeds in a low yield. This observation was rather unexpected and there is no obvious and straightforward explanation.

One explanation for the slow and low-yield crosslinking reaction could be inefficient hybridization of **43** with **46** with a concomitant suicide reaction of **43**. Indeed, MALDI-TOF analysis of HPLC fraction IV indicates a product with a mass of 2178.6 corresponding to **43** minus chloride. This mass indicates either a product resulting from a suicide reaction of **43** or unreacted **43** with the chloro ligand being removed during the MALDI-TOF measurement (fragmentation). However, as hybridization of PNA with deoxyoligonucleotides is usually fast and strong and as DNA / PNA hybrids of comparable length have melting temperatures of 313 K[168] it is expected that hybridization of **43** with **46** should be efficient.

An alternative explanation for the slow interstrand crosslink formation could be restricted rotation of the platinated N-terminal guanine around the N9-C9 bond in **43**. The formation of an interstrand crosslink between **43** and **46** requires the rotation of the platinated guanine residue in **43** around the N9-C9 bond to place the *trans*-$(NH_3)_2$Pt(II)Cl unit in proximity to the *N7*-position of the opposite 3´guanine. Slow nucleobase rotation around the N9-C9 bond has been observed for the protected PNA monomer **32** and building block **33** (cf. section 4.1.2.1 of this chapter). If the rotation of the platinated N-terminal guanine around the N9-C9 bond in **43** is also restricted this could indeed effect the rate and yield of the crosslinking reaction of **43** with **46**.

A third explanation could be that the *trans*-$(NH_3)_2$Pt(II) interstrand crosslink within a PNA / DNA duplex would induce too much steric distortion so that crosslink formation is not favourable. PNA / DNA duplex structures differ significantly from DNA duplex structures[167] and the steric effect of a *trans*-$(NH_3)_2$Pt(II) interstrand crosslink within a PNA / DNA duplex can differ significantly from that within a DNA duplex. An answer to these questions is not

yet available. For a detailed investigation of these features molecular modelling studies would be necessary.

## 6 Conclusions

Section 3 of this chapter describes the development of a solid-phase approach towards the synthesis of monofunctionally *trans*-Pt(II) modified homopyrimidine PNA oligomers. Building block **9** was quantitatively conjugated to the N-terminal amino group of the immobilized homopyrimidine PNA pentamer (**30**) (Scheme 2). In principle, this method allows the sequence-independent and site-specific monofunctional *trans*-Pt(II) modification of PNA oligomers. However, building block **9** has been shown to be incompatible with the forced ammonolysis conditions required for removal of the G-*i*Bu base protecting groups.[130] Therefore, this method is mainly suited for the synthesis of monofunctionally *trans*-Pt(II) modified homopyrimidine PNA sequences.

In section 4 of this chapter the development of a solid-phase synthesis method for the synthesis of monofunctionally *trans*-Pt(II) modified mixed purine / pyrimidine PNA oligomers is reported. This method involved first the design and synthesis of the *trans*-Pt(II) modified PNA building block **33** which has been shown to be entirely compatible with the applied PNA synthesis protocol according to method IV (Scheme 1). By contrast to solid-phase PNA synthesis according to method II and III (Scheme 1) method IV involves an acid-labile linker and acid-labile base protecting groups. Thus, removal of the base protecting groups and cleavage from the solid support is achieved under acidic conditions instead of ammonolysis. This difference renders method IV advantageous since the synthesized preplatinated building blocks are better compatible with acid treatment.

Building block **33** has been conjugated to the N-terminus of three different immobilized PNA sequences to yield the monofunctionally *trans*-Pt(II) modified PNA oligomers **43**, **44** and **45** in acceptable yields of 40 – 60 %. The major side-products in all coupling experiments were the respective unplatinated PNA (n-1)-mers, indicating that coupling of building block **33** to an immobilized PNA oligomer is somewhat less efficient compared to an unplatinated Fmoc / N-Bhoc protected PNA monomer. Reasons for this observation have been discussed but based on the experimental data an ultimate explanation is not possible. Despite this minor drawback the coupling yields obtained are still quite satisfactory. Furthermore, the

monofunctionally *trans*-Pt(II) modified PNA oligomers **43**, **44** and **45** have been successfully purified by reversed-phase HPLC. Thus, the method developed gives a practicable access to the synthesis of monofunctionally *trans*-Pt(II) modified mixed purine / pyrimidine oligonucleotide analogues of *any* desired sequence for potential application *both* in antigene *and* antisense strategy.

The monofunctionally *trans*-Pt(II) modified PNA oligomer **43** undergoes a crosslinking reaction with the complementary DNA sequence **46** yielding a *trans*-$(NH_3)_2$Pt(II) crosslinked PNA / DNA duplex as evidenced by MALDI-TOF mass spectrometry. The location of the interstrand crosslink has not unambiguously been established but the results of the gel-electrophoretic studies strongly suggest that it is located between the N-terminal guanine of the PNA part and the 3´guanine of 5´d(GCGAATG) (**46**). Thus, it can be assumed that sequence-specific recognition between **43** and **46** takes place prior to formation of a site-specific interstrand crosslink. The resulting structure is very likely the *trans*-$(NH_3)_2$Pt(II) crosslinked PNA / DNA duplex **47**.

The fact that **43** performs a sequence-specific crosslinking reaction with a complementary deoxyoligonucleotide demonstrates the potential application of the newly synthesized monofunctionally *trans*-Pt(II) modified PNA oligomers **43**, **44** and **45** in antisense strategy. It again underscores the impact of the developed solid-phase synthesis approach described in section 4 of this chapter.

# Chapter IV Effect of Pt(II) coordination to *N1* of adenine on Hoogsteen hydrogen bonding with thymine

## 1 Introduction

In DNA, the *N7* sites of guanine and adenine nucleobases are the major binding sites for the antitumor drug cisplatin.[169] The major coordination product is the 1,2 d(GpG) intrastrand crosslink followed by the 1,2 d(ApG) intrastrand crosslink. Interestingly, the latter is at least five times more mutagenic than the major d(GpG) adduct.[170]

Apart from the resulting geometric distortion of DNA, which is reasonably well investigated,[171] the Pt(II) electrophile effects electronic features of the coordinated nucleobase resulting in potential alteration of H bonding properties and base stacking. The effect caused by the electron withdrawing Pt(II) moiety on purines is e.g. reflected in significant changes of acid-base properties. For example, binding of Pt(II) to the guanine *N7* position acidifies the proton at the *N1* position by 1.5 - 2 log units.[166] As for adenine, an acidification of the *N1* position of approximately one logarithmical unit has been observed.[80]

A *N7*-platinated guanine within a DNA duplex still forms a Watson-Crick pair with cytosine, which has been manifested by means of NMR studies[173] and X-ray crystallography.[174-176] Furthermore, in a crystal, the model nucleobase 1-MeC was found to form Watson-Crick hydrogen bonds to the model compound *trans*-[Pt($NH_2CH_3$)$_2$(9-MeGH-*N7*)(1-MeC-*N3*)]$X_2$.[81] In solution, concentration-dependent $^1$H NMR studies of several *N7*-platinated guanine complexes and 1-MeC in DMSO demonstrated that Pt(II) binding at *N7* even stabilizes the Watson-Crick G / C pair, as demonstrated by an increase of the association constant.[177,178] These results are in agreement with theoretical studies, according to which metal ion binding to *N7* of guanine was calculated to stabilize the Watson-Crick G / C base pair in general.[179-181]

For adenine, it was proposed that metal ion binding at *N7* effects hydrogen bonding little[181] or not at all.[182] So far, no empirical studies exist adressing the question as to what extent *N1*- or *N7*-coordinated Pt(II) influences the Hoogsteen or Watson-Crick hydrogen bonding properties of adenine with thymine. In general, A / T base pairs possess a lower stability than G / C base pairs. As a consequence, observation of hydrogen bonds between A and T is not possible in hydrogen bonding solvents like DMSO.[183] The poor hydrogen-

bonding solvent chloroform, however, has been shown to be a convenient medium for investigation of hydrogen bonding between chloroform-soluble adenine and thymine derivatives.[184] An investigation of hydrogen bonding properties of a platinated adenine with thymine should also be possible in this solvent if chloroform-soluble Pt(II)-adenine complexes were available. With regard to the fact that the plethora of adenine model compounds that have so far been synthesized,[185,186] do not fulfil this criterion, the synthesis of chloroform-soluble Pt(II)-adenine complexes is required before hydrogen bonding studies can be conducted.

## 2 Synthesis and characterization of the chloroform-soluble complexes *trans*-[Pt($NH_2CH_3$)$_2$(CHMA)(CHMT)]$^+NO_3^-$ (50) and *trans*-[Pt($NH_2CH_3$)$_2$(CHMT)(TBS-ado)]$^+BF_4^-$ (51)

### 2.1 Synthesis

Pt(II) binding to naturally occurring adenine nucleobases and their *N9*-blocked model compounds mostly occurs through the endocyclic *N1* and *N7* nitrogen atoms.[187] Rarely, binding to *N3* is observed.[188] From model chemistry it is known that for Pt(II) the coordination behaviour is governed by pH. At acidic pH the most basic site *N1* ($pK_a \cong 4$) is protonated and consequently Pt(II) coordination takes place preferentially at the *N7* position. At $pH \geq 4$, when both *N1* and *N7* are deprotonated, usually a mixture of linkage isomers is formed. For example, monofunctional Pt(II)dien distributes almost equally between the *N7* and *N1* sites in neutral adeosine, and in 5´AMP it slightly favors the *N7* site.[189,190]

Reasons for the distribution patterns with Pt(II) are not yet very well understood, although it appears that the exocyclic amino group exercises a steric hindrance, which is larger for metals approaching *N1* than *N7*.[191-194] Similarly, ancillary ligands already bonded to Pt(II) effect the distribution between the two endocyclic nitrogens.[195] The adenine *N1* position is the themodynamically more stable binding site for Pt(II) as compared to *N7*. In agreement with this, migration of a monofunctional Pt(II) moiety from the *N7* to the *N1* position at high temperatures has been observed.[196]

So far, all platination reactions in combination with adenine model nucleobases have been carried out in an aqueous medium. Not much is known about coordination of Pt(II) to this base in an aprotic solvent.

In order to achieve solubility of Pt(II)-adenine complexes in chloroform, a prerequisite for hydrogen bonding studies, highly lipophilic adenine derivatives as ligands are required. To this end, the adenine derivatives 9-*N*-cyclohexylmethyladenine (CHMA, **48**) and 2´,3´,5´-tris-(*tert*-butyldimethylsilyl)-adenosine (TBS-ado, **49**) have first been synthesized.

Subsequently, **48** and **49** have been reacted with *trans*-$[Pt(NH_2CH_3)_2(CHMT)(DMF)]^+NO_3^-$ (**7b**) and *trans*-$[Pt(NH_2CH_3)_2(CHMT)(DMF)]^+BF_4^-$ (**7a**), respectively, in DMF to yield the chloroform-soluble complexes **50** and **51** (Scheme 1). Surprisingly, in both cases platination proceeds with high regioselectivity yielding the respective *N1*-linkage isomers *trans*-$[Pt(NH_2CH_3)_2(CHMA)(CHMT)]^+NO_3^-$ (**50**) and *trans*-$[Pt(NH_2CH_3)_2(CHMA)(TBS\text{-}ado)]^+BF_4^-$ (**51**) (Scheme 1).

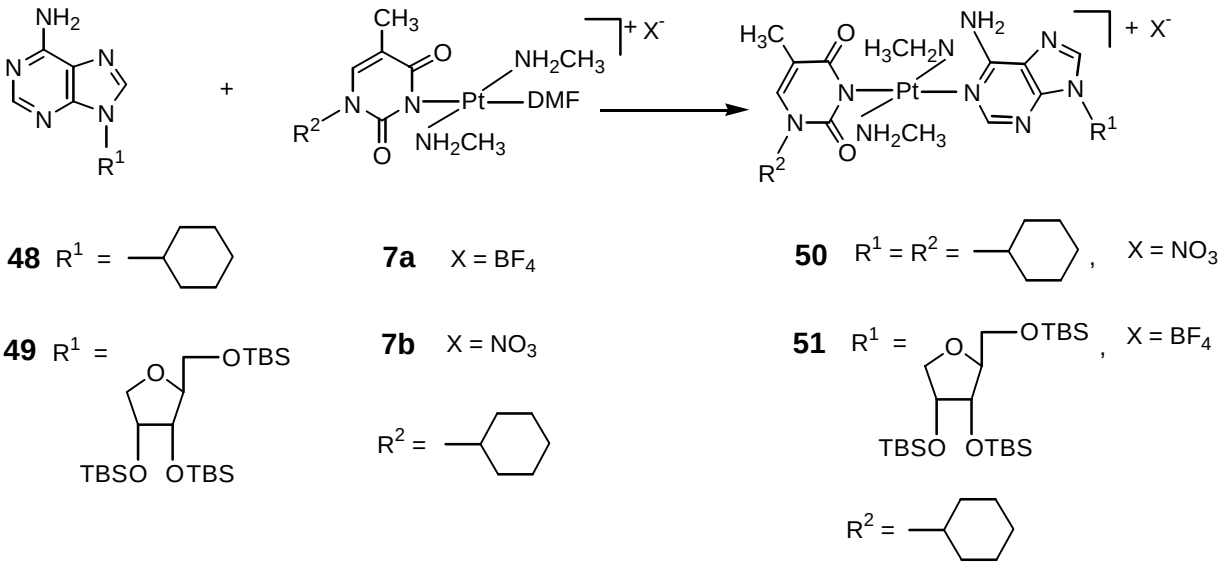


Scheme 1: Synthesis of **50** and **51** by reaction of **48** with **7b** and **49** with **7a**.

## 2.2 NMR spectroscopic characterization

### 2.2.1 *Trans*-[Pt($NH_2CH_3$)$_2$(CHMA)(CHMT)]$^+NO_3^-$ (50)

*Trans*-[Pt($NH_2CH_3$)$_2$(CHMA)(CHMT)]$^+NO_3^-$ (**50**) has been fully characterized by NMR spectroscopic methods. Tables 1, 2 and 3 list the $^1$H, $^{13}$C and $^{195}$Pt NMR data for compounds **48** and **50**. The $^{195}$Pt NMR spectrum of **50** in deuterated methanol shows one signal at -2584 ppm which is consistent with a $PtN_4$ coordination sphere.[135,136]

Table 1: $^1$H NMR data for **48** and **50**

| | A-H2 | A-H8 | A-N9-$CH_2$ | A-6-$NH_2$ | T-H6 | T-$CH_3$ | T-N1-$CH_2$ | Pt-$NH_2$ | Pt-$NH_2C\mathit{H}_3$ |
|---|---|---|---|---|---|---|---|---|---|
| **48**[a] | s, 8.37 | s, 7.75 | d, 4.02 | s, 5.61 | | | | | |
| **48**[b] | s, 8.19 | s, 8.15 | d, 4.06 | s, 7.18 | | | | | |
| **48**[c] | s, 8.18 | s, 8.08 | d, 4.06 | n.o. | | | | | |
| **50**[a] | s, 8.69 | s, 7.63 | d, 3.94 | s, 9.07 | s, 6.91 | s, 1.70 | d, 3.65 | m, 5.13; m, 4.50 | t, 2.21 |
| **50**[b] | s, 8.85 | s, 8.44 | d, 4.15 | s, 9.30 | s, 7.38 | s, 1.82 | d, 3.50 | m, 5.11 | t, 2.24 |
| **50**[c] | s, 9.0 | 8.19 | d, 4.12 | n.o. | s, 7.32 | s, 1.92 | d, 3.64 | m, 4.55 | t, 2.15 |

[a] $CDCl_3$, [b] DMF-$d_7$, [c] $CD_3OD$; n.o. = not observed

Table 2: $^{13}$C NMR data for **48** and **50**

| | A-C6 | A-C2 | A-C4 | A-C8 | A-C5 | A-C9 | T-C5 | T-C6 | T-CO(4) | T-CO(2) |
|---|---|---|---|---|---|---|---|---|---|---|
| **48**[a] | 155.6 | 152.9 | 150.3 | 140.9 | 119.6 | 50.0 | | | | |
| **50**[b] | 157.6 | 155.3 | 149.4 | 144.5 | 120.5 | 51.1 | 109.8 | 143.0 | 174.0 | 159.0 |

[a] $CDCl_3$, [b] $CD_3OD$

Table 3: $^{195}$Pt NMR data for **50**

| solvent | $CDCl_3$ | $CD_3OD$ | DMF-$d_7$ |
|---|---|---|---|
| δ (ppm) | - 2599 | - 2584 | - 2594 |

Compared to free CHMA (**48**) in $CDCl_3$, the A-H2 resonance in **50** has been shifted downfield by 0.32 ppm, whereas the A-H8 proton undergoes a slight upfield shift of 0.11 ppm. Furthermore, a remarkable downfield shift of 3.46 ppm for the resonance of the exocyclic amino protons is observed in **50**.

In DMF-$d_7$, the low-field shifts of the A-H2 and A-H8 resonance in **50** amount to 0.66 and 0.29 ppm, respectively, compared to **48**. Furthermore, a downfield shift of 2.12 ppm for the resonance of the exocyclic amino protons in **50** is observed.

In $CD_3OD$, low-field shifts of 0.81 ppm for A-H2 and 0.11 ppm for A-H8 are observed for **50**, in agreement with reported data.[196-199]

Coordination of Pt(II) to the *N1*-position in **50** is evidenced by two-dimensional NMR experiments, a $^{195}$Pt-$^{1}$H HMQC experiment and pH$^*$-dependent $^{1}$H NMR measurements. Figure 1 displays the $^{1}$H,$^{1}$H NOESY spectrum of **50**. The A-H8 proton is identified by its crosspeak with the A-N9-$CH_2$ protons whereas the A-H2 proton shows crosspeaks to the amino protons and the methyl group protons of the methylamine ligands. Furthermore, as expected, the T-H6 resonance in **50** exhibits crosspeaks to the T-N1-$CH_2$ and the T-5-$CH_3$ resonances.

A long-range $^{1}$H, $^{13}$C experiment (Figure 2) reveals the expected coupling of A-H2 with A-C2 ($^{1}$J), A-C4 ($^{3}$J) and A-C6 ($^{3}$J) as well as of A-H8 with A-C8 ($^{1}$J), A-C4 ($^{3}$J), A-C5 ($^{3}$J), and A-C9 ($^{3}$J). The assignment of the $^{13}$C NMR resonances (Table 2) of the CHMA ligand is based on literature data for 9-*N*-methyladenine[200,201] as well as for [Pt(dien)(ado-*N1*)].[196]

Finally, the $^{1}$H,$^{195}$Pt HMQC experiment (Figure 3) shows coupling ($^{3}$J = 20 Hz) between A-H2 and the $^{195}$Pt resonance.

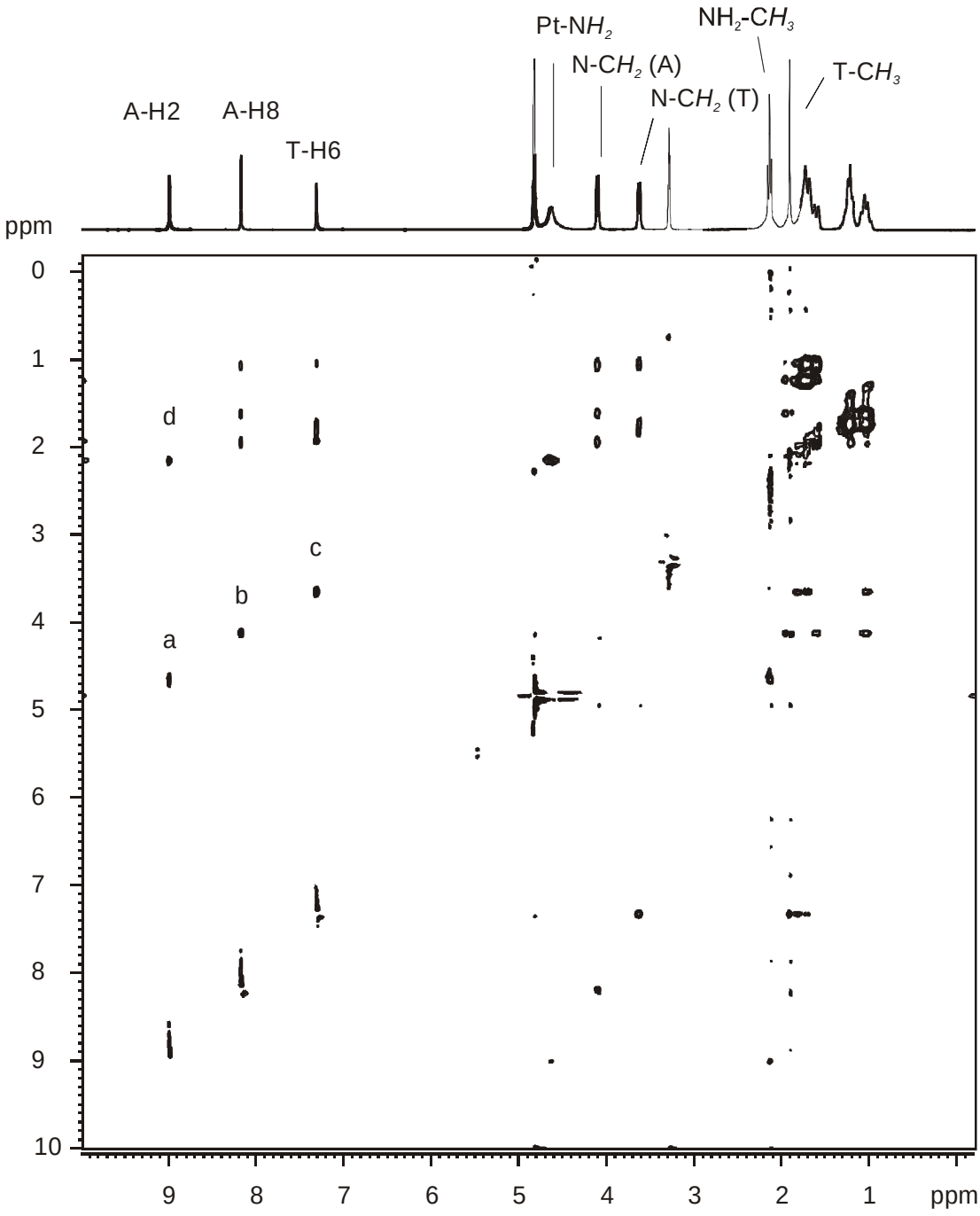


Figure 1: $^1$H, $^1$H NOESY spectrum of **50** in $CD_3OD$;
crosspeaks: a: A-H2 / Pt-$NH_2$, b: A-H8 / A-N9-$CH_2$, c: T-H6 / T-N1-$CH_2$,
d: A-H2 / Pt-$NH_2C$*H*$_3$.

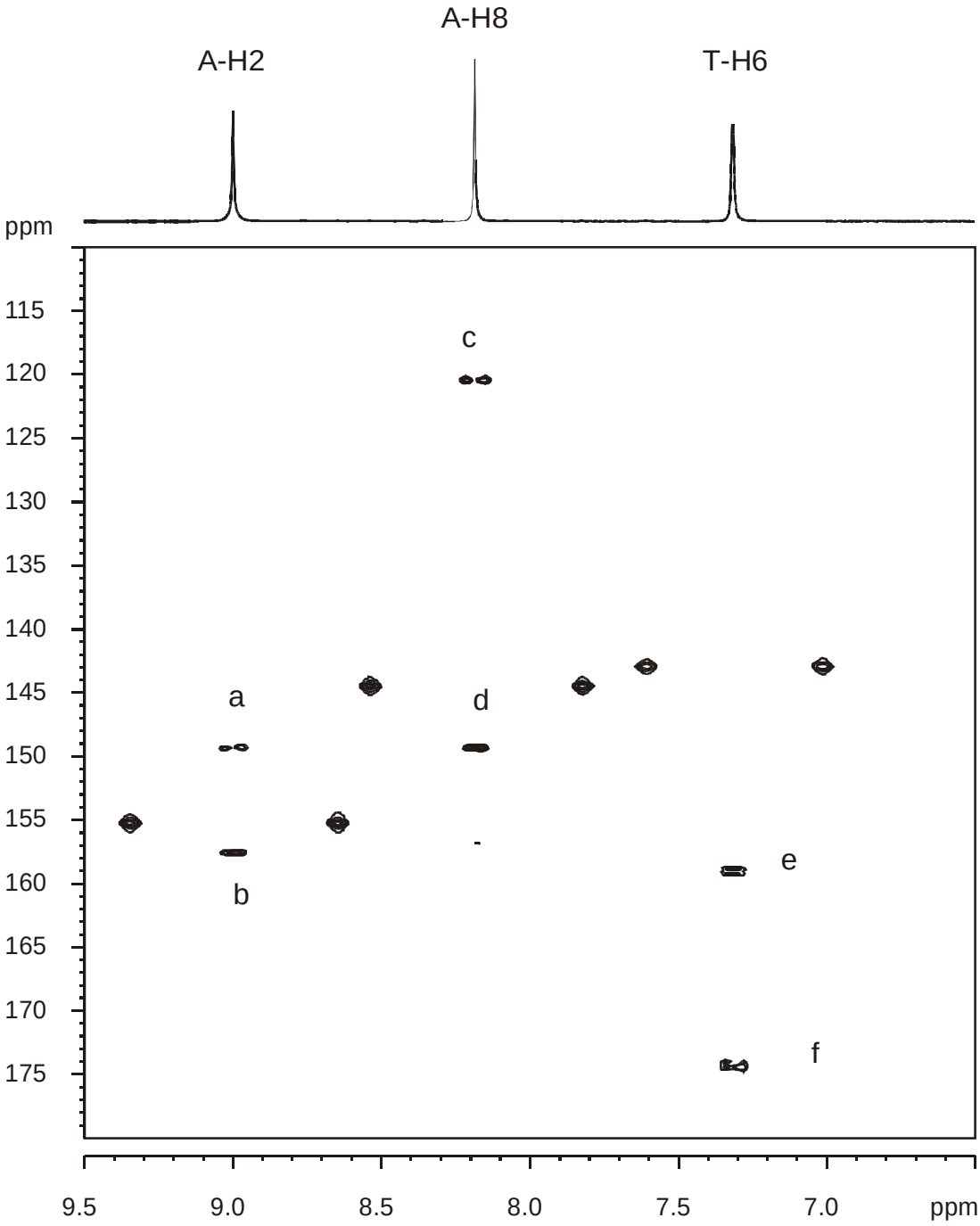


Figure 2: Long-range $^{13}C$, $^{1}H$ COSY spectrum of **50** in $CD_3OD$;
a: A-H2 / A-C4 ($^{3}J$), b: A-H2 / A-C6 ($^{3}J$), c: A-H8 / A-C5 ($^{3}J$),
d: A-H8 / A-C4 ($^{3}J$), e: T-H6 / T-CO(2) ($^{3}J$), f: T-H6 / T-CO(4) ($^{3}J$).

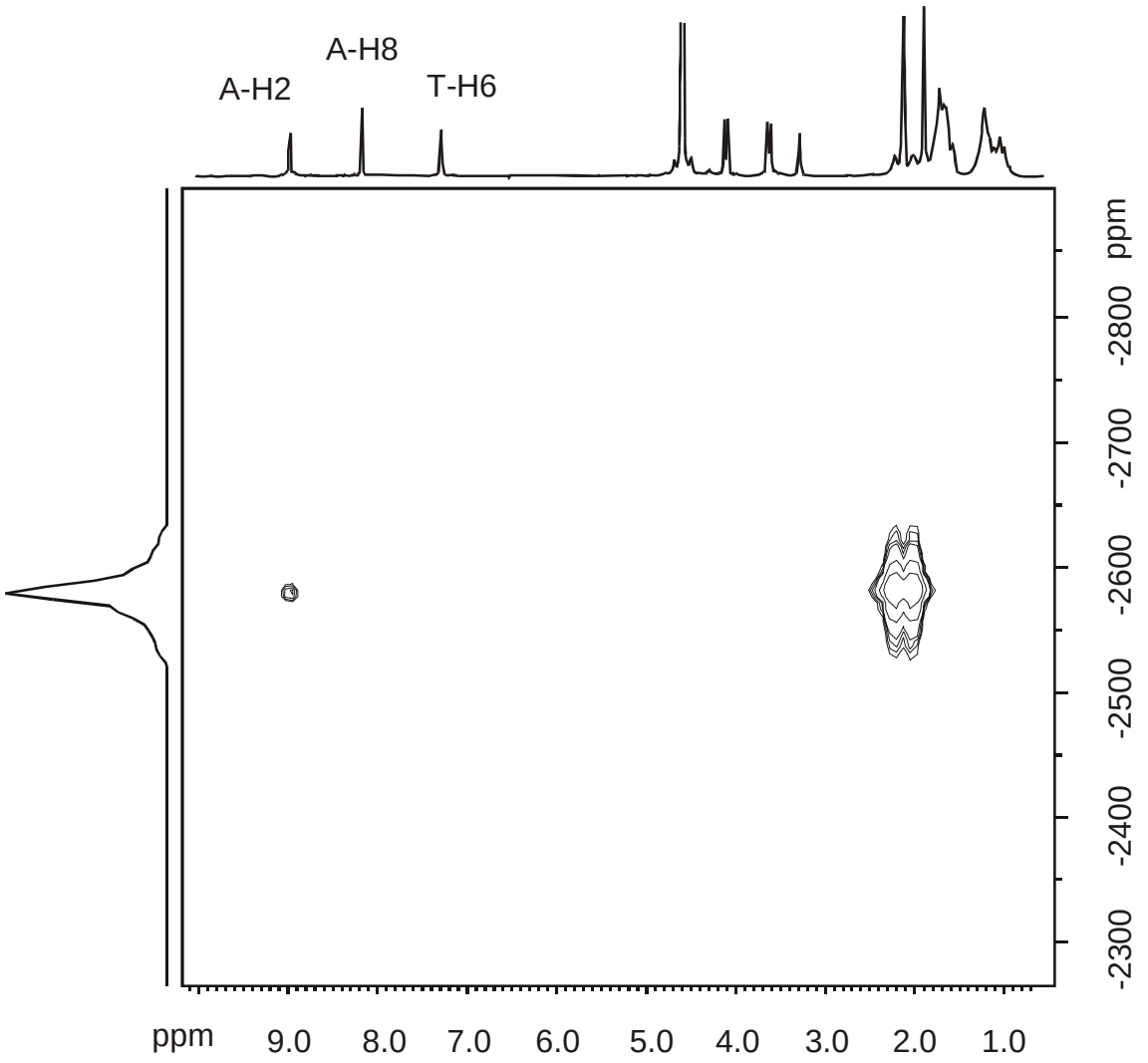


Figure 3: $^{1}H,^{195}Pt$ HMQC spectrum of **50** in $CD_3OD$.

Coordination of Pt(II) to the adenine *N1* position in **50** was furthermore evidenced by $pH^*$-dependent $^{1}H$ NMR measurements (Figure 4). At a characteristically low pH the A-H8 resonance of **50** undergoes a large downfield shift due to protonation of the A-*N7* position whereas the effect on the $^{1}H$ chemical shift of the A-H2 resonance is less pronounced (Figure 4). From the $pH^*$-dependent $^{1}H$ NMR chemical shifts of the A-H2 and A-H8 resonances of **50** in $D_2O$ a $pK_a$ value of 0.9 for (de)protonation of the A-*N7* position has been derived, in agreement with results for similar compounds.[80]

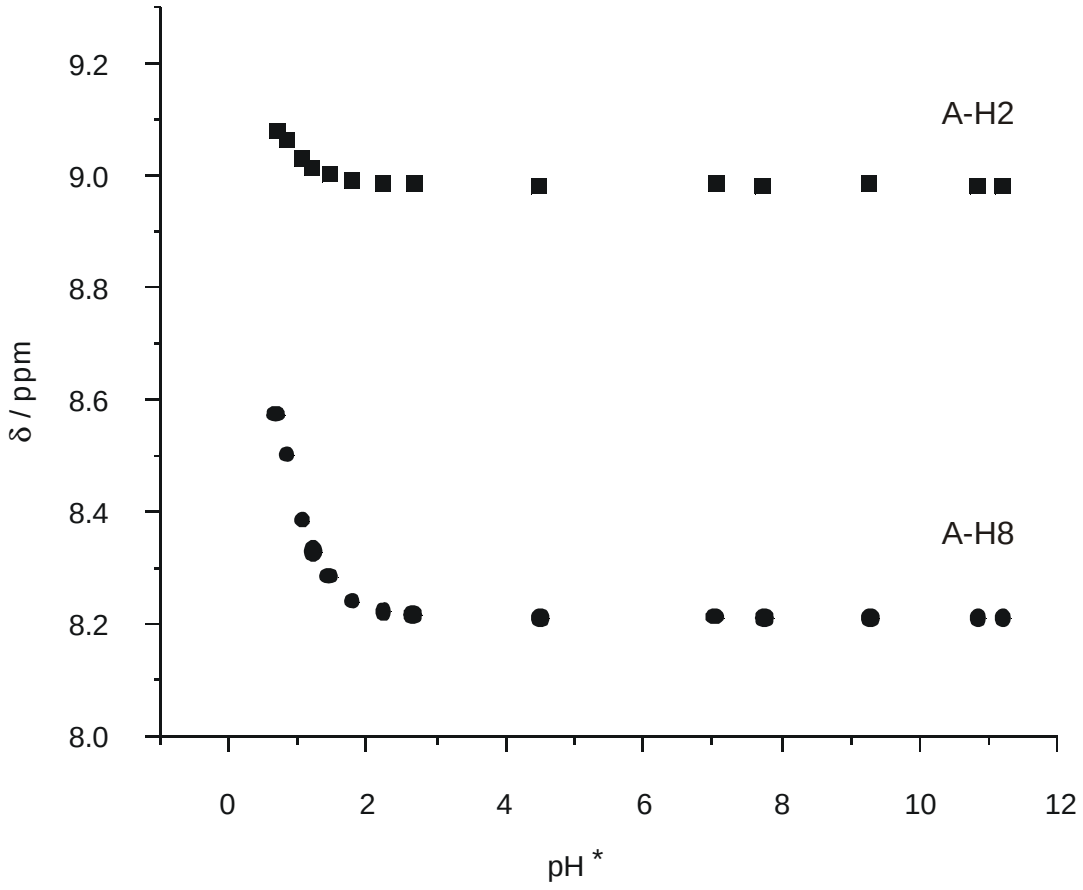


Figure 4: pH*-dependence of the A-H2 and A-H8 $^1$H NMR resonances of **50**.

Temperature-dependent $^1$H NMR studies of complex **50** have been carried out in $D_2O$. In $D_2O$, A-H2 occurs as two resonances (1:1) up to ca. 318 K, irrespective of pH* (Figure 5). Above this temperature, coalescence takes place and this process is fully reversible. A similar splitting of A-H2 in related complexes has been reported earlier[80] and is assigned to hindered rotation of the nucleobases about the Pt-N bonds. This hindered rotation depends on the presence of methylamine ligands (the $NH_3$ analogues do not display this behaviour) and the solvent water. The role of water could be to bridge exocyclic groups of the two *trans*-positioned bases, as seen in the X-ray crystal structure of *trans*-[Pt($NH_2CH_3$)$_2$(1-MeT)(9-MeA-*N1*)]$ClO_4$·3.25$H_2O$.[80] While direct hydrogen bonding between the exocyclic groups of the two bases is excluded on steric grounds (distance ca. 4 Å), the dual function of a water molecule to act as a H bond acceptor for A-N(6)$H_2$ and a H donor for T-*O4* or T-*O2* is ideal for this purpose. The rate of rotation at the coalescence point can be estimated to $k_c = 2.22\ \Delta\nu = 27.33$ Hz. Furthermore, the rotational barrier at the coalescence temperature is calculated to 69.30 kJ mol$^{-1}$.[172]

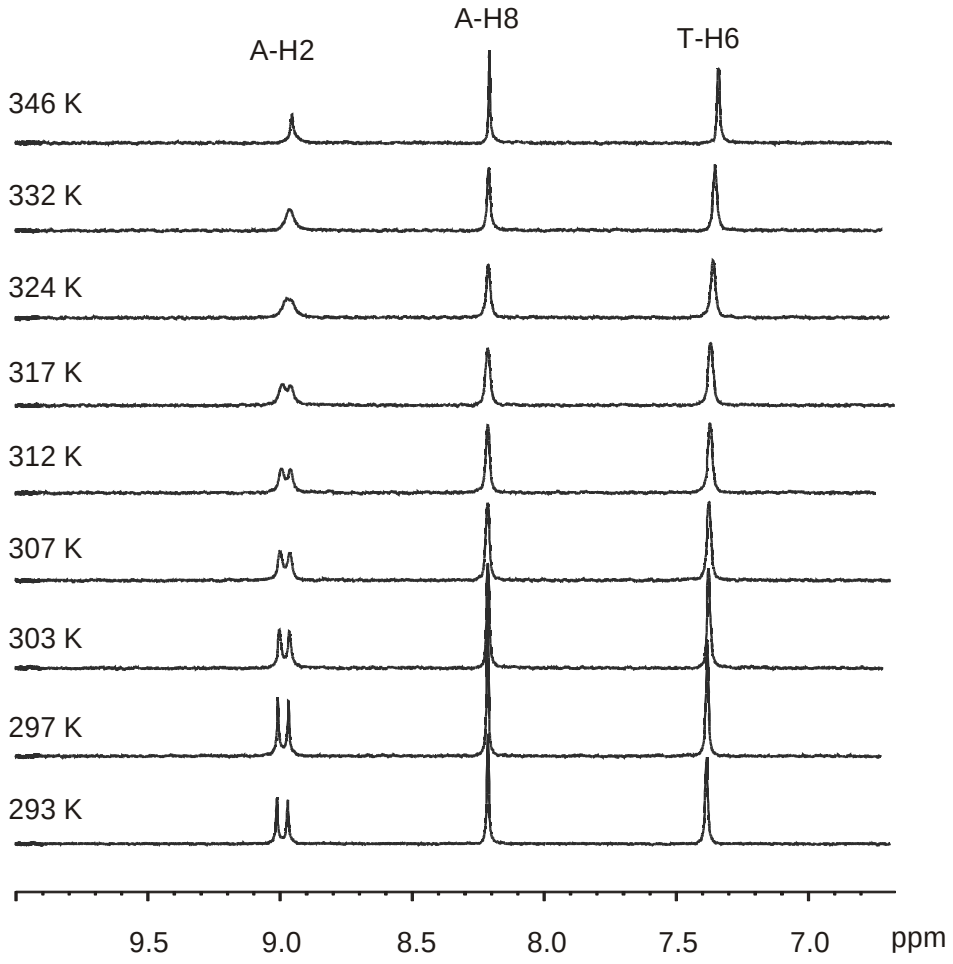


Figure 5: Temperature-dependent $^{1}H$ NMR spectra of **50** in $D_2O$.

### 2.2.2 *Trans*-[Pt(NH$_2$CH$_3$)$_2$(CHMT)(TBS-ado)]$^{+}$BF$_4^{-}$ (51)

All signals in *trans*-[Pt(NH$_2$CH$_3$)$_2$(CHMT)(TBS-ado)]$^{+}$BF$_4^{-}$ (**51**) have been assigned by two-dimensional NMR spectroscopy. Thus, A-H8 in **51** is identified by its crosspeaks with the H1´, H2´ and H3´protons of the ribose moiety in the $^{1}H$, $^{1}H$ NOESY spectrum (Figure 6). The A-H2 resonance exhibits crosspeaks to the resonances of the amino protons and the methyl protons of the methylamine ligands. A long range $^{1}H$, $^{13}C$ COSY experiment (Figure 7) shows the expected coupling of A-H8 with A-C8 ($^{1}J$), A-C4 ($^{3}J$), A-C5 ($^{3}J$), whereas A-H2 displays couplings with A-C2 ($^{1}J$), A-C4 ($^{3}J$) and A-C6. The assignment of the $^{13}C$ NMR resonances of the TBS-ado ligand of **51** (Table 5) is based on literature data for adenosine and [Pt(dien)(ado-*N1*)]$^{2+}$.[196]

The $^{195}$Pt NMR spectrum of **51** in $CD_3OD$ shows one signal at -2580 ppm which is comparable with the $^{195}$Pt NMR spectrum of **50** in the same solvent and consistent with a $PtN_4$ coordination sphere.[135,136]

The $^{1}$H NMR spectrum of **51** in $CDCl_3$ (Table 4) shows characteristic low-field shifts of 0.5 ppm for the A-H2 resonance and 0.09 ppm for the A-H8 resonance compared to the free ligand TBS-ado (**49**) in the same solvent.[199-201] The protons of the exocyclic amino group of **51** show a very significant low-field shift of 3.25 ppm compared to free TBS-ado (**49**).

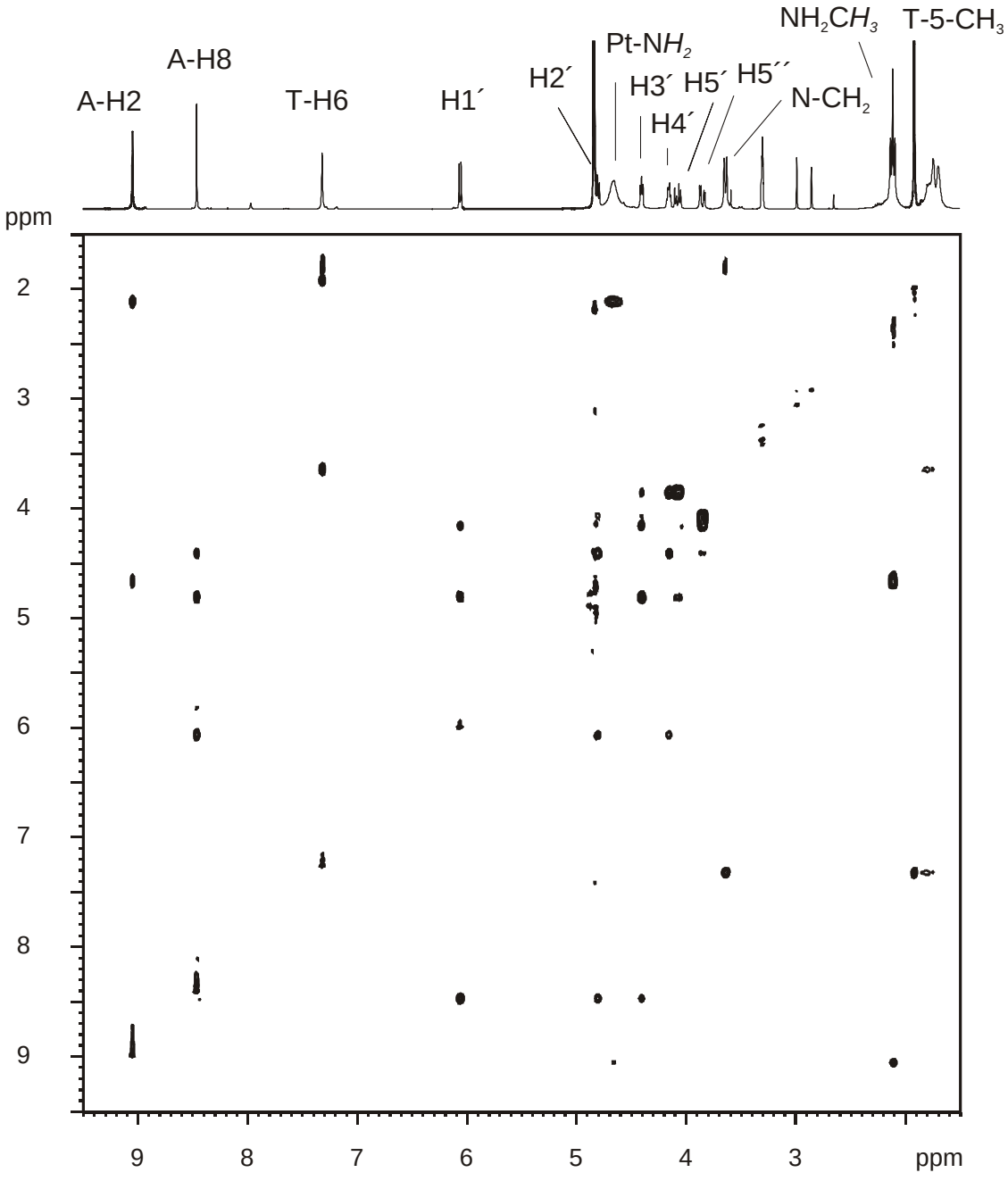


Figure 6: $^{1}$H, $^{1}$H NOESY spectrum of **51** in $CD_3OD$.

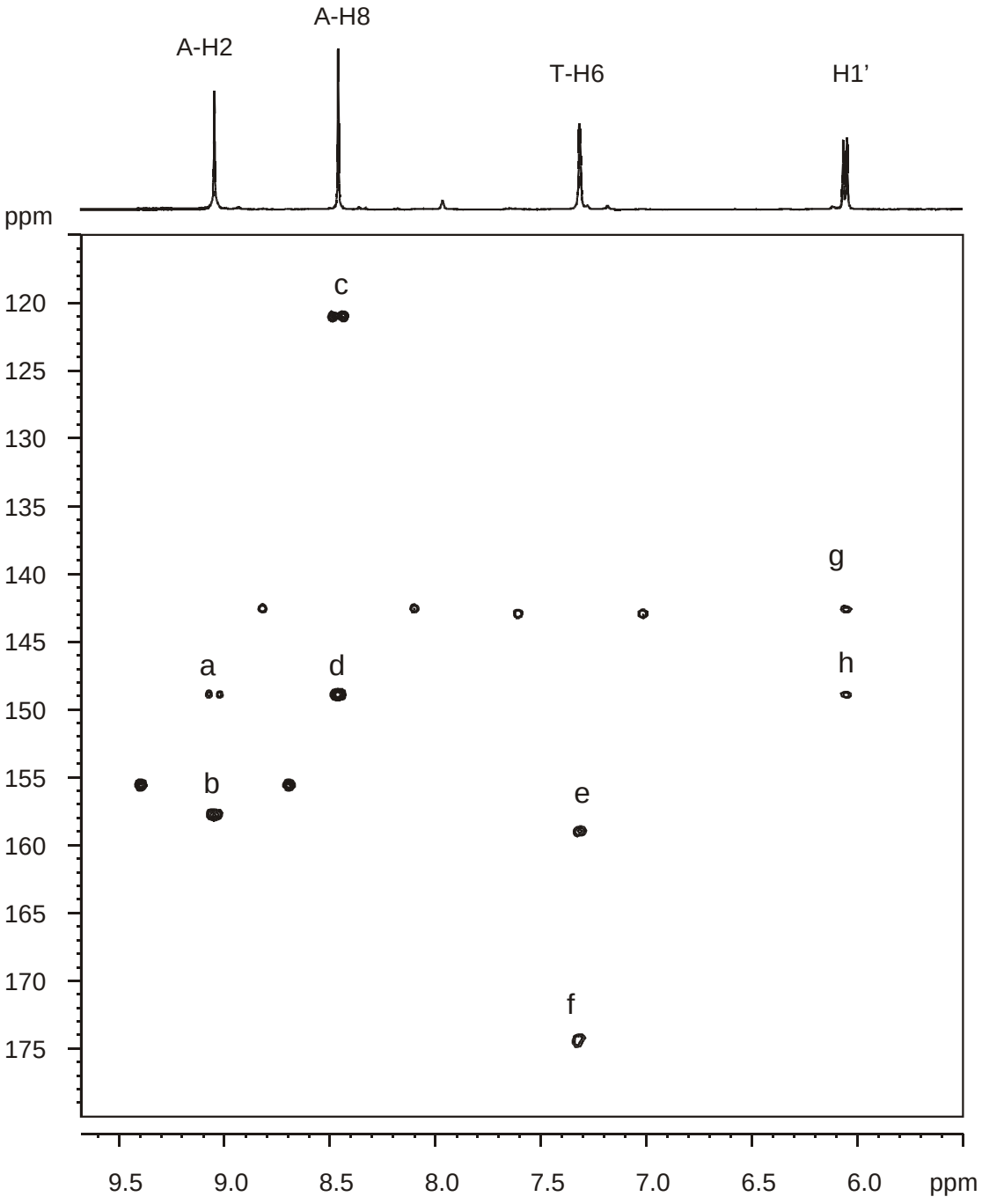


Figure 7: $^{13}C$, $^{1}H$ long-range COSY spectrum of **51**; a: A-H2 / A-C4 ($^{3}J$), b: A-H2 / A-C6 ($^{3}J$), c: A-H8 / A-C5 ($^{3}J$), d: A-H8 / A-C4 ($^{3}J$), e: T-H6 / T-CO(2), f: T-H6 / T-CO(4), g: H1´/ A-C8, f: H1´ / A-C4.

Table 4: $^{1}$H NMR data for **49** and **51**

| | A-H2 | A-H8 | A-6-$NH_2$ | T-H6 | T-5-$CH_3$ | Pt-$NH_2$ | Pt-$NH_2C\mathit{H}_3$ |
|---|---|---|---|---|---|---|---|
| **49**[a] | s, 8.16 | s, 8.34 | s, 5.51 | - | - | - | - |
| **51**[a] | s, 8.66 | s, 8.43 | s, 8.76 | s, 6.92 | s, 1.92 | m, 4.47,<br>m, 3.82 | t, 2.27,<br>t, 2,10 |
| **51**[b] | s, 9.05 | s, 8.46 | n.o. | s, 7.32 | s, 1.91 | m, 4.65 | t, 2.11 |

Table 4 (continued)

| | H1´ | H2´ | H3´ | H4´ | H5´ | H5´´ |
|---|---|---|---|---|---|---|
| **49**[a] | d, 6.02 | dd, 4.69 | dd, 4.32 | m, 4.12 | dd, 4.03 | dd, 3.79 |
| **51**[a] | d, 5.95 | * | * | * | dd, 3.66 | dd, 3.52 |
| **51**[b] | d, 6.06 | dd, 4.71 | t, 4.40 | m, 4.16 | dd, 4.07 | dd, 3.55 |

[a] $CDCl_3$, [b] $CD_3OD$; * not assignable due to overlap

Table 5: $^{13}$C NMR data for **51**

| | A-C6 | A-C2 | A-C4 | A-C8 | A-C5 | T-C5 | T-C6 | T-CO(4) | T-CO(2) |
|---|---|---|---|---|---|---|---|---|---|
| **51**[b] | 157.7 | 155.6 | 148.9 | 142.6 | 121.6 | 110.5 | 142.9 | 174.4 | 158.9 |

Table 5 (continued)

| | C1´ | C2´ | C3´ | C4´ | C5´ |
|---|---|---|---|---|---|
| **51**[b] | 89.7 | 77.0 | 73.6 | 87.3 | 63.8 |

[b] $CD_3OD$

## 2.3 Discussion

The reactions of **48** and **49** with *trans*-[Pt($NH_2CH_3$)$_2$(CHMT)(DMF)]$^+NO_3^-$ (**7b**) and *trans*-[Pt($NH_2CH_3$)$_2$(CHMT)(DMF)]$^+BF_4^-$ (**7a**), respectively, in DMF lead with high regioselectivity to formation of the respective *N1*-linkage isomers *trans*-[Pt($NH_2CH_3$)$_2$(CHMA)(CHMT)]$^+NO_3^-$ (**50**) and *trans*-[Pt($NH_2CH_3$)$_2$(CHMA)(TBS-ado)]$^+BF_4^-$ (**51**) (Scheme 1). The reason for this coordination behaviour is not straightforward. In the analoguous reaction of *trans*-[Pt($NH_2CH_3$)$_2$(1-MeT)($H_2O$)]$^+$ with 9-*N*-methyladenine in aqueous solution (pH 5.5, 48 h, 60 °C) only a slight preference for the adenine *N1* position as the Pt(II) coordination site has been observed.[80] Thus, solvent effects may influence the coordination behaviour. Furthermore, the DMF ligand within **7a** and **7b** is sterically more demanding than the aqua ligand in *trans*-[Pt($NH_2CH_3$)$_2$(1-MeT)($H_2O$)]$^+$ which may influence the distribution between *N1* and *N7* platination. Based on the experimental data an explanation for the observed regioselective *N1* platination of the adenine derivatives **48** and **49** is not available.

# 3 Investigation of hydrogen bonding interactions of the *N1*-platinated complexes 50 and 51 with 1-*N*-cyclohexylmethylthymine (5)

## 3.1 General considerations

A prediction to what extent Pt(II) binding to adenine *N1* will effect the Hoogsteen hydrogen bonding properties of adenine with the complementary thymine, is difficult. On the one hand, an acidification of the protons of the exocyclic amino group is expected, resulting in an increase of the hydrogen bond donating ability. On the other hand, the electron-withdrawing Pt(II) decreases the basicity of the A-*N7* position and therefore its hydrogen bond accepting ability.

The thymine derivative **5** can be hydrogen-bonded to **50** and **51** both according to Hoogsteen and reverse Hoogsteen geometry (Figure 8). The nucleobase triple in which **5** forms Hoogsteen hydrogen bonds to **50** (or **51**) represents a model of a metalated nucleobase triple within parallel triplex DNA in which the two strands of the Watson-Crick duplex are crosslinked by a *trans*-$a_2$Pt(II) moiety (cf. chapters I and III). Thus, also from this point of view an investigation of the alteration of hydrogen bonding properties due to platination seems relevant.

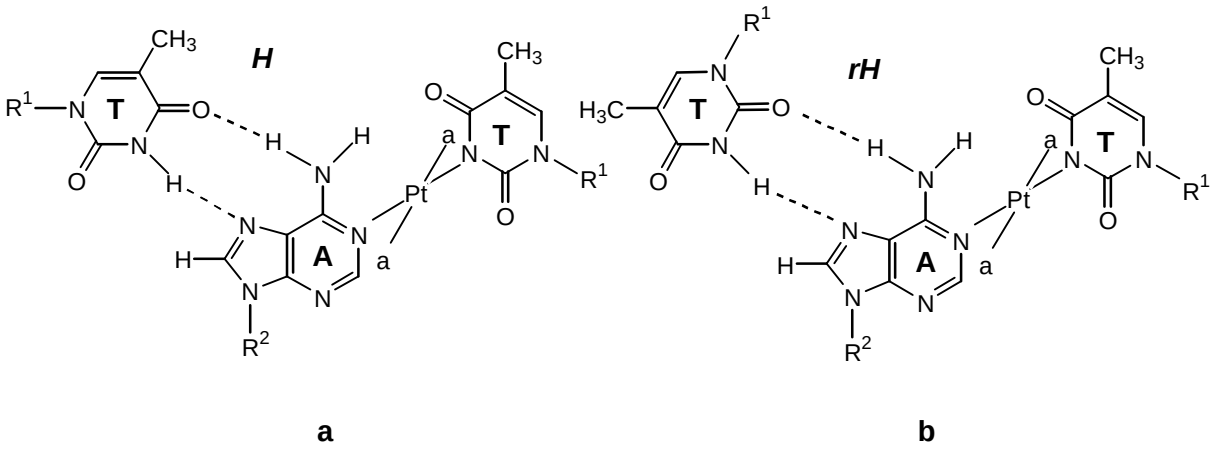


Figure 8: Hydrogen-bonded associates of **50** and **51** with **5** according to a) Hoogsteen geometry and b) reverse Hoogsteen geometry.

### 3.2 Concentration-dependent $^1$H NMR studies in $CDCl_3$

$^1$H NMR chemical shifts of H-bonded protons can be used as indicators of the hydrogen bond strength.[202] Thus, H bond formation results in downfield shifts of the protons involved. From concentration-dependent $^1$H NMR measurements equilibrium constants for the association of the respective species can be derived. However, it has to be taken into account that $^1$H NMR data obtained at RT represent averages over all coexisting H-bonded associates and do not allow a detailed evaluation of type and relative population of these in solution.

In order to study the influence of Pt(II) bound to the adenine *N1* position on the overall association with thymine, concentration-dependent $^1$H NMR measurements of an equimolar mixture of **50** and 1-*N*-cyclohexylmethylthymine (**5**) in deuterated chloroform were carried out. For comparison, concentration-dependent $^1$H NMR measurements of an equimolar mixture of CHMA (**48**) and **5** as well as pure **5** (Figure 9) were performed at RT.

From Figure 9 it is evident that upon dilution of the equimolar **48** / **5** mixture, both the T-NH (curve a) and the A-$NH_2$ resonances (curve e) undergo significant $^1$H NMR highfield shifts. The highfield shift of 2.84 ppm for the T-NH resonance is more pronounced than that of 0.71 ppm observed for the A-$NH_2$ resonance. This is largely due to the fact that for the two A-$NH_2$ protons only an averaged signal is observed. From these data, an association constant of 56.5 ± 9 $M^{-1}$ was calculated (Table 6), which is in agreement with reported data.[203]

Upon dilution of the solution of **5** in $CDCl_3$, the T-NH resonance similarly shifts to higher field (Figure 9). The concentration-dependent highfield shift of 0.86 ppm is significantly less pronounced than for the T-NH resonance in the **5** / **48** mixture. Furthermore, the T-NH resonance of pure **5** in $CDCl_3$ appears at all concentrations at higher field than the T-NH resonance of the **5** / **48** mixture. This illustrates that hydrogen bonds between homodimers of **5** are weaker than that in **5** / **48** pairs. An association constant of 4.72 ± 0.23 $M^{-1}$ for the self-association of **5** has been calculated (Table 6), again in agreement with literature data.[203-205]

Upon dilution of the equimolar **50** / **5** mixture, only a highfield shift of the T-NH resonance of 1.18 ppm occurs, whereas the chemical shift of the A-$NH_2$ resonance remains largely unaffected and actually undergoes a slight *downfield* shift of 0.09 ppm (Figure 9). The concentration-dependent $^1$H NMR chemical shift of the T-NH proton in the **50** / **5** mixture is almost the same as for pure **5**. The T-NH resonance of **5** in the **50** / **5** mixture appears at only slightly lower field compared to the T-NH resonance of the pure **5** solution. This observation leads to the conclusion that within the **50** / **5** mixture the T-NH of **5** is not engaged in strong

hydrogen bonds like e.g. in the **48** / **5** mixture. However, hydrogen bonding interactions between **50** and **5** might be present to some extent to account for the slight downfield shift of the T-NH relative to the T-NH of the pure **5** solution.

Taken together, the observations suggest that hydrogen bonding interactions between **50** and **5** are minimal and that **5** undergoes self-association rather than pairing with **50** in a Hoogsteen or reverse Hoogsteen type fashion.

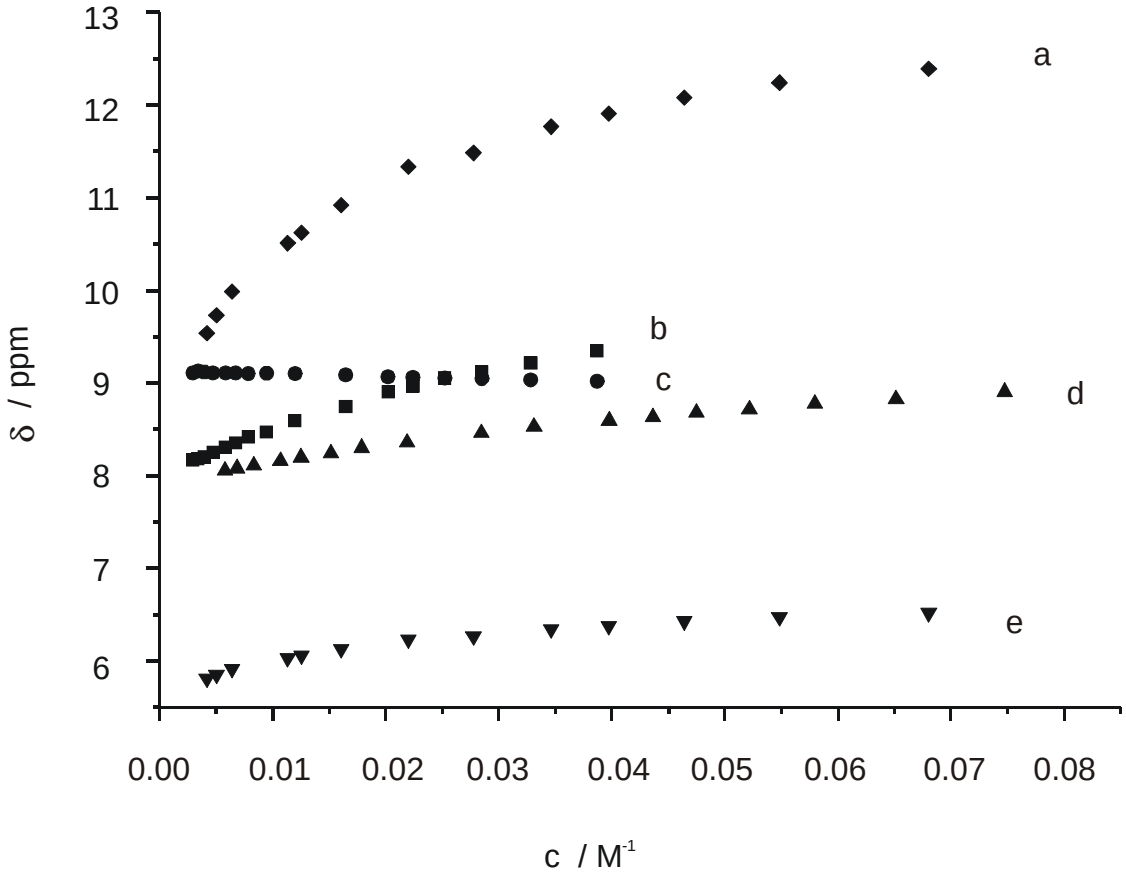


Figure 9: Concentration-dependent chemical shifts of the T-NH and A-$NH_2$ protons a: T-NH (**48** / **5**), b: T-NH (**50** / **5**), c: A-$NH_2$ (**50** / **5**), d: T-NH (**5** / **5**), e: A-$NH_2$ (**48** / **5**).

Table 6 : association constants

| | |
|---|---|
| A / T | $56.5 \pm 9\ M^{-1}$ |
| T / T | $4.72 \pm 0.23\ M^{-1}$ |

### 3.3 Temperature-dependent $^1$H NMR studies in $CDCl_3$

If hydrogen bonds according to the Hoogsteen or reverse Hoogsteen pattern between **50** and **5** and **51** and **5** were present at low temperatures, both the T-NH and the A-$NH_2$ resonances should undergo highfield shifts upon raising the temperature. To this end, temperature-dependent $^1$H NMR spectra of equimolar **50** / **5** and **51** / **5** mixtures in $CDCl_3$ have been recorded (Figure 10).

Figure 10 shows the temperature-dependent $^1$H NMR spectra of an equimolar **50** / **5** mixture in $CDCl_3$. Upon raising the temperature, only the T-NH resonance shifts to higher field, whereas the A-$NH_2$ resonance remains largely unaffected. Below 270 K the A-$NH_2$ resonance initially splits up into two and eventually into three resonances. This is probably due to hindered rotation of the exocyclic amino group in combination with hindered nucleobase rotation. It is noted that its chemical shift virtually does not change. Above 285 K the T-NH resonance even appears at higher field than the A-$NH_2$ resonance.

A similar temperature dependence of the T-NH and the A-$NH_2$ resonances is seen for the equimolar **51** / **5** mixture in $CDCl_3$ (Figure 11). In Figure 11 the temperature-dependent shifts of the T-NH resonance for the equimolar **50** / **5** and **51** / **5** mixtures as well as for pure **5** in $CDCl_3$ are summarized. It is evident, that despite some differences in absolute values, in all three cases the temperature-dependent shifts of the T-NH resonances are rather similar. The T-NH resonance of **5** within the **50** / **5** and the **51** / **5** mixtures appears at all temperatures at slightly lower field than the T-NH resonance of the pure **5** system. This could be due to the presence of a minimal amount of hydrogen bonding interactions between **50** and **5** as well as between **51** and **5**. However, the observation that the concentration-dependence of the T-NH resonance is almost the same as for the pure **5** leads to the conclusion that in the presence of **50** and **51**, self-association of 1-*N*-cyclohexylmethylthymine (**5**) prevails.

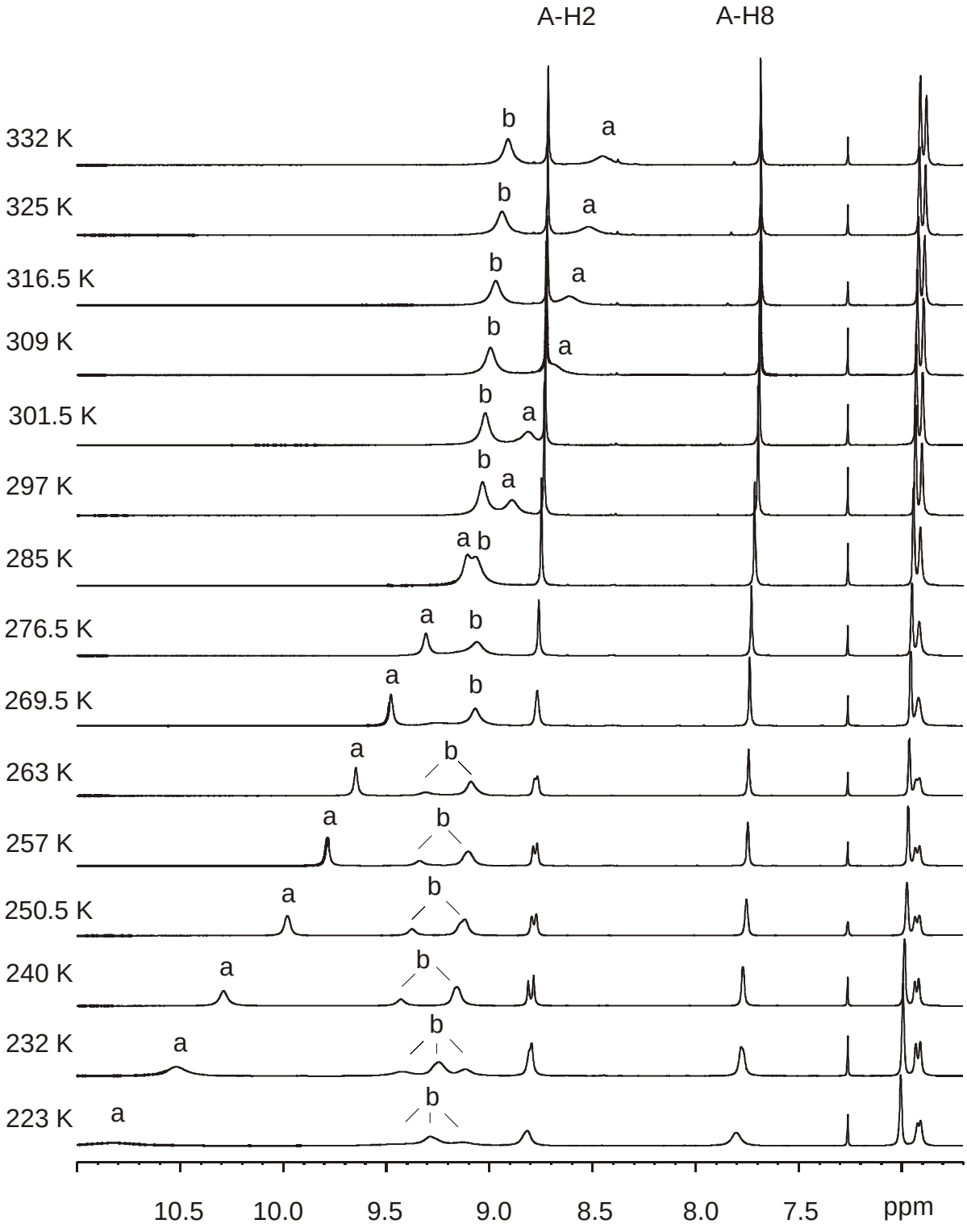


Figure 10: Temperature-dependent $^{1}H$ NMR spectra of an equimolar **50** / **5** mixture in $CDCl_3$; a: T-NH, b: A-$NH_2$.

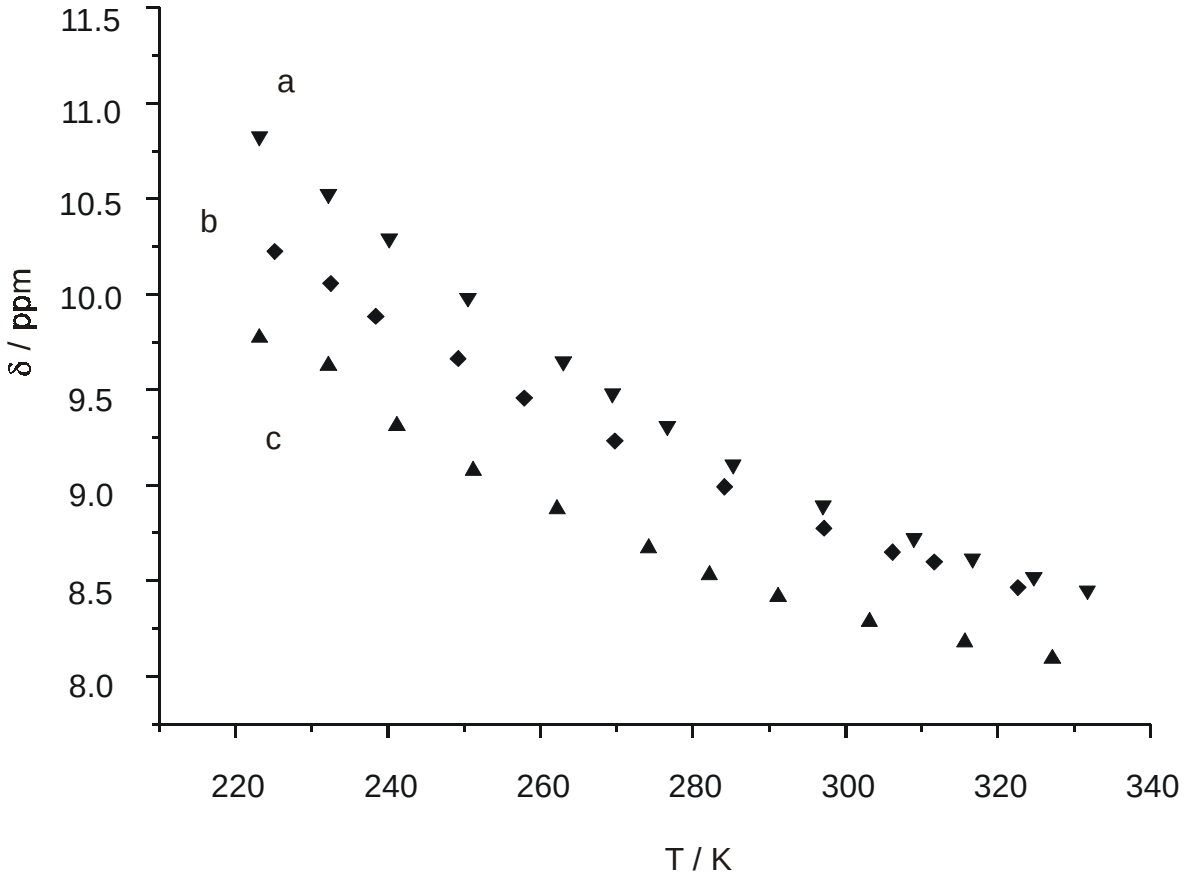


Figure 11: Temperature dependence of the T-NH resonance of **5** within equimolar mixtures of a: **50** / **5**, b: **51** / **5** and c: **5** / **5** in $CDCl_3$.

## 3.4 Investigation of hydrogen bonding between 51 and 3´,5´-diacetyl-2´-deoxyuridine (52) within a slow exchange regime

### 3.4.1 Low temperature $^1$H NMR spectroscopy

For a more detailed study of hydrogen bonding between **51** and the uridine derivative 3´,5´-diacetyl-2´-deoxyuridine (**52**) one- and two-dimensional $^1$H NMR spectroscopy at low temperatures down to 128 K in a freon mixture[206-208] was applied by Dr. K. Weisz at the Freie Univesität, Berlin, Germany. At these low temperatures, any coexisting hydrogen-bonded associates are in slow exchange which allows an analysis of the preferred association modes of **51** with **52** by $^1$H,$^1$H NOESY spectroscopy. No crosspeaks due to chemical exchange are supposed to appear and thus the NOE contacts directly identify protons in close spatial proximity. Recently, the preferred association modes within U / U homodimers and A / U heterodimers have been established by this method.[209,210]

$^1$H NMR measurements of a 1:2-mixture of **51** and 3´,5´-diacetyl-2´deoxyuridine (**52**) were carried out in freon at various temperatures from 273 K down to 128 K (Figure 12). Figure 12 shows that until 193 K only one uridine imino resonance at 11.7 ppm is present which originates from hydrogen-bonded homodimers of **52**. At 153 K additional uridine imino resonances at 14.01 and 13.58 ppm are observable. At 128 K in total four different uridine imino resonances with chemical shifts of 14.41, 14.01, 13.58 and 13.51 ppm (marked as a, b, c, d in Figure 12) are observable which, based on NOE connectivities (see below), must arise from hydrogen-bonded **51** / **52** pairs. In addition, at 128 K two uridine NH resonances at 12.2 and 11.7 ppm are observable which originate from homodimers of **52**[209] (marked as e and f in Figure 12). The resonances at 13.51 (d) and 14.41 ppm (a) disappear above 133 K indicating that they arise from kinetically labile associates, whereas the signals at 13.58 (c) and 14.01 ppm (b) are in slow exchange already at 153 K, reflecting their relative kinetic stability.

From the integrals of the NMR signals at 153 K it has been calculated that approximately 40 % of **52** are associated with **51** and that the remaining 60 % represent homodimers of **52**. With regard to the fact that two equivalents of **52** are present in the mixture this means that approximately only 80 % of **51** are associated with **52** and that also free, non-hydrogen bonded **51** is present in the mixture.

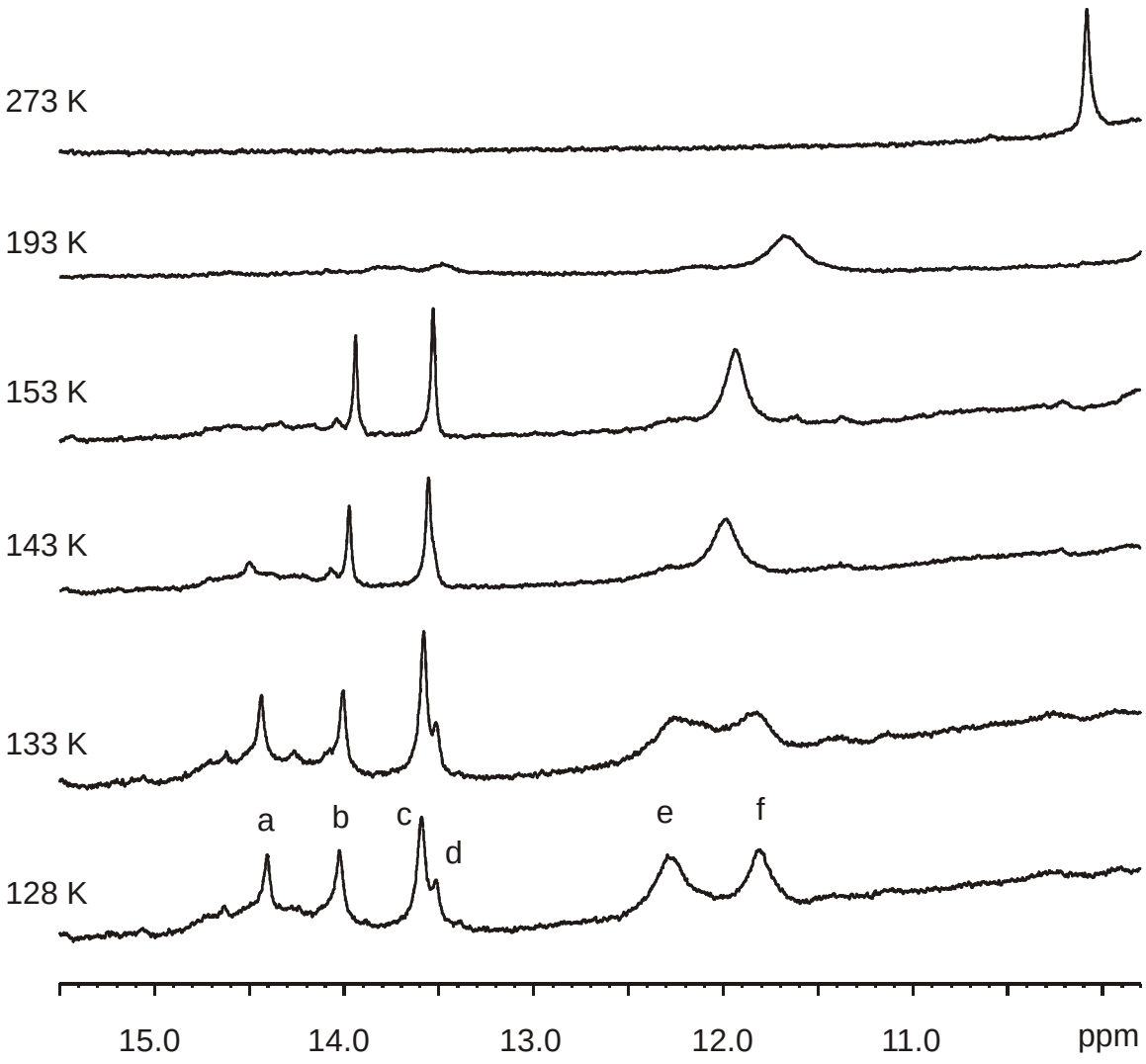


Figure 12: Low field portions of $^{1}$H NMR spectra of a **51** / **52** (1 / 2) mixture in freon at various temperatures; a: U-NH (14.41 ppm), b: U-NH (14.01 ppm), c: U-NH (13.58 ppm), d: U-NH (13.51 ppm), d: U-NH (12.2 ppm), U-NH (11.7 ppm).

In order to establish the association geometries of the hydrogen-bonded **51** / **52** pairs a $^{1}$H,$^{1}$H NOESY spectrum was recorded at 128 K in freon (Figure 14). In **51** / **52** pairs with Hoogsteen or reverse Hoogsteen geometry crosspeaks of the uridine NH proton of **52** with the A-$NH_2$ protons and the A-H8 proton of **51** should appear (Figure 13). A-H8 resonances can be identified by their NOE contacts with the H1´, H2´and H3´-sugar protons.

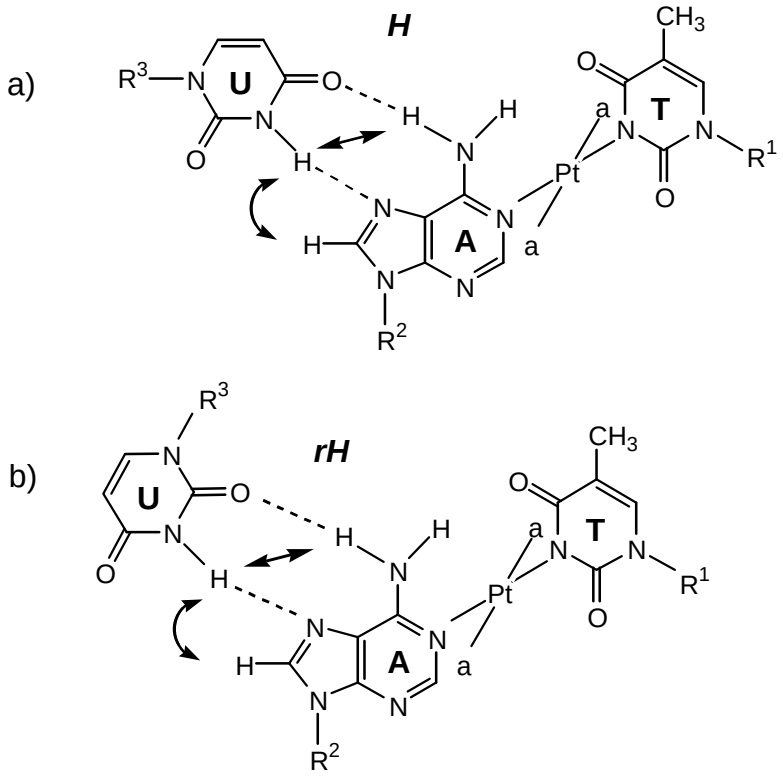


Figure 13: Expected NOE contacts within a **51** / **52** pair with a) Hoogsteen and b) reverse Hoogsteen geometry; a = $NH_2CH_3$, $R^1$ = cyclohexylmethyl, $R^2$ = 2´,3´,5´-tris-(*tert*-butyldimethylsilyl)-ribose, $R^3$ = 3´,5´-diacetyl-2´deoxyribose.

Figure 14 shows portions of the $^1$H, $^1$H NOESY spectrum of a **51** / **52** mixture in freon at 128 K. The uridine NH resonance at 13.58 ppm exhibits crosspeaks to the A-H8 resonance at 8.35 ppm and to A-$NH_2$ resonances at 8.69 and 9.18 ppm. The U-NH resonance at 14.01 ppm exhibits crosspeaks to the A-H8 resonance at 8.78 ppm and to A-$NH_2$ resonances at 8.98 and 9.64 ppm. The resonances at 8.35 and 8.78 ppm have been identified as A-H8 resonances through their crosspeaks to H1´, H2´ and H3´-sugar protons (Figure 14). Based on these NOE connectivities the uridine imino resonances at 13.58 ppm and 14.01 ppm have tentatively been assigned to arise from hydrogen-bonded **51** / **52** pairs with Hoogsteen and reverse Hoogsteen geometry. A differentiation between these two geometries is not possible on the basis of the NOE connectivities.

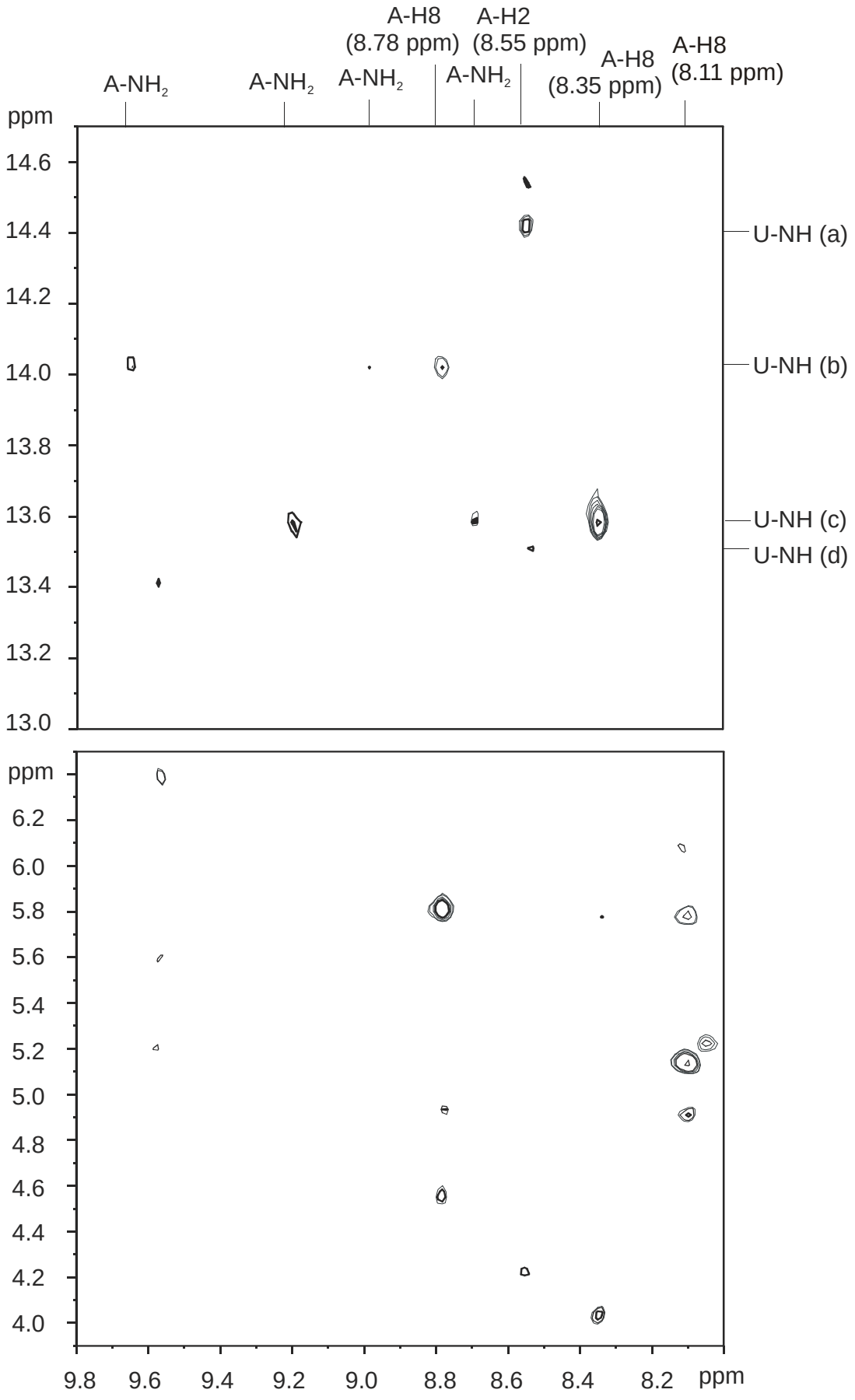


Figure 14: Portions of the NOESY spectrum of the **51** / **52** mixture in freon at 128 K.

The kinetically labile U-NH resonances at 13.51 and 14.41 ppm must arise from U-NH protons which are engaged in strong hydrogen bonding interactions (stronger than formed within **52** homodimers) as they appear at rather low field These resonances exhibit no crosspeaks to exocyclic A-$NH_2$ resonances of **51** but only a crosspeak to a resonance at 8.55 ppm. This resonance at 8.55 ppm is tentatively assigned to the A-H2 resonance of **51** as it shows no crosspeaks to sugar protons. The only crosspeak is to a resonance at 4.1 ppm, which is tentatively assigned to the resonance for the amino protons of the methylamine ligands. At first glance, the presence of crosspeaks between the resonance at 8.55 ppm and the two uridine imino resonances at 13.51 and 14.41 ppm is not immediately evident. One possible explanation could be hydrogen bond formation between a uridine NH proton and the *O4* atom of the CHMT ligand in **51** (Figure 15). Platination of the *N3* position of thymine increases the $pK_a$ value of the T-*O4* position significantly[94-98] and therefore increases its hydrogen bond accepting ability. Thus, a hydrogen bond between a uridine NH and *O4* of the CHMT ligand should be comparatively strong which would account for the observed low-field shift of the uridine NH resonance. Furthermore, the presence of such a hydrogen bond could explain the observed crosspeak between the putative A-H2 resonance at 8.55 ppm and the two uridine NH resonances at 13.51 and 14.41 ppm. An associate like the one depicted in Figure 15 would be stabilized by only one hydrogen bond, which would explain its kinetic lability.

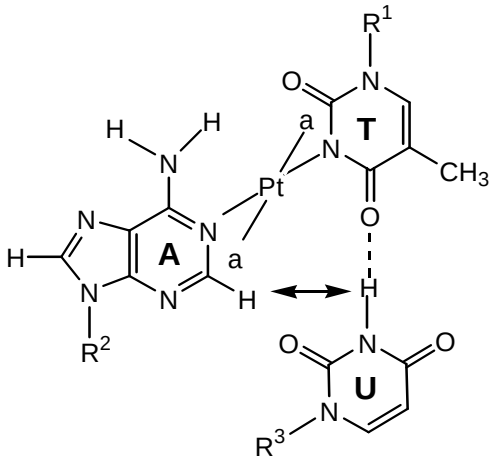


Figure 15: Possible hydrogen bond between the uridine NH of **52** and *O4* of the CHMT ligand within **51**; a = $NH_2CH_3$, $R^1$ = cyclohexylmethyl, $R^2$ = 2´,3´,5´-tris-(*tert*-butyldimethylsilyl)-ribose, $R^3$ = 3´,5´-diacetyl-2´deoxyribose.

The resonance at 8.11 ppm is, based on its NOE contacts to the sugar protons (Figure 14), unambiguously assigned to a A-H8 resonance. As it exhibits no crosspeak to uridine NH resonances it is assigned to the A-H8 resonance originating from free, non-hydrogen bonded **51**. Thus, **51** is not quantitatively associated with **52**.

### 3.4.2 Determination of the $^1J_{NH}$ coupling constant

$^{15}N$ labelled uracil derivatives can be used to probe hydrogen bonding interactions, since the $^1J_{NH}$ coupling constant is a direct measure for the strength of a hydrogen bond. There is a strong linear correlation between the chemical shift of the imino proton and the $^1J_{NH}$ coupling constant for imino groups hydrogen-bonded to a nitrogen acceptor.[211] Normally, the $^1J_{NH}$ couplings range from approximately -84 to -89 Hz.[211] A decrease in the absolute size of the $^1J_{NH}$ coupling correlates with a downfield shift of the imino proton and indicates a gradual shift of the proton from the donor to the acceptor with a concomitant lengthening of the covalent NH bond.[211] Variations of approximately 4 Hz upon hydrogen bond formation have been observed so far.[212-214] For an adenine-uracil base pair analogue in chloroform, the formation of the base pair resulted in a decrease in $|^1J_{NH}|$ from 91.3 to 87.5 Hz.[215]

In a mixture of **51** and 3-$^{15}N$-labelled 3´,5´-diacetyl-2´deoxyuridine in freon at 133-138 K a $^1J_{NH}$ coupling constant of 87.6 Hz has been determined for both the putative Hoogsteen and reverse Hoogsteen base pair geometries. This compares with a $^1J_{NH}$ coupling constant of 84 Hz measured for the unplatinated Hoogsteen A / U pair.[210] Low temperature $^1H$ NMR studies in freon show furthermore that the uridine NH resonances of both the **51** / **52** Hoogsteen and reverse Hoogsteen pairs appear at higher field than the uridine NH resonance of the unplatinated Hoogsteen A / U pair.[210] Both observations are consistent with a decrease of the strength of the hydrogen bond between *N7* of **51** and NH of **52** compared to the unplatinated Hoogsteen A / U pair. This result was not unexpected in that coordination of the Pt(II) electrophile at the A-*N1* position in **51** decreases the basicity of the A-*N7* position and thus diminishes its hydrogen bond accepting ability. Information on the strength of the hydrogen bond between the exocyclic A-$NH_2$ protons and a carbonyl group of the uracil base within **52** is, unfortunately, not available. For a quantitative evaluation of the strength of this hydrogen bond a $^{15}N$ label has to be introduced into the exocyclic amino group. In this case, the $^1J_{NH}$ coupling constant would be a measure for the hydrogen bond strength between the protons of the exocyclic amino group and *O2* or *O4* of **52**.

Table 7: $^{1}J_{NH}$ coupling constants in an unplatinated Hoogsteen A / U pair and a **51** / **52** pair

| | $^{1}J_{NH}$ | δ (ppm) U-NH |
|---|---|---|
| A / U (H) | 84 Hz[210] | 14.32[210] |
| **51** / **52** (H, rH) | 87.6 Hz | 13.58, 14.01 |

## 4 Discussion

Concentration-dependent $^{1}$H NMR measurements in chloroform at room temperature suggest that in the presence of **50**, 1-*N*-cyclohexylmethylthymine (**5**) undergoes self-association rather than Hoogsteen or reverse Hoogsteen pairing with **50**. The concentration-dependent shift of the T-NH resonance of **5** in the **50** / **5** mixture is of the same order of magnitude as for pure **5** in $CDCl_3$.

Similarly, temperature-dependent $^{1}$H NMR measurements in $CDCl_3$ show that down to 220 K in the presence of **50** and **51,** 1-*N*-cyclohexylmethylthymine (**5**) undergoes self-association rather than forming hydrogen bonds to **50** and **51**. The temperature-dependent shift of the T-NH resonance in the **50** / **5** and the **51** / **5** mixtures is again of the same order of magnitude as for pure **5**.

In agreement with this observation, low temperature $^{1}$H NMR measurements of a **51** / **52** mixture in freon only show homodimers of **52** up to 193 K. Only below 153 K two kinds of hydrogen-bonded **51** / **52** heterodimers have been detected in addition to homodimers of **52**. The **51** / **52** heterodimers have, based on NOE connectivities, tentatively been assigned as **51** / **52** pairs with Hoogsteen and reverse Hoogsteen geometry. Below 143 K two additional kinetically labile uridine NH resonances appear which cannot be assigned unambiguously. From these low temperature measurements it is furthermore evident that **51** is not quantitatively associated with **52** but that a small amount of free **51** is present.

One feature which could effect the formation of hydrogen bonds between **50** and **5** as well as between **51** and **52** could be the formation of ion pairs of **50** and **51** with their respective counterions. It is feasible that in $CDCl_3$, the nitrate and tetrafluoroborate counterions are not well solvated and rather hydrogen-bonded to the protons of the exocyclic amino groups in **50** and **51**, respectively. In this case, hydrogen bond formation between **50** and **5** as well as between **51** and **52** would be hindered, so that indeed self-association of **5** would prevail. Furthermore, it is known that the dielectric constant of freon mixtures significantly increases at very low temperatures.[216] If at these low temperatures the increased

polarity of the solvent leads to a better solvation of the $BF_4^-$ counter ion, the observed existence of hydrogen-bonded **51** / **52** heterodimers at 153 K could be rationalized.

In conclusion, the question has to be raised if the conditions applied are appropriate for a detection of hydrogen bonds of the *N1*-platinated adenine derivatives **50** and **51** to the thymine and uridine derivatives **5** and **52**. Hydrogen bond formation in $CDCl_3$ can, in principle, also be troubled by residual traces of water, which can never be completely removed. However, if relevant, this problem should also effect pairing between the free bases **48** and **5**. This is apparently not the case.

The ultimate way to gain information on the alteration of the Hoogsteen hydrogen bonding strength within a *N1*-platinated adenine / thymine pair compared to a non-platinated A / T pair, would be to introduce a $^{15}N$ label into the exocyclic amino group of the *N1*-platinated adenine derivative. In this case, the absolute value of the $^1J_{NH}$ coupling constant would reflect the strength of the hydrogen bond between the protons of the exocyclic amino group and T-CO(4). It could be estimated to what extent the expected increase of the hydrogen bond strength compensates the observed weakening of the hydrogen bond between A-*N7* and uridine NH. In this way, information on the overall change of the hydrogen bond strength in a *N1*-platinated adenine / thymine pair would be available.

# C Experimental Section

## 1 Starting compounds and general procedures

$K_2PtCl_4$ was purchased from Heraeus. *Trans*-$[Pt(NH_3)_2Cl_2]$,[217] *trans*-$[Pt(NH_2CH_3)_2Cl_2]$,[218] *trans*-$[Pt(NH_3)_2(1\text{-MeT})Cl]$[80], 1-*N*-cyclohexylmethylthymine (**5**)[133] 1-*N*-methylthymine,[219] 9-*N*-cyclohexylmethyladenine (**48**)[220] and 2´,3´,5´-tris-(*tert*-butyldimethylsilyl)-adenosine (**49**)[221] have been synthesized according to literature procedures. Bromomethylcyclohexane was from Fluka, adenine and thymine have been purchased from Acros and Aldrich, respectively. Oligonucleotides were synthesized in the group of Prof. J.H. van Boom, Leiden University, Leiden, The Netherlands, or purchased from Oswel, Southampton, England. Methanol, DMF and dioxane were dried over molecular sieves (3 Å and 4 Å) prior to use. Acetonitrile used for HPLC was HPLC grade. All other chemicals were p.a. grade and used without further purification. Deutrated solvents were purchased from Sigma and Deutero. All reactions involving silver nitrate or silver tetrafluoroborate were carried out under exclusion of daylight. Millipore water was obtained using a MilliQ Plus apparatus.

Compounds for which an elemental analysis is not reported were fully characterized by NMR and ESI MS.

Automated DNA synthesis was carried out on a Gene Assembler Special DNA synthesizer (Pharmacia, Sweden) according to the phosphoramidite method.[130] Protected nucleoside phosphoramidites were obtained from PerSeptive Biosystems (USA). Deoxyribonucleoside building blocks immobilized on CPG were obtained from PerSeptive Biosystems (30 µmol / g). *O*-NPT was synthesized according to a published procedure.[222]

Solid-phase PNA synthesis was performed on a 433A Peptide Synthesizer (Applied Biosystems) using as the solid-support PEG-PS resin functionalized with a RINK linker or on a Pharmacia Gene Assembler using highly cross-linked polystyrene beads as the solid-support. Fmoc / N-acyl protected PNA monomers were provided by the group of Prof. J. H. van Boom. The Fmoc / N-Bhoc protected PNA monomers were obtained from PE Biosystems. Fmoc / Boc protected L-lysine was from NovaBiochem. TFA and *m*-cresol were from Fluka.

## 2 Analytical methods

### NMR spectroscopy

$^{1}$H NMR spectra were recorded on Bruker DPX 300 (300.13 MHz) or DMX 600 (600.13 MHz) spectrometers using a 5 mm multi-nucleus probe. A variable temperature unit was used to keep the temperature constant. Chemical shifts (δ) are given in ppm relative to tetramethylsilane (TMS), when measured in $CDCl_3$ or sodium-3-(trimethylsilyl)propansulfonate (TSP), when measured in $D_2O$. $^{13}$C NMR spectra were recorded on a Bruker DPX 300 spectrometer (75.48 MHz) and calibrated externally to TMS. $^{31}$P NMR spectra were measured on a Bruker DPX 300 spectrometer (121.50 MHz) using 85 % $H_3PO_4$ as external standard. $^{195}$Pt NMR spectra were recorded on a Bruker DPX 300 spectrometer (64.38 MHz) using $K_2PtCl_4$ (δ = -1614 ppm) as an external standard.

### Concentration-dependent $^{1}$H NMR measurements and determination of the association constant

In the dilution experiments a 1:1 mixture of the two components in $CDCl_3$ was diluted stepwise in the concentration range 80 – 5 mM and each time a $^{1}$H NMR spectrum was recorded. The measurements were carried out at 296 K under argon atmosphere in deuterated chloroform that had been dried over 4 Å molecular sieves. The added amount of $CDCl_3$ was weighed every time. The concentration-dependent shift of the NH protons involved in hydrogen bonding were fitted with a non-linear least squares program after Newton-Gauss.[177,223] Three independent dilution experiments were performed and evaluated for each system.

### Measurement of pH / pD values

pH measurements were carried out at 298 K with a Radiometer PHM 80 pH meter using a Hamilton combination glass electrode. The pH meter was calibrated with Fischer-certified buffer solutions of pH 4.00, pH 7.00 and pH 11.00.

The pD value of solutions in $D_2O$ was calculated by addition of 0.4 units to the measured value ($pD = pH^* + 0.4$).[224] For determination of $pK_a$ values the uncorrected pH value ($pH^*$) was used.

**UV spectroscopy**

UV spectra were measured on a Lambda 15 Perkin-Elmer spectrometer. Melting curves were measured using heatable quartz cuvetts. The heating rate was 1 °C $min^{-1}$.

**ESI mass spectrometry and LC MS**

ESI mass spectra were recorded on a Finnigan MAT TSQ-70 instrument equipped with a custom-made Electrospray interface. LC MS analysis was carried out on a Jasco LC MS system with mass detection on a Perkin Elmer Sciex API 165 equipped with an Electrospray Interface. In both cases positively charged ions were detected.

The ESI MS spectrum of the *trans*-$(NH_3)_2$Pt(II) crosslinked triple helix **4** was measured on a Finnigan LCQ Deca instrument. Negatively charged ions were detected.

**MALDI-TOF mass spectrometry**

MALDI TOF MS spectra were obtained on a PE-Biosystems Voyager DE-PRO MALDI-TOF mass spectrometer, equipped with delayed extraction and a reflector. Samples were irradiated with short pulses of a nitrogen laser emitting at 337 nm. The matrix used was 3-hydroxy-picolinic acid (3-HPA). The matrix solution consisted of 8/1 3-HPA (10 mg/ml in water/acetonitrile 1/1) / diammonium citrate (50 mg/ml in water). The samples were diluted to 10 pmol/µl and mixed 1/1 with matrix solution. 1 µl of this solution was put on the target and allowed to dry.

**Elemental analysis**

Elemental analysis was carried out on an Elemental Analyzer CHNS-932 (LECO) or 1106 (Carlo Strumentazione).

**HPLC / FPLC**

HPLC analysis and purifications were carried out on a Jasco HPLC system. FPLC analysis was carried out on a Pharmacia FPLC instrument using a MonoQ column. FPLC Buffers (pH 12): A, 100 mM NaOH; B, 100 mM NaOH in 1.2 M NaCl.

**Gel electrophoresis**

Gel electrophoresis was carried out on a 24% Acrylamide/Bisacrylamide gel (19:1) under denaturing conditions (7 M urea, 1 M Tris-Borate-EDTA Buffer, 3 h, 3000 V).

## 3 Synthesis

***Trans*-[Pt($NH_3$)$_2${5´d(G-*N7*-$T_2CTC_2TC$)}{(5´d(G-*N7*-$A_2GAG_2AGCT_2GCTC_2TCT_2C$)}]$^{27-}$ (4)**

5.89 x $10^{-4}$ mmol of *trans*-[Pt($NH_3$)$_2$Cl($D_2O$)]$^+NO_3^-$, obtained *in situ* by reaction of *trans*-[Pt($NH_3$)$_2$$Cl_2$] with one equivalent of $AgNO_3$ in water at RT overnight,[89] was reacted with 1.66 mg (5.89 x $10^{-4}$ mmol) of 5´d($GT_2CTC_2TC$) (**1**) at pH* 3.2 at RT in $D_2O$ to yield after 48 h *trans*-[Pt($NH_3$)$_2${5´d(G-*N7*-$T_2CTC_2TC$)}Cl]$^{7-}$ (**2**). Compound **2** was lyophilized and reacted with 6.35 mg (8.84 x $10^{-4}$ mmol) of 5´d($GA_2GAG_2AGCT_2GCTC_2TCT_2C$)$^{21-}$ (**3**) at pH* 4.8 at RT in 1.5 ml of a 100 mM $NaClO_4$ and 5 mM $Mg(ClO_4)_2$ solution. After 72 h the reaction was complete and yielded *trans*-[Pt($NH_3$)$_2${5´d(G-*N7*-$T_2CTC_2TC$)}{(5´d(G-*N7*-$A_2GAG_2AGCT_2GCTC_2TCT_2C$)}]$^{27-}$ (**4**) as the major product. Compound **4** was isolated by reversed-phase HPLC using an Alltech Alltima C18 5µ (10 x 250 mm) column. A gradient elution (11→19 % B in 40 min) was applied by building up a gradient starting with buffer A (50 mM TEAA) and applying buffer B (50 mM TEAA in 75 % acetonitrile) with a flow rate of 5 ml/min. Subsequently, **4** was converted into the $Na^+$ form by running it over a Dowex column.
ESI MS: m/z 1597 ($M^{6-}$/6), 1917 ($M^{5-}$/5), 2396 ($M^{4-}$/4).

**1-*N*-cyclohexylmethylthymine (5)**

6.076 g (48.2 mmol) of thymine and 6.667 g (48.2 mmol) of $K_2CO_3$ were suspended in 150 ml of DMSO and stirred for 1 h at room temperature. 2.224 ml (15.9 mmol) of bromomethylcyclohexane was added and the reaction mixture stirred for 3 h at 70° C and then for 14 h at RT. KBr was removed by filtration. 200 ml of water were added to the filtrate and the solution was extracted 3 times with 150 ml of dichloromethane. Purification of the crude product by silica gel chromatography (eluent: dichloromethane/methanol, 100 / 0 to 97.5 / 2.5, v / v) afforded 1.68 g (47 %) pure 1-*N*-cyclohexylmethylthymine (**5**).

$^1$H NMR ($CDCl_3$, δ, ppm): 8.42 (s, N(3)H), 6.93 (d, $^4$J = 1.12 Hz, H6), 3.52 (d, $^3$J = 7.11 Hz, T-N1-$CH_2$), 1.92 (d, $^4$J = 1.07 Hz, T-5-$CH_3$), 1.70, 1.21, 0.96 (m, cyclohexylmethyl)

$^{13}$C NMR ($CDCl_3$, δ, ppm): 164.24 (C-4), 151.1 (C-2), 141.0 (C-6), 110.05 (C-5), 54.52 ($CH_2N$), 37.29, 30.36, 26.14, 25.52, (cyclohexyl), 12.30 (T-5-$CH_3$);

ESI MS: m/z 223 ($M^+$);

elemental analysis: found (calculated): C: 64.7 (64.8), H: 8.1 (8.1), N: 12.5 (12.6).

**K(1-*N*-cyclohexylmethylthyminate) (6)**

To a suspension of 0.799 g (3.594 mmol) 1-*N*-cyclohexylmethythymine in 20 ml millipore water was added 0.2015 g (3.591 mmol) of potassium hydroxide (KOH) and 30 ml of ethanol. The solution was stirred for 1 h at RT and subsequently the solvents were evaporated. The residue was dissolved in dioxane / water (1/1, v/v) and freeze-dried to yield 0.908 g (97 %) of K(1-*N*-cyclohexylmethylthyminate) (**6**).

***Trans*-[Pt($NH_2CH_3$)$_2$(CHMT)Cl] (7)**

To 0.502 g (1.531 mmol) of *trans*-[Pt($NH_2CH_3$)$_2$$Cl_2$] in 30 ml of DMF was added 0.247 g (1.454 mmol) of $AgNO_3$ and the reaction mixture stirred overnight. AgCl was filtered off and 0.4402 g (1.691 mmol) of K(CHMT) (**6**) was added. The reaction mixture was stirred at RT for 3 d. DMF was largely removed *in vacuo*. Addition of diethylether lead to isolation of 0.555 g (70.5 %) of analytically pure *trans*-[Pt($NH_2CH_3$)$_2$(CHMT)Cl] (**7**).

$^{1}$H NMR ($CDCl_3$, δ, ppm): 6.85 (d, $^{4}$J = 1.01 Hz, H6), 4.19 (s, Pt-$NH_2$), 3.52 (d, $^{3}$J = 7.20 Hz, T-N1-$CH_2$), 2.37 (t, $^{3}$J = 6.51 Hz, Pt-$NH_2C\mathit{H}_3$), 1.89 (d, $^{4}$J = 0.86 Hz, T-5-$CH_3$), 1.75, 1.21, 0.96 (m, cyclohexyl);

$^{195}$Pt NMR ($CDCl_3$, δ, ppm): - 2338;

IR ($\tilde{\nu}$, $cm^{-1}$): 3272, 3193, 3107, 2928, 2851, 1664, 1633, 1571, 1461, 1438, 1354, 1097, 774, 586, 464, 337;

ESI MS: m/z 515 ($M^+$);

elemental analysis: found (calculated): C: 32.7 (32.7), H: 5.3 (5.3), N: 11.0 (10.9).

### *Trans*-$[Pt(NH_2CH_3)_2(CHMT)\{NH_2(CH_2)_6OH\}]^+Cl^-$ (8)

To 0.259 g (0.504 mmol) of *trans*-[$Pt(NH_2CH_3)_2$(CHMT)Cl] (**7**) in 30 ml of methanol and 20 ml of $H_2O$ was added 0.0612 g (0.522 mmol) of 6-amino-1-hexanol and the reaction mixture was stirred for 3 d at 60 °C under argon atmosphere. The solvents were removed *in vacuo* and the residue washed with boiling diethylether to remove residual 6-amino-1-hexanol. This procedure yielded 0.222 g (70 %) analytically pure **8**.

$^{1}$H NMR ($CDCl_3$, δ, ppm): 6.85 (d, $^{4}$J = 0.78 Hz, H6), 6.06 (m, $NH_2$ (ahol)), 5.02 (m, Pt-$NH_2$), 3.64 (t, $^{3}$J = 6.23 Hz, α-$CH_2$ (ahol)), 3.50 (d, $^{3}$J = 6.97 Hz, $NCH_2$(CHMT)), 2.86 (m, ξ-$CH_2$ (ahol)), 2.39 (t, $^{3}$J = 6.12 Hz, Pt-$NH_2C\mathit{H}_3$), 1.80 (T-5-$CH_3$), 1.98, 1.67, 1.44, 1,20, 0.90, (m, ahol, cyclohexyl);

$^{195}$Pt NMR (δ, ppm): - 2607 ($CD_3OD$), -2597 ($CDCl_3$);

ESI MS: m/z 595 ($M^+$);

IR ($\tilde{\nu}$, $cm^{-1}$): 3179, 2923, 2852, 1661, 1633, 1558, 1539, 1455, 1346, 1329, 1084, 1054, 1027, 1004, 787, 589, 496, 451.

### *Trans*-$[Pt(NH_2CH_3)_2(CHMT)(gly\text{-}\mathit{N})]^+BF_4^-$ (9)

To a solution of 0.130 g (0.253 mmol) of *trans*-[$Pt(NH_2CH_3)_2$(CHMT)Cl] (**7**) in 10 ml DMF was added 0.047 mg (0.241 mmol) of $AgBF_4$ and the reaction mixture stirred for 7 h. AgCl was filtered off and 0.018 g (0.240 mmol) of glycine in a small amount of water was

added. The reaction mixture was stirred for 2 d at RT. After removal of DMF *in vacuo* 0.106 g (65.8 %) of analytically pure *trans*-[Pt($NH_2CH_3$)$_2$(CHMT)(gly-*N*) ]$^+BF_4^-$ (**9**) were obtained.

$^1$H NMR ($CD_3OD$, δ, ppm): 7.25 (d, $^4J$ = 1.0 Hz, H6), 5.22 (m, $NH_2$ (gly)), 4.57 (m, Pt-$NH_2$), 3.58 (d, $^3J$ = 7.21 Hz, $NCH_2$(CHMT)), 3.51 (s, $CH_2$ (gly)), 2.26 (t, $^3J$ = 6.2 Hz, Pt-$NH_2C\mathit{H}_3$), 1.86 (d, $^4J$ = 0.83 Hz, T-5-$CH_3$), 1.73, 1.19 ,1.013 (m, cyclohexylmethyl);

$^{195}$Pt NMR ($CD_3OD$, δ, ppm): - 2605;

IR (ϑ̃, $cm^{-1}$): 3178, 2924, 2852, 1661, 1634, 1557, 1540, 1455, 1346, 1084, 1054, 1027, 1004, 782, 587, 496, 451;

ESI MS: m/z 553 ($M^+$);

elemental analysis: found (calculated): C: 30.9 (30.0), H: 5.3 (5.0), N: 11.4 (10.9).

### *Trans*-[Pt($NH_3$)$_2$(1-MeT)(gly-*N*)]$^+NO_3^-$ (10)

To a suspension of 0.115 g (0.285 mmol) of *trans*-[Pt($NH_3$)$_2$(1-MeT)Cl] in 10.5 ml $H_2O$ was added 0.044 g (0.259 mmol) of $AgNO_3$ and the reaction mixture was stirred for 17 h at 40 °C. AgCl was filtered off and 0.016 g (0.213 mmol) of glycine was added. The reaction mixture was stirred for 72 h at 60 °C with the pH being kept at 7.5 by addition of KOH solution. After filtration, the reaction mixture was lyophilyzed and the residue recrystallized from a mixture of water and acetone to give 0.088 g (70 %) of analytically pure *trans*-[Pt($NH_3$)$_2$(1-MeT)(gly-*N*)]$^+NO_3^-$ (**10**).

$^1$H NMR ($D_2O$, δ, ppm): 7.27 (d, $^4J$ = 0.96 Hz, H6), 4.95 (s, $NH_2$(gly)), 3.83 (s, Pt-$NH_3$), 3.41 (t, $^3J$ = 6.5 Hz, $CH_2$(gly)), 3.30 (s, T-N1-$CH_3$), 1.81 (s, T-5-$CH_3$);

$^{195}$Pt NMR ($D_2O$, δ, ppm): - 2557;

IR (ϑ̃, $cm^{-1}$): 3182, 2926, 2854, 1661, 1634, 1557, 1442, 1354, 1051, 773, 606, 464.

### *Trans*-[Pt($NH_2CH_3$)$_2$(CHMT){$NH_2(CH_2)_6O(PO_3H)$-dT-5´-*O*-DMTr}]$^+$ (13)

To a solution of 8.5 mg (13.5 µmol) of *trans*-[Pt($NH_2CH_3$)$_2$(CHMT){$NH_2(CH_2)_6OH$}]$^+Cl^-$ (**8**) in dioxane was added 13 µmol of 5´-*O*-DMTr-deoxythymidine-3´-phosphoramidite (**12**) and *o*-NPT (53.5 µmol) in acetonitrile. After 10 min an aqueous solution of $I_2$/collidine was added. The solvents were removed and the

residue dissolved in 1000 µl methanol containing 200 µl of concentrated aqueous ammonia. After 10 h at 20 °C, the sample was freeze-dried and purified by reverse-phase HPLC (Alltima C 18 column, 50 mmol aqueous ammonium bicarbonate/acetonitrile buffer, gradient: 40-70 % acetonitrile) to give *trans*-[Pt($NH_2CH_3$)$_2$(CHMT){$NH_2(CH_2)_6O(PO_3H)$-dT-5´-*O*-DMTr}]$^+$ (**13**).

$^1$H NMR ($CD_3OD$, δ, ppm): 7.68 (s, H6, (dT)), 7.42, 7.30, 7.23, 6.87 (m, DMT) 7.24 (s, H6, (CHMT)), 6.38 (dd, $^3$J = 5.80 Hz, $^3$J = 8.29 Hz, H1´), 5.02 (t, H3´), 4.50 (m, Pt-$NH_2$), 4.26 (q, H4´), 3.82 (t, $^3$J = 6.1 Hz, α-$CH_2$ (ahol)), 3.77 (s, $OCH_3$), 3.58 (d, $^3$J = 7.25 Hz, $NCH_2$(CHMT)), 3.43 (m, H5´, H5´´), 2.77 (m, ξ-$CH_2$ (ahol)), 2.58 (m, H2´´), 2.46 (m, H2´), 2.26 (t, $^3$J = 6.5 Hz, Pt-$NH_2C\mathit{H_3}$), 1.87 (s, T-5-$CH_3$ (CHMT)), 1.30 (s, T-5-$CH_3$ (dT)), 1.66 1.44, 1.22, 0.89 (m, ahol, cyclohexylmethyl);

$^{195}$Pt NMR ($CD_3OD$, δ, ppm): $\delta$ = -2621;

$^{31}$P NMR ($CD_3OD$, δ, ppm): $\delta$ = 0.18;

LC MS: m/z = 1201.5 ($M^+$).

### *Trans*-[Pt($NH_2CH_3$)$_2$(CHMT){$NH_2(CH_2)_6O(PO_3H)$-dT-5´-OH}]$^+$ (14)

To the purified *trans*-[Pt($NH_2CH_3$)$_2$(CHMT){$NH_2(CH_2)_6O(PO_3H)$-dT-5´-O-DMTr}]$^+$ (**13**) was added 800 µl of concentrated acetic acid and the reaction mixture was shaken for 1 h at RT. The sample was freeze-dried and to the residue 500 µl of millipore water was added. Subsequently, the sample was freeze-dried again and 500 µl of millipore water were added. The supernatant solution was removed and freeze-dried. This procedure yielded pure *trans*-[Pt($NH_2CH_3$)$_2$(CHMT){$NH_2(CH_2)_6O(PO_3H)$-dT-5´-OH}]$^+$ (**14**).

ESI MS: m/z 900 ($M^+$).

### *Trans*-[Pt($NH_2CH_3$)$_2${$NH_2(CH_2)_6O(PO_3H)$-dT-5´-OH}Cl]$^+$ (15)

*Trans*-[Pt($NH_2CH_3$)$_2$(CHMT){$NH_2(CH_2)_6O(PO_3H)$-dT-5´-OH}]$^+$ (**14**) was subjected to DCl (pD 2.2, 40 °C) to yield *trans*-[Pt($NH_2CH_3$)$_2${$NH_2(CH_2)_6O(PO_3H)$-dT-5´-OH}Cl]$^+$ (**15**) after 108 h.

$^{195}$Pt NMR: -2312 ppm;

ESI MS: m/z 713 ($M^+$).

### *Trans*-[Pt($NH_2CH_3$)$_2$(CHMT){$NH_2(CH_2)_6O(PO_3H)dT_4$-3´-OH}]$^+$ (22) and *Trans*-[Pt($NH_2CH_3$)$_2$(CHMT){$NH_2(CH_2)_6O(PO_3H)d(T_3CTC_2TC)$-3´-OH}]$^+$ (23)

Immobilized $dT_4$ (**16**) and 5´d($T_3CTC_2TC$) (**19**) (0.2 μmol) were synthesized on a Gene Assembler (Pharmacia) following a standard protocol[130] and phosphitylated by treating it twice for 30 min with a 1.0 M **11** / 1.2 M D*i*PEA solution in acetonitrile. The immobilized 5´-phosphoramidites **16b** and **19b** were reacted with *trans*-[Pt($NH_2CH_3$)$_2$(CHMT){$NH_2(CH_2)_6OH$}]$^+Cl^-$ (**8**) [15 μmol, 0.05 M solution in dioxane/acetonitrile (1/1)] in the presence of *o*-NPT (30 μmol, 0.2 M solution in acetonitrile). Decyanoethylation and release from the solid-support were achieved by treatment with concentrated aqueous ammonia for 12 h at 20 °C.

LC-MS analysis of the crude products was carried out on a PE Sciex API 165 mass unit connected to a Jasco HPLC system. HPLC analysis was performed using a Merck LiChrosphere 100 RP18 column (pore size 5 μm, diameter 4 mm, length 250 mm) and 10 mM aqueous ammonium acetate / acetonitrile (gradient: 5-50% acetonitrile) buffer.

As for conjugation of **8** to **16a,** the coupled product **22** was found in the ESI MS at m/z 1812 ($M^+$) and 906 ($M^{2+}$/2). Additionally, tetrathymidylic acid and the corresponding 5´amidate **16b** were detected at m/z 1155.6 ($M^+$) and m/z 1318.5 ($M^+$), respectively.
As for conjugation of **8** to **19a** the coupled product **23** was found in the ESI-MS at m/z 1638 ($M^{2+}$/2) and 1091.8 ($M^{3+}$/3). Additionally, masses for d($T_3CTC_2TC$)-5´phosphate and d($T_3CTC_2TC$)-5´OH have been detected at m/z 1349 ($M^{2+}$/2) and 1309 ($M^{2+}$/2), repectively.

### *Trans*-[Pt($NH_2CH_3$)$_2${$NH_2(CH_2)_6O(PO_3H)dT_4$-3´-OH}Cl]$^+$ (24) and *Trans*-[Pt($NH_2CH_3$)$_2${$NH_2(CH_2)_6O(PO_3H)d(T_3CTC_2TC)$-3´-OH}Cl]$^+$ (25)

Compounds **22** and **23** have been subjected to pH 2.3 at 40 °C for 48 h yielding the monofunctionally *trans*-Pt(II) modified tetranucleotide **24** and nonanucleotide **25** as evidenced by LC MS.

ESI MS: **24**: 1625.5 ($M^+$), 813 ($M^{2+}$/2); **25**: 1545 ($M^{2+}$/2)

***Trans*-[Pt($NH_2CH_3$)$_2$(CHMT){$NH_2CH_2CONH(CH_2)_6O(PO_3H)$d($T_2CTC_2TC$)-3´-OH}]$^+$ (29)**

Fully protected 5´d($T_2CTC_2TC$) was assembled on a 1.0 μmol scale and reacted with $MMTrHN(CH_2)_6OP\{(OCH_2CH_2CN)N(iPr)_2\}$ (**26**) under the influence of *o*-NPT yielding, after treatment with TCA, compound **28**. Immobilized **28** was transferred into a syringe. A solution of 15.71 mg (24.5 μmol) of *trans*-[Pt($NH_2CH_3$)$_2$(CHMT)(gly-N)]$^+BF_4^-$ (**9**), 8.706 g (22.9 μmol) of HATU and 50 μl of D*i*PEA in 450 μl DMF was added and the reaction mixture was shaken for 2 h yielding immobilized **29**. After washing with DMF and dichloromethane **29** was deprotected and cleaved from the solid-support by treatment with concentrated aqueous ammonia for 20 h at RT. The coupling yield was around 60 % as gauged by LC MS. Compound **29** was purified by reversed-phase HPLC using an Alltima C18 column (5 μm pore size, length: 250 mm, diameter: 10.0 mm). A gradient elution (14→22 % B in 5 CV) was performed by building up a gradient starting with buffer A (50 mM TEAA) and applying buffer B (acetonitrile) with a flow rate of 1 ml/min.
ESI MS: m/z 1513 ($M^{2+}$/2), 1009.7 ($M^{3+}$/3).

***Trans*-[Pt($NH_2CH_3$)$_2$(CHMT)($NH_2CH_2CONHc_5$-gly)]$^+$ (31)**

Solid-phase PNA synthesis was performed on a Pharmacia Gene Assembler using highly cross-linked polystyrene beads as the solid-support (loading 26 - 28 μmol/g) on a 1 μmol scale. The support was functionalized with a glycine moiety via a 4-hydroxymethylbenzoic acid linker. Assembly of $c_5$ was performed using solutions of 0.3 M of Fmoc/N-acyl protected PNA monomers in DMF, 0.3 M D*i*PEA in acetonitrile/DMF (1/1, v/v). Prior to coupling the monomers were pre-activated for 1 min by mixing equal amounts of the PNA monomer (15 eq per μmol support), HATU and D*i*PEA solutions. The protocol for one PNA chain extension cycle consisted of (1) wash: acetonitrile/DMF (1/1, v/v), 2.5 ml; (2) coupling: PNA + HATU + D*i*PEA in acetonitrile/DMF (1/1, v/v), 15 min; (3) wash: acetonitrile/DMF (1/1, v/v), 2.5 ml; (4) capping: $Ac_2O$/2,6-lutidine/N-methylimidazole/tetrahydrofuran (1/1/1/7, v/v/v/v), 2.0 ml; (5) wash: acetonitrile/DMF (1/1, v/v), 2.5 ml. The immobilized fully protected $c_5$ (**30**) was transferred into a syringe and a solution of 15.71 mg (24.5 μmol) of *trans*-[Pt($NH_2CH_3$)$_2$(CHMT)(gly-N)]$^+BF_4^-$ (**9**), 19.36 mg (22.9 μmol) HATU and 50 μl of a

0.9 M D*i*PEA solution in DMF was added. The reaction mixture was shaken for 2 h. After washing the solid-support with 3 ml of DMF and 3 ml of $CH_2Cl_2$ a capping procedure ($Ac_2O$/2,6-lutidine/N-methylimidazole/tetrahydrofuran (1/1/1/7, v/v/v/v)) was carried out followed by washing with 3 ml of DMF and 3 ml of $CH_2Cl_2$. The resin was dried in the air. Deprotection and cleavage of the platinated PNA oligomer (**31**) from the solid-support was achieved by treatment with methanolic ammonia for 20 h at RT. Compound **31** was purified by reversed-phase HPLC using an Alltima C18 column (5 μm pore size, length: 250 mm, diameter: 10.0 mm). A gradient elution (10→25 %B in 5 CV) was performed by building up a gradient starting with buffer A (50 mM TEAA) and applying buffer B (acetonitrile) with a flow rate of 1 ml/min. The coupling yield was 36 % as gauged by LC MS.
ESI MS: m/z 1866.2 ($M^+$), 933.2 ($M^{2+}$/2).

### *Trans*-[Pt(NH$_3$)$_2$(Fmoc/N-Bhoc G)Cl]$^+$BF$_4^-$ (33)

To a solution of 0.049 g (0.163 mmol) of *trans*-[$Pt(NH_3)_2Cl_2$] in 2.5 ml of DMF was added 0.031 g (0.159 mmol) of $AgBF_4$ and the reaction mixture stirred overnight at RT. AgCl was removed by filtration and 0.119 g (0.160 mmol) of Fmoc/N-Bhoc G PNA monomer (**32**) was added. After stirring for 1 d at RT, DMF was removed *in vacuo* yielding 0.151 g (84 %) of crystalline *trans*-[$Pt(NH_3)_2$(Fmoc/N-Bhoc G)Cl]$^+BF_4^-$ (**33**).
$^1$H NMR (DMF-$d_7$, δ, ppm): 8.83 (ma), 8.81 (mi) (H8, rotamers), 8.0-6.98 (m, Fmoc, Bhoc), 5.51 (ma), 5.30 (mi) (G-N9-$CH_2$, rotamers), 4.30, (m, Pt-$NH_3$);
$^{195}$Pt NMR (DMF-$d_7$,δ, ppm): = -2289;
ESI-MS: *m/z*: 1006 ($M^+$);
elemental analysis: found (calculated): C: 43.9 (43.8), H: 3.8 (3.8), N: 11.5 (11.8).

### *Trans*-[Pt(NH$_2$CH$_3$)$_2$(CHMT)(Fmoc/N-Bhoc G)]$^+$BF$_4^-$ (34)

To a solution of 0.053 g (0.103 mmol) of *trans*-[$Pt(NH_2CH_3)_2$(CHMT)Cl] (**7**) in 3 ml of DMF was added 0.019 g (0.098 mmol) of $AgBF_4$ and the reaction mixture stirred overnight at RT. After removal of AgCl by filtration 0.074 g (0.100 mmol) of Fmoc/Bhoc-PNA G (**32**) was added to the filtrate and the reaction mixture stirred for 2 d at RT. DMF was removed *in*

*vacuo* to give 0.108 g (80 %) of crystalline *trans*-[Pt($NH_2CH_3$)$_2$(CHMT)(Fmoc/N-Bhoc G)]$^+BF_4^-$ (**34**).

$^{195}$Pt NMR: (DMF-$d_7$, δ, ppm):- 2476;

ESI-MS: m/z 1219 ($M^+$);

elemental analysis: found (calculated): C: 49.3 (49.6), H: 4.7 (4.8), N: 12.0 (11.8).

**Monofunctionally *trans*-Pt(II) modified PNA oligomers 43, 44 and 45**

Solid-phase PNA synthesis was performed on a 433A Peptide Synthesizer (Applied Biosystems) using as the solid-support PEG-PS resin functionalized with a RINK linker (loading 0.2 mmol/g) on a 1 μmol scale. Assembly of the monofunctionally *trans*-Pt(II) modified PNA oligomers **43**, **44**, and **45** was performed using solutions of 0.1 M Fmoc/N-Bhoc protected PNA monomers (and Fmoc / Boc protected L-lysine in case of **44**) and *trans*-[Pt($NH_3$)$_2$(Fmoc/N-Bhoc G)Cl]$^+BF_4^-$ (**33**) in NMP. Prior to coupling the monomers were pre-activated for 1 min by mixing equal amounts of the PNA monomer (25 eq per μmol support), HATU and D*i*PEA solutions. At the beginning of the PNA assembly the Rink-functionalized PEG-PS resin was washed with $CH_2Cl_2$ (5 x 2 ml) and NMP (5 x 1.5 ml). The protocol for one PNA chain extension cycle constisted of (1) Fmoc deprotection: 20 % piperidine in NMP (1 ml, 1 x 1 min, 4 x 0.5 min), (2) wash: NMP (5 x 1.5 ml), (3) coupling: PNA + HATU + D*i*PEA in NMP, 15 min; (4) wash: NMP (5 x 0.5 ml) (5) capping: 0.5 M $Ac_2O$/0.125 M D*i*PEA in NMP, (6) wash: NMP (5 x 0.5 ml). At the end, a final Fmoc protection was carried out (20 % piperidine in NMP (1 ml, 1 x 1 min, 4 x 0.5 min)) followed by a final wash (5 x 1.5 ml NMP, 5 x 2 ml $CH_2Cl_2$). The resin was air-dried. Deprotection and cleavage from the solid-support was accomplished by treatment with TFA/*m*-cresol (4/1 v/v) for 1 h. LC-MS analysis of the crude products was carried out on a PE Sciex API 165 mass unit connected to a Jasco HPLC system. HPLC analysis was performed using an Alltech Alltima C18 column (pore size 5 μm, diameter 4.6 mm, length 150 mm). A gradient elution (0→25 %B in 30 min) was performed by building up a gradient starting with buffer A (1 % TFA) and applying buffer B (1 % TFA in 75 % acetonitrile) with a flow rate of 1 ml/min. Compounds **43**, **44** and **45** were purified by reversed-phase HPLC using an Alltech Alltima C18 5μ (10 x 250 mm) column. A gradient elution (9→16 %B in 40 min) was performed by building up a gradient starting with buffer A (1 % TFA) and applying buffer B (1 % TFA in

75 % acetonitrile) with a flow rate of 5 ml/min. The purity of compounds **43**, **44** and **45** was established by LC MS under the same conditions as used for analysis of the crude products.

ESI MS: **43**: m/z 2215 ($M^+$), 1108 ($M^{2+}/2$), 739 ($M^{3+}/3$)

**44**: m/z 1172 ($M^{2+}/2$), 782 ($M^{3+}/3$)

**45**: m/z 2741 ($M^+$), 1371 ($M^{2+}/2$), 914 ($M^{3+}/3$)

***Trans*-[Pt(NH$_3$)$_2$(g-*N7*-attcgc){3´d(G-*N7*-TAAGCG)}]$^{2+}$ (47)**

2.572 x $10^{-8}$ mol of **43** were reacted with 5.145 x $10^{-8}$ mol of 5´d(GCGAATG) (**46**) in 500 µl of a 0.1 M $NaClO_4$ solution at pH 6.5 at RT. In order to increase the solubility of **43**, 100 µl of DMF were added and the reaction mixture left for 11 d at RT. Compound **47** was purified by reversed-phase HPLC using an Alltech Alltima C18 5µ (4.6 x 150 mm) column. A gradient elution (0→23 %B in 40 min) was performed by building up a gradient starting with buffer A (50 mM TEAA) and applying buffer B (50 mM TEAA in 75 % acetonitrile) with a flow rate of 5 ml/min.

MALDI-TOF MS: m/z 4325 ($M^+$).

**9-*N*-cyclohexylmethyladenine (48)**

10.09 g (74.7 mmol) of adenine and 2.15 g (89.6 mmol) of NaH were suspended in 300 ml of DMF and stirred for 1 h at room temperature. 9.6 ml (69.3 mmol) of bromomethylcyclohexane was added and the reaction mixture stirred for 3 h at 70 °C and then for 14 h at RT. NaBr was removed by filtration over a glass filter. 200 ml water was added to the filtrate and the solution extracted with methylene chloride (3 x 150 ml). The organic layer was washed with water and the crude product purified by silica gel chromatography (eluent: dichloromethane / methanol 100 / 0 to 95 / 5, v / v) to give 2.11 g (12.2 %) pure 9-*N*-cyclohexyladenine.

$^1$H NMR ($CDCl_3$, δ, ppm): 8.37 (s, H2), 7.75 (s, H8), 4.09 (d, A-N9-$CH_2$), 5.61 (s, A-6-$NH_2$)

$^{13}$C NMR ($CDCl_3$, δ, ppm): 155.59 (C-6), 152.94 (C-2), 150.29 (C-4), 140.88 (C-8) 119.58 (C-5), 50.0 ($CH_2$N), 38.17, 30.58, 26.09, 25.46 (cyclohexyl);

ESI MS: m/z 232 ($M^+$);

elemental analysis: found (calculated): C: 62.3 (62.4), H: 7.4 (7.4), N: 30.3 (30.4).

### *Trans*-[Pt($NH_2CH_3$)$_2$(CHMA)(CHMT)]$^+NO_3^-$ (50)

To a solution of 0.189 g (0.368 mmol) of *trans*-[Pt($NH_2CH_3$)$_2$(CHMT)Cl] (**7**) in 11 ml of DMF was added a solution of 0.060 g (0.353 mmol) of $AgNO_3$ in 4 ml DMF and the reaction mixture was stirred for 6 h. AgCl was filtered off and 0.086 g (0.372 mmol) of 9-*N*-cyclohexylmethyladenine (**48**) was added and the reaction mixture stirred for 24 h. DMF was largely removed *in vacuo* and the product was recrystallized in methanol / diethylether (1/20, v/v) to give 0.100 g (35 %) of analytically pure *trans*-[Pt($NH_2CH_3$)$_2$(CHMA)(CHMT)]$^+NO_3^-$ (**50**).

$^1$H NMR ($CD_3OD$, δ, ppm): 9.04 (s, A-H2), 8.19 (s, A-H8), 7.35 (d, $^4$J = 0.95 Hz, T-H6), 4.55 (m, Pt-$NH_2$), 4.11 (d, $^3$J = 7.22 Hz, A-N9-$CH_2$), 3.64 (d, $^3$J = 6.82 Hz, T-N1-$CH_2$), 1.92 (d, $^4$J = 0.58 Hz, T-5-$CH_3$), 2.15 (t, $^3$J = 6.24 Hz, Pt-$NH_2$-C*H*$_3$); 1.70, 1.22, 1.06 (m, cyclohexyl);

$^1$H NMR ($CDCl_3$, δ, ppm): 9.074 (s, A-6-$NH_2$), 8.69 (s, A-H2), 7.63 (s, A-H8), 6.91 (s, T-H6), 5.13, 4.50 (m, Pt-$NH_2$), 3.94 (d, $^3$J = 7.09 Hz, A-N9-$CH_2$), 3.65 (d, $^3$J = 6.73 Hz, T-N1-$CH_2$), 1.70 (s, T-5-$CH_3$), 2.21 (t, $^3$J = 6.20 Hz, Pt-$NH_2$-C*H*$_3$); 1.75, 1.22, 1.06 (m, cyclohexyl);

$^1$H NMR (DMF-$d_7$, δ, ppm): 9.30 (s, A-6-$NH_2$), 8.85 (s, A-H2), 8.44 (s, A-H8), 7.38 (s, T-H6), 5.11 (m, Pt-$NH_2$), 4.15 (d, A-N9-$CH_2$), 3.50 (d, T-N1-$CH_2$), 2.24 (t, $^3$J = 6.10 Hz, Pt-$NH_2$-C*H*$_3$), 1.82 (s, T-5-$CH_3$), 1.70, 1.22, 1.06 (m, cyclohexyl);

$^{13}$C NMR ($CD_3OD$, δ, ppm): 157.6 (A-C6), 155.3 (A-C2), 149.4 (A-C4), 144.5 (A-C8), 120.5 (A-C5), 51.1 (A-C9), 109.8 (T-C5), 143.0 (T-C6), 174.0 (T-CO(4)), 159.0 (T-CO(2));

$^{195}$Pt NMR (δ, ppm): - 2594 (DMF-$d_7$), -2584 ($CD_3OD$), -2599 ($CDCl_3$);

ESI MS: m/z 709 ($M^+$);

elemental analysis: found (calculated): C: 40.3 (40.5), H: 5.6 (5.8), N: 18.0 (18.2).

***Trans*-[Pt($NH_2CH_3$)$_2$(CHMT)(TBS-ado)]$^+BF_4^-$ (51)**

To a solution of 0.095 g (0.185 mmol) of *trans*-[Pt($NH_2CH_3$)$_2$(CHMT)Cl] (**7**) in 5 ml DMF was added a solution of 0.034 g (0.175 mmol) of $AgBF_4$ in 1 ml of DMF and the reaction mixture was stirred for 10 h. AgCl was filtered off and 0.106 g (0.174 mmol) of TBS-ado (**49**) was added. The reaction mixture was stirred for 48 h. DMF was removed *in vacuo* and the residue recrystallized in diethylether / pentane to give 0.120 g (55.4 %) of analytically pure *trans*-[Pt($NH_2CH_3$)$_2$(CHMT)(TBs-ado)]$^+BF_4^-$ (**51**).

$^1$H NMR ($CD_3OD$, δ, ppm): 9.05 (s, A-H2), 8.46 (s, A-H8), 7.32 (d, $^4$J = 1.02 Hz, T-H6), 6.06 (d, $^3$J = 5.55 Hz, H1´), 4.65 (m, Pt-$NH_2$), 4.40 (t, $^3$J = 3.5 Hz, H3´), 4.16 (m, H4´), 4.07 (dd, $^3$J = 4.86 Hz, $^2$J = 11.31 Hz, H5´), 3.55 (dd, 3.85, $^3$J = 3.10 Hz, $^2$J = 11.31 Hz, H5´´), 3.64 (d, $^3$J = 7.05 Hz, T-N1-$CH_2$), 2.11 (t, $^3$J = 6.0 Hz, Pt-$NH_2C\mathit{H}_3$), 1.91 (s, T-5-$CH_3$), 1.80, 1.22 (m, cyclohexyl) 0.90, 0.75, 0.09, 0.07, 0.06, 0.03 (s, TBDMS);

$^1$H NMR ($CDCl_3$, δ, ppm): 8.76 (s, A-6-$NH_2$), 8.66 (s, A-H2), 8.43 (s, A-H8), 6.92 (s, T-H6), 5.95 (H1´), 4.47, 3.82 (m, Pt-$NH_2$), 3.66 (dd, $^3$J = 7.10 Hz, $^2$J = 13.55 Hz, H5´), 3.52 (dd, $^3$J = 6.6 Hz, $^2$J = 13.55 Hz, H5´´), 2.27, 2.10 (t, $^3$J = 6.35 Hz, $^3$J = 6.03 Hz, Pt-$NH_2C\mathit{H}_3$), 1.92 (s, T-5-$CH_3$), 0.90, 0.86, 0.10, 0.01, -0.02, (s, TBDMS);

$^{13}$C NMR ($CD_3OD$, δ, ppm): 157.7 (A-C6), 155.6 (A-C2), 148.9 (A-C4), 142.6 (A-C8), 121.5 (A-C5), 110.5 (T-C5), 142.9 (T-C6), 174.4 (T-CO(4)), 158.9 (T-CO(2)); 89,7 (C1´). 77.0 (C2´), 73.6 (C3´), 87.3 (C4´), 63.8 (C5´);

$^{195}$Pt NMR (DMF-$d_7$, δ, ppm): -2580;

IR ($\tilde{\nu}$, $cm^{-1}$): 3274, 2930, 2858, 1652, 1568, 1464, 1253, 1359, 1253, 1069, 1000, 836.1, 778, 670, 648, 591, 460;

elemental analysis: found (calculated): C: 42.6 (42.9), H: 6.8 (7.0), N: 10.7 (10.7).

# D Summary

The central aim of this thesis was to develop new methods for the synthesis of monofunctionally *trans*-Pt(II) modified deoxyoligonucleotide or deoxyoligonucleotide analogues by making use of solid-phase synthesis methodologies. A further aim was to assess the potential application of these platinated oligonucleotide (analogues) in antigene and antisense strategy. To this end, model crosslinking reactions with double- and single-stranded deoxyoligonucleotide targets were carried out.

Chapter I demonstrates the general applicability of monofunctionally *trans*-Pt(II) modified homopyrimidine oligonucleotides in antigene strategy. The monofunctionally *trans*-Pt(II) modified deoxyoligonucleotide **2**, obtained by post-synthetic *trans*-Pt(II) modification of the pyrimidine-rich deoxyoligonucleotide **1** in solution, has been shown to recognize a specific homopurine target within the double-stranded DNA fragment **3** with subsequent formation of a *trans*-Pt(II) interstrand crosslink at a defined site (Figure 1). The resulting *trans*-$(NH_3)_2$Pt(II)-bridged DNA triple helix **4** was characterized by gel-electrophoretic studies, ESI MS and UV spectroscopy. It was demonstrated that, in comparison to the respective unplatinated triplex **1•3**, the thermal stability of **4** was significantly increased by the *trans*-$(NH_3)_2$Pt(II) interstrand crosslink.

With respect to antigene strategy this means that, in principle, homopurine sequences in double-stranded DNA can be targeted sequence-specifically and crosslinked irreversibly to monofunctionally *trans*-Pt(II) modified antigene oligonucleotides. The crosslinked triple helical adducts possess a greater thermal stability which results in increased steric blockage of the target sequence by the antigene oligonucleotide. In this way it should in principle be possible to influence the process of transcription in a highly specific manner.

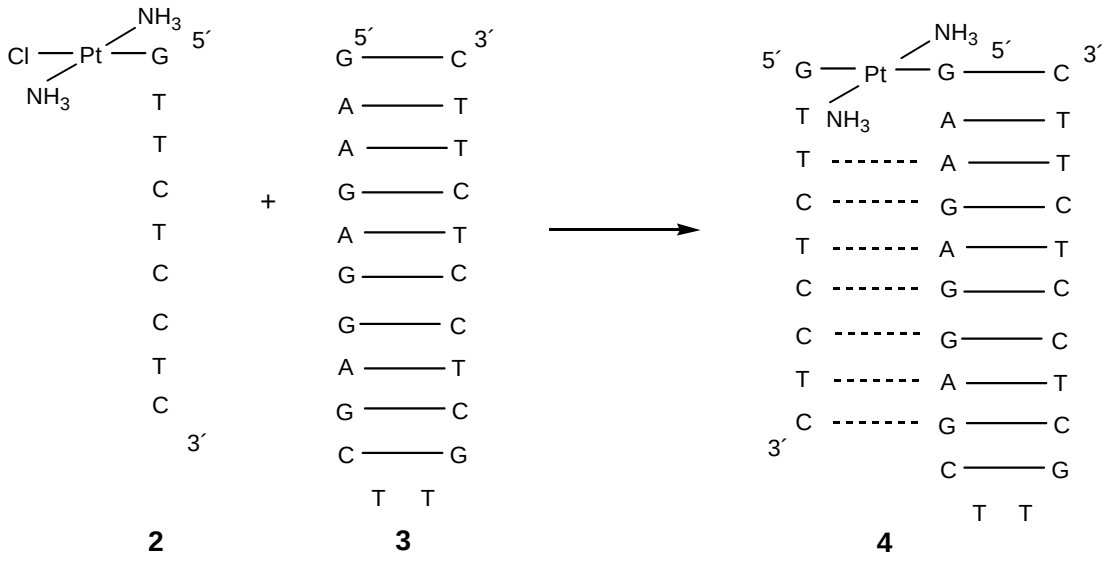


Figure 1: Formation of the *trans*-$(NH_3)_2$Pt(II) crosslinked DNA triple helix **4** by sequence-specific crosslinking reaction of the monofunctionally *trans*-Pt(II) modified oligonucleotide **2** with the DNA target **3**.

In Chapter II novel solid-phase methodologies for the synthesis of monofunctionally *trans*-Pt(II) modified homopyrimidine deoxyoligonucleotides are described. These methodologies involved the synthesis of the preplatinated building blocks **8** and **9**. Building blocks **8** and **9** have been conjugated to the 5´-terminus of deoxyoligonucleotides via a phosphate bond and an amide bond, respectively (Figure 2). The CHMT ligand in both **8** and **9** serves as a protecting group. After conjugation of **8** and **9** to oligonucleotides it can be substituted with a chloro ligand, thereby affording monofunctionally *trans*-Pt(II) modified oligonucleotides. A drawback associated with these methodologies is that the post-synthetic removal of the CHMT protecting group and its exchange by a chloro ligand requires a rather low pH, which may effect depurination reactions.[151] Therefore, this method is restricted to the synthesis of monofunctionally *trans*-Pt(II) modified homopyrimidine deoxyoligonucleotides for potential use mainly in antigene strategy.

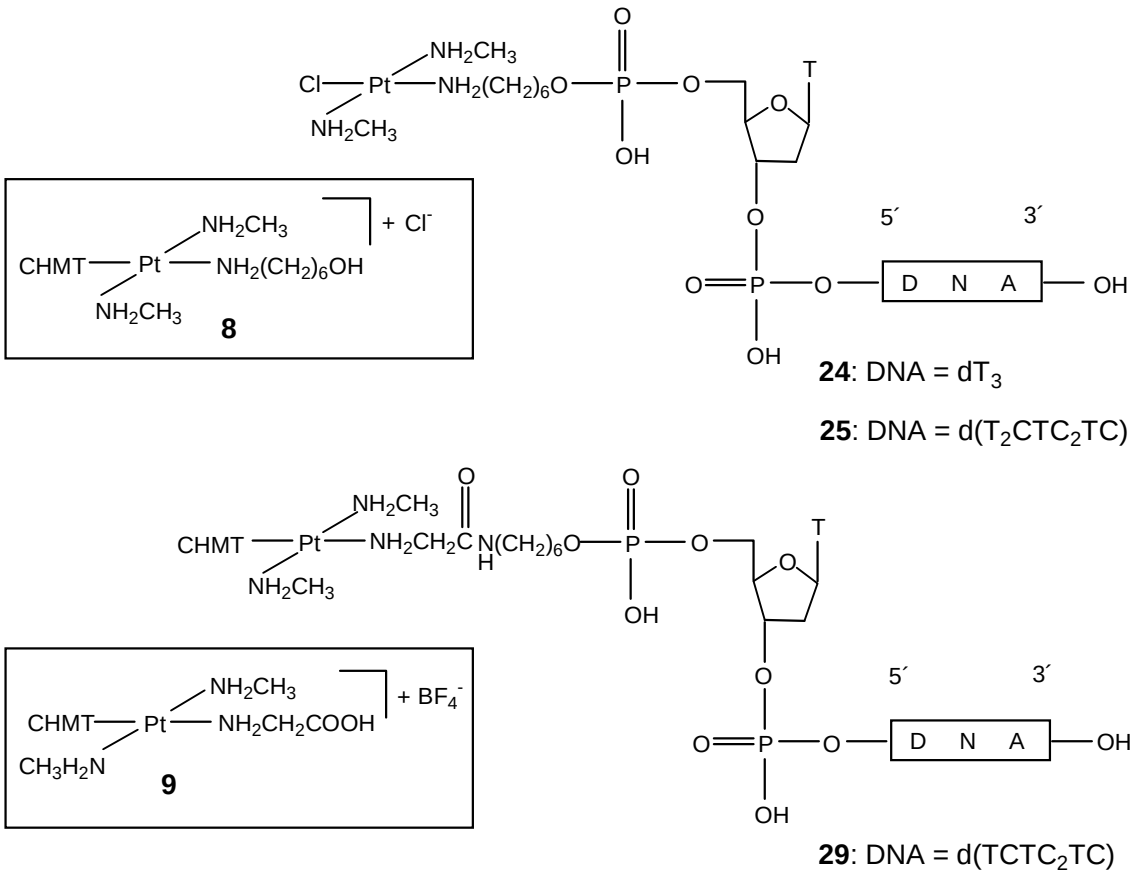


Figure 2: Solid-phase synthesis of monofunctionally *trans*-Pt(II) modified oligonucleotides by conjugation of building blocks **8** and **9** to the 5´-terminus of deoxyoligonucleotides.

Chapter III descibes a novel solid-phase methodology for the synthesis of monofunctionally *trans*-Pt(II) modified mixed pyrimidine / purine PNA oligomers. The design and synthesis of the preplatinated PNA building block **33**, which was shown to be compatible with solid-phase PNA synthesis, was an essential prerequisite. Incorporation of **33** in two different PNA oligomers and a PNA-peptide conjugate by solid-phase PNA synthesis yielded the monofunctionally *trans*-Pt(II) modified PNA oligomers **43**, **44** and **45** (Figure 3).

The potential use of these monofunctionally *trans*-Pt(II) modified PNA oligomers in antisense strategy has been demonstrated by a model crosslinking reaction in which *trans*-$[(NH_3)_2Pt(g\text{-}N7\text{-}attcgc)Cl]^+$ (**43**) has been reacted with the complementary oligonucleotide 5´d(GCGAATG) (**46**). As shown by MALDI TOF MS in combination with a hydroxyl radical footprinting experiment, this crosslinking reaction proceeded sequence-specifically, yielding, albeit in low yield, the *trans*-$(NH_3)_2Pt(II)$ crosslinked PNA / DNA duplex **47** (Figure 3).

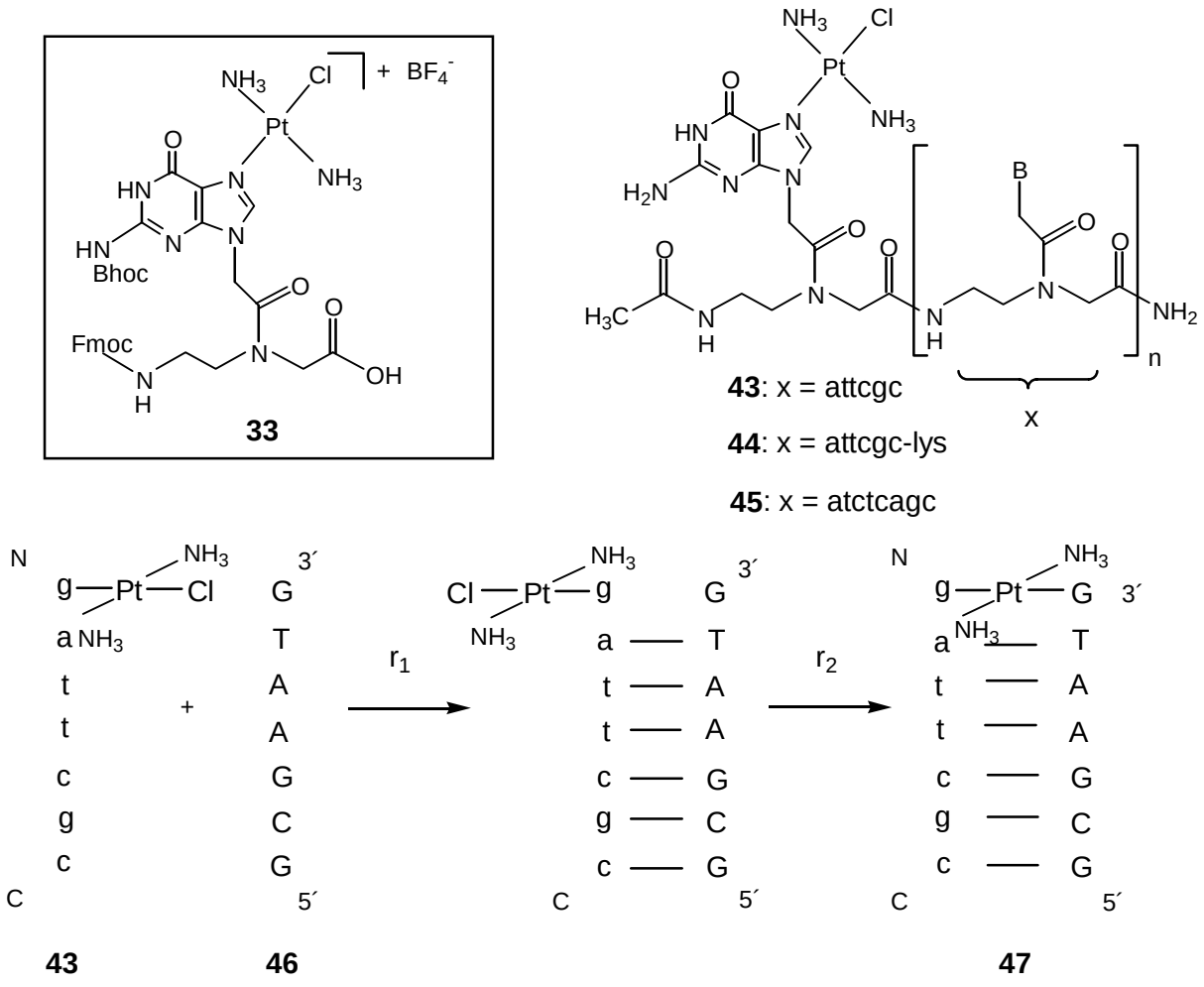


Figure 3: Solid-phase synthesis of monofunctionally *trans*-Pt(II) modified PNA oligomers **43**, **44** and **45** by incorporation of **33** in PNA oligomers and crosslinking reaction of **43** with the deoxyoligonucleotide target **46**.

Thus, the novel solid-phase methodology developed allows the facile synthesis of highly sequence-specific antisense drugs with crosslinking ability. The synthesized monofunctionally *trans*-Pt(II) modified PNA oligomers contain all four natural nucleobases and are not susceptible to enzymatic degradation. From these two points of view these potential antisense drugs are superior to the monofunctionally *trans*-Pt(II) modified deoxyoligonucleotides obtained by the methodologies described in chapter II. The methodology described in chapter III thus represents a facile and powerful new alternative towards the synthesis of specifically platinated oligonucleotide analogues with potential application both in antigene and antisense strategy.

Chapter IV deals with hydrogen bonding abilities of nucleobases involved in a *trans*-Pt(II) interstrand crosslink within a DNA triplex in which the two strands of the Watson-Crick duplex are crosslinked. As model compounds, the two chloroform-soluble *trans*-$a_2$Pt(II) crosslinked Watson-Crick A / T base pairs **50** and **51**, in which the hydrogen bond between A-*N1* and T-*N3* has been replaced by a linear *trans*-$a_2$Pt(II) unit, have been synthesized. The ability of these model compounds to perform Hoogsteen or reverse Hoogsteen hydrogen bonds with the chloroform-soluble thymine derivative 1-*N*-cyclohexylmethylthymine (**5**) has been investigated in the non-hydrogen bonding solvent chloroform (Figure 4). It has been found that in $CDCl_3$ in the presence of **50** and **51**, 1-*N*-cyclohexylmethylthymine (**5**) rather undergoes self-association than performing Hoogsteen or reverse Hoogsteen hydrogen bonds with **50** and **51**. By constrast, in equimolar mixtures of **5** and the unplatinated adenine derivative **48** in $CDCl_3$ hydrogen bonding interactions between **5** and **48** are definitely present as shown by concentration-dependent $^1$H NMR measurements.

Low temperature $^1$H NMR measurements of a mixture of **51** and the uridine derivative **52** in freon (Figure 4) show down to 193 K only the presence of homodimers of **52**. Only at 153 K two kinds of hydrogen-bonded **51** / **52** heterodimers in almost equal populations are observable. The **51** / **52** heterodimers have, based on NOE connectivities, been assigned as **51** / **52** pairs with Hoogsteen and reverse Hoogsteen geometries.

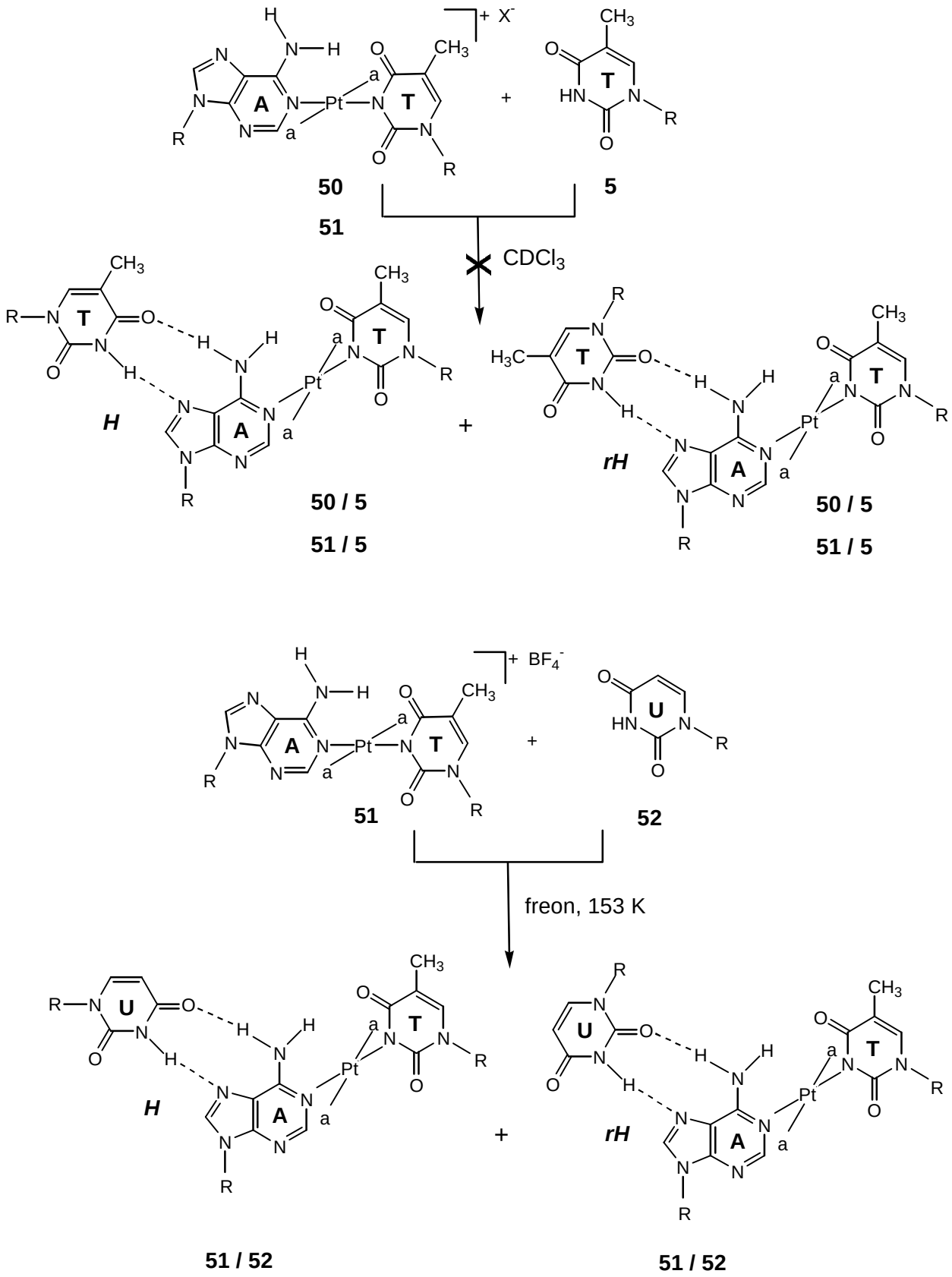


Figure 4: Hydrogen bonding interactions between **50** and **51** and **5** in $CDCl_3$ and **51** and **52** in freon.

## Zusammenfassung

Das Hauptziel dieser Arbeit war die Entwicklung neuer Methoden zur Synthese monofunktionell *trans*-Pt(II) modifizierter Deoxyoligonukleotide bzw. Deoxyoligonukleotid-Analoga. Ein Schwerpunkt lag dabei in der Anwendung von Methoden der Festphasensynthese. Ein weiteres Ziel war es, anhand von Modell-Crosslinking-Reaktionen Erkenntnisse über eine mögliche Anwendung der neuartig hergestellten monofunktionell *trans*-Pt(II) modifizierten Deoxyoligonukleotide bzw. deren Analoga in der Antigen- und Antisense-Strategie zu gewinnen.

Kapitel I zeigt die prinzipielle Anwendbarkeit von monofunktionell *trans*-Pt(II) modifizierten Deoxyoligonukleotiden in der Antigen-Strategie. Das monofunktionell *trans*-Pt(II) modifizierte Deoxyoligonukleotid **2**, welches durch direkte Transplatin-Modifikation des Deoxyoligonukleotids **1** in Lösung erhalten wurde, erkennt spezifisch eine Homopurinsequenz innerhalb des DNA-Fragmentes **3**. Nachfolgend kommt es zur regiospezifischen Ausbildung eines *trans*-$(NH_3)_2$Pt(II) interstrand crosslinks (Abb. 1). Das Produkt dieser Crosslinking-Reaktion ist die *trans*-$(NH_3)_2$Pt(II) verknüpfte DNA Tripelhelix **4**, welche durch gelelektrophoretische Untersuchungen, ESI-Massenspektrometrie sowie UV-Spektroskopie identifiziert bzw. charakterisiert wurde. Es zeigte sich, daß aufgrund der Verknüpfung durch den *trans*-$(NH_3)_2$Pt(II) interstrand crosslink die platinierte Triplex **4** eine größere thermische Stabilität besitzt als die entsprechende unplatinierte Triplex **1•3**.

Im Hinblick auf die Antigen-Strategie bedeuten die Ergebnisse, daß es prinzipiell möglich ist, durch Einsatz monofunktionell *trans*-Pt(II) modifizierter Oligonukleotide Homopurinsequenzen innerhalb doppelsträngiger DNA Fragmente sequenzspezifisch zu erkennen und diese durch Ausbildung eines interstrand crosslinks irreversibel mit dem Antigen-Oligonukleotid zu verknüpfen. Die entsprechenden tripelhelicalen Strukturen besitzen eine erhöhte thermische Stabilität, wodurch die sterische Blockierung der Zielsequenz verstärkt wird. Auf diese Art und Weise sollte es prinzipiell möglich sein, den Prozeß der Transkription gezielt zu beeinflussen.

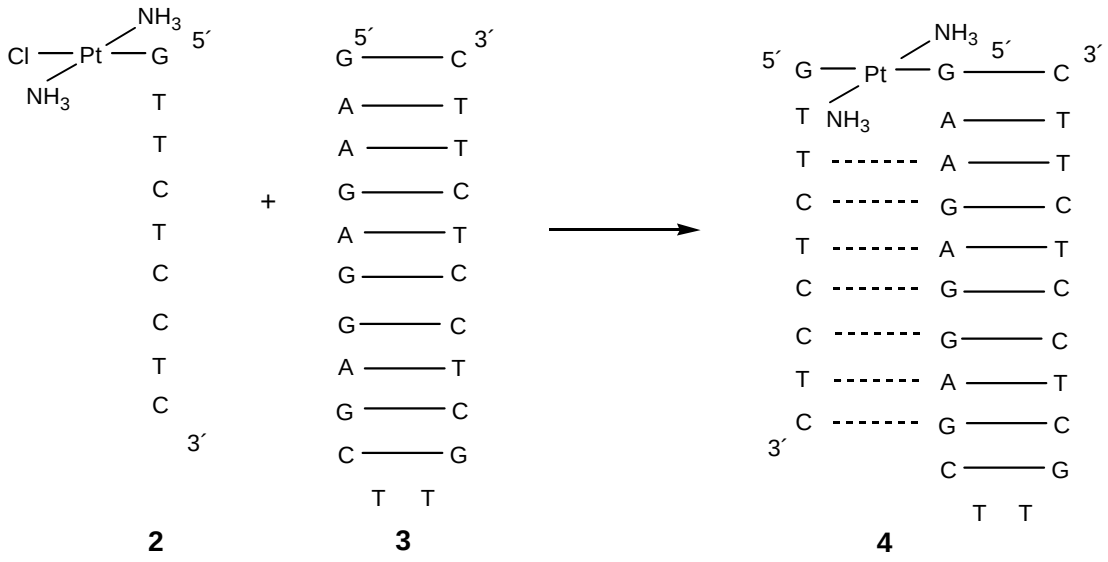


Abb. 1: Bildung der *trans*-$(NH_3)_2$Pt(II) verknüpften DNA Tripelhelix **4** durch sequenzspezifisches Crosslinking des monofunktionell *trans*-Pt(II) modifizierten Oligonukleotids **2** mit dem DNA Fragment **3**.

In Kapitel II werden neue Methoden zur Festphasensynthese monofunktionell *trans*-Pt(II) modifizierter Homopyrimidin Oligonukleotide beschrieben. Hierzu war zunächst die Synthese der platinierten Bausteine **8** und **9** notwendig. Nachfolgend wurden **8** und **9** dann über einen ihrer Liganden durch eine Phosphodiester- bzw. Amid-Bindung an das 5´-Ende eines Oligonukleotids gekuppelt (Abb. 2). Der CHMT Ligand in **8** und **9** dient als Schutzgruppe, welche die Kompatibilität der Bausteine mit den Bedingungen der automatisierten DNA Synthese leistet. Nach der Kupplung der Bausteine **8** und **9** an ein Oligonukleotid kann diese Schutzgruppe entfernt und gegen einen Chloroliganden ausgetauscht werden, wobei die gewünschten monofunktionell *trans*-Pt(II) modifizierten Oligonukleotide entstehen. Ein Nachteil besteht darin, daß zur Entfernung des CHMT Liganden saure Bedingungen (pH 2) erforderlich sind. Da unter diesen Bedingungen Depurinierungsreaktionen auftreten, sind die beschriebenen Methoden nur zur Synthese monofunktionell *trans*-Pt(II) modifizierter Homopyrimidin Oligonukleotide geeignet. Die beschriebenen Methoden können daher hauptsächlich zur Synthese möglicher Antigen-Reagentien genutzt werden.

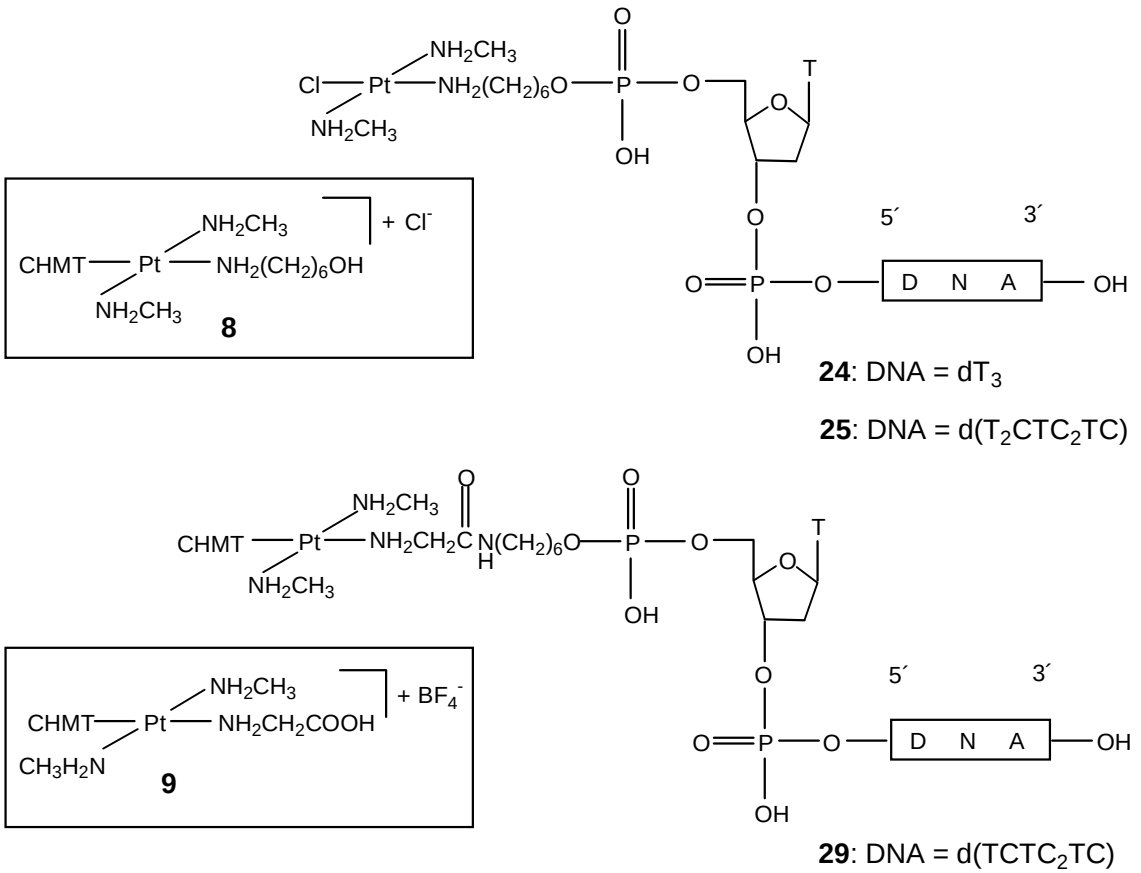


Abb. 2: Festphasensynthese monofunktionell *trans*-Pt(II) modifizierter Oligonukleotide durch Kupplung der platinierten Bausteine **8** und **9** an das 5´-Ende von Deoxyoligonukleotiden.

Kapitel III beschreibt die Entwicklung einer neuartigen Methode zur Festphasensynthese monofunktionell *trans*-Pt(II) modifizierter Hetero-PNA-Oligomere. Hierzu war zunächst die Synthese des platinierten PNA-Bausteins **33** erforderlich. Mit Hilfe der automatisierten PNA-Synthese wurde **33** in zwei verschiedene PNA-Oligomere und ein PNA-Peptid-Conjugat eingebaut und so die monofunktionell *trans*-Pt(II) modifizierten PNA-Oligomere **43**, **44** und **45** synthetisiert (Abb. 3). Die mögliche Anwendung dieser monofunktionell *trans*-Pt(II) modifizierten PNA-Oligomere in der Antisense-Strategie wurde anhand einer Modell-Crosslinking-Reaktion demonstriert. Zu diesem Zweck wurde *trans*-[$(NH_3)_2$Pt(g-*N7*-attcgc)Cl]$^+$ (**43**) mit dem komplementären Deoxyoligonukleotid 5´d(GCGAATG) (**46**) umgesetzt. Diese Reaktion führte in moderater Ausbeute zur sequenzspezifischen Ausbildung eines interstrand crosslinks unter Bildung der *trans*-$(NH_3)_2$Pt(II) verknüpften DNA / PNA Duplex **47.**

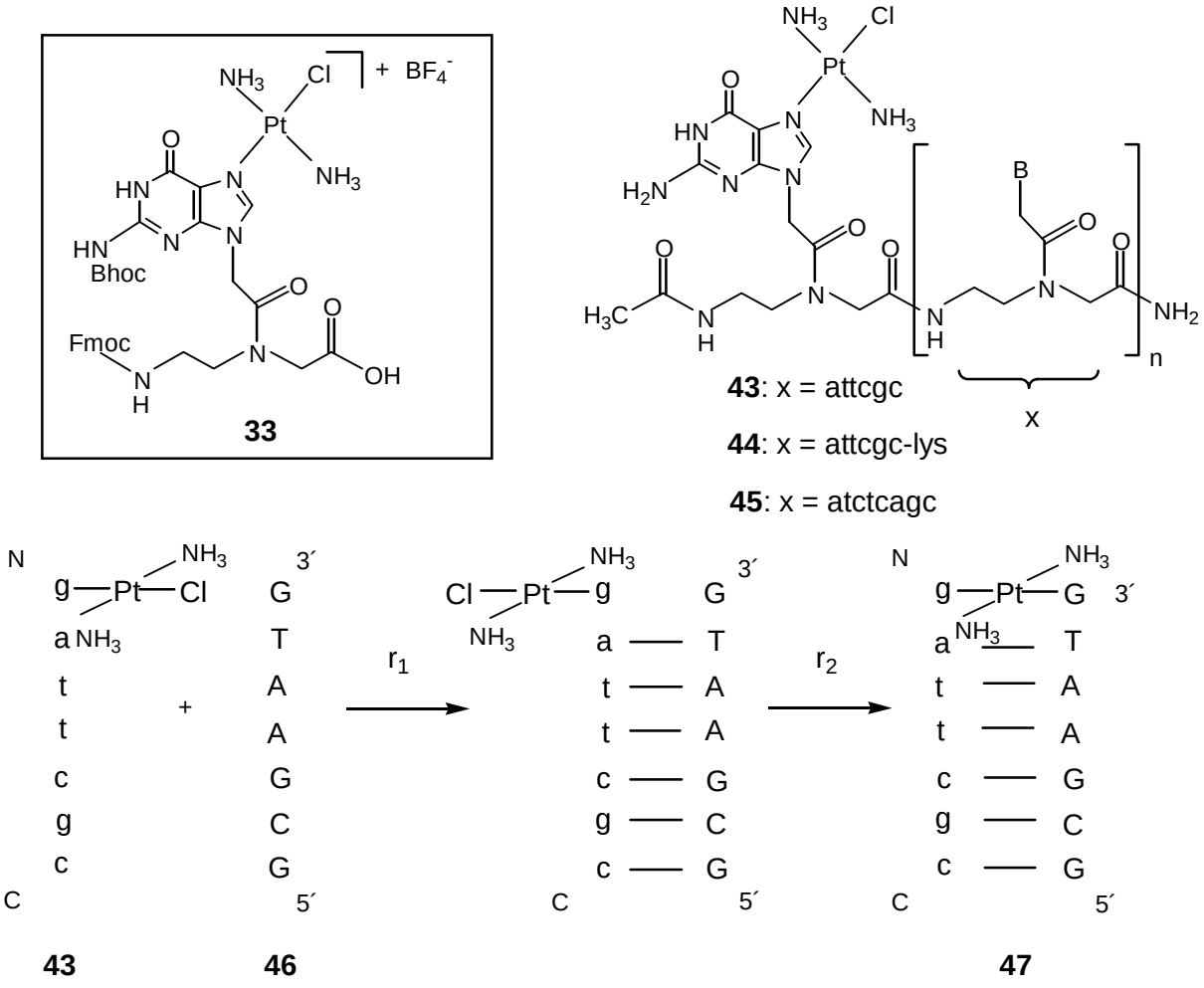


Abb. 3: Festphasensynthese monofunktionell *trans*-Pt(II) modifizierter PNA-Oligomere durch Einbau von **33** in PNA-Oligomere und sequenzspezifische Verknüpfung von **43** mit dem Deoxyoligonukleotid **46**.

Die in Kapitel III beschriebene Methode erlaubt somit eine relativ unproblematische Synthese von hochgradig sequenzspezifischen monofunktionell *trans*-Pt(II) modifizierten Antisense-Reagentien. Im Unterschied zu der in Kapitel II vorgestellten Methode bietet sie den Vorteil, daß auch die Synthese monofunktionell *trans*-Pt(II) modifizierter Heterosequenzen möglich ist, welche bei einer möglichen *in vivo* Anwendung aufgrund der speziellen Eigenschaften von PNA zusätzlich stabil gegen enzymatischen Abbau sind. Daher wird durch die Entwicklung der in Kapitel III beschriebenen Methode ein wichtiger Beitrag zur Synthese speziell platinierter Oligonukleotid-Analoga für potentielle Anwendungen in der Antigen- und Antisense-Strategie geleistet.

Kapitel IV befaßt sich mit der Fähigkeit zur Ausbildung von Wasserstoffbrücken von Nukleobasen, welche in einem interstrand crosslink innerhalb einer DNA Tripelhelix, in welcher die beiden Watson-Crick Stränge verknüpft sind, involviert sind. Als Modellverbindungen wurden die chloroformlöslichen *trans*-$a_2$Pt(II) ($a = NH_2CH_3$) verknüpften Watson-Crick A / T Basenpaare **50** und **51** synthetisiert, in welchen die Wasserstoffbrücke zwischen A-*N1* und T-*N3* gegen eine lineare *trans*-$a_2$Pt(II) Einheit ersetzt wurde. Die Fähigkeit dieser Modellverbindungen zur Ausbildung von Hoogsteen- bzw. reversen Hoogsteen-Wasserstoffbrücken mit dem chloroformlöslichen Thyminderivat 1-*N*-cyclohexylmethylthymin (**5**) wurde in dem nicht wasserstoffbrückenbildenden Solvens Chloroform untersucht (Abb. 4). Es stellte sich heraus, daß in Gegenwart von **50** und **51**, 1-*N*-cyclohexylmethylthymin (**5**) eher Selbstassoziation eingeht als Hoogsteen- oder reverse Hoogsteen-Wasserstoffbrücken mit **50** und **51** auszubilden. Zwischen dem unplatinierten Adeninderivat **48** und dem Thyminderivat **5** werden in $CDCl_3$ dagegen sehr wohl Wasserstoffbrücken ausgebildet, wie anhand von konzentrationsabhängigen $^1$H NMR Messungen gezeigt wurde.

Tieftemperatur- $^1$H NMR-Messungen eines Gemisches von **51** und dem Uridinderivat **52** in Freon (Abb. 4) zeigen bis 193 K nur das Vorhandensein wasserstoffbrückengebundener Homodimere von **52**. Erst bei 153 K wird das Vorhandensein zweier verschiedener wasserstoffbrückengebundener **51** / **52** Heterodimere beobachtet. Aufgrund eines $^1$H,$^1$H NOESY Experimentes konnten diese Heterodimere **51** / **52** Paaren mit Hoogsteen- bzw. reverser Hoogsteen-Geometrie zugeordnet werden.

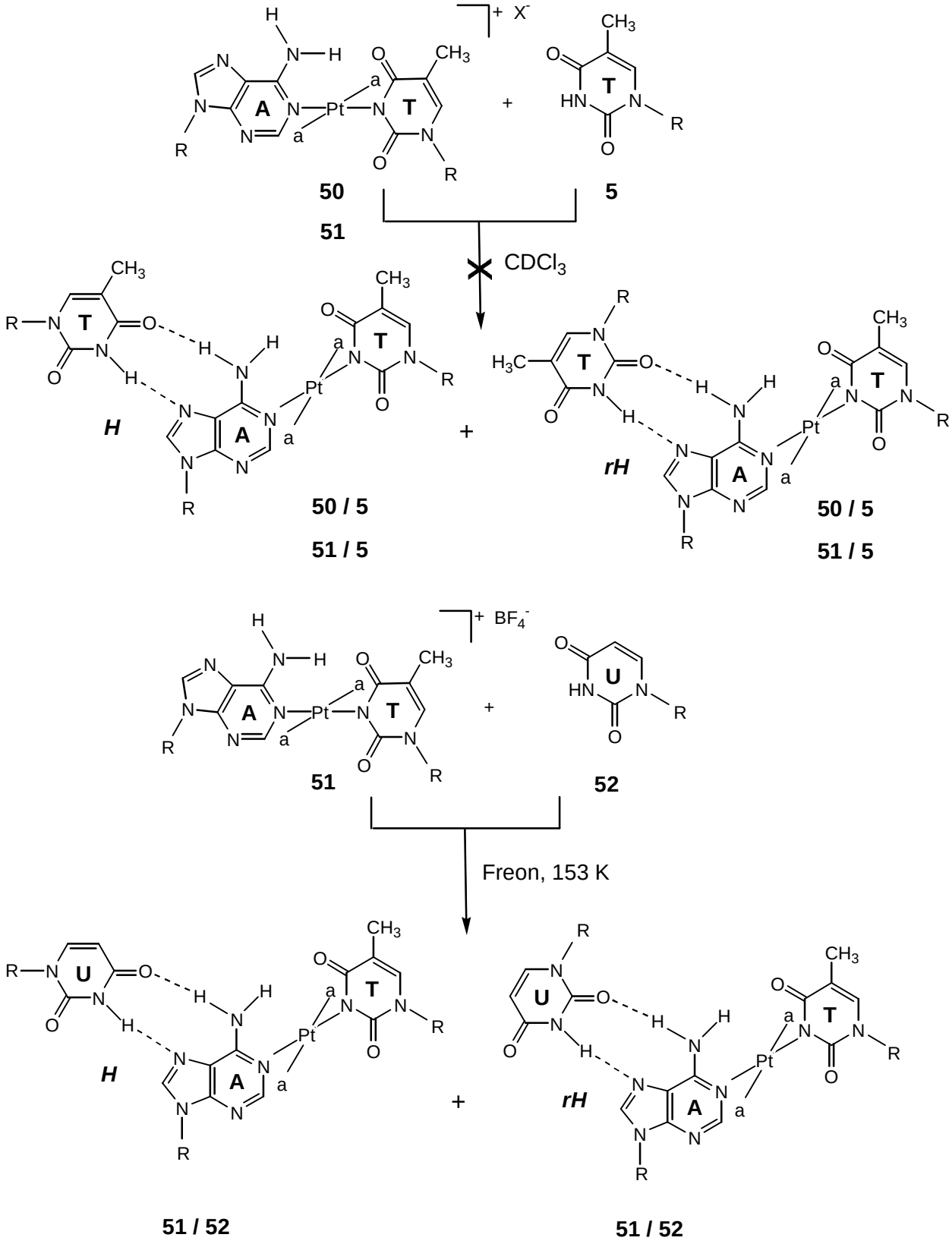


Abb. 4: Wasserstoffbrückenwechselwirkungen zwischen **50** bzw. **51** und **5** in $CDCl_3$ und zwischen **51** und **52** in Freon.

# E Appendix

## 1 References


1 L. Stryer, Biochemistry, 4th Ed., W.H. Freeman and Company, New York, **1995**.

2 J.W. Trauger, E.E. Baird, P.B. Dervan, Nature **1996**, *382*, 559.

3 J.M. Gottesfeld, L. Neely, J.W. Trauger, E.E. Baird, P.B. Dervan, Nature **1997**, *387*, 202.

4 L.A. Dickinson, R.J. Gulizia, J.W. Trauger, E.E. Baird, D.E. Mosier, J.M. Gottesfeld, P.B. Dervan, Proc. Natl. Acad. Sci. USA **1998**, *95*, 12890.

5 P.C. Zamecnik, M.L. Stephenson, Proc. Natl. Acad. Sci. USA **1978**, *75*, 280.

6 M.L. Stephenson, P.C. Zamecnik, Proc. Natl. Acad. Sci. USA **1978**, *75*, 285.

7 P.S. Miller, C.H. Agris, L. Aurelian, K.R. Blake, S.A. Glave, S.-B. Lin, A. Murakami, M.P. Reddy, C.C. Smith, S.A. Spitz, P.O.P. Ts`o, in Molecular Mechanims of carcinogenic and antitumor activity (Eds. C. Chagas, B. Pullman), Adenine Press, Schenectady, **1987**, p. 169.

8 V.N. Soyfer, V.N. Potaman, Triple Helical Nucleic Acids, Springer-Verlag, New York, Berlin, Heidelberg, **1996**.

9 K.M. Vasquez, J.H. Wilson, Trends Biochem. Sci. **1998**, *23*, 4.

10 N.T. Thuong, C. Hélène, Angew. Chem. Int. Ed. **1993**, *32*, 666.

11 V.A. Malkov, O.N. Voloshin, V.N. Soyfer, M.D. Frank-Kamenetskii, Nucleic Acids Res. **1993**, *21*, 585.

12 V.N. Potaman, V.N. Soyfer, J. Biomol. Struct. Dyn. **1994**, *11*, 1035.

13 M. Cooney, G. Czernuszewicz, E.H. Postel, S.J. Flint, M.E. Hogan, Science **1988**, *241*, 456.

14 M. Grigoriev, D. Praseuth, A.L. Guieysse, P. Robin, N.T. Thuong, C. Hélène, A. Harel-Bellan, Proc. Natl. Acad. Sci. USA **1993**, *90*, 3501.

15 M. Grigoriev, D. Praseuth, A.L. Guieysse, P. Robin, N.T. Thuong, C. Hélène, A. Harel-Bellan, C. R. Acad. Sci. III **1993**, *316*, 492.

16 S. Ritchie, F.M. Boyd, J. Wong, K. Bonham, J. Biol. Chem. **2000**, *275*, 847.

17 M. Faria, C. Wood, C. Perroualt, J.S.Nelson, A. Winter, M. White, C. Hélène. C. Giovannangeli, Proc. Natl. Acad. Sci. USA **2000**, *97*, 3862.

18 C. Bailey, D.L. Weeks, Nucleic Acids Res. **2000**, *28*, 1154.

19 S. Kuznetsova, S. Ait-Si-Ali, I. Nagibneva, F. Troalen, J.P. Le Villain, A. Harel-Bellan, F. Svinarchuk, Nucleic Acids Res. **1999**, *27*, 3995.

20 G. Wang, D.D. Levy, M.M. Seidman, P.M. Glazer, Mol. Cell. Biol. **1995**, *15*, 1759.

21 G. Wang, M.M. Seidman, P.M. Glazer, Science **1996**, *271*, 802.

22 K.M. Vasquez, G. Wang, P.A. Havre, P.M. Glazer, Nucleic Acids Res. **1999**, *27*, 1176.

23 K.M. Vasquez, L. Narayanan, P.M. Glazer, Science **2000**, *290*, 530.

24 D. Praseuth, A.L. Guieysse, C. Hélène, Biochim. Biophys. Acta **1999**, *1489*, 181, and refs. therein.

25 K.R. Fox, Curr. Med. Chem. **2000**, *7*, 17, and refs. therein.

26 D. M. Gowers, K.R. Fox, Nucleic Acids Res. **1999**, *27*, 1569, and refs. therein.

27 C. Escudé, J.-S. Sun, M. Rougee, T. Garestier, C. Hélène, C.R. Acad. Sci. Paris III **1992**, *315*, 521.

28 B. Couenoud, F. Casset, D. Hüsken, F. Natt, R. Wolf, K. Altman, P. Martin, H. Moser, Angew. Chem. Int. Ed. **1998**, *37*, 1288.

29 S.M. Gryaznov, Biochim. Biophys. Acta **1999**, *1489*, 131, and refs. therein.

30 P.E. Nielsen, Perspect. Drug Discov. Design **1996**, *4*, 76.

31 M. Egholm, O. Buchardt, L. Christensen, C. Behrens, S.M. Freier, D.A. Driver, R.H. Berg, S.K. Kim, B. Nordén, P.E. Nielsen, Nature **1993**, *365*, 566.

32 S. Tomac, M. Sarkar, T. Ratilainen, P. Wittung, P.E. Nielsen, B. Nordén, A. Gräslund, J. Am. Chem. Soc. **1996**, *118*, 5544.

33 P.E. Nielsen, M. Egholm, R.H. Berg, O. Buchardt, Science **1991**, *254*, 1497.

34 D.Y. Cherny, B.P. Belotserkovskii, M.D. Frank-Kamenetskii, M. Egholm, O. Buchardt, R.H. Berg, P.E. Nielsen, Proc. Natl. Acad. Sci. USA **1993**, *90*, 1667.

35 P.E. Nielsen, M. Egholm, O. Buchardt, J. Mol. Recognition **1994**, *7*, 165.

36 M.C. Griffith, L.M. Risen, M.J. Greig, E.A. Lesnik, K.G. Sprankle, R.H. Griffey, J.S. Kiely, S.M. Freier, J. Am. Chem. Soc. **1995**, *117*, 831.

37 M. Egholm, L. Christensen, K.L. Dueholm, O. Buchardt, J. Coull, P.E. Nielsen, Nucleic Acids Res. **1995**, *23*, 217.

38 T.A. Vickers, M.C. Griffith, K. Ramasamy, L.M. Risen, S.M. Freier, Nucleic Acids Res. **1995**, *23*, 3003.

39 P.E. Nielsen, M. Egholm, R.H. Berg, O. Buchardt, Nucleic Acids Res. **1993**, *21*, 197.

40 J.C. Hanvey, N.J. Peffer, J.E. Bisi, S.A. Thomson, R. Cadilla, J.A. Josey, D.J. Ricca, C.F. Hassman, M.A. Bonham, K.G. Au, S.G. Carter, D.A. Bruckenstein, A.L. Boyd, S.A. Noble, L.E. Babiss, Science **1992**, *258*, 1481.

41 P.E. Nielsen, M. Egholm, O. Buchardt, Gene **1994**, *149*, 139.

42 R.W. Taylor, P.F. Chinnery, D.M. Turnbull, R.N. Lightowlers, Nature Genet. **1997**, *15*, 212.

43 B. Wittung, J. Kajanus, K. Edwards, P. Nielsen, B. Norden, G. Malmstroem, FEBS Lett. **1995**, *365*, 27.

44 S. Basu, E. Wickstrom, Bioconjugate Chem. **1997**, *8*, 481.

45 G. Cutrona, E.M. Carpaneto, M. Ulivi, S. Roncella, O. Landt, M. Ferrarini, L.C. Boffa, Nature Biotech. **2000**, *18*, 300.

46 A.F. Faruqi, M. Egholm, P.M. Glazer, Proc. Natl. Acad. Sci. USA **1998**, *95*, 1398.

47 G. Wang, X. Xu, B. Pace, D.A. Dean, P.M. Glazer, P. Chan, S.R. Goodman, I. Shokolenko, Nucleic Acids Res. **1999**, *27*, 2806.

48 J.F. Milligan, M.D. Matteucci, J.C. Martin, J. Med. Chem. **1993**, *36*, 1923.

49 C.A. Stein, A.M. Krieg, Antisense Res. Dev. **1994**, *4*, 67.

50 A. de Mesmaeker, K.-H. Altman, A. Waldner, S. Wendeborn, Curr. Op. Struct. Biol. **1995**, *5*, 343.

51 B.F. Baker, B.P. Monia, Biochim. Biophys. Acta **1999**, *1489*, 3.

52 M. Manoharan, Biochim. Biophys. Acta **1999**, *1489*, 117.

53 O. Heidenreich, S. Gryaznov, M. Nerenberg, Nucleic Acids Res. **1997**, *25*, 776.

54 M.A. Bonham, S. Brown, A.L. Boyd, P.H. Brown, D.A. Bruckenstein, J.C. Hanvey, S.A. Thomson, A. Pipe, F. Hassman, J.E. Bisi, B.C. Froehler, M.D. Matteucci, R.W. Wagner, S.A. Noble, L.E. Babiss, Nucleic Acids Res. **1995**, *23*, 1197.

55 J.E. Gee, I. Robbins, A.C. van der Laan, J.H. van Boom, C. Colombier, M. Leng, A.R. Raible, J.S. Nelson, B. Lebleu, Antisense & Nucleic Acid Drug Development **1998**, *8*, 103.

56 H. Knudsen, P.E. Nielsen, Nucleic Acids Res. **1996**, *24*, 494.

57 C. Gambacorti-Passerini, L. Mologni, C. Bertazzoli, P. le Coutre, E. Marchesi, F. Grignani, P.E. Nielsen, Blood **1996**, *88*, 1411.

58 E. Uhlmann, D.W. Will, G. Breipohl, D. Langner, A. Ryte, Angew. Chem. Int. Ed. Engl. **1996**, *35*, 2632.

59 E. Uhlmann, P. Peyman, G. Breipohl, D.W. Will, Angew. Chem. Int. Ed. Engl. **1998**, *37*, 2796.

60 E. Uhlmann, Biol. Chem. **1998**, *379*, 1045.

61 J.C. Verheijen, B.A.L.M. Deiman, E. Yeheskiely, G.A. van der Marel, J.H. van Boom, Angew. Chem. Int. Ed. **2000**, *39*, 369.

62 T. Hermann, D.J. Patel, Science **2000**, *287*, 820, and refs. therein.

63 M. Boidot-Forget, M. Chassignol, M. Takasugi, T.T. Nguyen, C. Hélène, Gene **1988**, *72*, 361.

64 J.C. François, T. Saison-Behmoaras, C. Barbier, M. Chassignol, N.T. Thuong, C. Hélène, Proc. Natl. Acad. Sci. USA **1989**, *86*, 9702.

65 P. Bigey, G. Pratviel, B. Meunier, Nucleic Acids Res. **1995**, *23*, 3894, and refs. therein.

66 P. Bigey, S.H. Sönnichsen, B. Meunier, P.E. Nielsen, Bioconjugate Chem. **1997**, *8*, 267.

67 B.N. Trawick, A.T. Daniher, J.K. Bashkin, Chem. Rev. **1998**, *98*, 939, and refs. therein.

68 V.V. Vlassov, V.V. Gorn, E.M. Ivanova, S.A. Kazakov, S.V. Mamaev, FEBS Lett. **1983**, *162*, 286.

69 B.C.F. Chu, L.E. Orgel, Nucleic Acids Res. **1989**, *17*, 4783.

70 B.C.F. Chu, L.E. Orgel, Nucleic Acids Res. **1990**, *18*, 5163.

71 E.S. Gruff, L.E. Orgel, Nucleic Acids Res. **1991**, *24*, 6849.

72 A. Eastman, Biohemistry **1985**, *24*, 5027.

73 V. Brabec, M. Leng, Proc. Natl. Acad. Sci. USA **1993**, *90*, 5345.

74 H. Huang, L. Zhu, B.R. Reid, G.P. Drobny, P.B. Hopkins, Science **1995**, *270*, 1842.

75 F. Paquet, C. Perez, M. Leng, G. Lancelot, J.M. Malinge, J. Biomol. Struct. Dyn. **1996**, *14*, 67.

76 F. Coste, J.M. Malinge, L. Serre, W. Sheppard, M. Roth, M. Leng, C. Zelwer, Nucleic Acids Res. **1999**, *27*, 1837.

77 V. Brabec, M. Síp, M. Leng, Biochemistry **1993**, *32*, 11676.

78 F. Paquet, M. Boudvillain, G. Lancelot, M. Leng, Nucleic Acids Res. **1999**, *27*, 4261.

79 B. Andersen, E. Bernal-Mendez, M. Leng, E. Sletten, Eur. J. Inorg. Chem. **2000**, 1201.

80 O. Krizanovic, M. Sabat, R. Beyerle-Pfnür, B. Lippert, J. Am. Chem. Soc. **1993**, *115*, 5538.

81 I. Dieter-Wurm, M. Sabat, B. Lippert, J. Am. Chem. Soc. **1992**, *114*, 357.

82 S. Metzger, A. Erxleben, B. Lippert, J. Biol. Inorg. Chem. **1997**, *2*, 256.

83 S. Metzger, B. Lippert, J. Am. Chem. Soc. **1996**, *118*, 12467.

84 R.K.O. Sigel, M. Sabat, E. Freisinger, A. Mower, B. Lippert, Inorg. Chem. **1999**, *38*, 1481.

85 M. Boudvillain, M. Guérin, R. Dalbiès, T. Saison-Behmoaras, M. Leng, Biochemistry **1997**, *36*, 2925.

86 J.E. Gee, I. Robbins, A.C. van der Laan, J.H. van Boom, C. Colombier, M. Leng, A.R. Raible, J.S. Nelson, B. Lebleu, Antisense & Nucleic Acid Drug Development **1998**, *8*, 103.

87 K. Aupeix-Scheidler, S. Chabas, L. Bidou, J.-P. Rousset, M. Leng, J.-J. Toulmé, Nucleic Acids Res. **2000**, *28*, 438.

88 R. Dalbiès, D. Payet, M. Leng, Proc. Natl. Acad. Sci. USA **1994**, *91*, 8147.

89 M.B.L. Janik, B. Lippert, J. Biol. Inorg. Chem. **1999**, *4*, 645.

90 J. Müller, M. Drumm, M. Boudvillain, M. Leng, E. Sletten, B. Lippert, J. Biol. Inorg. Chem. **2000**, *5*, 603.

91 C. Colombier, B. Lippert, M. Leng, Nucleic Acids Res. **1996**, *24*, 4519.

92 J. Reedijk, Chem. Commun. **1996**, 801, and refs. therein.

93 U. Berghoff, K. Schmidt, M. Janik, G. Schröder, B. Lippert, Inorg. Chim. Acta **1998**, *269*, 135.

94 B. Lippert, Inorg. Chim. Acta **1981**, *55*, 5.

95 B. Lippert, U. Thewalt, H. Schöllhorn, D.M.L. Goodgame, R.W. Rollins, Inorg. Chem. **1984**, *23*, 2807.

96 B. Lippert, D. Neugebauer, G. Raudaschl, Inorg. Chim. Acta **1983**, *78*, 161.

97 U. Thewalt, D. Neugebauer, B. Lippert, Inorg. Chem. **1984**, *23*, 1713.

98 H. Schöllhorn, U. Thewalt, B. Lippert, J. Am. Chem. Soc. **1989**, *111*, 7213.

99 J. Schliepe, U. Berghoff, B. Lippert, D. Cech, Angew. Chem. Int. Ed. Engl. **1996**, *35*, 646.

100 R. Manchanda, S.U. Dunham, S.J. Lippard, J. Am. Chem. Soc. **1996**, *118*, 5144.

101 S.I. Khan, A.E. Beilstein, M. Sykora, G.D. Smith, X. Hu, M.W. Grinstaff, Inorg. Chem. **1999,** *38*, 3922.

102 S.I. Khan, A.E. Beilstein, M. Tierney, M. Sykora, M.W. Grinstaff, Inorg. Chem. **1999**, *38*, 5999.

103 X. Hu, G.D. Smith, M. Sykora, S.J. Lee, M.W. Grinstaff, Inorg. Chem. **2000**, *39*, 2500.

104 A.E. Beilstein, M.W. Grinstaff, Chem. Commun. **2000**, 509.

105 F.D. Lewis, S.A. Helvoigt, R.L. Letsinger, Chem. Commun. **1999**, 327.

106 R.C. Mucic, M.K. Herrlein, C.A. Mirkin, R.L. Letsinger, Chem. Commun. **1996**, 555.

107 P.J. Dandliker, R.E. Holmlin, J.K. Barton, Science **1997**, *275*, 1465.

108 E. Meggers, D. Kusch, B. Giese, Helv. Chim. Acta **1997**, *80*, 640.

109 W. Bannwarth, W. Pfleiderer, F. Müller, Helv. Chim. Acta **1991**, *74*, 1991.

110 J. Hall, D. Hüsken, U. Pieles, H.E. Moser, R. Häner, Chem. & Biol. **1994**, *1*, 185.

111 G.E. Plum, D.S. Pilch, S.F. Singleton, K.J. Breslauer, Annu. Rev. Biophys. Biomol. Struct. **1995**, *24*, 319.

112 R.W. Roberts, D.M. Crothers, Proc. Natl. Acad. Sci. USA, **1996**, *93*, 4320.

113 J. Völker, H.D. Klump, Biochemistry **1994**, *33*, 13502.

114 J.H. Ippel, V. Lanzotti, A. Galeone, L. Mayol, J.E. van den Boogaard, J.E. Pikkemaat, C. Altona, J. Biomol. Struct. Dyn. **1992**, *9*, 821.

115 L. Kibler-Herzog, B. Kell, G. Zon, K. Shinozuka, S. Mizan, W.D. Wilson, Nucleic Acids Res. **1990**, *18*, 3545.

116 D.M. Noll, A.-F. Miller, P.S. Miller, J. .Am. Chem. Soc. **1996**, *118*, 8979.

117 J.L. Asensio, A.N. Lane, J. Dhesi, S. Bergqvist, T. Brown, J. Mol. Biol. **1998**, *275*, 811.

118 J.L. Asensio, R. Carr, A.N. Lane, J. Am. Chem. Soc. **1999**, *121*, 11063.

119 J. Völker, S.E. Osborne, G.D. Glick, K. Breslauer, Biochemistry **1997**, *36*, 756.

120 S.E. Osborne, R.J. Cain, G.D. Glick, J. Am. Chem. Soc. **1997**, *119*, 1171.

121 R.B. Martin, Met. Ions Biol. Syst. **1996**, *32*, 61.

122 T.D. Tullius, B.A. Dombroski, Proc. Natl. Acad. Sci. USA, **1986**, *83*, 5469.

123 C. Bull, G.J. Mc Clune, J.A. Fee, J. Am. Chem. Soc. **1983**, *105*, 5290.

124 W. Knapp Pogozelski, T.D. Tullius, Chem. Rev. **1998**, *98*, 1089, and refs. therein.

125 E. Bernal-Méndez, J. Sun, F. González-Vilchez, M. Leng, New. J. Chem. **1998**, 1479.

126 S.J. Lippard, J.M. Berg in Principles of Bioinorganic Chemistry, University Science Books, Mill Valley, USA, **1994**.

127 D.P. Bancroft, C.A. Lepre, S.J. Lippard, J. Am. Chem. Soc. **1990**, *112*, 6860.

128 A. Eastman, M.A. Barry, Biochemistry **1987**, *26*, 3303.

129 K.S. Schmidt, D.V. Filippov, N.J. Meeuwenoord, G.A. van der Marel, J.H. van Boom, B. Lippert, J. Reedijk, Angew. Chem. Int. Ed. Engl. **2000**, *39*, 375.

130 M.J. Gait in An Introduction to Modern Methods of DNA Synthesis (Ed. M.J. Gait), IRL Press, Oxford, **1984**, pp. 1-22.

131 U. Berghoff, Ph. D. Thesis, Universität Dortmund, **1995**.

132 S. Ren, L. Cai, B.M. Segal, J. Chem. Soc., Dalton Trans. **1999**, 1413.

133 D.T. Browne, J. Eisinger, N.J. Leonard, J. Am. Chem. Soc. **1968**, *90*, 7302.

134 C.J.L. Lock, P. Pilon, B. Lippert, Acta Cryst. Sect. B **1979**, *35*, 2533.

135 L.S. Hollis, A.R. Amundsen, E.W. Stern, J. Med. Chem. **1989**, *32*, 128.

136 P.S. Pregosin in Annual Reports on NMR spectroscopy (Ed. G.A. Webb), Academic Press, London **1986**, *17*, 285.

137 B. Lippert, D. Neugebauer, Inorg. Chim. Acta **1980**, *46*, 171.

138 F.D. Rochon, R. Melanson, Acta Cryst. Sect. B, **1982**, *38* 1133.

139 R. Kuroda, S. Neidle, I.M. Ismail, P.J. Sadler, J. Chem. Soc. Dalton Trans. **1983**, 823.

140 Y.N. Kukushkin, V.B. Ukraintsev, A.I. Mokhov, Russ. J. Inorg. Chem. **1971**, *16*, 879.

141 F. Schwarz, B. Lippert, A. Iakovidis, N. Hadjiliadis, Inorg, Chim. Acta, **1990**, *168*, 275.

142 F.J. Pesch, H. Preut, B. Lippert, Inorg, Chim. Acta, **1990**, *169*, 195.

143 A. Iakovidis, N. Hadjiliadis, J.F. Britten, I.S. Butler, F. Schwarz, B. Lippert, Inorg, Chim. Acta, **1991**, *184*, 209.

144 T.G. Appleton, J.R. Hall, S.F. Ralph, Aust. J. Chem. **1986**, *39*, 1347.

145 S.J.S. Kerrison, P.J. Sadler, J. Chem. Soc. Chem. Commun. **1977**, 861.

146 Z. Zhang, J.Y. Tang, Tetrahedron Lett. **1996**, *37*, 331.

147 F.D. Lewis, S.A. Helvoigt, R.L. Letsinger, J. Chem. Soc. Chem. Commun. **1999**, 327.

148 T. Kempe, W.I. Sundquist, F. Chow, S.L. Hu, Nucleic Acids Res. **1985**, *13*, 45.

149 E. Kuyl-Yeheskiely, C.M. Tromp, A.H. Schaeffer, G.A. van der Marel, J.H. van Boom, Nucleic Acids Res. **1987**, *15*, 1807.

150 E. Kuyl-Yeheskiely, C.M. Tromp, A.W.M. Lefeber, G.A. van der Marel, J.H. van Boom, Tetrahedron **1988**, *44*, 6515.

151 J.A. Zoltewicz, D.F. Clark, T.W. Sharpless, G. Grahe, J. Am. Chem. Soc. **1970**, *92*, 1741.

152 J. Robles, S.B. Rajur, L.W. McLaughlin, J. Am. Chem. Soc. **1996**, *118*, 5820.

153 K. Wiederholt, S.B. Rajur, J. Giuliano, M.J. O´Donnel, L.W. McLauhglin, J. Am. Chem. Soc. **1996**, *118*, 7055.

154 S.B. Rajur, J. Robles, K. Wiederholt, R.G. Kuimelis, L.W. McLaughlin, J. Org. Chem. **1997**,*62*, 523.

155 V.V. Demidov, V.N. Potaman, M.D. Frank-Kamenetskii, M. Egholm, O. Buchardt, S.H. Sönnichsen, P.E. Nielsen, Biochem. Pharmacol. **1994**, *48*, 1310.

156 M. Egholm, O. Buchardt, P.E. Nielsen, R.H. Berg, J. Am. Chem. Soc. **1992**, *114*, 1895.

157 K.L. Dueholm, M. Egholm, C. Behrens, L. Christensen, H.F. Hansen, T. Vulpius, K.H. Petersen, R.H. Berg, P.E. Nielsen, O. Buchardt, J. Org. Chem. **1994**, *59*, 5767.

158 T. Koch, H.F. Hansen, P. Andersen, T. Larsen, H.G. Batz, K. Ottensen, H. Ørum, J. Pept. Res. **1997**, *49*, 80.

159 F. Bergmann, W. Bannwarth, S. Tam, Tetrahedron Lett. **1995**, *36*, 6823.

160 D.W. Will, G. Breipohl, D. Langner, J. Knolle, E. Uhlmann, Tetrahedron, **1995**, *51*, 12069.

161 A.C. van der Laan, R. Brill, R. Kuimelis, E. Kuyl-Yeheskiely, J.H. van Boom, Tetrahedron Lett. **1997**, *38*, 2249.

162 R. Casale, I.S. Jensen, M. Egholm in Peptide Nucleic Acids: Protocols and Applications (Eds. P.E. Nielsen, M. Egholm), Horizon Scientific Press, Wymondham, UK **1999**, pp. 39 – 50.

163 G.Y.H. Chu, S. Mansy, R.E. Duncan, R.S. Tobias, J. Am. Chem. Soc. **1978**, *100*, 593.

164 S.-M. Chen, V. Mohan, J.S. Kiely, M.C. Griffith, R.H. Griffey, Tetrahedron Lett., **1994**, *35*, 5105.

165 M.S. Bernatowicz, S.B. Daniels, H. Köster, Tetrahedron Lett. **1989**, *30*, 4645.

166 G. Schröder, B. Lippert, M. Sabat, D.J.C. Lock, R. Faggiani, B. Song, H. Sigel, J. Chem. Soc. Dalton Trans., **1995**, 3767.

167 M. Eriksson, P.E. Nielsen, Nature Struct. Biol. **1996**, *3*, 410.

168 J.C. Verheijen, G.A. van der Marel, J.H. van Boom, N. Metzler-Nolte, Bioconjugate Chem. **2000**, *11*, 741.

169 A.M.J. Fichtinger-Schepmann, J.L. van der Veer, J.H.J. den Hartog, P.H.M. Lohmann, J. Reedijk, Biochemistry, **1985**, *24*, 707.

170 D. Burnouf, C. Gauthier, J.C. Chottard, R.P.P. Fuchs, Proc. Natl. Acad. Sci. USA **1990**, *87*, 6087.

171 E.R. Jamieson, S. J. Lippard, Chem. Rev. **1999**, *99*, 2467.

172 H. Günther, NMR spectroscopy, Wiley, New York **1980**.

173 D. Yang, S.S.G.E. van Boom, J. Reedijk, J.H. van Boom, A.H.-J. Wang, Biochemistry **1995**, *34*, 12912, and refs. therein.

174 P.M. Takahara, A.C. Rosenzweig, C.A. Frederick, S.J. Lippard, Nature (London) **1995**, *377*, 649.

175 P.M. Takahara, C.A. Frederick, S.J. Lippard, J. Am. Chem. Soc. **1996**, *118*, 12309.

176 R.M. Wing, P. Pjura, H.R. Drew, R.E. Dickerson, EMBO J. **1984**, *3*, 1201.

177 R.K.O. Sigel, B. Lippert, Chem. Commun. **1999**, 2167.

178 R.K.O. Sigel, E. Freisinger, B. Lippert, J. Biol. Inorg. Chem. **2000**, *5*, 287.

179 J. Sponer, J.V. Burda, M. Sabat, J. Leszczynski, P. Hobza, J. Phys. Chem. A **1998**, *102*, 5951.

180 J.V. Burda, J. Sponer, J. Leszczynski, P. Hobza, J. Phys. Chem. B **1997**, *101*, 9670.

181 E.H.S. Anwander, M.M. Probst, B.M. Rode, Biopolymers **1990**, *29*, 757.

182 J. Sponer, M. Sabat, J.V. Burda, A.M. Doody, J. Leszczynski, P. Hobza, J. Biomol. Struct. Dyn. **1998**, *16*, 139.

183 L. Katz, S. Penman, J. Mol. Biol. **1966**, *15*, 220.

184 H. Iwahashi, Y. Kyogoku, J. Am. Chem. Soc. **1967**, *89*, 496.

185 B. Lippert, J. Chem. Soc. Dalton Trans. **1997**, 3971, and refs. therein.

186 B. Lippert, Coord. Chem. Rev. **2000**, *200*, 487, and refs. therein.

187 R.B. Martin in Cisplatin: Chemistry and Biochemistry of a Leading Anticancer Drug, (Ed. B. Lippert), VHCA, Zürich and Wiley-VCH, Weinheim, **1999**, p.183.

188 C. Meiser, B. Song, E. Freisinger, M. Peilert, H. Sigel, B. Lippert, Chem. Eur. J. **1997**, *3*, 388.

189 M.C. Lim, R.B. Martin, J. Inorg. Nucl. Chem. **1976**, *38*, 1915.

190 R.B. Martin, Acc. Chem. Res. **1985**, *18*, 32.

191 R.B. Martin, Metal Ions Biol. Syst. **1996**, *32*, 61.

192 J. Arpalahti, H. Lonnberg, Inorg. Chim. Acta **1983**, *78*, 63.

193 M.D. Reily, L.G. Marzili, J. Am. Chem. Soc. **1986**, *108*, 6785.

194 J. Arpalahti, P. Lehikonen, Inorg. Chim. Acta **1989**, *159*, 115.

195 R. Beyerle-Pfnür, B. Brown, R. Faggiani, B. Lippert, C.J.L. Lock, Inorg. Chem. **1985**, *24*, 4001.

196 J. Arpalahti, K.D. Klika, R. Sillanpää, R. Kivekäs, J. Chem. Soc. Dalton Trans. **1998**, 1397.

197 R. Beyerle, B. Lippert, Inorg. Chim. Acta **1982**, *66*, 141.

198 J.H.J. den Hartog, H. van den Elst, J. Reedijk, J. Inorg. Biochem. **1984**, *21*, 83.

199 F. Schwarz, B. Lippert, H. Schöllhorn, U. Thewalt, Inorg. Chim. Acta **1990**, *176*, 113.

200 J.P. Charland, M.T. Phan Viet, M. St-Jacques, A.L. Beauchamp, J. Am. Chem. Soc. **1985**, *107*, 8202.

201 M.T. Chenon, R.J. Pugmire, D.M. Grant, R.P. Paniza, L.B. Townsend J. Am. Chem. Soc. **1975**, *97*, 4627.

202 S.-O. Shan, S. Loh, D. Herschlag, Science **1996**, *272*, 97.

203 H. Iwahashi, Y. Kyogoku, J. Am. Chem. Soc. **1977**, *99*, 7761.

204 G. Lancelot, C. Hélène, Nucleic Acids Res. **1979**, *6*, 1063.

205 Y. Kyogoku, R.C. Lord, A. Rich, Proc. Natl. Acad. Sci. USA **1967**, *57*, 250.

206 S.N. Smirnov, N.S. Golubev, G.S. Denisov, H. Benedict, P. Schah-Mohammedi, H.-H. Limbach, J. Am. Chem. Soc. **1996**, *118*, 4094.

207 N.S. Golubev, S.N. Smirnov, V.A. Gindin, G.S. Denisov, H. Benedict, H.-H. Limbach, J. Am. Chem. Soc. **1994**, *116*, 12055.

208 N.S. Golubev, G.S. Denisov, S.N. Smirnov, D.N. Shchepkin, H.-H. Limbach, Z. Phys. Chem. **1996**, *196*, 73.

209 A. Dunger, H.-H. Limbach, K. Weisz, Chem. Eur. J. **1998**, *4*, 621.

210 A. Dunger, H.-H. Limbach, K. Weisz, J. Am. Chem. Soc. **2000**, *122*, 10109.

211 A.J. Dingley, J.E. Masse, R.D. Peterson, M. Barfield, J. Feigon, S. Grzesiek, J. Am. Chem. Soc. **1999**, *121*, 6019.

212 L. Paollilo, E.D. Becker, J. Magn. Res. **1970**, *2*, 168.

213 T. Axenrod, P.S. Pregosin, M.J. Wieder, E.D. Becker, R.B. Bradley, G.W.A. Milne, J. Am. Chem. Soc. **1971**, *93*, 6536.

214 T. Axenrod, M.J. Wieder, J. Am. Chem. Soc. **1971**, *93*, 3541.

215 C.D. Poulter, C.L. Livingston, Tetrahedron Lett. **1979**, *9*, 755.

216 N.S. Golubev, I.G. Shenderovich, S.N. Smirnov, G.S. Denisov, H.-H. Limbach, Chem. Eur. J. **1999**, *5*, 492.

217 G.B. Kauffman, D.O. Cowan, Inorg. Synth. **1963**, *7*, 239.

218 J. Arpalahti, B. Lippert, H. Schöllhorn, U. Thewalt, Inorg. Chim Acta **1988**, *153*, 45.

219 T. Kistenmacher, M. Rossi, J.P. Caradonna, L.G. Marzilli, Adv. Mol. Rel. Interact. Processes **1979**, *15*, 119.

220 J.S. Nowick, J.S. Chen, G. Noronha, J. Am. Chem. Soc. **1993**, *115*, 7636.

221 K.K. Ogilvie, Can. J. Chem. **1973**, *51*, 3799.

222 D.V. Filippov, Ph.D. Thesis, Leiden University, **1998**.

223 H. Sigel, K.H. Scheller, V.M. Rheinberger, B. Fischer, J. Chem. Soc. Dalton Trans. **1980**, 1022.

224 R.B. Martin, Science **1963**, *139*, 1198.

## 2 Overview on described compounds

**1*** 5´d($GT_2CTC_2TC$)$^{8-}$

**2** *trans*-[$Pt(NH_3)_2${5´d(G-*N7*-$T_2CTC_2TC$)}Cl]$^{7-}$

**3*** 5´d($GA_2GAG_2AGCT_2GCTC_2TCT_2C$)$^{21-}$

**4** *trans*-[$Pt(NH_3)_2${5´d(G-*N7*-$T_2CTC_2TC$)}{(5´d(G-*N7*-$A_2GAG_2AGCT_2GCTC_2TCT_2C$)}]$^{27-}$

**5** 1-*N*-cyclohexylmethylthymine

**6** K(1-*N*-cyclohexylmethylthyminate)

**7** *trans*-[$Pt(NH_2CH_3)_2$(CHMT)Cl]

**7a**** *trans*-[$Pt(NH_2CH_3)_2$(CHMT)(DMF)]$^+BF_4^-$

**7b**** *trans*-[$Pt(NH_2CH_3)_2$(CHMT)(DMF)]$^+NO_3^-$

**8** *trans*-[$Pt(NH_2CH_3)_2$(CHMT){$NH_2(CH_2)_6OH$}]$^+Cl^-$

**8a**** *trans*-[$Pt(NH_2CH_3)_2$(CHMT){$NH_2(CH_2)_6$*O*-phosphoramidite }]$^+Cl^-$

**9** *trans*-[$Pt(NH_2CH_3)_2$(CHMT)(gly-*N*)]$^+BF_4^-$

**10** *trans*-[$Pt(NH_3)_2$(1-MeT)(gly-*N*)]$^+NO_3^-$

**11*** chloro(N,N-diisopropyl)-β-cyanoethoxyphosphine

**12*** 5´-*O*-DMTr-deoxythymidine-3´-phosphoramidite

**13** *trans*-[$Pt(NH_2CH_3)_2$(CHMT){$NH_2(CH_2)_6O(PO_3H)$-dT-5´-*O*-DMTr}]$^+$

**14** *trans*-[$Pt(NH_2CH_3)_2$(CHMT){$NH_2(CH_2)_6O(PO_3H)$-dT-5´-OH}]$^+$

**15** *trans*-[$Pt(NH_2CH_3)_2${$NH_2(CH_2)_6O(PO_3H)$-dT-5´-OH}Cl]$^+$

**16*** 5´-OH-$dT_4$-3´-CPG

**16a** 5´-phosphoramidite-$dT_4$-3´-CPG

**16b** 5´-phosphoramidate-$dT_4$-3´-OH

**17*** $DMTrO(CH_2)_5OH$

**18*** 5´-$HO(CH_2)_5OPO_3H$-$dT_4$-3´-OH

**19*** 5´-OH-d($T_3CTC_2TC$)-3´-CPG

**19a** 5´-phosphoramidite-d($T_3CTC_2TC$)-3´-CPG

**20** *trans*-[$Pt(NH_2CH_3)_2$(CHMT){$NH_2(CH_2)_6O(PO_3H)dT_4$-3´-CPG}]$^+$

**21** *trans*-[$Pt(NH_2CH_3)_2$(CHMT){$NH_2(CH_2)_6O(PO_3H)$d($T_3CTC_2TC$)-3´-CPG}]$^+$

**22** *trans*-[$Pt(NH_2CH_3)_2$(CHMT){$NH_2(CH_2)_6O(PO_3H)dT_4$-3´-OH}]$^+$

**23** *trans*-[$Pt(NH_2CH_3)_2$(CHMT){$NH_2(CH_2)_6O(PO_3H)$d($T_3CTC_2TC$)-3´-OH}]$^+$

**24** *trans*-[$Pt(NH_2CH_3)_2${$NH_2(CH_2)_6O(PO_3H)dT_4$-3´-OH}Cl]$^+$

**25** *trans*-[Pt($NH_2CH_3$)$_2${$NH_2(CH_2)_6O(PO_3H)$d($T_3CTC_2TC$)-3´-OH}Cl] $^+$

**26**$^*$ MMTrHN$(CH_2)_6$OP{($OCH_2CH_2CN$)(N(*i*Pr)$_2$}

**27**$^*$ 5´-OH-d($T_2CTC_2TC$)-3´-CPG

**28**$^*$ 5´-$NH_2(CH_2)_6O$-d($T_2CTC_2TC$)-3´-CPG

**29** *trans*-[Pt($NH_2CH_3$)$_2$(CHMT){($NH_2CH_2CONH(CH_2)_6O(PO_3H)$d($T_2CTC_2TC$)-3´-OH}]$^+$

**30**$^*$ $NH_2$-$c_5$-gly-HMBA-PS

**31** *trans*-[Pt($NH_2CH_3$)$_2$(CHMT)($NH_2CH_2CONH$-$c_5$-gly)]$^+$

**32**$^*$ N-[(*N2*-benzhydryloxycarbonylguanin-9-yl)acetyl]-
N-[2-{(9-fluorenylmethyloxycarbonyl)amino}ethyl]glycine
(Fmoc/N-Bhoc protected guanine PNA monomer)

**33** *trans*-[Pt($NH_3$)$_2$(Fmoc/N-Bhoc G)Cl]$^+$$BF_4^-$

**34** *trans*-[Pt($NH_3$)$_2$(CHMT)(Fmoc/N-Bhoc G)]$^+$$BF_4^-$

**35** Ac-gattcgc-Rink-PEG-PS;

**36** Ac-gattcgc-$NH_2$

**37** Fmoc-attcgc-Rink-PEG-PS

**38** Fmoc-attcgc-lys-Rink-PEG-PS

**39** Fmoc-atctcagc-Rink-PEG-PS

**40** *trans*-[Pt($NH_3$)$_2$Cl(Fmoc-g-*N7*-attcgc-Rink-PEG-PS)]$^+$

**41** *trans*-[Pt($NH_3$)$_2$Cl(Fmoc-g-*N7*-attcgc-lys-Rink-PEG-PS)]$^+$

**42** *trans*-[Pt($NH_3$)$_2$Cl(Fmoc-g-*N7*-atctcagc-Rink-PEG-PS)]$^+$

**43** *trans*-[Pt($NH_3$)$_2$Cl(Ac-g-*N7*-attcgc-$NH_2$)]$^+$

**44** *trans*-[Pt($NH_3$)$_2$Cl(Ac-g-*N7*-attcgc-lys-$NH_2$)]$^+$

**45** *trans*-[Pt($NH_3$)$_2$Cl(Ac-g-*N7*-atctcagc-$NH_2$)]$^+$

**46**$^*$ 5´d(GCGAATG)

**47** *trans*-[Pt($NH_3$)$_2$(Ac-g-*N7*-attcgc-$NH_2$){3´d(G-*N7*-TAAGCG}]$^{2+}$

**48** 9-*N*-cyclohexylmethyladenine

**49**$^*$ 2´,3´,5´-tris-(*tert*-butyldimethylsilyl)-adenosine

**50** *trans*-[Pt($NH_2CH_3$)$_2$(CHMA)(CHMT)]$^+$$NO_3^-$

**51** *trans*-[Pt($NH_2CH_3$)$_2$(CHMT)(TBS-ado)]$^+$$BF_4^-$

**52**$^§$ 3´,5´-diacetyl-2´-deoxyuridine

$^*$ not described for the first time

$^{**}$ not isolated

$^§$ provided by Dr. K. Weisz, FU Berlin

# Curriculum Vitae

## Personal details

| | |
|---|---|
| Name: | Kathrin Susanne Schmidt |
| Date of birth: | 21.10.1971 |
| Place of birth: | Unna |
| Nationality: | German |

## School

| | |
|---|---|
| 08/1978 - 06/1982 | Primary school: Grilloschule (Unna) |
| 08/1982 - 06/1991 | Grammar school: Geschwister-Scholl-Gymnasium (Unna) |
| 18.06.1991 | Final exam: Abitur |

## University

| | |
|---|---|
| 10/1991 - 09/1996 | Student of chemistry at the University of Dortmund, Dortmund, Germany |
| 13.10.1993 | Vordiplom |
| 03/1996 - 09/1996 | Master thesis in the workgroup of Prof. Dr. B. Lippert, University of Dortmund; Subject: "Synthesis of monofunctionally platinated oligonucleotides as interstrand crosslinking reagents in antigene strategy" |
| 27.09.1996 | Diplom |
| since 10/1996 | Ph. D. studentship in the workgroup of Prof. Dr. B. Lippert, University of Dortmund; Subject: “Solution- and solid-phase synthesis of monofunctionally *trans*-Pt(II) modified oligonucleotide (analogues) and their potential application in antigene and antisense strategy” |
| since 02/1997 | Work partly in the group of Prof. Dr. J. Reedijk and Prof. Dr. J.H. van Boom, Leiden University, Leiden, The Netherlands |